eman ta zabal zazu

Universidad del País Vasco
Euskal Herriko Unibertsitatea

Characterization of USP11 as a novel regulator of Hypoxia Inducible Factor α

Doctoral Thesis

Teresa Martín Mateos

2019

Characterization of USP11 as a novel regulator of Hypoxia Inducible Factor α

Teresa Martín Mateos

Doctoral Thesis 2019

Director: Dr. Edurne Berra

Doctorate Program: Molecular Biology and Biomedicine

Department: Biochemistry and Molecular Biology

University of Basque Country (UPV/EHU)

This work has been performed at the Centre for Cooperative Research in Biosciences (CIC bioGUNE) supported by the Spanish Government (BES_2014_070406, EEBB-1-17-12687, BFU_2013_46647_R, BFU_2016_76872_R) and RedHypox (SAF2017-90794-REDT)

Table of Contents

Abbreviations....11
Abstract....17
Resumen....19
Introduction....21
1 Hypoxia signalling pathway....23
1.1 Dealing with hypoxia....23
1.1.1 The family of HIF- a:....25
1.1.2 HIF-a regulation....26
2 Role of DUBs in hypoxia....33
2.1 Ubiquitin-mediated posttranslational modifications....33
2.2 DUBs that promote HIF-1a stability....35
2.3 DUBs regulated by hypoxia....36
2.4 USP11....38
2.4.1 Structure of USP11....38
2.4.2 Functional relevance of USP11 and direct targets....40
2.4.3 Regulation of USP11....43
Hypothesis and Aims....45
Materials and Methods....49
1 Materials....51
2 Methods....51
2.1 Molecular biology....51
2.1.1 Polymerase chain reaction (PCR)....51
2.1.2 RNA extraction and Reverse Transcriptase quantitative Polymerase Chain Reaction (RT-qPCR)....52
2.1.3 Mutagenesis....53
2.1.4 Restriction digestion....54
2.1.5 In-Fusion® HD cloning....54
2.1.6 Bacterial transformation....55
2.2 Cell biology....56
2.2.1 Cell culture and transfections....56
2.2.2 DNA transfections....56
2.2.3 siRNA transfections....56
2.2.4 GFP-Fluorescence detection....57
2.3 Biochemistry....58

2.3.1 Ribonucleoprotein immunoprecipitation (RIP) 58
2.3.2 Biotin pulldown assay 58
2.3.3 Luciferase assays 59
2.3.4 Cell fractionation 60
2.3.5 Western Blot 61
2.3.6 DUB activity assay 62
2.3.7 Ubiquitination assay 62
2.3.8 Co-immunoprecipitation assays 63
2.3.9 MassSpec (MS) analysis 64
2.4 Statistical Analysis 64
Results 65
1 RNAi screen of DUBs that modulate the hypoxia signalling cascade 67
1.1 Validation of the screening 67
1.1.1 Silencing efficacy of the selected candidates 67
1.1.2 Impact of the selected candidates in the induction of hypoxia target genes 69
2 USP11 is an activator of the hypoxia-signalling cascade 71
2.1 USP11 induces HIF target genes 71
2.2 USP11 accumulates HIF-1α but not HIF-2α 72
2.3 Searching HIF-1 and HIF-2 specific target genes 75
2.4 Mitoxantrone inhibits HIF-1α accumulation 82
3 HIF1α regulation by USP11 84
3.1 USP11 controls HIF1A mRNA 84
3.2 USP11 and HIF1A mRNA transcriptional regulation 85
3.3 USP11 and HIF1A mRNA stability 86
3.4 The impact of USP11 in HIF1A mRNA stability in MDA-MB-231 88
3.5 Searching for the ribonucleoprotein complex that controls HIF1A mRNA stability 90
3.5.1 hnRNPD activates the hypoxia-signalling cascade 93
3.6 hnRNPD and USP11 interact in cellulo 98
3.6.1 hnRNPD binds HIF1A mRNA 100
3.6.2 USP11 binds HIF1A mRNA 103
3.6.3 hnRNPD is not a direct target of USP11 104
4 Hypoxic regulation of the hnRNPD/USP11 ribonucleoprotein complex 107
4.1 Hypoxia and USP11 107

4.2 Hypoxia and hnRNPD 113
5 Relevance of USP11 in innate immune memory 115
Discussion: 119
1 RNAi screen of DUBs that modulate the hypoxia signalling cascade .121
2 USP11 is an activator of the hypoxia-signalling cascade.....123
3 HIF1α regulation by USP11 123
4 Hypoxic regulation of the hnRNPD/USP11 ribonucleoprotein complex 126
5 Relevance of USP11 in innate immune memory 127
6 Outlook and perspectives.....128
Conclusions.....131
Bibliography.....133
Apendix 1: Posters presented during the thesis.....167
Apendix 2: Scientific Contributions 171

Abbreviations

3'UTR: 3' untranslated region.
3D: three dimensions.
4E-BP1: eIF-4E binding protein 1.
5'UTR: 5' untranslated region.
AEBSF: 4-(2-aminoethyl) benzenesulfonyl fluoride hydrochloride.
AKT: Protein kinase B.
ALK5: Anaplastic lymphoma kinase 5.
AREs: AU-rich elements.
ATP: adenosine triphosphate.
BCa: Breast cancer
BCLAF1: Bcl-2-associated transcription factor.
bHLH: basic helix-loop-helix.
BNIP3: BCL2 Interacting Protein 3.
BRCA1: breast cancer 1.
CA9: Carbonic Anhydrase 9.
CDS: gene coding sequence.
CHIP: Carboxyl terminus of Hsp70-interacting protein.
cIAP-2: cellular inhibitor of apoptosis protein 2.
CITED-2: CBP/P300 Interacting Transactivator 2.
CMA: chaperone mediated autophagy.
CMV: cytomegalovirus.
CPEB: Cytoplasmic polyadenylation-element-binding protein.
C-TAD: carboxyl transactivation domains
Cul5: Cullin-5.
CXCR4: C-X-C chemokine receptor type 4.
CYLD: Ubiquitin carboxyl-terminal hydrolase CYLD.
DLBCL: diffuse large B-cell lymphoma.
DMEM: Dulbecco's Modified Eagles Medium.
DMOG: Dimetiloaxil glicine.
DNA: Deoxyribonucleic acid.
DNMT1: DNA Methyltransferase 1.
dNTPs: dideoxynucleotide.
DRB: 5,6-Dichlorobenzimidazole 1-β-D-ribofuranoside
DTT: Dithiothreitol.
DUBs: Deubiquitinases.
E2F1: Transcription factor E2F1.
eIF4B: Eukaryotic Translation Initiation Factor 4B.
ELK: ETS domain-containing protein.
EPAS1: Endothelial PAS domain-containing protein 1.
EPO: Erythropoietin.
ER: Endoplasmatic Reticulum.
ETS-1: Protein C-ets-1.
FANCD2: Fanconi anaemia group D2 protein.
Fbw7: F-box/WD repeat-containing protein 7.
FBXO11: F-box only protein 11.
FDA: Food and Drug Administration
FIH: Hypoxia-inducible factor 1-alpha inhibitor.
FOXO3: Forkhead box protein O3.
FYLIR: AEGEFYKLKIRTPQ peptide
GFP: Green fluorence protein
GSK3β: Glycogen synthase kinase 3 beta.
H2A: Histone 2A.
H2B: Histone 2B.
H3: Histone H3
HA: Influenza Haemagglutinin.
HEK293: human embryonic kidney cells.
HeLa: Henrietta Lacks cervix adenocarcinoma cells.
HES1: Transcription factor HES1.
HEY1: Hairy/enhancer-of-split related with YRPW motif protein 1.
HIF: Hypoxia Inducible Factor.
HIF-1 : HIF complex 1.
HIF-α : HIF alpha subunit.
HIF-β: HIF beta subunit.
HK2: Hexokinase 2.
hnRNPD: Heterogeneous nuclear ribonucleoprotein D0.
HPV-16E7: Human papillomavirus type 16 Protein E7.
HREs: Hypoxia Responsive Elements
HSC70: Heat shock cognate 70.
HSP90: Heat shock protein 90.
HuR: ELAV-like protein 1.

IKKβ: Inhibitor of nuclear factor kappa-B kinase subunit beta.
INK4a: Cyclin-dependent kinase 4 inhibitor A.
IRE: Iron-Responsive Elements.
IRP1: Iron Regulatory Protein 1
JAMM: ab1/Mov34/Mpr1 Pad1 N-terminal+ (MPN+) domain.
JmjC: Jumonji-C.
JNK: c-Jun N-terminal Kinases
KDM5A: lysine demethylase 5A.
KDM6A: lysine demethylase 6A.
KLHL20: Kelch-like protein 20
LAMP2A: Lysosome-associated membrane glycoprotein 2.
LOX1: Oxidized low-density lipoprotein receptor
MBD3: Methyl-CpG-binding domain protein 3.
MCPIP1: Monocyte chemotactic protein-induced protein 1.
Mdm2: E3 ubiquitin-protein ligase Mdm2.
Mgl-1: Mammalian lethal giant larvae-1.
MINDYs: Motif Interacting with Ub-containing Novel DUB family.
miRNAs: micro RNAs.
MITF: Microphthalmia-associated transcription factor.
MJDs: Josephins or Machado-Josephin Domain proteases
mRNA: Messenger RNA.
mTOR: Mammalian target of rapamycin.
Myc: Myc proto-oncogene protein.
NEDD8 : Neuronal precursor cell Expressed Developmentally Down regulated protein 8.
N-TAD: Amino transactivation domains.
N-terminal: amino terminal
NP: RNA replication complex proteins.
NuRD: Nucleosome Remodeling Deacetylase.
O_2: Oxygen
ODD: Oxygen-dependent degradation domain
OTUB1: OTU domain-containing ubiquitin aldehyde-binding protein 1.
OTUD4: OTU domain-containing ubiquitin aldehyde-binding protein 4.
OTUs: Ovarian Tumour Proteases
p21: cyclin-dependent kinase inhibitor 1
CBP: CREB-binding protein
P4HA1: Prolyl 4-hydroxylase subunit alpha-1.
p53: Cellular tumor antigen p53.
PARP: Poly ADP Ribose Polymerase.
PAS domains: Per-Arnt-Sim domain.
P-body: Processing Bodies.
PBS: Phosphate Buffer Saline.
PCNA: Proliferating Cell Nuclear Antigen.
PCOLCE: Procollagen C-endopeptidase enhancer 1.
PCR : Polymerase Chain Reaction.
PHD: HIF Prolyl Hydroxylases.
PHLPP: PH domain and Leucine rich repeat Protein Phosphatases.
PI3K: phosphatidylinositol-3-kinase
PML: Promyelocytic Leukemia Protein.
RARα: Retinoic Acid Receptor alpha.
PPP1CA: Serine/threonine-protein phosphatase PP1-alpha catalytic subunit.
PRC1: Polycomb repressive complex 1.
PRPF8: Pre-mRNA-processing-splicing factor 8.
PTB: Polypyrimidine Tract-Binding protein.
PTEN: Phosphatase and Tensin homolog.
RACK1: Receptor of activated protein C kinase 1.
RAE1: Ribonucleic Acid Export protein .1
RanBPM: Ran-binding protein 9.
RBPs: RNA Binding Proteins
RIP: Ribonucleoprotein Immunoprecipitation.
RNF4: RING finger protein 4.

ROS: Reactive Oxygen Species.
RT-qPCR: Reverse Transcriptase quantitative Polymerase Chain Reaction.
S6K1: p70 ribosomal protein S6 kinase 1.
SDS: Sodium Dodecyl Sulfate.
SDS-PAGE: Sodium dodecyl sulfate polyacrylamide gel electrophoresis
shRNAs: Small hairpins RNA.
Siah-2: Seven in absentia homolog 2.
siRNAs: Small interference RNA.
SLC2A1: Solute Carrier Family 2 Member 1.
SMAD3/4: Mothers against decapentaplegic homolog 3/4.
SNAI1: Protein snail homolog 1.
SOX9: Transcription factor SOX-9.
SSD: Small-scale duplication
STAMBPL1: STAM-binding protein-like 1.
STAT3: Signal transducer and activator of transcription 3.
SUMO: Small Ubiquitin-like MOdifier
TAK1: Orphan nuclear receptor TAK1.
TAp73: Tumor protein p73.
TGFBR2: Transforming growth factor beta receptor II.
TNF: Tumor necrosis factor.
TRAF6: TNF Receptor Associated Factor 6.
TTP: Tristetraprolin
UBLs: Ubiquitin-like.
UCHL: Ubiquitin carboxy-terminal hydrolase L1.
UCHs: Ubiquitin C-terminal Hydrolases
USP: Ubiquitin-specific protease.
UV: Ultraviolet
VEGFA: Vascular endothelial growth factor A.
VEGFR2: Vascular endothelial growth factor receptor 2.
VGLL4: Vestigial like family member 4
pVHL: Von Hippel-Lindau disease tumor suppressor.
WISP2: WNT1-inducible-signaling pathway protein 2.
XIAP: X-linked inhibitor of apoptosis protein.
XPC: Xeroderma pigmentosum, complementation group C.
ZUP1: Zinc finger-containing ubiquitin peptidase 1.
γH2AX: H2A histone family member.

Abstract

Adaptation to hypoxia is a puzzling and tightly regulated challenge. This adaptability involves a severe gene expression rewiring, which is mainly triggered by the Hypoxia Inducible transcription Factor (HIF). HIF acts as a heterodimer composed by a ubiquitously expressed β subunit (HIF-β) and to the O2-sensitive α subunit (HIF-α). Canonically, the regulation of the hypoxia signalling pathway mostly relies on HIF-α, which has been described to be exquisitely regulated through the Ubiquitin Proteasome System (UPS). Ubiquitin (Ub) conjugation is a reversible process that depends on both, Ub ligases to tag Ub moieties into the target proteins and deubiquitinating enzymes (DUBs) to remove them.

Because of the Ub conjugation' crucial role in the hypoxia pathway and in light with DUBs being druggable enzymes, we carried out an unbiased loss-of function screen to identify new DUBs modulating HIF signalling. Using this strategy, we identified 12 novel hypoxia-related DUBs. In this project, we have validated the hit candidates and further focused on USP11 characterization. We have shown that USP11 is required to sustain hypoxia-driven signalling. USP11 exclusively controls HIF-1α by regulating HIF1A mRNA stability. Indeed, USP11 binds the mRNA-binding protein, hnRNPD, forming a ribonucleoprotein complex that controls HIF1A mRNA turnover by hnRNPD-mediated interaction with HIF1A 3'UTR. Pharmacological inhibition of USP11, by using the FDA approved drug, Mitoxantrone, also exacerbates HIF1A turnover and prevents HIF-signalling without affecting EPAS1 mRNA. Consistent with the decrease in HIF1A mRNA upon hypoxia, we have shown that hypoxia inhibits USP11 activity and promotes hnRNPD/p37 nuclear accumulation. Therefore, USP11-mediated HIF1A post-transcriptional regulation reveals a new mechanism to fine tune HIF signalling and hypoxia adaptation, and might represent a new opportunity to understand the pathology of Lyme disease.

Resumen

La adaptación a hipoxia es un proceso complejo y regulado al detalle. Esta adaptación implica cambios sustanciales en la expresión génica que son, principalmente, orquestados por el factor de transcripción inducido por hipoxia (HIF por sus siglas en inglés). HIF es un hetero-dímero compuesto por una subunidad β (HIF-β), constitutiva, que se une a una subunidad α (HIF-α), sensible a los niveles de O2. La regulación canónica de la cascada de señalización activada por hipoxia depende en gran medida del control de la estabilidad de la proteína HIF-α. Dicha estabilidad está mediada por el denominado sistema ubicuitina proteasoma (UPS por sus siglas en inglés). La conjugación de ubicuitina (Ub) es una modificación reversible resultado de la acción de las Ub ligasas, responsables de añadir las moléculas de Ub sobre las proteínas dianas, y las enzimas desubicuitinantes (DUBs) que las eliminan.

Debido al papel crucial que juega la ubicuitinación en la modulación de la cascada de hipoxia y teniendo en cuenta que las DUBs son dianas farmacológicas, llevamos a cabo un rastreo génico a gran escala con el objetivo de identificar nuevas DUBs moduladoras de la respuesta a hipoxia. De este modo, identificamos 12 DUBs cuya función está relacionada con la cascada de señalización activada por hipoxia. En este proyecto hemos validado las enzimas candidatas y nos hemos centrado en la caracterización más detallada de USP11. Nuestros resultados demuestran que USP11 es necesaria para una correcta activación de la señalización por hipoxia. En efecto, USP11 controla específicamente HIF-1α mediante la regulación de la tasa de renovación del mRNA. Desde un punto de vista mecanístico, hemos puesto de manifiesto que USP11 une la proteína de unión al mRNA, hnRNPD, y forma un complejo ribonúcleo-proteico que controla la estabilidad del mRNA de HIF1A a través de la interacción de hnRNPD con la región 3'UTR. La inhibición farmacológica de USP11 al administrar mitoxantrone, un medicamento aprobado por la FDA, también aumenta la tasa de renovación del mRNA de HIF1A e inhibe la cascada de señalización activada por hipoxia sin

afectar los niveles del mRNA de EPAS1. De acuerdo con la disminución de los niveles del mRNA de HIF1A detectados en hipoxia crónica, hemos demostrado que la hipoxia inhibe la actividad de USP11 y promueve la acumulación nuclear de hnRNPD/p37. En conclusión, nuestros resultados ponen en evidencia que la regulación post-transcripcional del mRNA de HIF1A mediada por USP11 constituye un nuevo mecanismo de regulación de la señalización dependiente de HIF y la adaptación a hipoxia, y puede representar, además, una nueva oportunidad terapéutica para entender la patología de la enfermedad de Lyme.

Introduction

Oxygen (O_2), as the electron acceptor, is essential for all organisms that use oxidative phosphorylation as the principal source for ATP (adenosine triphosphate) production (aerobic organisms). Cellular O_2 levels may fluctuate but any reduction in O_2 availability (hypoxia), even when transient, prompts immediate adaptive responses. Indeed, high energy-consuming processes such as protein synthesis are transiently disrupted and thus, spare ATP can attend functions that are critical for cell survival. Cellular adaptation to hypoxia also comprises a transcriptional programme mainly driven by the Hypoxia Inducible Factor (HIF), which controls the expression of a cohort of target genes. In that manner, cells can survive under a low O_2-availability environment.

1 Hypoxia signalling pathway

1.1 Dealing with hypoxia

The oxygen, which started to accumulate in the atmosphere almost 2.5 billion years ago, has played a key role driving complexity and biodiversity. Hence, the organisms have developed elegant adaptive mechanisms to monitor oxygen levels and respond to changes in oxygen tension. Specialized sensory tissues, mainly glomus cells of the carotid body, chromaffin cells of the foetal adrenal medulla and neuroepithelial cells of the lungs, rapidly detect and respond to changes in oxygen availability for the global benefit of the whole organisms. Hypoxia is normally sensed at the carotid artery bifurcation by the carotid body, which sends nervous signals to the brain that result in the stimulation of breathing and heart rate in response to hypoxemia (López-Barneo *et al*, 2004).

Hypoxia adaptation at cellular level relies on the transcriptional up-regulation of a number of genes pointed to reduce O_2 demand and increase O_2 supply. Reduced O_2 consumption is achieved among others by switching the metabolism from mitochondrial oxidative phosphorylation to anaerobic glycolysis, while the increased O_2 delivery is promoted by favouring vascular tone and angiogenesis as well as iron metabolism and erythropoiesis (Mole & Ratcliffe, 2008). This adaptive response, orchestrated by HIF is essential for

proper embryonic development (Dunwoodie, 2009), wound healing (Zhang *et al*, 2010) or maintaining circadian rhythm (Adamovich *et al*, 2017). On the contrary, abnormal HIF activation has been related to human diseases including but not limited to hereditary erythrocytosis, pulmonary arterial hypertension or cancer (Semenza, 2012). More recently, the Jumonji-C (JmjC) family (particularly the lysine demethylase 5A (KDM5A) and the lysine demethylase 6A KDM6A) has been shown as essential mediator of the hypoxia signalling by regulating O_2-dependent histone methylation independently of the HIF pathway (Batie *et al*, 2019; Chakraborty *et al*, 2019).

Sponges and comb jellies lack key components of the HIF or any other HIF-like pathway (Mills *et al*, 2018). This suggests that this pathway evolved after the last common ancestor of all living animals. HIF transcription factor functions as a dimer consisted of a HIF-α and HIF-β subunits bound through their basic helix-loop-helix (bHLHL), which also provides DNA (Deoxyribonucleic Acid) binding capacity as well as the Per-Arnt-Sim (PAS) domains presents on their amino-terminal (N-terminal) region (Wang & Semenza, 1993; Jiang *et al*, 1996).

HIF functionality relies on the HIF-α subunit, which is constitutively expressed even though the protein half-life is extremely short in normoxia, less than 5 min (Moroz *et al*, 2009). In contrast, the expression of the HIF-β-subunit is constitutive. Accordingly, HIF-α but not HIF-β, contains an Oxygen-dependent Degradation Domain (ODD) in addition of two transactivation domains (amino transactivation domains (N-TAD) and carboxyl transactivation domain (C-TAD)) split by an inhibitory domain (ID)(Huang *et al*, 1998; Jiang *et al*, 1997a). HIF-α protein stability is mostly regulated by the ubiquitin-proteasome system in an oxygen-dependent manner through the ODD (Huang *et al*, 1998). Upon hypoxia, HIF-α protein is stabilized allowing the dimerization with the β-subunit and the binding to the Hypoxia Responsive Elements (HREs), which are enhancer motifs within the regulatory region of the target genes (Jiang *et al*, 1997b; Wang & Semenza, 1993).

1.1.1 The family of HIF- α:

The human HIF-α family is composed by three isoforms: HIF-1α, HIF-2α and HIF-3α, which are encoded by chromosomes 14q21–24, 2p16–21 and 19q13.13–13.2, respectively (Ema *et al*, 1997; Semenza & Wang, 1992). However, HIF-1α and HIF-2α are the main activators of the hypoxia pathway and share 48% overall amino acid identity. In particular, specially conserved are the bHLH and PAS domains that share 70% and 83% of homology, respectively (Hu *et al*, 2003) (Figure I1). In contrast, HIF-3α shares part of the N-terminal region but hold a unique TAD (Hara *et al*, 2001). HIF-3α up regulates *RhoC* and *ROCK1* transcription (Zhou *et al*, 2018) but it has been proposed to exert an inhibitory role on the hypoxia signalling cascade (Hara *et al*, 2001). Furthermore, multiple splice variants of HIF-3α have been described, and only the hHIF-3α1–3 splice variant contains an ODD (Maynard *et al*, 2003). Interestingly, *HIF-3A* gene expression is induced by HIF complex 1 (HIF-1) forming a negative feedback loop that may play an important role in the maintenance of the avascular cornea (Makino *et al*, 2001).

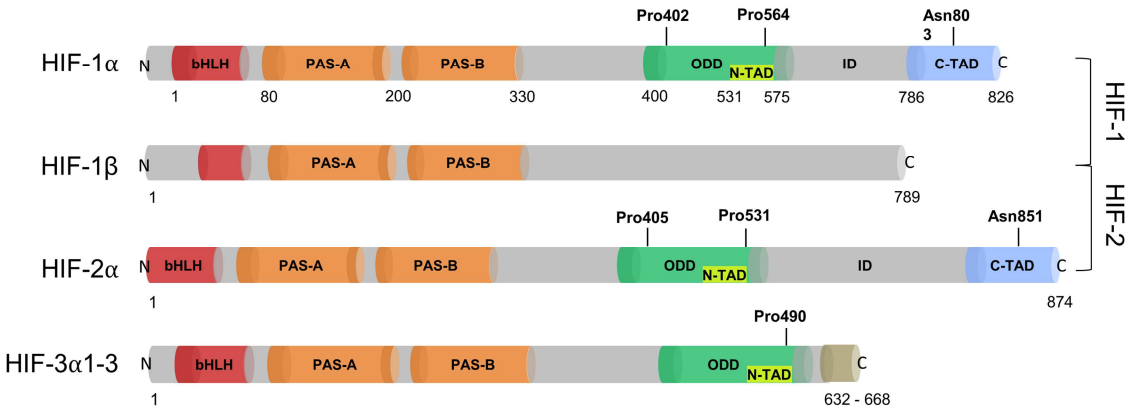

Figure I1: Schematic representation of HIF-1 and HIF-2 complexes along with hHIF-3α1–3 splice variants. Domain structure of hypoxia-inducible factor (HIF) subunits. The following domains are shown from N-terminal (N) to C-terminal (C): basic helix-loop-helix domain (bHLH), Per-Arnt-Sim homology domains (PAS A and B), O_2-dependent degradation domain (ODD), N- and C-terminal transactivation domains (TAD-N and TAD-C) and inhibitory domain (ID).

Great efforts have been devoted to distinguish specific functions for HIF-1 and HIF-2. While both are required for hypoxic adaptation in most cells, describing their individual roles and exclusive target genes remain controversial.

hif-1a$^{-/-}$ mice exhibit mid-gestation lethality and severe blood vessel defects (Iyer *et al*, 1998a) whereas *hif-2a*$^{-/-}$ mice, which also exhibit embryonic lethality, present a different phenotype with abnormal lung maturation, erythropoiesis and reduced levels of catecholamines leading to heart failure (Compernolle *et al*, 2002; Gruber *et al*, 2007; Tian *et al*, 1998). In addition, the *hif-2a* knock-in into the *hif-1a*$^{-/-}$ locus cannot compensate for HIF-1α function, clearly demonstrating that both isoforms play non-redundant roles at least during development (Covello *et al*, 2005). HIF-1 or HIF-2 are able to recognize similar core HREs, though HIF-2 only activates some of them (Mole *et al*, 2009). As such, O_2-deprived 786-O cells line (human clear cell renal carcinoma), which lack HIF-1α expression, responded to hypoxia but failed to induce glycolytic genes. In that regard, cooperation with additional transcription factors are essential for the hypoxic induction of some HIF target genes such as *EPO* (Erythropoietin), which is regulated by HIF-1 and SMAD3/4 (Mothers against decapentaplegic homolog 3/4)(Sánchez-Elsner *et al*, 2004). *VEGFR2* (Vascular Endothelial Growth Factor Receptor 2), which depends on HIF-2 and ETS-1 (Protein C-ets-1)(Elvert *et al*, 2003). Finally, *CITED-2 (*CBP/P300 Interacting Transactivator 2) and *WISP2 (*WNT1-inducible-signaling pathway protein 2) rely on both, HIF-2 and ELK (ETS domain-containing protein)(Aprelikova *et al*, 2006). In fact, the repertoire of HIF target genes is highly cell-type dependent, with only a small number of HIF-regulated genes conserved across all cell types (Ortiz-Barahona *et al*, 2010).

1.1.2 HIF-α regulation

According to the essential role of the HIF complex, the regulation of the HIF-α subunit is an intricate and tightly regulated pathway, in which converge sophisticated mechanisms that have been lately classified as canonical or non-canonical mechanisms.

1.1.2.1 Canonical HIF-α regulation

A family of oxygen sensors drives the canonical pathway. Among them, the PHDs (also known as EGg-Laying abnormal Nine, EGLN, o HIF Prolyl Hydroxylases, HPHs), which belong to the largest family of 2-oxoglutarate and iron-dependent dioxygenases, were the first to be described (Ivan *et al*, 2001;

Jaakkola *et al*, 2001). As such oxygen sensors, PHDs possess low oxygen affinity (Km≅ 230-250μM) meaning that even small changes in O_2 availability strongly impact their activity (Hirsilä *et al*, 2003).

These enzymes hydroxylate Pro-402 and Pro-564 residues, located within the ODD of HIF-1α (Pro-405 and Pro-531 in the case of HIF-2α) using O_2 and 2-oxoglutarate as co-substrates, and Fe^{2+} and ascorbate as cofactors (Bruick & McKnight, 2001; Epstein *et al*, 2001). In normoxia, the hydroxylation of the above-mentioned prolines is the signal for the Von Hippel-Lindau disease tumor suppressor (pVHL)-Ub E3-Ligase complex to polyubiquitinate HIF-α and therefore, target it for proteasomal degradation (Maxwell *et al*, 1999; Ohh *et al*, 2000). However, the activity of these enzymes is compromised upon low O_2, HIF-α is neither hydroxylated nor ubiquitinated and therefore, HIF-α is stabilized (Figure I2).

The family of PHDs holds 3 members: PHD1, PHD2 and PHD3, which differentially contributes to HIF-α regulation. PHD2 and PHD3 show higher activity for HIF-α than PHD1(Huang *et al*, 2002; Tuckerman *et al*, 2004). Moreover, PHD2 is the major regulator of HIF-1α in normoxia, and its inactivation is sufficient to unleash the adaptive response to hypoxia (Berra *et al*, 2003; Minamishima *et al*, 2008). In addition, the spare O_2 from the mitochondrial switch off upon chronic hypoxia is sufficient to reactivate all the three isoforms. Thus, PHD1, 2 and 3 contribute to HIF-α degradation and avoid the harmful consequences of a sustained activation of HIF pathway (Ginouves *et al*, 2008).

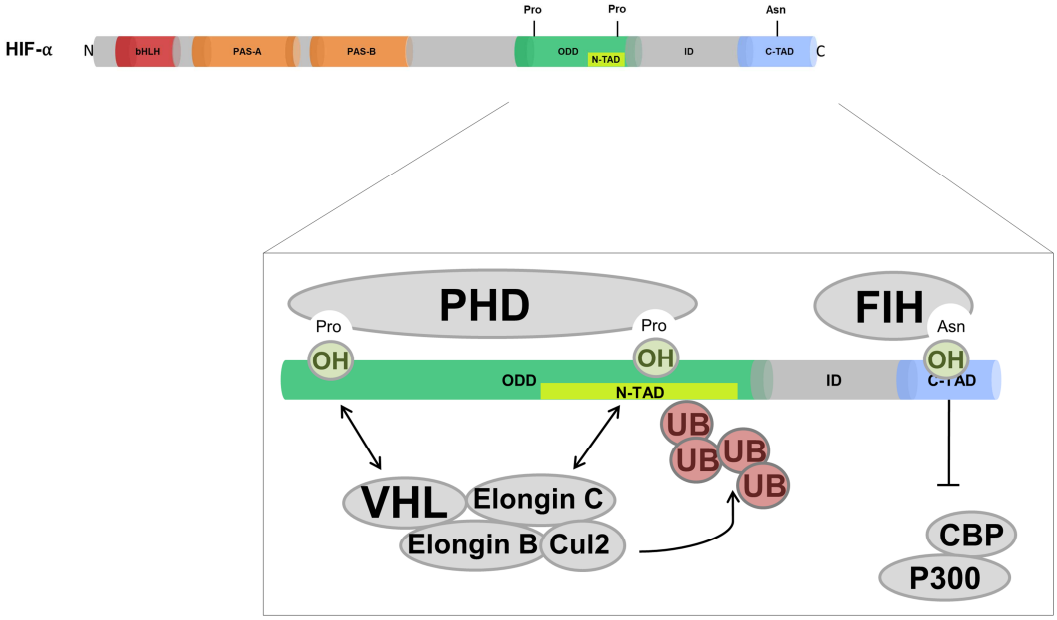

Figure I2: Schematic representation of the HIF-α canonical regulation. PHDs hydroxilate two proline residues (Pro) recognized by VHL that recruits the ElonginC-ElonginB-CUL2 E3-ubiquitin complex to ubiquitinate HIF-α. This polyubiquitination signals for proteasome-dependent degradadion. FIH in turn, hydroxylates Asparagine (N803), which inhibits the recruitment of CBP and P300 co-activators.

Shortly after, other member of the 2-oxoglutarate and iron-dependent dioxygenases, Hypoxia-inducible factor 1-alpha inhibitor (FIH), was described as an essential factor to repress HIF transcriptional activity (Lando *et al*, 2002; Mahon *et al*, 2001). FIH has a lower affinity for O_2 than that of the PHDs (Km≅ 90 ±20μM)(Koivunen *et al*, 2004), though its catalytic activity is still sensitive to cellular O_2 fluctuations. In that manner, FIH hydroxylates HIF-1α Asp-803 (and HIF-2α Asp-851) within the C-TAD domain and impairs the recruitment of the transcriptional co-activators p300/CBP during normoxia (Figure I2).

Therefore, the dual hydroxylation, by the PHDs and FIH, maintains HIF-α unstable and HIF transcriptionally inactive in well oxygenated cells, whereas HIF-α becomes stable and HIF transcriptionally active when pO_2 drops.

1.1.2.2 Non-Canonical HIF-α regulation

As mentioned previously, both, the PHDs, in terms of protein stability and FIH, which regulates transcriptional activity, mainly execute the canonical HIF-α regulation. However, HIF-α regulation is also extended to gene expression, mRNA (messenger RNA) turnover and even, further PHDs/pVHL-independent protein stability regulation.

1.1.2.2.1 Transcriptional regulation

Analysis of the murine *hif1a* promoter revealed two independent and functional transcription starting sites proceeded by a GC rich region (500 bp with 68% CG). This structure is similar to that of housekeeping promoters pointing to a rather steady transcriptional regulation (Luo *et al*, 1997). However, NFκB (Nuclear factor NF-kappa-B p105 subunit) was reported to up regulate *HIF1A* transcription through Lipopolysaccharide-triggered AMPK (5'-AMP-activated protein kinase) activation in monocytes and macrophages (Frede *et al*, 2006) or through Reactive Oxygen Species (ROS) activation in Human Embryonic Kidney cells (HEK293) (Bonello *et al*, 2007). Likewise, Inhibitor of nuclear factor kappa-B kinase subunit beta (IKKβ)-responsive NF-κB is essential for *HIF1A* up regulation, which is crucial to ensure a successfully innate immune response (Rius *et al*, 2008). Melanoma cells have been described to transcriptionally up-regulate *HIF1A* mRNA through MITF (Microphthalmia-associated transcription factor) (Buscà *et al*, 2005) and STAT3 (Signal transducer and activator of transcription 3) (Xu *et al*, 2005). This *HIF1A* mRNA up-regulation is reversed by the STAT3 inhibitor vanillin (Park *et al*, 2017). Also, *HIF1A* transcription is increased in acute promyelocytic leukaemia through Promyelocytic Leukemia Protein-Retinoic Acid Receptor alpha fusion protein (PML-RARα) (Coltella *et al*, 2014). Moreover, *HIF1A* transcription has been shown to be induced in breast cancer compared to benign tumours or epithelial cells due to hypomethylation of the *HIF1A* promoter (Li *et al*, 2019). Very recently, BCLAF1 (Bcl-2-associated transcription factor) has been proposed as an essential transcription factor for *HIF1A* up-regulation in hepatocellular carcinoma (Wen *et al*, 2019).

In the case of Endothelial PAS domain-containing protein 1(*EPAS1),* it has been reported to be transcriptionally up regulated by Sirtuin1 in response to hypoxia (Dioum *et al*, 2009). Similarly, *EPAS1* transcription was enhanced by MBD3 (Methyl-CpG-binding domain protein 3) through demethylation of CpG islands located in the proximity of the transcription starting site in MDA-MB-468 cells (Cui *et al*, 2016). In addition, *EPAS1* has been shown to be demethylated upon hypoxia by its own target DNMT1 (DNA Methyltransferase 1) in a positive feedback loop (Xu *et al*, 2018). In terms of regulation by transcription factors,

only E2F1 (Transcription factor E2F1) been validates as an inductor of *EPAS1* transcription (Moniz *et al*, 2015). Interestingly, *EPAS1* promoter single nucleotide polymorphisms may contribute the high altitude adaptive mechanisms among Tibetans (Peng *et al*, 2017).

1.1.2.2.2 mRNA splicing

Several *HIF1A* alternative spliced isoforms arise by skipping particular exons among the 15 that encode *HIF1A,* though the molecular mechanisms underlying these splicing events are completely unknown (Iyer *et al*, 1998b). HIF-1α^{417}, HIF-1α^{785}, HIF-1α^{557}, HIF-1α^{516}, HIF-1α^{736} spliced variants are generated by skipping exon 10, 11, 12, 11 and 12 and 14, respectively (Lee *et al*, 2004; Chun *et al*, 2003, 2001, 2002; Gothié *et al*, 2000). Such alternative splicing mostly provokes frame shifts that repress transcriptional activity. By contrast, no results have been published about *EPAS1* alternative splicing.

1.1.2.2.3 mRNA translation

Global inhibition of protein synthesis “translational arrest” has been classically recognized as a fundamental adaptation to hypoxia as mRNA translation is an energy costly process that consumes up to 70% of the ATP synthesized by the cells (Pontes *et al*, 2015).

HIF1A mRNA has been reported to decrease during hypoxia while HIF-1α protein continues translating (Thomas & Johannes, 2007). More in detail, *HIF1A* mRNA is decreased from the polysomal fraction while being increased into the endoplasmic reticulum (ER) fraction suggesting that the successful *HIF1A* translation required for hypoxia adaptation takes places into the ER-associated ribosomes (Staudacher *et al*, 2015). This mechanism is reminiscent of genes such as *P4HA1* (Prolyl 4-Hydroxylase subunit alpha-1)*, HK2* (Hexokinase 2) and *VEGFA* (Vascular endothelial growth factor A) that have been shown to ensure its translation towards the ER ribosomes (Staudacher *et al*, 2015).

HIF1A translation can be up regulated under normoxic conditions by activation of the mammalian Target Of Rapamycin (mTOR) through phosphatidylinositol-3-kinase (PI3K) pathway, which phosphorylates and activates p70 ribosomal protein S6 kinase 1(S6K1). As a result, eIF-4E binding

protein 1 (4E-BP1) is activated and promotes *HIF1A* translation in colon and prostate cancer cells (Pore *et al*, 2006; Zhong *et al*, 2000). Besides, up-regulation of *HIF1A* translation through mTOR in MCF-7 human breast cancer cells line dependens on the *HIF1A* 5' untranslated region (5'UTR) (Laughner *et al*, 2001). Interestingly, mTOR complexes differentially regulate HIF isoforms. Indeed, mTORC1 and mTORC2 control *HIF1A* translation while *EPAS1* is exclusively regulated by mTORC2 (Toschi *et al*, 2008; Mohlin *et al*, 2015). Moreover, insulin has been found to activate Cytoplasmic polyadenylation-element-binding protein (CPEB) 1 and 2, which binds to *HIF1A* 3' untranslated region (3'UTR) to increase its translation (Hägele *et al*, 2009). Moreover, the presence of Iron-Responsive Elements (IREs) within the 5'-UTR of *EPAS1* blocks translation in normoxia, while hypoxia impairs the Iron Regulatory Protein 1 (IRP1)/IRE interaction allowing the efficient translation of *EPAS1* (Sanchez *et al*, 2007; Zimmer *et al*, 2008).

1.1.2.2.4 mRNA stability

RBPs (RNA Binding Proteins) by recognizing conserved sequences within the target mRNAs control transcripts' fate. One of the conserved sequences is the AU-rich elements (AREs), which are regions of 50–150 nucleotide rich in adenosine and uridine bases located within the 3′-UTR (Barreau *et al*, 2005). One common feature of the ARE-containing genes is their temporal expression profile (Hao & Baltimore, 2009). In the case of the hypoxic adaptive program, it has been reported that ARE-containing transcripts are significantly enriched among total transcripts upon hypoxia (de Toeuf *et al*, 2018).

HIF1A contains a relatively long 3'UTR sequence (1197 bp) that includes at least eight ARE motifs (AUUUA)(Yasuda *et al*, 2014a), which makes it highly susceptible to recruit RBPs. As such, *HIF1A* mRNA has been shown to be stabilized by USP52/PAN2, ELAV-like protein 1 (HuR) and Nucleolin (Bett *et al*, 2013a; Sheflin *et al*, 2004; Zhang *et al*, 2012a; Cheng *et al*, 2014a). Furthermore, *HIF1A* is destabilized by Tristetraprolin (TTP), Polypyrimidine Tract-Binding protein (PTB) and a methyltransferase called F-box only protein 11 (FBXO11) (Kim *et al*, 2010; Chamboredon *et al*, 2011c; Wang & Lin, 2009; Ju *et al*, 2015a).

Competition of RBP with non-coding RNAs add and additional layer of regulation dictating transcripts fate (Shin *et al*, 2017; Wang *et al*, 2016). As such, several microRNAs (miRNAs) that directly or indirectly target *HIF1A* have been described and contribute to either *HIF1A* mRNA degradation or stabilization: miR-424, miR-199a, miR-155, and the miR-17/92 cluster (Ghosh *et al*, 2010; Rane *et al*, 2009; Taguchi *et al*, 2008; Bruning *et al*, 2011). In addition, *EPAS1* is down regulated by miR-148a and miR-20b (Giraud-Triboult *et al*, 2011; Taibi *et al*, 2017).

1.1.2.2.5 Non canonical regulation of HIF-a protein stability

In addition to the canonical O_2/PHD/pVHL-mediated regulation of HIF-α stability, it has been reported that Cul5 (Cullin-5) is recruited by HSP90 (Heat Shock Protein 90) and triggers HIF-1α proteasome-dependent degradation (Ehrlich *et al*, 2009). By contrast, RACK1 (Receptor of activated protein C kinase 1) bound to HSP90 prevents the recruitment of the elongin C/B Ub E3 ligase complex and thus, stabilize HIF-α in normoxic conditions (Liu *et al*, 2007; Paatero *et al*, 2012). HSP70 (Heat shock 70 kDa protein 1A) has been reported to mediate HIF-1α (but not HIF-2α) degradation upon chronic hypoxia, through the recruitment of CHIP (Carboxy terminus of Hsp70-interacting protein) (Luo *et al*, 2010). Moreover, p53 (Cellular tumour antigen p53) and PTEN (Phosphatase and Tensin homolog) stabilize HIF-1α by impairing the binding of the E3 ubiquitin-protein ligase Mdm2 (Ravi *et al*, 2000; Joshi *et al*, 2014a). Similarly, TAp73 (Tumor protein p73) and BRCA1 (Lys-63-specific deubiquitinase BRCC36) were reported to promote HIF-α proteasome-mediated degradation independently of VHL, though direct HIF-α ubiquitination has not been demonstrated (Amelio *et al*, 2015; Kang *et al*, 2006). HAF (hypoxia-associated factor) targets HIF-1α but not HIF-2α for proteasome-dependent degradation independently of oxygen levels (Koh *et al*, 2008). By contrast, TRAF6 (TNF Receptor Associated Factor 6) increases HIF-1α polyK-63 ubiquitination and protects it from proteasome degradation (Sun *et al*, 2013). In addition, the Fbw7 (F-box/WD repeat-containing protein 7) Ub-E3 ligase ubiquitinates and degrades HIF-1α after GSK3β (Glycogen synthase kinase 3 beta) phosphorylation, and both, Fbw7 and GSK3β down-regulation enhance cell proliferation and colony formation (Flugel *et al*, 2012).

HIF-1α protein stability is also governed by the lysosomal degradation pathway. As such, HSC70 (Heat Shock Cognate 70) and LAMP2A (Lysosome-associated membrane glycoprotein 2), two key effectors of the chaperone-mediated autophagy (CMA), enhance HIF-1α lysosomal degradation (Hubbi *et al*, 2013).

Finally, several deubiquitinating enzymes have been related with the stability of HIF-α proteins (*See section 2.2*).

2 Role of DUBs in hypoxia

2.1 Ubiquitin-mediated posttranslational modifications

Ubiquitination, ubiquitin conjugation as a signal for proteasomal degradation was first discovered by Goldstein in 1975 (Goldstein *et al*, 1975). Until then, proteins were thought to be long-lived. Ubiquitin conjugation relies on the covalent attachment of Ubiquitin (Ub), a highly conserved 76 amino acid protein, to most commonly a lysine residue of the target substrate through the Ub C-terminal di-glycine (Gly-Gly) motif. Ubiquitin conjugation is one of the most common protein posttranslational modifications, and translates into changes of protein activity and/or stability (Swatek & Komander, 2016).

Ubiquitination is a multi-step cascade that involves three types of enzymes (Hershko *et al*, 1983). In the first step, Ub is activated by an E1 Ub-activating enzyme. Next, the activated Ub is transferred to the active site of an E2 Ub-conjugating enzyme that, in turn, shifts the Ub into an E3 Ub-ligase that catalyses the ligation of Ub to the target protein. The human genome codes for two E1s, around 30 E2s and more than 600 E3s, which illustrates the wide variety of targets and the number of cellular processes modulated by ubiquitination (Senft *et al*, 2018). Furthermore, Ub-like proteins (UBLs), which exhibit similar three-dimensional structures and include, among others, SUMO (Small Ubiquitin-like MOdifier) and NEDD8 (Neuronal precursor cell Expressed Developmentally Down regulated protein 8) are encoded to function as signalling tags modulating several cellular functions (van der Veen & Ploegh,

2012).

Ub conjugation might occur on a single or multiple lysine residue(s) of the target protein, resulting in mono-ubiquitination (mono-Ub) or multi-ubiquitination (multi-Ub), respectively (Petroski & Deshaies, 2005). Moreover, Ub can form polypeptide chains (poly-Ub) by the covalent attachment of subsequent Ubs into one of its seven internal lysine residues (Lys6, Lys11, Lys27, Lys29, Lys33, Lys48 or Lys63) forming homotypic poly-Ub chains (Pickart & Fushman, 2004). In addition, heterotypic poly-Ub chains can be formed by branched Ub or mixed chains including different combination of UBLs, such as Ub-SUMO hybrid chains (Guzzo & Matunis, 2013).

Such a diversity of ubiquitin chains opens the possibility for a great range of signals to modulate cellular processes. For example, mono and multi-Ub has been reported to regulate endocytosis, protein transport, DNA repair and histone modulation among other functions (Hicke, 2001; Ramanathan & Ye, 2012; Haglund *et al*, 2003). Regarding poly-Ub chains, Lys6- and Lys27-chains have been related to mitophagy, nuclear translocation and DNA damage responses (Akutsu *et al*, 2016). Lys11-, Lys29- and Lys33- Ub chains have been linked to cell cycle regulation, WNT/β-catenin signalling, and cellular trafficking and kinase signalling, respectively(Akutsu *et al*, 2016). Moreover, Ub Lys48- and Lys63-chains are the best characterised so far. Indeed, Ub Lys48-Ub chains mostly target proteins for proteasomal degradation, while Ub Lys63-Ub chains allow fast and reversible formation of signalling complexes (Yau & Rape, 2016; Wong & Cuervo, 2010).

As most of the post-translational modifications, Ub conjugation is a reversible process. Deubiquitinating enzymes or deubiquitinases (DUBs) oppose to E3 Ub-ligases activity by removing Ub moieties from protein substrates (Clague *et al*, 2013). DUBs catalyse the hydrolysis of the isopeptide bond between Ub and the target protein or between Ub moieties in the context of poly-Ub chains. Besides counteracting the action of the Ub E3 ligases, DUBs are proteases that process Ub precursors (Clague *et al*, 2019). DUBs are classified into seven different groups depending on the architecture of their catalytic centre. Among them, the family of JAMM (Ab1/Mov34/Mpr1 Pad1 N-terminal+ (MPN+)) domain

(also known as MPN) are zinc-dependent metalloproteinases while the other six families are conventional cysteine proteases: Ubiquitin-Specific Protease (USPs), Ubiquitin C-terminal Hydrolases (UCHs), Ovarian Tumour Proteases (OTUs), Machado-Josephin Domain proteases (MJDs) (also known as Josephins), Motif Interacting with Ub-containing Novel DUB family (MINDYs) and Zinc finger-containing Ubiquitin Peptidase 1 (ZUP1)(Clague *et al*, 2019).

2.2 DUBs that promote HIF-1α stability

Protein homeostasis is crucial for fitting cell proteome to face environmental stresses as hypoxia. In particular, HIF is primarily regulated by ubiquitination and consequently, several DUBs have been reported to modulate its activity (Figure I3): USP20 was the first DUB reported to directly deubiquitinate HIF-1α and therefore, preventing its proteasomal degradation (Li *et al*, 2005). Since then, USP8, MCPIP1 (Monocyte chemotactic protein-induced protein 1) and UCHL1 (Ubiquitin carboxy-terminal hydrolase L1) have been also reported to directly bind and deubiquitinate HIF-1α (Troilo *et al*, 2014; Sun *et al*, 2018a; Goto *et al*, 2015).

Interestingly, USP7 plays a dual role on HIF-1 activity. USP7 not only deubiquitinates and stabilizes HIF-1α but also promotes HIF-1 transcriptional activity by regulating CBP ubiquitination and histone 3 (H3) lysine 56 acetylation (Wu *et al*, 2016a).

USP19, a DUB implicated in ER stress responses was also reported to bind HIF-1α through its N-terminal region. Thus, USP19 integrates ER and hypoxic stress by promoting HIF-1α deubiquitination and stabilization (Altun *et al*, 2012).

USP28 deubiquitinates and stabilized HIF-1α by directly binding and antagonizing Fbw7 Ub E3-ligase activity, which is recruited by GSK-3β phosphorylation (Flugel *et al*, 2012). In this manner, HIF-1 activity can be modulated in normoxic conditions through GSK-3β phosphorylation in response to growth factors and nutrient availability (Maurer *et al*, 2014).

It is noteworthy the dual role of Cezanne in the control of HIF-α subunits. Indeed, Cezanne directly deubiquitinates HIF-1α preventing its chaperon-

dependent degradation but also controls HIF-2α expression by regulating the stability of E2F1 (Bremm *et al*, 2014b; Moniz *et al*, 2015).

More recently, we have identified USP29 as a novel DUB for HIF-1α and HIF-2α. Indeed, our data clearly show that USP29 binds and deubiquitinates HIF-α subunits independently of PHDs/VHL-mediated ubiquitination (Schober *et al.,* manuscript in preparation).

Although not directly related to the control of HIF protein stability, a Processing Bodie (P-body) component, the pseudo-DUB USP52, has been shown to be essential for hypoxic HIF-1α accumulation as it enhances *HIF1A* mRNA stability (Bett *et al*, 2013b).

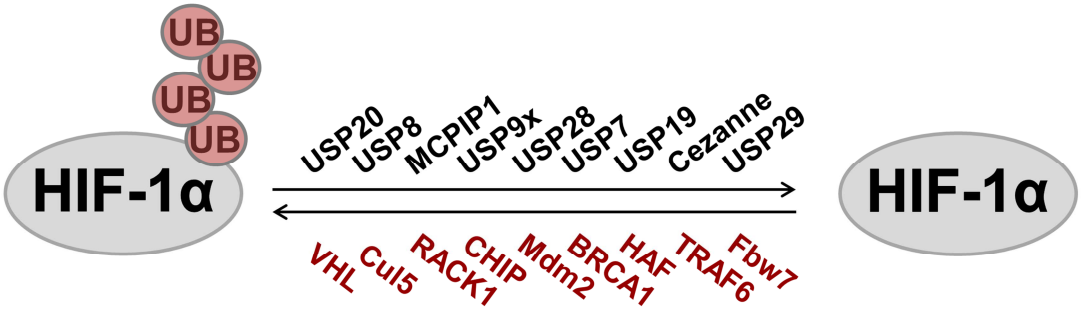

Figure I3: Squematic sumary of HIF-1α ubiquitination regulatory proteins. DUBs are presented in black and Ub E3-ligases are represented in red.

2.3 DUBs regulated by hypoxia

Not only DUBs regulate the hypoxia signalling pathway, but also hypoxia controls DUBs (Figure I4). Until now, most of the reported regulation of DUBs by hypoxia has been described at transcriptional level and especially in the context of cancer. In this regard, several DUBs have been shown to be down regulated. In glioma, this is the case for USP1, USP10 and USP14 whose mRNA levels decrease after overnight hypoxic incubation (3% O_2) (Minchenko *et al*, 2016). These three DUBs regulate essential proteins such as FANCD2 (Fanconi Anemia group D2 protein) and PCNA (Proliferating Cell Nuclear Antigen) (Nijman *et al*, 2005; Huang *et al*, 2006), p53 (Yuan *et al*, 2010) and CXCR4 (C-X-C chemokine receptor type 4) (Mines *et al*, 2009). Hypoxia,

through the transcriptional repressors SNAI1 (Protein snail homolog 1) and HES1 (transcription factor HES-1), has also been reported to down regulate CYLD (Ubiquitin carboxyl-terminal hydrolase CYLD) mRNA, boosting pro-inflammatory responses in glioblastoma multiforme (Guo *et al*, 2014). In addition, USP13 mRNA expression is attenuated in melanoma cells during hypoxia, which unexpectedly correlates with an increase in Siah-2 (Seven in absentia homolog 2) activity (Scortegagna *et al*, 2011). Colon cancer cells also exhibit a reduced transcription of USP46 mRNA during hypoxia that promotes tumour chemotherapy resistance (Wen *et al*, 2013). In this regard, down-regulation of USP46 forces the degradation of PHLPP (PH domain and Leucine rich repeat Protein Phosphatases), a Ser/Thr protein phosphatase, which functions as a tumour suppressor (Cheng *et al*, 2013; Wen *et al*, 2013). The expression of USP28 has been reported to be down regulated in liver as well as in breast cancer cell lines upon hypoxia. Interestingly, such decline correlates with poor survival outcomes (Richter *et al*, 2018). On the contrary, USP47 mRNA is up regulated by hypoxia through SOX9 (Transcription factor SOX-9) promoting SNAI1 stabilization and thus, epithelial-to-mesenchymal transition in colorectal cancer cells (Choi *et al*, 2017).

In a non-tumour context, USP8 has reported to be up-regulated upon intermittent hypoxia/reoxygenation conditions to foster the inflammatory response of renal tubular epithelial cells through TAK1 (Orphan nuclear receptor TAK1) stabilisation (Zhang *et al*, 2018b). Also, UCHL1 is up regulated by both, HIF-1 and HIF-2, upon hypoxia and promotes apoptosis after neuronal ischemic encephalopathy (Wu *et al*, 2016b). Moreover, hypoxia induces Cezanne via p38 mitogen-activated protein kinase-dependent transcriptional and post-transcriptional mechanisms in the murine kidney, in vascular, glomerular endothelial cells, podocytes, and epithelial cells (Luong *et al*, 2013).

Regardless of the transcriptional regulation, hypoxia also promotes the down-regulation of CYLD protein levels in a proteasome-dependent manner (Guo *et al*, 2014; An *et al*, 2008). Moreover, OTUB1 (OTU domain-containing ubiquitin aldehyde-binding protein 1) has been reported as a substrate for FIH, although hydroxylation does not affect its stability or enzymatic activity, it affects OTUB1 interaction landscape (Scholz *et al*, 2016). Hypoxia, by inactivating

PHD1, facilitates UPS9x-mediated deubiquitination and therefore, FOXO3a (Forkhead box protein O3) stabilisation (Zheng *et al*, 2014).

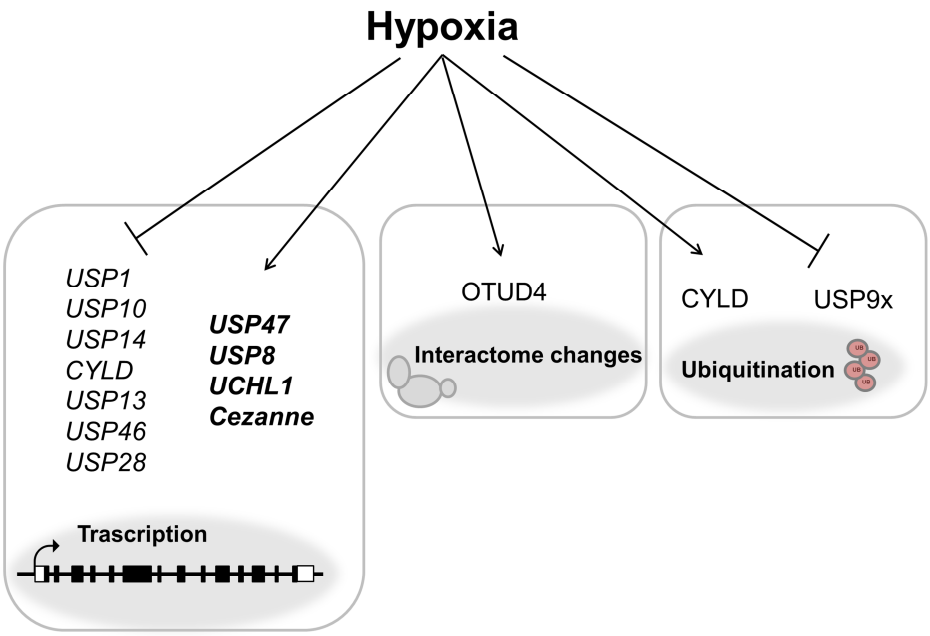

Figure I4: Squematic summary of the DUBs regulated by hypoxia. Hypoxia regulates transcription, induces changes on interacting parterns or changes ubiquitination pattern of the indicated DUBs.

2.4 USP11

2.4.1 Structure of USP11

Among all the DUBs, the family of USPs includes about sixty enzymes that share a common structured catalytic domain called USP fold (Hu *et al*, 2002). The USP domain is shaped resembling an open hand exposing its thumb, palm and fingers. The catalytic triad, based on Cys (thumb) and His/Asp residues (Palm), cut the isopeptide bond between two Ub molecules. The Ub molecule locates on the USP over the fingers, which hold the distal Ub part, and the palm that grasps the proximal Ub moiety (Ye *et al*, 2009) (Figure I5).

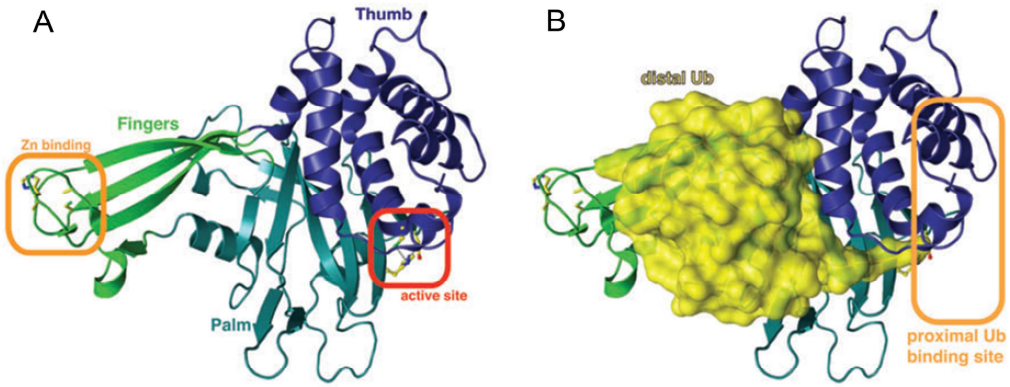

Figure I5: 3D USP domain structure. A) The USP domain structure of USP7 where Fingers (in green), Thumb (in blue) and Palm (light blue) are indicated along with the active site position. **B)** The Ub location on USP domain where proximal Ub can be observed located near the USP active site (Figure from Ye et al, 2009)

USP11, also known as UHX1, lies in a gene cluster on chromosome Xp21.2–p11.2 and encodes a protein of 963 Aa (Swanson *et al*, 1996). Phylogenetic studies indicate that USP11 arose from a small-scale duplication (SSD) event involving USP4-encoding region, which occurred in the common ancestor of bony fishes represented by gar, fugu, zebrafish and coelacanth (421.75 to 416 million of years ago). USP11 shares 44.6% of amino acid identity with USP4 that, in turns, exhibits 56.9% identity with USP15 from which it split after a previous whole genome duplication event (Vlasschaert *et al*, 2015). USP11 has been lost multiple times throughout vertebrate evolution. Indeed, in select fish, reptile and mammalian genomes, the syntenic loci where USP11 habitually resides hosts USP11 pseudogenes in lieu of functional genes. The variable retention or the loss of USP11 suggests that it is dispensable, which is in accordance with the viability of the *usp11*$^{-/-}$ mouse model (Park *et al*, 2019). However, the faster evolution and functional divergence of USP11, which corroborates well with reported trends for SSD-derived paralogs, precludes its functional interchangeability with its ancestor USP4.

The three dimensions (3D) structure of USP11 is only available for the N-terminal region (Harper *et al*, 2014). Similar to USP4 and USP15, it has been described that USP11 N-terminal region contains a DUSP-UBL (DU) domain, though it is longer, more disordered and more hydrophobic (rich in alanine). In

fact, the DUSP-UBL domain of USP11 does not mediate the regulatory functions such as enzyme-substrate interactions that have been structurally modelled for mammalian USP4 and USP15 (Faesen *et al*, 2012; Harper *et al*, 2014) (Figure I6).

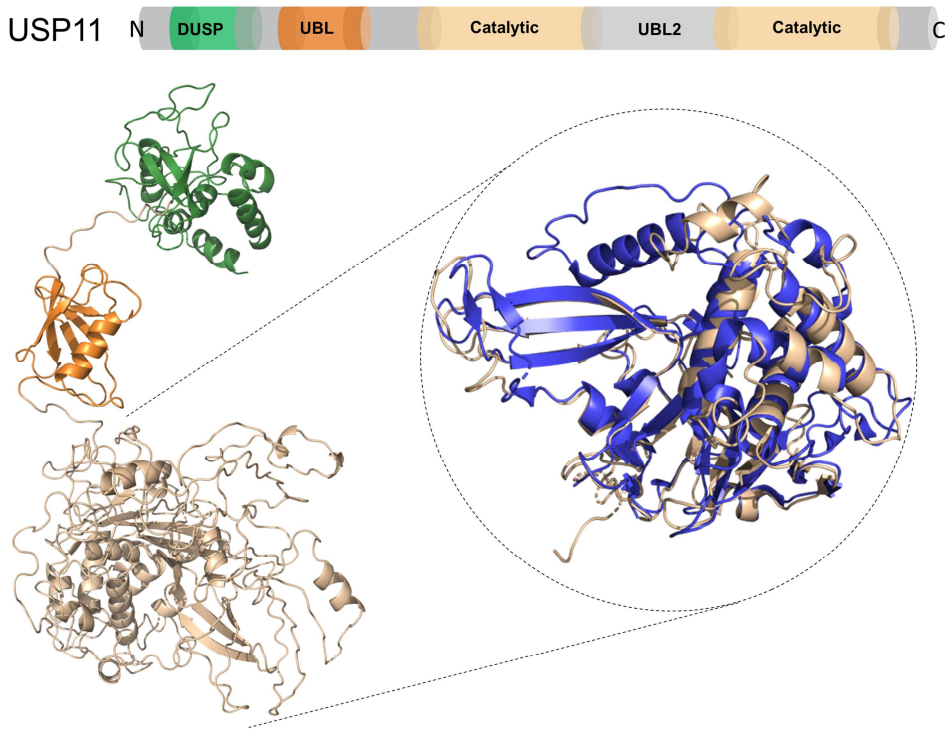

Figure I6: Modelization of USP11 3D structure. Schematic representation of USP11 DU domain DUSP in green and UBL1 in orange) followed by *in silico* modelization of USP11 structure using Phyre2 (Protein Homology/analog Y Recognition Engine V 2.0). USP domain is represented in light yellow. The hihgly structural homology between the modeled USP11 USP domain and the crystalized USP4 USP domain (blue) is shown in the inset.

The catalytic domain of USP11 is split in two parts, D1 and D2, both required for enzymatic activity. Regarding its activity, USP11 has been described to preferentially cleave Lys63, Lys6, Lys33 and Lys11 rather than Lys27, Lys29 or Lys48 Ub chains (Harper *et al*, 2014). Moreover, USP11 has been reported to cleave Ub-SUMO hybrid chains counteracting RNF4 (RING finger protein 4) activity (Hendriks *et al*, 2015a).

2.4.2 *Functional relevance of USP11 and direct targets*

RanBPM (Ran-binding protein 9) was the first USP11 target identified. Indeed, ubiquitin conjugation to RanBPM was inhibited in a dose-dependent manner by the addition of recombinant USP11 (Ideguchi *et al*, 2002).

Subsequently, many different targets have been described but the role of USP11 remains still controversial (Figure I7).

USP11 functions as an upstream regulator of IKKα (Inhibitor of nuclear factor kappa-B kinase subunit alpha) -p53 signalling pathway in response to TNF (Tumour necrosis factor) (Yamaguchi *et al*, 2007; Sun *et al*, 2010). The stability of LPAR1 (Lysophosphatidic acid receptor 1) is also up-regulated by USP11, which enhances LPAR1-mediated pro-inflammatory effects (Zhao *et al*, 2016). USP11 inhibits influenza virus genomic RNA replication by deubiquitinating NP (RNA replication complex protein) (Liao *et al*, 2010). USP11 has been extensively related to cell cycle regulation and DNA damage response. In this context, p21 (cyclin-dependent kinase inhibitor 1) and RAE1 (Ribonucleic Acid Export protein 1), a protein involved in spindle assembly checkpoint regulation and bipolar spindle formation, have been reported to be direct USP11 deubiquitination targets (Stockum *et al*, 2018a; Deng *et al*, 2018). USP11 also acts as a histone deubiquitinase to catalyse γH2AX (H2A histone family member), H2A (histone 2A) and H2B (histone 2B) deubiquitination in complex with NuRD (Nucleosome Remodelling Deacetylase) (Yu *et al*, 2016; Ting *et al*, 2019). DNA damages responses are also promoted by USP11 through the stabilization of p53, BRCA2 (Breast cancer type 2 susceptibility protein) and XPC (Xeroderma pigmentosum, complementation group C) (Ke *et al*, 2014; Shah *et al*, 2017; Schoenfeld *et al*, 2004).

High levels of USP11 expression in breast tumours correlate with a higher risk of recurrence and death (Bayraktar *et al*, 2013; Lim *et al*, 2016). Interestingly, silencing of USP11 displayed synthetic lethality with PARP (Poly ADP Ribose Polymerase) inhibitors in pancreatic cancer (Wiltshire *et al*, 2010a). Furthermore, USP11 expression is increased in pancreatic tumours compared to healthy tissue and related with poor prognosis in hepatocellular carcinoma (Zhang *et al*, 2018a). USP11 has been reported to deubiquitinate and stabilize PML, thereby counteracting the functions of PML ubiquitin ligases RNF4 and KLHL20 (Kelch-like protein 20)-Cul3 (Cullin 3)-Roc1 (E3 ubiquitin-protein ligase RBX1) complex. In accordance, USP11 confers multiple malignant characteristics of aggressive glioma, including proliferation, invasiveness and

tumour growth in an orthotropic mouse model, but also potentiates self-renewal, tumour-forming capacity and therapeutic resistance of patient-derived glioma-initiating cells (Wu *et al*, 2014). USP11 has also been shown crucial to promote epithelial-mesenchymal plasticity in breast and ovarian cancers, and USP11 expression correlated with poor prognosis. Mechanistically, USP11 has been shown to deubiquitinate type I TGFβ (Transforming growth factor beta) receptor (also known as ALK5 (Anaplastic lymphoma kinase 5)) as well as TGFβ receptor II and Snail1 (Garcia *et al*, 2018; Wang *et al*, 2018b). Moreover, USP11 controls Smac (mitochondrial-derived activator of caspases) mimetic-induced degradation of cellular inhibitor of cIAP-2 (apoptosis protein 2) and therefore, down-regulation of USP11 sensitizes cancer cells to apoptosis induced by TRAIL (TNF-related apoptosis-inducing ligand) and suppressed tumour growth (Lee *et al*, 2015). USP11, via stabilization of XIAP (X-linked inhibitor of apoptosis protein), also promotes tumour initiation and progression by inhibiting apoptosis (Zhou *et al*, 2017). In addition, eIF4B (Eukaryotic Translation Initiation Factor 4B) has been reported as a bonafide substrate of USP11, which stabilizes and enhances eIF4B activity, and thus promotes oncogenic translation in diffuse large B-cell lymphoma (DLBCL) (Kapadia *et al*, 2018). USP11 also prevents E2F1 degradation in the nuclei. Indeed, downregulation of USP11 reduces E2F1 stability and protein levels, thereby decreasing Peg10 mRNA levels, which in turns, suppresses cell proliferation and wound healing in lung epithelial cells (Wang *et al*, 2018a). USP11 can greatly increase the steady state level of HPV-16E7 (Human papillomavirus type 16 Protein E7), a major transforming protein, which has been implicated in the development of cervical cancer by reducing ubiquitination and attenuating E7 degradation (Lin *et al*, 2008). More recently, USP11 has been reported to stabilize PPP1CA (Serine/threonine-protein phosphatase PP1-alpha catalytic subunit) by deubiquitinating and protecting it from proteasome-mediated degradation. Besides, the USP11/PPP1CA complex promoted colorectal cancer progression by activating the ERK (Extracellular signal-regulated kinase)/MAPK(Mitogen-activated protein kinase) signalling pathway (Sun *et al*, 2019).

As indicated above, most of the reports favour a tumour promoting role for USP11. However, several papers display opposite results and claim that USP11

functions as a tumour suppressor. In this context, USP11 has been reported to control PTEN in prostate cancer (Park *et al*, 2019). Furthermore, Mgl-1 (Mammalian lethal giant larvae-1 protein), which controls cell polarity and differentiation of progenitor cells, is also a substrate for USP11, and, RanBPM functions as scaffolding in this reaction (Lim *et al*, 2016). USP11 was also proposed as tumour suppressor through the stabilization of VGLL4 (Vestigial Like Family Member 4), which promotes cell growth, migration, and invasion in a YAP-dependent manner (Zhang *et al*, 2016b). Finally, by regulating the ubiquitination status of Sce, a PRC1 (Polycomb repressive complex 1) protein, USP11 contributes to repress the tumour suppressor INK4a (Cyclin-dependent kinase 4 inhibitor A) (Maertens *et al*, 2010) (Figure I7).

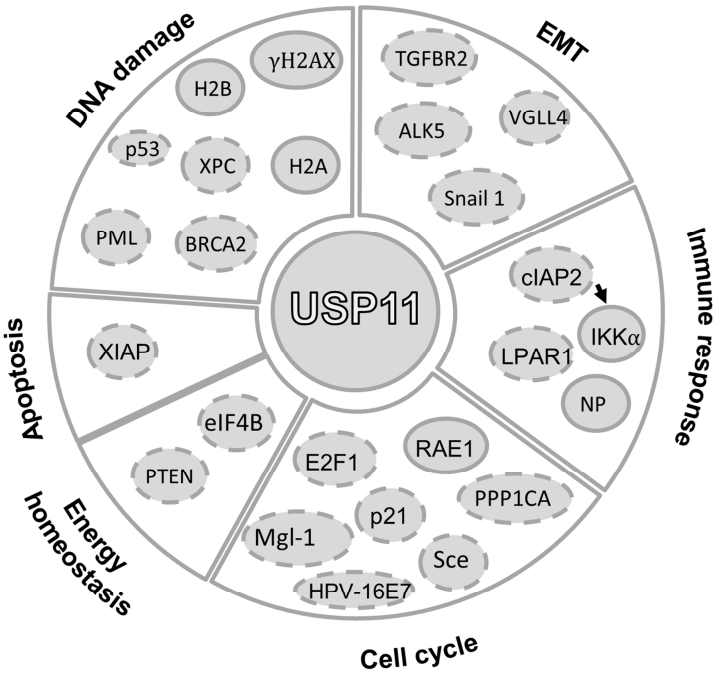

Figure I7: Squematic summary of the proteins reported in the literature as regulated by USP11. Targets whose protein stability has been shwon to be regulated by USP11 (dot-lines) while targets whose regulation does not involve proteasomal degradation (continue-lines).

2.4.3 Regulation of USP11

At the mRNA levels, USP11 has been reported be transcriptionally induced by the TNF/ JNK (c-Jun N-terminal Kinases) pathway (Lee *et al*, 2015) suggesting a feed forward regulatory mechanism on TNF-induced NF-ĸB

activation (Sun *et al*, 2010). In addition, USP11 mRNA levels are up regulated by the PTEN-FOXO pathway depicting an additional Yin-Yang regulatory mechanism (Park *et al*, 2019). By contrast, USP11 is transcriptionally repressed in glioma cells by the Notch effector HEY1 (Hairy/enhancer-of-split related with YRPW motif protein 1) (Wu *et al*, 2014). Furthermore, USP11 protein levels seem to be down regulated upon chronic ultraviolet (UV) exposure in mouse skin and also within mice and humans skin tumours (Shah *et al*, 2017).

Interestingly, USP11 catalytic activity has been reported to be dependent on the PI3K/mTOR/S6K1 pathway. Specifically, S6K1 phosphorylates USP11 Ser-452, though apparently conflicting observations raised from *in vitro* and cell-based deubiquitination assays (Kapadia *et al*, 2018). While the impact on USP11 regulation is unknown, additional phosphorylation sites (Tyr551, Tyr554, Tyr607 and Tyr 608) have been identified in several large-scale studies (Hornbeck *et al*, 2012).

Two main pharmacological inhibitors of USP11 have been described to date. Firstly, Mitoxantrone, which is an FDA (Food and Drug Administration)-approved drug for breast, prostate cancer, blood neoplasias and multiple sclerosis (Chegini & Safa, 1987; Wiseman & Spencer, 1997; Saini *et al*, 2019; Miller, 2000). Mitoxantrone has indeed been successfully tested as USP11 inhibitor on pancreatic cancer (Burkhart *et al*, 2013). Moreover, Mitoxantrone reverts USP11-mediated protein stabilization of LPA1 and TGFβ receptor II, providing mechanistic evidences for the use of such inhibitor to lessen lung injury ad pulmonary fibrosis, respectively (Zhao *et al*, 2016; Jacko *et al*, 2016). More recently, a unique peptide (FYLIR) has been identified by next generation phage display (NGPD). FYLIR binds USP11 UBL domain with micromolar affinity (K_D ≅7-8 µM). This peptide seems to affect cell-viability and cell cycle in a cell type specific manner. Thus, further characterization is needed to clarify the pharmacological interest of this peptide as a USP11 inhibitor (Spiliotopoulos *et al*, 2019).

Hypothesis and Aims

The hypoxia signalling pathway, and specifically HIF-1α, is deregulated in many diseases (Semenza, 2012). Hence, there is great interest in designing new drugs to modulate HIF-1 signalling (to increase or decrease its expression and activity) depending on the pathological context.

Ubiquitination plays a central role in HIF-signalling. As most of the post-translational modifications, ubiquitination is a reversible process catalysed by the family of deubiquitinating enzymes (DUBs). To address their direct or indirect implication in HIF signalling, we performed an unbiased loss-of function screen targeting all the Human DUBs. As a result, we newly identified 12 candidate DUBs involved in HIF-dependent transcriptional activation. The validation and further characterization of the candidates constitute the principal objective of the present *Doctoral Thesis*.

The specific objectives of the project are:

1. To validate the implication of our candidate DUBs in the modulation of the hypoxia signalling pathway (using independent RNAi (RNA interference) strategies and analysing the expression levels of endogenous hypoxia-regulated genes) and to select at least one candidate for further characterization (Section 1 and Section 2)

2. To understand the molecular mechanisms underlying USP11-mediated regulation of HIF-signalling (Section 3)

3. To analyse the potential crosstalk between hypoxia and USP11 (Section 4)

4. To evaluate the physio-pathological relevance of USP11 (Section 5).

Materials and Methods

1 Materials

Chemicals and small interference RNA (siRNAs) were purchased from Sigma-Aldrich unless stated otherwise. All tissue culture media were purchased from Gibco. Custom oligo primers were purchased from Invitrogen and Metabion International AG.

Mammalian expression plasmids CMV-βgal, Myc-HIF-1α and Myc-HIF-2α were inventoried in Edurne Berra's laboratory. FLAG-ubiquitin, GFP-USP11, *HIF1A* 3'UTR-LUC, *HIF1A* promoter-LUC, pTRIPZ-plasmids (pTRIZ-p37, pTRIZ-p40, pTRIZ-p42 and pTRIZ-p45) and FLAG-plasmids (FLAG-p37, FLAG-p40, FLAG-p42 and FLAG-p45) were kindly provided by Prof Ugo Mayor(Lee *et al*, 2014), Michael J. Clague(Urbé *et al*, 2012), Jean J. Feige(Chamboredon *et al*, 2011a), Carine Michiels(Minet *et al*, 1999), Robert J. Schneider(Lu *et al*, 2006) and Myriam Gorospe(Sarkar *et al*, 2003b), respectively.

2 Methods

2.1 Molecular biology

2.1.1 Polymerase chain reaction (PCR)

Polymerase chain reaction is used to exponentially amplify double-stranded DNA from single or doubled stranded DNA template. Primers anneal to complimentary target DNA and enable DNA polymerase to synthesize new DNA molecules replicating the target sequence. Modification of primers allows the introduction of point mutations, restriction enzyme sites, flanking sequences or tags.

DNA was amplified via PCR using KOD Hot Start DNA Polymerase (EMD Millipore). After an initial denaturation step for 5 minutes at 95 °C, 30 cycles using the following scheme were performed: 1). denaturation: 95 °C for 20 seconds; 2). annealing: primer-dependent melting temperature (Tm) for 15 seconds: 3). elongation: 70 °C for 30-90 seconds (according to the amplicon length); 4). final elongation: 70 °C for 10 minutes.

2.1.2 *RNA extraction and Reverse Transcriptase quantitative Polymerase Chain Reaction (RT-qPCR)*

RNA was extracted from cells using Qiagen's RNeasy Mini Kit as described in the manufacturer's protocol. 1 µg RNA was used as template for Reverse Transcription (RT) with qScript™ cDNA SuperMix (Quanta Biosciences). 1/40th of the reaction was subsequently analysed by qPCR amplification with FastStart Universal Master Mix (Roche) and using specific primer sets (Table M1). PCR cycles were set as follows: 10 minutes at 95 °C, 40 cycles of 15 seconds at 95 °C and 1 minute at 60 °C with a final cycle of 5 seconds at 55 °C and 50 seconds at 95 °C.

Table M1: Listing of qPCR primer sequences.

Oligos qPCR			
Target	*Sequence (5'→ 3')*	*Target*	*Sequence (5'→ 3')*
aHIF	**F:** GGAGTCAGGAGACTTGAGCTT	***PCOLCE***	**F:** CCTCCGGAGAAAACAGAGG
	R: TGAGTGAAGCAGTTCTCAGAC		**R:** GCTGGCACAGAAGTTGCTCT
AKAP12	**F:** CACTCAGGTTCCAGCCGATT	***PDGFRB***	**F:** CACCTCCTCAACCATCTCCT
	R: ACCTCGGCTAAGCCCTTTTC		**F:** TCTGGCTCTGGTTCGTCCT
ANGPL4	**F:** TCCACCGACCTCCCGTTAG	***PHD2***	**F:** AGCTGGTCAGCCAGAAGAGT
	R: CTGTTCTGAGCCTTGAGTTGTG		**R:** GCCCTCGATCCAGGTGATCT
BNIP3	**F:** GAATTTCTGAAAGTTTTCCTTCCA	***PPAP2B***	**F:** TTCTGGCAGGATTTGCTCAA
	R: TTGTCAGACGCCTTCCAATA		**R:** AGGGAGAGCGTCGTCTTAGTCTT
CA9	**F:** GAAAACAGTGCCTATGAGCAGTTG	***PRPF8***	**F:** CCCCTAAGGCTCAAAAGAAGA
	R: TCCTGGGACCTGAGTCTCTGA		**R:** AAGGTTGAGCATGTTGTAGC
COL18A1	**F:** GAAGTCGAGGAGCAGACCA	***RAE1***	**F:** GTTCGCAAACTCCTCAGACC
	R: CCCACGTGGAGACAGAATC		**R:** TGTTCCAAACAGGCTCATTTT
ELAVL1	**F:** GTCCAGAGGGGTTGCGTTTA	***RBM15B***	**F:** AGGAACTCCAGGTTCTGCTG
	R: TTGGCTGCAAACTTCACTGC		**R:** CAGGTGTCACTCATGCTACCTT
EPAS1	**F:** GTCACCAGAACTTGTGC	***RNF4***	**F:** TGGTGAGCAGTGACGATGAG
	R: CAAAGATGCTGTTCATGG		**R:** TGGCGTTTCTGGGAGTATGG
EPO	**F:** TCATCTGTGACAGCCGAGTC	***RPLP0***	**F:** CAGATTGGCTACCCAACTGTT
	R: TTTGGTGTCTGGGACAGTGA		**R:** GGCCAGGACTCCTTTGTACC
FBOXO11	**F:** TCAAATAGTGACCCAACAATAAGG	***SLC2A1***	**F:** GGTTGTGCCATACTCATGACC
	R: TCAATAAGGCCTCGTCCATC		**R:** CAGATAGGACATCCAGGGTAGC
GAPDH	**F:** AACTT TGGCATTGTGGAAGG	***SLC7A5***	**F:** GGAACATTGTGCTGGCATTATACA
	R: GGATGCAGGGATGATGTTCT		**R:** CCTCTGTGACGAAATTCAAGTAATTC
GPR116	**F:** AAGCGGAACATGAAATCAGC	***STAMBPL1***	**F:** AAAAATTGGAGCATCAGAGATT
	R: TTGCCAAGGATGACATTAACC		**R:** GAAACTGCTCCGATTCTAGCT
GSN	**F:** GAGTGCACGTGTCTGAGGAG	***TXNIP***	**F:** GATCACCGATTGGAGAGCCC
	R: GGTACCTGCAGGCAGAGC		**R:** TGCAGGGATCCACCTCAGTA
HIF1A	**F:** CTGCAACATGGAAGGTATTGCA	***UCHL5***	**F:** AAGTGGCAGCCAGGAGA

	R: TACCCACACTGAGGTTGGTTACTG		**R:** GGCTTGAGTAGCACAAGCAT
HIF1A pre-mRNA	**F:** CTCTACTGGCTCAGCCCTCT **R:** CCACATGGAGTCCTGCCTAA	***USP10***	**F:** CAAAACCCCGACAAGCTC **R:** TGTAAATATATGTGGGCTCAAAG
hnRNPD	**F:** GGGUCCCUCUGAAGUUUAATT **R:** UUAAACUUCAGAGGGACCCTT	***USP11***	**F:** CAGGCATTGCAGGCTTAGT **R:** CACTGCTAGGAGGAGACACG
LOX1	**F:** GGATACGGCACTGGCTACTT **R:** GACGCCTGGATGTAGTAGGG	***USP13***	**F:** CCACCCGGAATTCTCCT **R:** CATCGCTTGGGTTTTCTGA
MDM2	**F:** GACTCCAAGCGCGAAAAC **R:** GGTGGTTACAGCACCATCAGT	***USP16***	**F:** TGGGAAAGAAACGGACAAA **R:** TGTGTCTGCACACAGGTTCTA
MEF2C	**F:** TGTCTGTAGTGAATAAAAGTGGGAAA **R:** TTACTGAATTGTCTGCAAAATACAAA	***USP32***	**F:** TGTGTATGTTACCCTCACTGATG **R:** CAATGATGTCTGATTCCTCCA
NCL	**F:** CCACTTGTCCGCTTCACA **R:** TCTTGGGGTCACCTTGATTT	***USP40***	**F:** CTGTCCTCACAGCCTTAGC **R:** ACCTGGACATCCAGCACTG
OCT4	**F:** GCTTAGCTTCAAGAACATGTGTA **R:** CTCTCACTCGGTTCTCGAT	***USP47***	**F:** TGGAGACGAGAAAGCCTGAT **R:** CAACAACATGAACTTTCACCATC
OTUD4	**F:** GAGATTCAGAACAGAGATGAACAG **R:** GCTGACTGATTGACTGATGAG	***VEGFA***	**F:** GAGATGAGCTTCCTACAGCAC **R:** TCACCGCCTCGGCTTGTCACAT

2.1.3 Mutagenesis

QuikChange® II XL Site-Directed Mutagenesis Kit (Agilent Technologies) was used to introduce single or multiple point mutations from double-stranded DNA plasmids. The mutations were introduced by amplification of 100 ng of template DNA with 0.25 µM forward and reverse primers (Table M2), in the presence of 1x reaction buffer, 6% (v/v) Quick solution®, 0.1mM dideoxynucleotide (dNTPs), and 1.25 units of PfuUltra HF DNA Polymerase. PCR cycles were set as follows: 1 minute at 95 °C, 18 cycles of 50 seconds at 95 °C (denaturation), 50 seconds at 60 °C (annealing) and 7 minutes at 68 °C (elongation) with a final elongation cycle of 7 minutes at 68 °C. Template DNA was digested with 5 units of Dpn1 for 1h at 37 °C, and subsequently one sixth of the reaction was transformed into competent XL10-Gold (Agilent Technologies) cells.

Table M2: Summary of the primers used for plasmid mutagenesis.

QuikChange® II XL Site-Directed Mutagenesis		
Vector	*AA change*	*Sequence (5'→ 3')*
GFP-USP11 C/S	**C318S**	F: ccaatctgggcaacacaagcttcatgaactcggccctg R: cagggccgagttcatgaagcttgtgttgcccagattgg
GFP-USP11 S/A	**S452A**	F: aaccacaaacggcggaacgatgctgtgatcgtggacactttcc R: ggaaagtgtccacgatcacagcatcgttccgccgtttgtggtt

2.1.4 Restriction digestion

Restriction digestion is a process in which DNA is cleaved at specific 4-8 bp long palindromic sequences. This process is accomplished by incubation of the target DNA molecule with the restriction enzyme(s) of choice that recognize and cut at specific nucleotides.

Restriction digestions were carried out incubating 10 units of enzyme per µg of DNA in appropriate buffer for at least 1 hour at 37 °C. DNA fragments were separated by size on agarose gels containing SYBR® Safe DNA Gel Stain for visualization of DNA under UV exposure. Agarose gel percentage was chosen depending on expected DNA fragment size between 0.7 and 2%.

2.1.5 In-Fusion® HD cloning

In-Fusion® HD Cloning (Clontech) was used to insert cDNAs into different expression vectors taking advantage of the DNA recombination technology. In that manner, the destination vector was linearized by single or double digestion, while the insert was amplified by PCR using specific primers that creates complementary overhangs to the vector backbone at the site of insertion. Next, linearized vector and PCR product were gel-purified with a gel purification kit (QIAEX® II from Qiagen) and the In-Fusion® reaction was set up using an insert: vector-ratio of 4:1. After that, In-Fusion reaction was diluted 1:10, and 2.5 µl were transformed into 50µl of competent *Stellar*™ cells. Cloned plasmids and strategies are summarized in Table M3.

Table M3: Summary of the strategies used to clone the indicated plamsids.

In-Fusion® HD Cloning primer			
Final vector	*Insert donor*	*Vector acceptor*	*Sequence (5'→ 3')*
HA-USP11	**pEGFP-GW-JJ-USP11**	*HA*-USP29	**F**:GCCTGGGAGGACCTTATGCAGTAGCCCCGCGACTGTTT **R**:AAGTTCTCAGGATCTCAATTAACATCCATGAACTCAGAGC
Myc-clover-p37	**pTRIZ-p37**	*Myc-clover*-HIFDM	**F**:ACGAGCTGTACAAGGCCTCGGAGGAGCAGTTCGGC **R**:TTAATTAAGGTACCGGTATGGTTTGTAGCTATTTTGATG
Myc-clover-p40	**pTRIZ-p40**	*Myc-clover*-HIFDM	**F**:ACGAGCTGTACAAGGCCTCGGAGGAGCAGTTCGGC **R**:TTAATTAAGGTACCGGTATGGTTTGTAGCTATTTTGATG
Myc-clover-p42	**pTRIZ-p42**	*Myc-clover*-HIFDM	**F**:ACGAGCTGTACAAGGCCTCGGAGGAGCAGTTCGGC **R**:TTAATTAAGGTACCGGTATGGTTTGTAGCTATTTTGATG
Myc-clover-p45	**pTRIZ-p45**	*Myc-clover*-HIFDM	**F**:ACGAGCTGTACAAGGCCTCGGAGGAGCAGTTCGGC **R**:TTAATTAAGGTACCGGTATGGTTTGTAGCTATTTTGATG

2.1.6 Bacterial transformation.

Amplification of plasmid DNA was carried out by transforming the DNA into chemically competent *E. coli* XL10-Gold (Agilent Technologies) or *Stellar*™ (Clontech) cells. Therefore, the plasmid needed to contain a bacterial origin of replication and an antibiotic resistance for selection purposes. 5ng of plasmid DNA were incubated with 50µl of competent bacteria for 30 minutes on ice. Bacteria were then heat-shocked in a 42 °C water bath for 45 seconds and after 2 minutes on ice, 500µl of SOC-medium was added. Bacteria were allowed to grow for 1 hour at 37 °C in a shaker (220 rpm) before plating 1:10 and 9:10 of the culture onto LB plates containing the selection antibiotic (50µg/ml kanamycin or 100µg/ml ampicillin). Plates were incubated overnight at 37 °C and single colonies were picked and inoculated into 5 and 200 ml of antibiotic containing LB-medium for mini-cultures and maxi-cultures, respectively, and allowed to grow for 16 hours. The GeneJET Plasmid Miniprep Kit (Thermo Fisher Scientific) or the QIAGEN® Plasmid Maxi Kit were used for plasmid purification from mini- and maxi-cultures, respectively.

All plasmids were verified by enzymatic digestion and/or sequencing with appropriate primers from STABvida (Table M4).

Table M4: Summary of the primers used for sequencing .

Sequencing primers	
Vector	*Sequence (5'→ 3')*
HA-USP11	**F**:CGCAAATGGGCGGTAGGCGTG **Internal**:CCCACTGGGCATGAAGGGTG **R:**CCCTTGTATCACCATGGACCC
GFP-USP11*	**F**: CATGGTCCTGCTGGAGTTCGTG
GFP-USP11 S/A	**F**: CATGGTCCTGCTGGAGTTCGTG
Myc-clover-p37,p40,p42 and p45	**F:** CGCAAATGGGCGGTAGGCGTG **R**: GTCTGACGTGGCAGCGCTC

2.2 Cell biology

2.2.1 Cell culture and transfections

HEK293 and MDA-MB-231 cell lines (Metastatic breast adenocarcinoma cells) and A375 cells line (malignant melanoma cells) cells were cultured in Dulbecco's Modified Eagle Medium (DMEM) + GlutaMAX™ supplemented with 5% FBS at 37 °C and 5% O_2. 80% sub-confluent plates were trypsinised and cells for experiments were plated at a density of 31600 cells/cm^2 or 42000 cells/cm^2, respectively. Hypoxic incubation was carried out in an *Invivo* O_2 400 chamber (Baker Ruskin) equipped with an I-CO_2N_2IC gas mixer (Baker Ruskin).

2.2.2 DNA transfections

After 24 hours, cells were transfected using Lipofectamine® 2000 (Thermo-Fisher Scientific) at a Lipofectamine:DNA ratio of 2:1 using Opti-MEM medium. Then, transfection mix was added to the culture media and incubated during 24 hours for HEK293 cell line. In the case of MDA-MB-231 cells, were incubated with the transfection mix for 6 hours before medium change. Cells were harvested 24 hours post-transfection, unless stated otherwise, to be further processed.

2.2.3 siRNA transfections

In order to silence the expression of the target genes, cells were transfected with 20nM siRNAs (Table M5). The first transfection of the siRNAs with Lipofectamine® 2000 (3µl Lipofectamine® 2000) was made in suspension at the moment of plating. 24h later, the cells were transfected again with the siRNAs (and eventually with the corresponding DNA) after a medium change. Cells were harvested 48h after the first transfection to be further processed.

Table M4: Summary of the siRNA sequences.

siRNAs		
Target	*Sequence (5'→3')*	*Reference*
Control	CUACAUCCCGAUCGAUGAUGdTdT	Lab validated
HIF1A	AAAGGACAAGUCACCACAGGAdTdT	Lab validated
EPAS1	UAUCAUUGGGUACAUUUGCdTdT	Lab validated

UCHL5	GCAGUUAAUACCACUAGUAdTdT	(Nishi *et al*, 2014)
USP10	CACAGCUUCUGUUGACUCUdTdT	(Bomberger *et al*, 2011)
USP11.1	ACCGAUUCUAUUGGCCUAGUAdTdT	(Wiltshire *et al*, 2010b)
USP11.2	GAUUCUAUUGGCCUAGUAUdTdT	Lab validated
USP13	CUACGAGCAACGAAUAAUAdTdT	(Liu *et al*, 2011)
USP16	UAUCAGAUCUGGAGUGUGAdTdT	(Joo *et al*, 2007)
USP32	UAUCAGAUCUGGAGUGUGAdTdT	Lab validated
USP40	CUGAAGAGAAGCAAGUUAAdTdT	Lab validated
USP47	GCAACGAUUUCUCCAAUGA dTdT	Lab validated
OTUD4	UGGCCUGUAUUCACUAUCUUC dTdT	(Zhao *et al*, 2015)
STAMBPL1	CAAGAAUAUUUGCAAAGCAdTdT	(Lavorgna & Harhaj, 2012)
PRPF8	GGGCCAAGUUCCUGGACUAdTdT	(Kurtovic-Kozaric *et al*, 2015)
hnRNPD	AAGAUCCUAUCACAGGGCGAUdTdT	(Yoon *et al*, 2014)
RBM15B	GGUCGCAACCCCAUUAAGAUAdTdT	(Majerciak *et al*, 2010)
RAE1	GCAGUAACCAAGCGAUACAdTdT	(Cuende *et al*, 2008)
FBOXO11	AGUCCAUACCAACUUCGUAGAdTdT	(Ju *et al*, 2015b)
RNF4	CACCAGUUGUUCUCAGGAACCdTdT	(Tan *et al*, 2015)
NCL	CGGUGAAAUUGAUGGAAAUdTdT	(Reyes-Reyes *et al*, 2015)
ELAVL1	AAGAGGCAAUUACCAGUUUCAdTdT	(Kim *et al*, 2015)

2.2.4 GFP-Fluorescence detection

HeLa cell line (Henrietta Lacks cervix adenocarcinoma cells) were seeded and transfected on microscope coverslips, and fixed using 3% paraformaldehyde during 30 minutes at 37 °C. Then, cells were permeabilised during 5 minutes with 0.2% Triton X-100 diluted into Phosphate Buffer Saline (PBS). After that, cells were washed and blocked with a solution containing 0.2% gelatine and 2% bovine serum albumin diluted into PBS. Finally, cells were incubated with DAPI nuclear staining (SIGMA) (5mg/ml) diluted into blocking solution (1:1000) during 15 minutes before fixing the coverslips into microscope slides (MENZEL-GLÄSER) using fluoromount (SIGMA). Cells were visualized using Axio Imager D1 (ZEISS) and images were capture using the Axiocam HRm (ZEISS) camera equipped with AxioVision Rel 4.8. Software.

2.3 Biochemistry

2.3.1 Ribonucleoprotein immunoprecipitation (RIP)

The association of endogenous hnRNPD and USP11 with endogenous mRNAs in HEK293 cells was assessed using Myriam Gorospe's lab protocol from National Institute on Aging (NIA) (Abdelmohsen *et al*, 2007). Briefly, cells were lysed in 20mM Tris-HCl at pH 7.5, 100mM KCl, 5mM $MgCl_2$, and 0.5% NP-40 for 10 minutes on ice and centrifuged at 15,000 g for 10 minutes at 4 °C. The supernatants were incubated with protein A Dynabeads coated with anti-hnRNPD (Millipore), anti-USP11 (Abcam) or with control IgG (Santa Cruz Biotechnology) antibodies for 2 h at 4 °C. The beads were washed with NT2 buffer (50mM Tris-HCl [pH 7.5], 150mM NaCl, 1mM $MgCl_2$, 0.05% NP-40), followed by incubation with 20 units of RNase-free DNase I for 15 minutes at 37 °C to remove the DNA. The RNA from the IP samples was extracted using TRIzol (Invitrogen) following the manufacturer's protocol and then used for cDNA synthesis followed by qPCR analysis.

2.3.2 Biotin pulldown assay

DNA templates overlapping the whole sequence of *HIF1A* mRNA were synthesized by PCR from cDNA generated from HEK293 total mRNA by RT following Myriam Gorospe's lab protocol from National Institute on Aging (NIA) (Abdelmohsen *et al*, 2007). All of the forward primers (F) contained the T7 RNA polymerase promoter (T7, AGTAATACGACTCACTATAGGG) at their 5' end (Table M6).

The PCR products overlapping *HIF1A* mRNA sequence were purified using NucAway Spin columns (ThermoFisher) and used for preparing biotinylated RNA transcripts using the MaxiScript T7 *in vitro* transcription kit (Ambion). 500 µg of total protein cell lysate was incubated with 5 µg of purified biotinylated transcripts for 30 minutes at room temperature, followed by isolation of RNP complexes using streptavidin-coupled Dynabeads (Invitrogen). The presence of hnRNPD in the pulldown complexes was assessed by Western blot analysis.

Table M6: Summary of the primers used to amplify by PCR the different *HIF1A* mRNA probes for *in vitro* transcription

HIF1A mRNA primer fragments		
Probe	*Sequence (5'→3')*	*Length*
5'UTR (1)	**F:** CCTCAGCTCCTCAGTGCACA **R:** GCCCTCCATGGTGAATCG	313 bp
CR (2)	**F:** ATTCACCATGGAGGGCGC **R:** TGTCCTGTGGTGACTTGTCC	918 bp
CR (3)	**F:** GGACAAGTCACCACAGGACA **R:** TGCTTCTGTGTCTTCAGCAAA	747 bp
CR (4)	**F:** TGATGACCAGCAACTTGAGG **R:** TGGGTAGGAGATGGAGATGC	678 bp
CR (5)	**F:** GCCACCACTGATGAATTAAA **R:** GCTCAGTTAACTTGATCCAAAGC	629 bp
3'UTR (5)	**F:** GTTAACTGAGCTTTTTCTTAATT **R:** GCTGTCTGTGATCCAGCATT	210 bp
3'UTR (6)	**F:** CACAGACAGCTCATTTTCTC **R:** GCTGGCAAAGCATTATTATTTATGTA	250 bp
3'UTR (7)	**F:** CTTTGCCAGCAGTACGTGGT **R:** CCCATTTAAATAATAAACCATACAGC	209 bp
3'UTR (8)	**F:** TTTAAATGGGTAAAGCCATT **R:** ACCAACAGGGTAGGCAGAAC	222 bp
3'UTR (9)	**F:** GCCTACCCTGTTGGTATAAAG **R:** GCCTGGTCCACAGAAGATGT	337 bp

2.3.3 *Luciferase assays*

To measure luciferase activity Steadylite plus™ High Sensitivity Luminescence Reporter Gene Assay System (PerkinElmer) commercial kit was used. Cells were collected in 100µl/1.1cm^2 of lysis buffer (25mM Tris phosphate, 8mM $MgCl_2$, 1% Triton X-100 and 15% Glycerol and 0.5mM Dithiothreitol (DTT). 20µL of cellular extracts were loaded into opaque 96 well plates (Optiplate 96 white, Perkin Elmer) and 40µL of reacting substrate (Steadylite plus substrate solution, PerkinElmer) and 50µL of PBS 1x were added. The mix was incubated during 15 minutes at room temperature protected from light. Then, luciferase activity was measures using a luminometer plate reader (Veritas Microplate Luminometer, Turner Biosystems) controlled by software Veritas 1.3.1 version. In parallel and to normalize, β-galactosidase activity was measured to normalize using Galacto-light Plus

system (Applied Biosystems) commercial kit. Hence, 10µL of sample were loaded into opaque 96 well plates (Optiplate 96 white, Perkin Elmer) and 50µL of reacting substrate that contains Galacto reagent (1:100) into dilution buffer (Applied Biosystems). The mix was incubated during 60 minutes at room temperature protected from light. After that, 75µL of Accelerator-II were added (Applied Biosystems). Then, β-galactosidase activity was measured using the same luminometer. Luciferase activity is expressed as relative values (luciferase/β-galactosidase).

2.3.4 *Cell fractionation*

Cells were tripsinized, washed in PBS and counted. $8x10^6$ cells were suspended into 400µL of cold buffer A freshly prepared (10mM HEPES pH 7.9, 10mM KCl, 1.5mM $MgCl_2$, 0.34M sucrose, 10% glycerol, 1mM DTT, 1ug/ml aprotinin, 1ug/ml leupeptin, 1ug/ml pepstatin, 0,1mM AEBSF (4-(2-aminoethyl) benzenesulfonyl fluoride hydrochloride), 1mM O-Vanadate, 10mM NaF and 2mM NEM (N-Ethylmaleimide)). 1/10 fraction from the lysate was stored into Laemli 2x (1:1 ratio) and kept for whole cellular extract analysis. After that 0.1% Triton X-100 was added to the lysate, incubated for 5 minutes incubation on ice and subsequently centrifuged (4 minutes at 1 300g at 4 °C). Then, supernatant was recovered and centrifuged for additional 15 minutes at 20 000g at 4 ºC. The clarified supernatant (cytoplasm fraction) was stored into Laemli 2x (1:1 ratio) and kept for analysis, and the pellet was discharged. The pellet from the initial centrifugation was washed in buffer A and lysed in one volume of buffer B freshly prepared (3mM EDTA, 0.2mM EGTA, 1mM DTT, 1ug/ml aprotinin, 1ug/ml leupeptin, 1ug/ml pepstatin, 0.1mM AEBSF, 1mM o-vanadate, 10mM NaF and 2mM NEM) by incubation during 30 minutes at 4 ºC. The lysate was then centrifuged for 5 minutes at 1 700g at 4 ºC. Finally, the supernatant (nuclear fraction) was recovered into a new eppendorf and stored into Laemli 2x (1:1 ratio) for analysis. All fractions were sonicated (15 sec, 10% amplitude) and quantified using DC™ Protein Assay (BioRad). 20 ug of each fraction was migrated into self-cast SDS (Sodium Dodecyl Sulfate) polyacrylamide (Bio-Rad) gels (7.5 %, 10 % or 12 %).

2.3.5 Western Blot

Cells were lysed in 200µl/8.8 cm^2 of 1.5x Laemmli (50mM Tris-HCl pH 6.8, 1.25% SDS and 15% glycerol) and the lysates were frozen, boiled at 95 °C for 15 minutes and then sonicated during 5 seconds. Protein quantification was performed with the DC™ Protein Assay (BioRad). Between 10 and 40µg of protein were loaded on elf-cast SDS polyacrylamide (Bio-Rad) gels (7.5 %, 10 % or 12 %) or 4-15% gradient gels (Bio-Rad) and migrated on 1x Tris/Glycine/SDS running buffer (BioRad) at 160V for 90 minutes and 100V for 60 minutes, respectively. Then, proteins were transferred into a PVDF-membrane (EMD Millipore) at 100V for 1h at 4 °C using 1x Tris/Glycine transfer buffer (Bio-Rad). Membranes were stained with amidoblack, air-dried, rehydrated by washing with ethanol, 2 washes with TNT (50mM Tris-HCl pH 7.4, 150mM NaCl, 0.1 % Triton X-100) and 1 wash with TN (50mM Tris-HCl pH 7.4, 150mM NaCl). The membrane was then blocked for 1 hour with 5% skimmed milk in TN and incubated with the primary antibody (diluted in 5% milk in TN) at 4 °C overnight (Table M7). After 3 washes with TNT, 1 wash with TN and a short blocking step (5% skimmed milk in TN), membranes were incubated with the HRP-conjugated secondary antibody for 1h. After further washing steps, home-made ECL (1:1; solution A: 100mM Tris-HCl pH 8.5, 0.4mM coumaric acid, 2.5mM luminol; solution B: 100mM Tris-HCl, 2% H_2O_2) was incubated on the membranes for 1 minutes and signal was detected with Amersham Hyperfilm ECL (GE Healthcare Life Sciences).

Table M7: Summary of the antibodies used for WBs.

Antibodies			
Target	*Reference*	*Dilution*	*Secondary*
β-actin	Sigma A5441	1 : 50 000	mouse 1 : 20000
CAIX	clone MN75, Bayer	1 : 1 000	mouse 1 : 5000
FLAG M2-HRP	Sigma A8592	1 : 1 000	-
GFP	Roche 11 814 460 001	1 : 1 000	mouse 1 : 5000
HA	Covance 16B12	1 : 10 000	mouse 1 : 10 000
HIF-1α	Home-made (Richard et al, 1999)	1 : 5 000	rabbit 1 : 5000
HIF-2α	Home-made	1 : 1 000	rabbit 1 : 5000
hnRNPD	Millipore #07-260	1 : 5 000	rabbit 1 : 5000
PHD2	Home-made (Berra et al, 2003)	1 : 1 000	rabbit 1 : 5000
pRS6K1	Cell Signaling 9234	1 : 1 000	rabbit 1 : 5000
pRS6	Cell Signaling 2215S	1 : 10 000	rabbit 1 : 5000
RS6K1	Cell Signaling 2708	1 : 1 000	rabbit 1 : 5000

RS6	Cell Signaling 2317S	1 : 1 000	mouse 1 : 5000
Tubulin	SIGMA T9026	1 : 10 000	mouse 1 : 10 000
USP11	Abcam ab109232	1: 5 000	rabbit 1 : 5000
AMPKα2	Cell Signaling 2757	1 : 1 000	rabbit 1 : 5000

2ndary antibodies	
anti-mouse-HRP	Promega W4021
anti-rabbit-HRP	Promega W4011

2.3.6 *DUB activity assay*

This assay is based on HA-Ubiquitin Vinyl Sulfone (Boston Biochem), which is an N-terminal HA-tagged ubiquitin that acts as a potent, irreversible and specific inhibitor of most deubiquitinating enzymes (DUBs) including ubiquitin-specific proteases (USPs).

HEK293 cells were transfected with the different GFP-USP11 constructs during 24 hours before additional 24 hours incubation in normoxia or hypoxia. After that, cell were lysate with 200µl of HR buffer (50Mm Tris pH 7.5, 5mM $MgCl_2$, 250mM sucrose (fresh), 1mM DTT, 2mM ATP, 1mM AEBSF, 25mM β-glycerol phosphate, 1mM O-Vanadate and 50mM NaF) under mechanical disintegration with a 27G syringe. After 3 minutes of centrifugation at 1500 rpm, supernatants were collected and protein quantified. 0, 1µg of HA-Ubiquitin Vinyl Sulfone probe was incubated with 50µg of protein for 2 hours at 25 ºC shaking at 1250 rpm in a thermomixer. Once the reaction was finished, Laemli buffer was added to store the samples. The extracts were migrated in duplicates in on self-cast SDS polyacrylamide gels, and membranes were probed with the corresponding antibodies.

2.3.7 *Ubiquitination assay*

The assay has been adapted from (Lee *et al*, 2014). Briefly HEK293 cells were co-transfected with FLAG-Ubiquitin and GFP-tagged protein of interest and then, treated 24h post-transfection with 10µM MG132 for 2-4h prior to lysis in order to accumulate ubiquitinated proteins. Lysis was done on ice from 3.5 cm dishes with 300 µl lysis buffer (50mM Tris-HCl pH 7.5, 150mM NaCl, 1mM EDTA, 0.5% Triton X-100, 40mM β-Glycerol phosphate, 1µg/ml Leupeptin, 1µg/ml Aprotinin, 1µg/ml Pepstatin A, 7mg/ml NEM). Lysates were centrifuged

for 15 minutes at 13000 g at 4 ºC, and the supernatant was diluted with dilution buffer (50mM Tris-HCl pH 7.5, 150mM NaCl, 1mM EDTA, 40mM β-Glycerol phosphate, 1µg/ml Leupeptin, 1µg/ml Aprotinin, 1µg/ml Pepstatin A, 7mg/ml NEM) to reduce detergent concentration to 0.2%. The diluted lysate was incubated for 2.5h at RT with 15µl pre-washed GFP-traps® (Chromotek). Then, beads were washed with 500µl of dilution buffer and subjected to 3 stringent washes in denaturing conditions with 8M urea in PBS 1% SDS, followed by one wash in PBS 1% SDS. GFP-proteins were then eluted from the beads by boiling 10 minutes in elution buffer (250mM Tris-HCl pH 7.5, 40% glycerol, 4% SDS, 0.2% bromophenol blue, 5% β-mercaptoethanol). The input and the eluate (two times) were migrated on pre-cast 4-15% Tris-glycine gradient gels, and membranes were probed with anti-GFP (input and pull-downed proteins to validate the pull-down) and anti-FLAG M2-HRP (to visualize the proteins conjugated with the ubiquitin-tagged) antibodies, respectively.

2.3.8 Co-immunoprecipitation assays

HEK293 cells were transfected with the GFP-tagged protein of interest and 24h post-transfection cells were lysed on ice with lysis buffer (50mM Tris-HCl (pH 8), 120mM NaCl, 1mM EDTA, 1% IGEPAL CA-630, 40mM β-Glycerolphosphate, 1µg/ml Leupeptin, 1µg/ml Aprotinin, 1µg/ml Pepstatin A). Lysates were centrifuged for 15 minutes at 13 000 g at 4 ºC, and the supernatant was diluted with Co-IP buffer buffer (50mM Tris-HCl (pH 8), 120mM NaCl, 1mM EDTA, 40mM β-Glycerolphosphate, 1µg/ml Leupeptin, 1µg/ml Aprotinin, 1µg/ml Pepstatin A) to reduce detergent concentration to 0.2%. The diluted lysate was incubated for 1h at 4 ºC with 15µl pre-washed bab-20 (Chromotek) beads for pre-clearing. The lysate was then incubated with 15µl pre-washed GFP-traps® overnight at 4 ºC. The beads were subjected to 3 washes of 30 minutes with dilution buffer and 1 washing with PBS, before the bound proteins were eluted from the beads by boiling them for 10 minutes in elution buffer (250mM Tris-HCl pH 7.5, 40% glycerol, 4% SDS, 0.2% bromophenol blue, 5% β-mercaptoethanol). Input samples and eluates were analysed by Western Blot.

2.3.9 *MassSpec (MS) analysis*

For MS analysis samples were prepared as described in the *Ubiquitination assay* section but scaling up to three 10cm-dishes per condition (approximately 12 mg protein) and analysed in the Proteomics Facility from Servicios Generales de Investigación (SGIker-UPV/EHU). The samples were separated by SDS-PAGE and specific bands were cut out and digested individually with trypsin. Peptides were loaded onto an EASY-nLC 1200 liquid chromatography system interfaced with a Q Exactive HF-X mass spectrometer (Thermo Scientific) via a nanospray flex ion source and processed using MaxQuant software (version 1.5.3.17)(Cox & Mann, 2008) and the internal search engine Andromeda searching (Cox *et al*, 2011) against the UniProt database restricted to *Homo sapiens* entries (Human). Carbamidomethylation (C) was set as fixed modification whereas Met oxidation, protein N-terminal acetylation and Lys GlyGly (not C-term) were defined as variable modifications. Enzyme specificity was set to trypsin, allowing the maximum of three missed cleavages. The minimum peptide length was set to seven amino acids. The false discovery rate for peptides and proteins was set to 1%. Normalized spectral protein label-free quantification (LFQ) intensities were calculated using the MaxLFQ algorithm(Cox *et al*, 2014). MaxQuant output data was analysed with the Perseus module (version 1.5.6.0)(Tyanova *et al*, 2016). Proteins only identified by site, contaminants, reverse hits and proteins with no unique peptides and/or no intensity were removed.

2.4 Statistical Analysis

All experiments were performed at least three times as biological replicates to ensure adequate statistical power.

Unless stated otherwise, data is as means ± S.E.M of each group of experiments.

For *in vitro* experiments, normal distribution was assumed and Student T-test was applied for two component comparisons. One sample T-test with corresponding hypothetical value 1 was used for statistical analysis using GraphPad Prism 8.2.1 software.

Results

1 RNAi screen of DUBs that modulate the hypoxia signalling cascade

A loss of function DUBs screen was previously performed in our laboratory. It comprised a library of small hairpins RNA (shRNAs) targeting all the DUBs encoded by the human genome with predicted catalytic activity. Hence, pools of three different shRNAs were transfected into HeLa cells together with an HRE-luciferase reporter gene and a CMV-βgal as a normalizer. After that, the cells were exposed to either normoxia or hypoxia and luciferase activity was used as a read out of HIF-dependent transcriptional activation. The experiment was carried out three times in triplicates, and several DUBs were shown to have an effect on HIF activity. The above-mentioned set of experiments was the beginning of this PhD thesis, which started validating the top "hits" identified.

1.1 Validation of the screening

Hits selection was decided based on the Z-score of the shDUB-driven luciferase activity perturbation compared to shControl (data not shown). Thereby, 11 DUBs were selected and further validated using independent siRNAs sequences on HEK293 cells. Indeed, the hypoxic induction of endogenous HIF target genes measured by RT-qPCR was used as a read-out of HIF activation.

1.1.1 Silencing efficacy of the selected candidates

Specific siRNAs were designed against *OTUD4 (*OTU domain-containing ubiquitin aldehyde-binding protein 4), *PRPF8 (*Pre-mRNA-processing-splicing factor 8), *STAMBPL1* (STAM-binding protein-like 1), *UCHL5 (*Ubiquitin carboxyl-terminal hydrolase isozyme L5) *USP10*, *USP11*, *USP13*, *USP16*, *USP32*, *USP40* and *USP47*. To test them, HEK293 cells were transfected with the corresponding siRNA for 48 hours and incubated in either normoxia or hypoxia overnight before harvesting. Without exception, each DUB was significantly knocked down in both conditions (Figure R1A). In addition, it is important to

notice that *PRPF8*, *USP10* and *USP16* mRNA expression was down regulated upon hypoxia (Figure R1B).

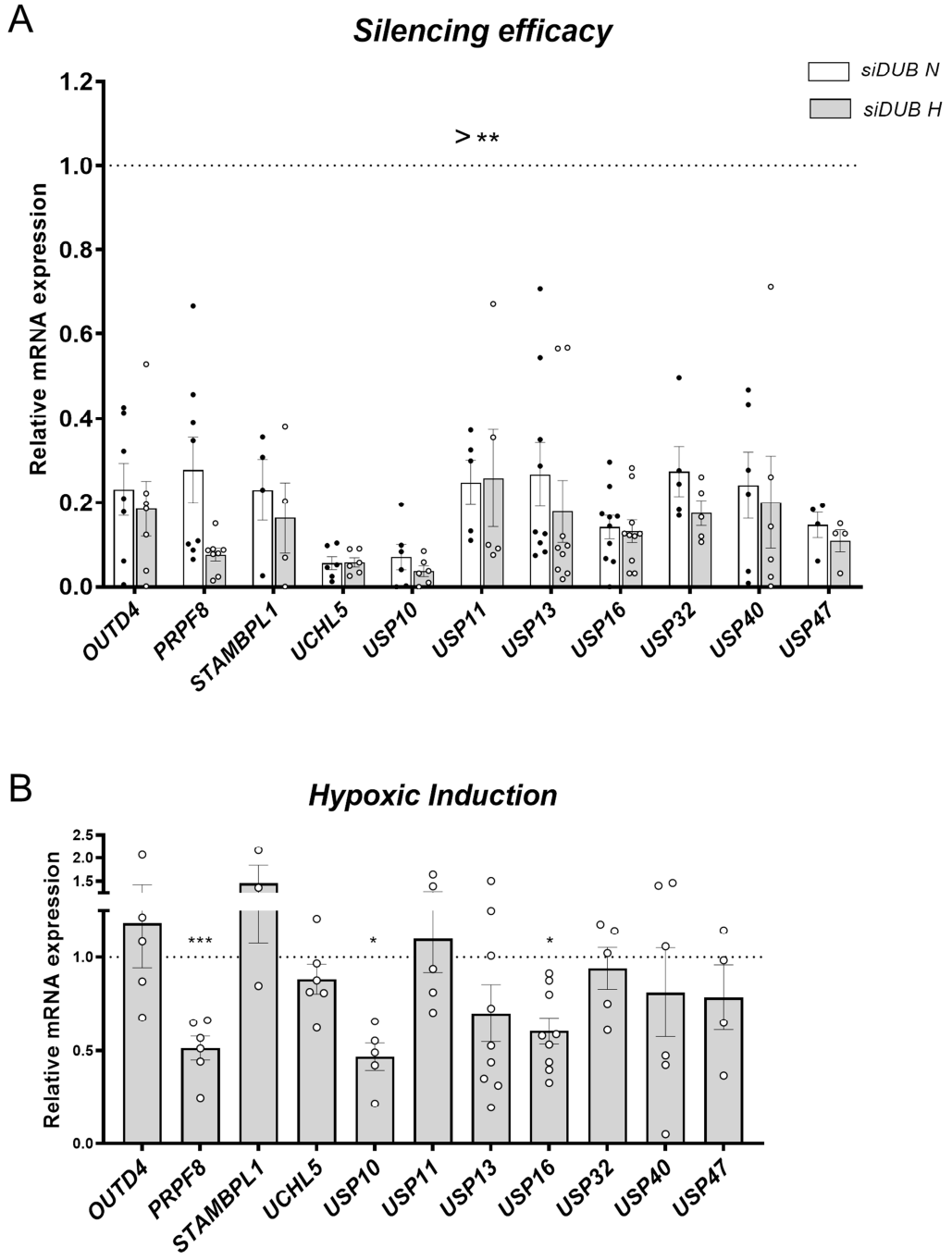

Figure R1: DUB screening validation. HEK293 cells were transfected with *siC* (Control) or *siRNAs* targeting each of the selected DUBs during 48 hours. Then, after overnight normoxic (N; 20% O_2) or hypoxic (H; 1% O_2) incubation, mRNA levels were analysed by RT-qPCR. Results are normalized to *RPLP0* following $2^{-\Delta\Delta Ct}$ method**. A)** Silencing efficacy. Results are represented as relative values to normoxic or hypoxic control cells (dotted line). **B)** Hypoxic induction of *DUBs'* mRNA levels. Results are represented as relative values to normoxic control cells (dotted line). Figures show the values corresponding to average ± s.e.m. (*p<0,03, ** p<0,0021, ***p<0,0002. One sample T-test)

1.1.2 Impact of the selected candidates in the induction of hypoxia target genes

Once the silencing of each DUB was confirmed, the effect over the hypoxia signalling cascade was assessed by measuring the hypoxic induction of two well described HIF target genes: *BNIP3* (BCL2 Interacting Protein 3) and *CA9* (Carbonic Anhydrase 9).

As a result, *OTUD4*, *STAMBPL1*, *USP32*, *USP40* and *USP47* were discarded as regulators of the hypoxia-cascade, since their silencing yielded no significant effect on *BNIP3* and *CA9* mRNA hypoxic induction (Figure R2A).

In the case of *PRPF8* and *USP13*, their silencing significantly reduced *BNIP3* hypoxic induction, whereas *CA9* induction was not modified. Surprisingly, *USP10* and *USP16* knockdown yielded conflicting results: hypoxic induction of *BNIP3* was decrease in the case of *USP16* silencing, while *USP10* knockdown seemed to have little effect on *BNIP3* hypoxic induction. By contrast, *CA9* induction was significantly increased upon both, *USP10* and *USP16* silencing (Figure R2A). In view of these results, and with the aim of shedding light upon HIF activity in the above-mentioned contexts, we analysed two additional HIF target genes: *LOX1* and *SLC2A1.* Unfortunately, the results of the hypoxic induction of *LOX1* or *SLC2A1* upon *PRPF8*, *USP13, USP10* or *USP16* silencing did not clarify their role on hypoxia signalling pathway, as mostly mild effect could be detected and only *USP16* silencing produced a significant decrease (Figure R2B).

Concerning *UCHL5* and *USP11* silencing, both DUBs emerged as required to sustain the hypoxic induction of both *BNIP3* and *CA9* (Figure R2A) and therefore, as strong candidates for further characterization

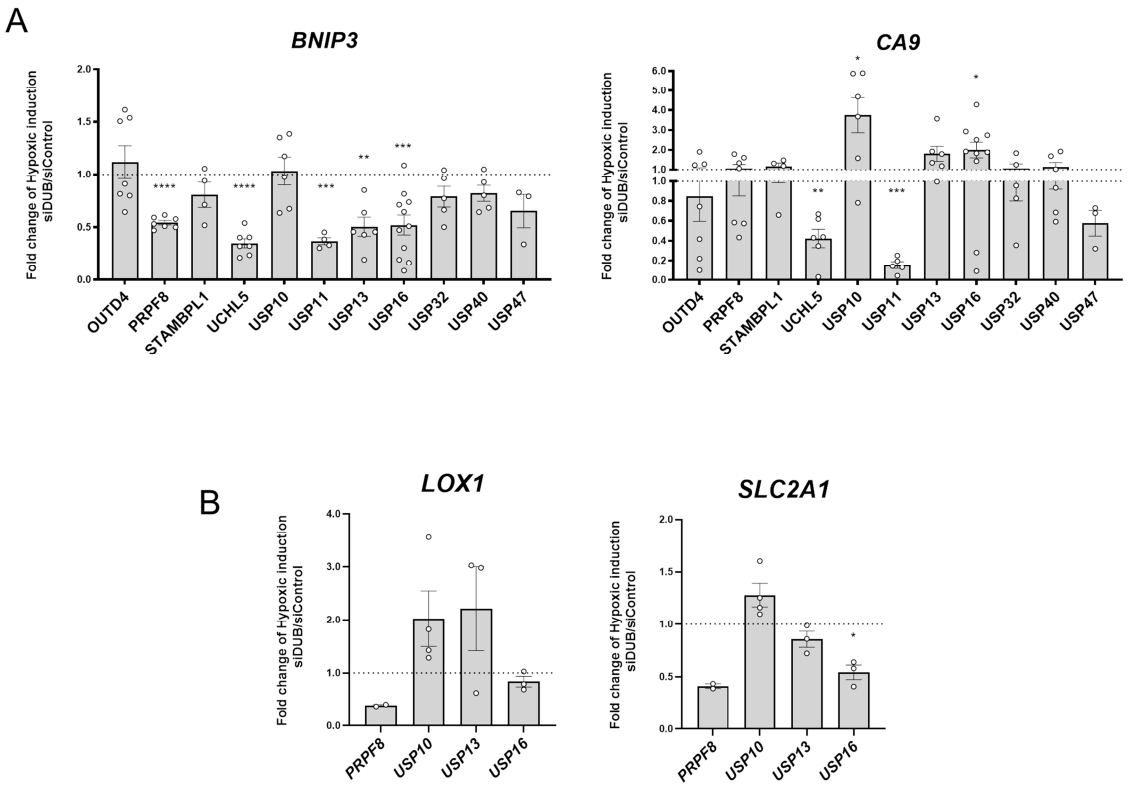

Figure R2: Validation of selected *DUB*s on the hypoxic induction of HIF target genes. HEK293 cells were transfected with *siC* (Control) or *siRNAs* against each of the selected DUBs during 48 hours. Then, after overnight normoxic (N; 20% O_2) or hypoxic (H; 1% O_2) incubation, mRNA levels were analysed by RT-qPCR.: **A)** *BNIP3* and *CA9*; **B)** *LOX1* and. Results are normalized to *RPLP0* following $2^{-\Delta\Delta Ct}$ method and represented as relative values to hypoxic control cells (dotted line). Figure shows the values corresponding to average ± s.e.m. (*p<0,03, ** p<0,0021, ***p<0,0002, ***p<0,0001. One sample T-test)

The initial DUBs screen and the validation indicated that *UCHL5* and *USP11* are necessary for an adequate hypoxic response. However, how these DUBs are activating the hypoxia-signalling pathway, the detailed molecular mechanisms and the target proteins involved needed to be investigated. Henceforth, the aim of my research project has been to characterize the molecular mechanism by which USP11 activates the hypoxia-signalling pathway.

2 USP11 is an activator of the hypoxia-signalling cascade.

2.1 USP11 induces HIF target genes

An additional siRNA sequence targeting *USP11* was used to confirm the activating role of this DUB towards the hypoxia signalling pathway. As expected, the hypoxic induction of three HIF target genes (*BNIP3*, *CA9* and *SLC2A1)* was significantly blocked silencing *USP11* with the two independent sequences (Figure R3).

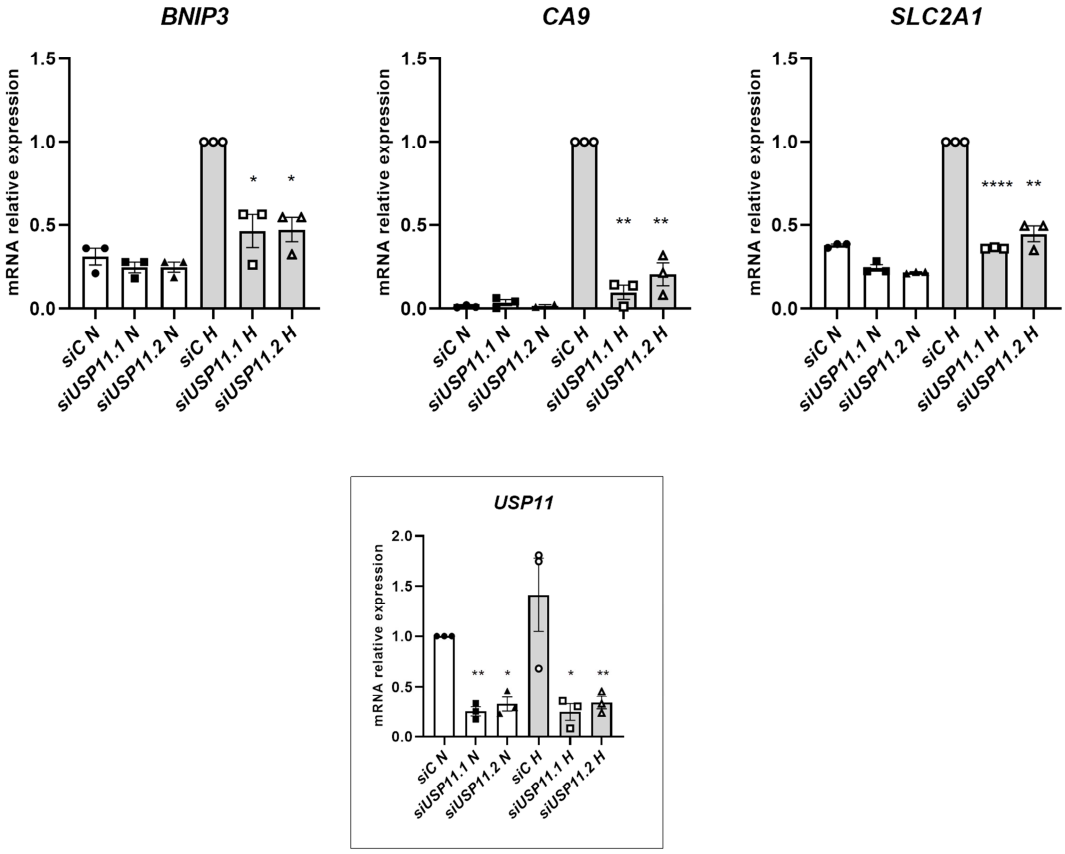

Figure R3: *BNIP3*, *CA9* and *SLC2A1* hypoxic induction is blocked upon *USP11* knockdown. HEK293 cells were transfected with *siC* (control), *siUSP11.1* or *siUSP11.2* during 48 hours. Then, after overnight normoxic (N; 20% O_2) or hypoxic (H; 1% O_2) incubation, mRNA levels were analysed by RT-qPCR. Results are normalized to *RPLP0* following $2^{-\Delta\Delta Ct}$ method and represented as relative values to hypoxic control cells in the case of the HIF target genes. Silencing efficacy is represented on the inset as relative values to normoxic control cells. Figure shows the values corresponding to average ± S.E.M. (*p<0,03, **p<0,0021, ****p<0,0001. One sample T-test)

2.2 *USP11 accumulates HIF-1α but not HIF-2α*

Our first attempt to decipher the molecular mechanisms underlying the activating role of USP11 on the hypoxia-driven signalling was to evaluate the status of the HIF transcription factors, which are the master regulators of the pathway. In that regard, our data clearly demonstrated that *USP11* silencing blocked the hypoxic accumulation of HIF-1α as well as its downstream target EGLN1/PHD2. This effect was indeed specific for the HIF-1α isoform, as HIF-2α protein levels appeared even increased (Figure R4).

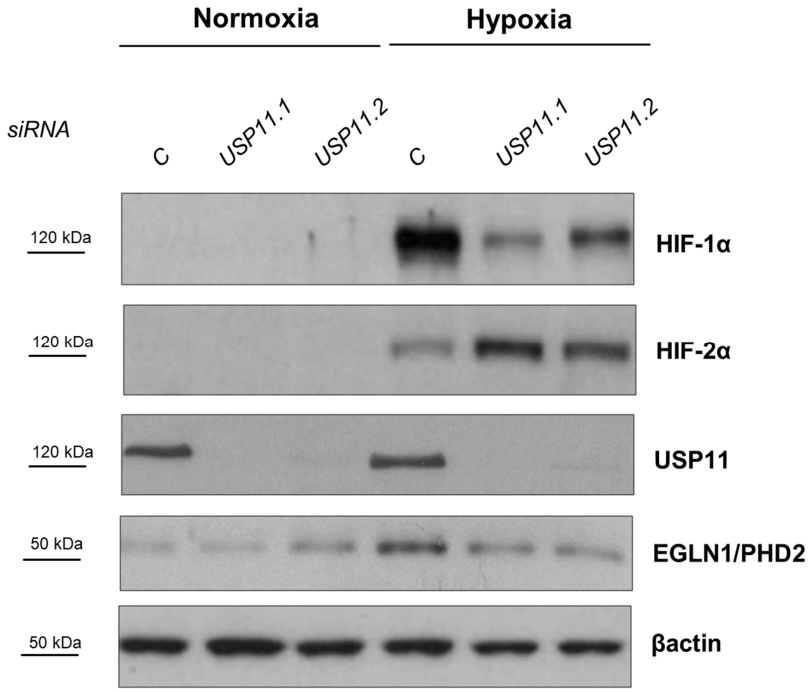

Figure R4: **USP11 knockdown specifically decreases HIF-1α hypoxic accumulation.** HEK293 cells were transfected with *siC* (control), *siUSP11.1* or *siUSP11.2* during 48 hours. After overnight normoxic (N; 20% O_2) or hypoxic (H; 1% O_2) incubation, cells were harvested and protein levels were analysed by western blot analysis using the indicated antibodies. β-actin was used as a loading control. This is a representative figure of at least three independent experiments.

HIF-dependent activation and HIF-1α regulation by USP11 seemed quite robust but had been only observed in HeLa and HEK293 cells so far. Thus, USP11 effect on the hypoxia signalling cascade was also studied in different cell lines, and in particular in melanoma and breast cancer cells. Indeed, USP11 expression was knockdown in MDA-MB-231 and A375 cells lines. There was a significant impairment on the hypoxic accumulation of HIF-1α as well as its downstream targets CA9 or EGLN1/PHD2 upon USP11 silencing in both, MDA-MB-231 and A375 cells (Figure R5).

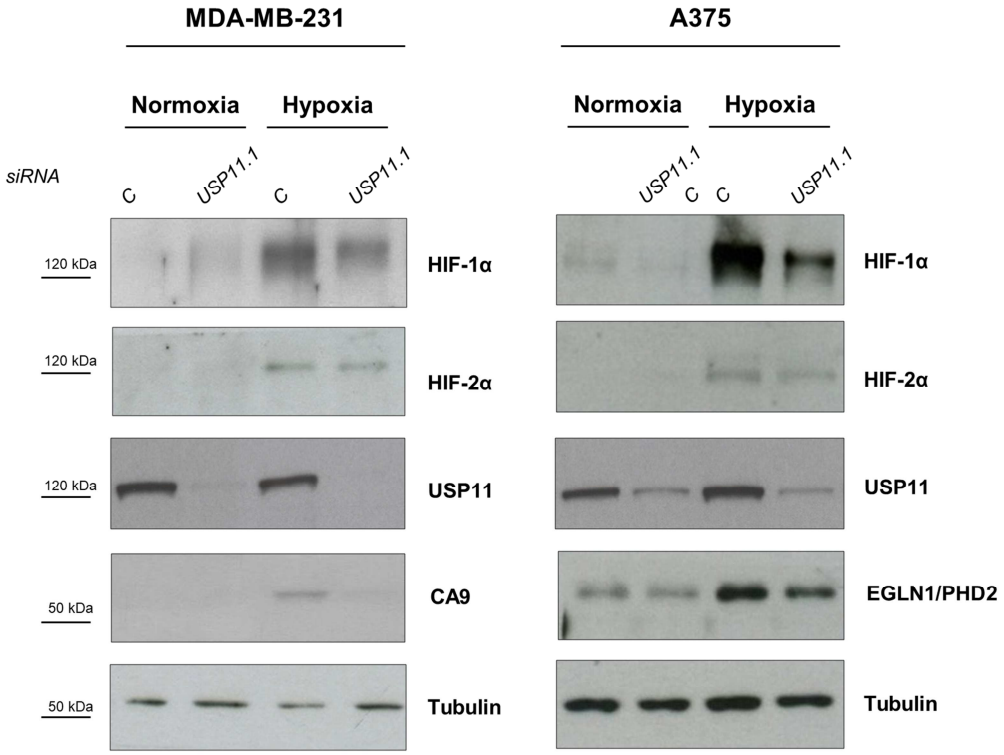

Figure R5: **USP11 knockdown specifically decreases HIF-1α hypoxic accumulation in MDA-MB-231 and A375 cells.** MDA-MB-231 and A375 cell lines were transfected with *siC* (control) or *siUSP11.1* during 48 hours. After overnight normoxic (N; 20% O_2) or hypoxic (H; 1% O_2) incubation, cells were collected and protein levels were analysed by western blot analysis using the indicated antibodies. Tubulin was used as a loading control. This is a representative figure of at least three independent experiments.

According to the results obtained at cellular level, the hypoxic induction of HIF-1 target genes mRNA was significantly decreased upon USP11 silencing in MDA-MB-231 and A375 cell lines (Figure R6A and B respectively).

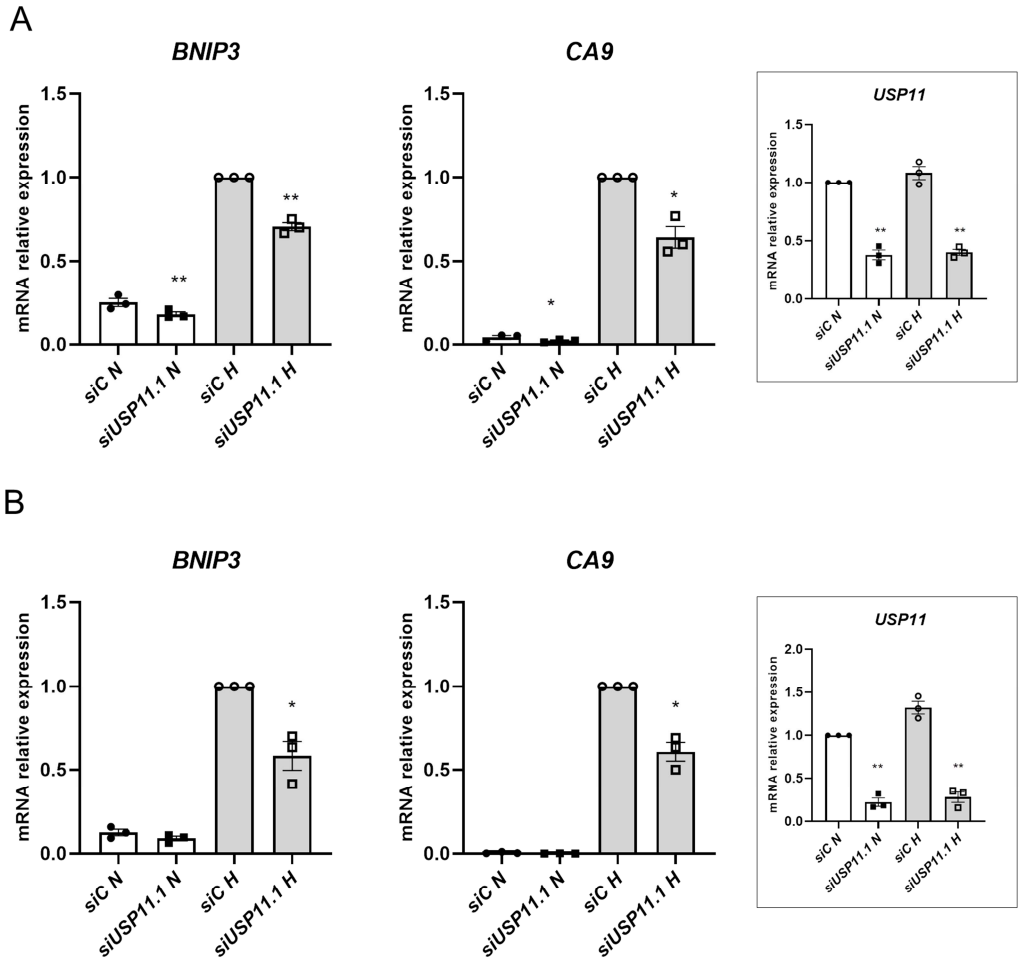

Figure R6: ***BNIP3* and *CA9* hypoxic induction is blocked upon *USP11* knockdown in MDA-MB-231 and A375 cells. A)** MDA-MB-231 and **B)** A375 cell lines were transfected with *siC* (control) or *siUSP11.1* during 48 hours. Then, after overnight normoxic (N; 20% O_2) or hypoxic (H; 1% O_2) incubation, mRNA levels were analysed by RT-qPCR. Results are normalized to *RPLP0* following $2^{-\Delta\Delta Ct}$ method and represented as relative values to hypoxic control cells in the case of the HIF target genes. Silencing efficacy is represented on the inset as relative values to normoxic control cells. Figure shows the values corresponding to average ± S.E.M.. (*p<0,03, **p<0,0021. One sample T-test)

2.3 Searching HIF-1 and HIF-2 specific target genes

The activating role of USP11 appeared to be exclusively mediated through HIF-1α. With the purpose of confirming these data, we analysed the impact of USP11 in the expression of HIF-1 and HIF-2 specific target genes in our cellular models following two different strategies.

For the first one, we based the analysis on data previously reported in the literature. Thus, we selected *LOX1* (He *et al*, 2015), *POU5F1* (Xu *et al*, 2012), *EPO* (Su *et al*, 2015), *SLC7A5* (Elorza *et al*, 2012) and *ANGPTL4* (Takano *et al*, 2014) *as* HIF-2 target genes along with *BNIP3* (Dhingra *et al*, 2014), *CA9* (Shafee *et al*, 2009) and *SLC2A1* (Joshi *et al*, 2014b), which are described to be HIF-1-dependent. To validate their selectivity, both HIF-1α and HIF-2α were independently knockdown in three cell lines: HEK293, MDA-MB-231 and A375. In our settings, the hypoxic induction of *BNIP3, CA9, SLC2A1* and *ANGPL4* was controlled by HIF-1 in HEK293 cells. However, both HIF isoforms mediated *LOX1* hypoxic induction whereas *POU5F1, EPO and SLC7A5* mRNAs were not induced in this model (Figure R7). In the context of the MDA-MB-231 cell line, *BNIP3, CA9, SLC2A1, LOX1* and *ANGPL4* mRNAs were induced upon hypoxia. Furthermore, HIF-1 mediated the induction of *BNIP3, CA9, SLC2A1* and *LOX1,* though the expression of *ANGPL4* appears to be independent of HIF-1 or HIF-2 (Figure R8). Regarding A375 cells, not only *BNIP3, CA9* and *SLC2A1* but also *EPO* and *ANGPTL4* hypoxic regulation was exclusively controlled by HIF-1. Surprisingly, hypoxia induced *SLC7A5* mRNA independently of HIF isoforms and the expression of *LOX1* and *POU5F1* was not regulated by hypoxia in this cell line (Figure R9)

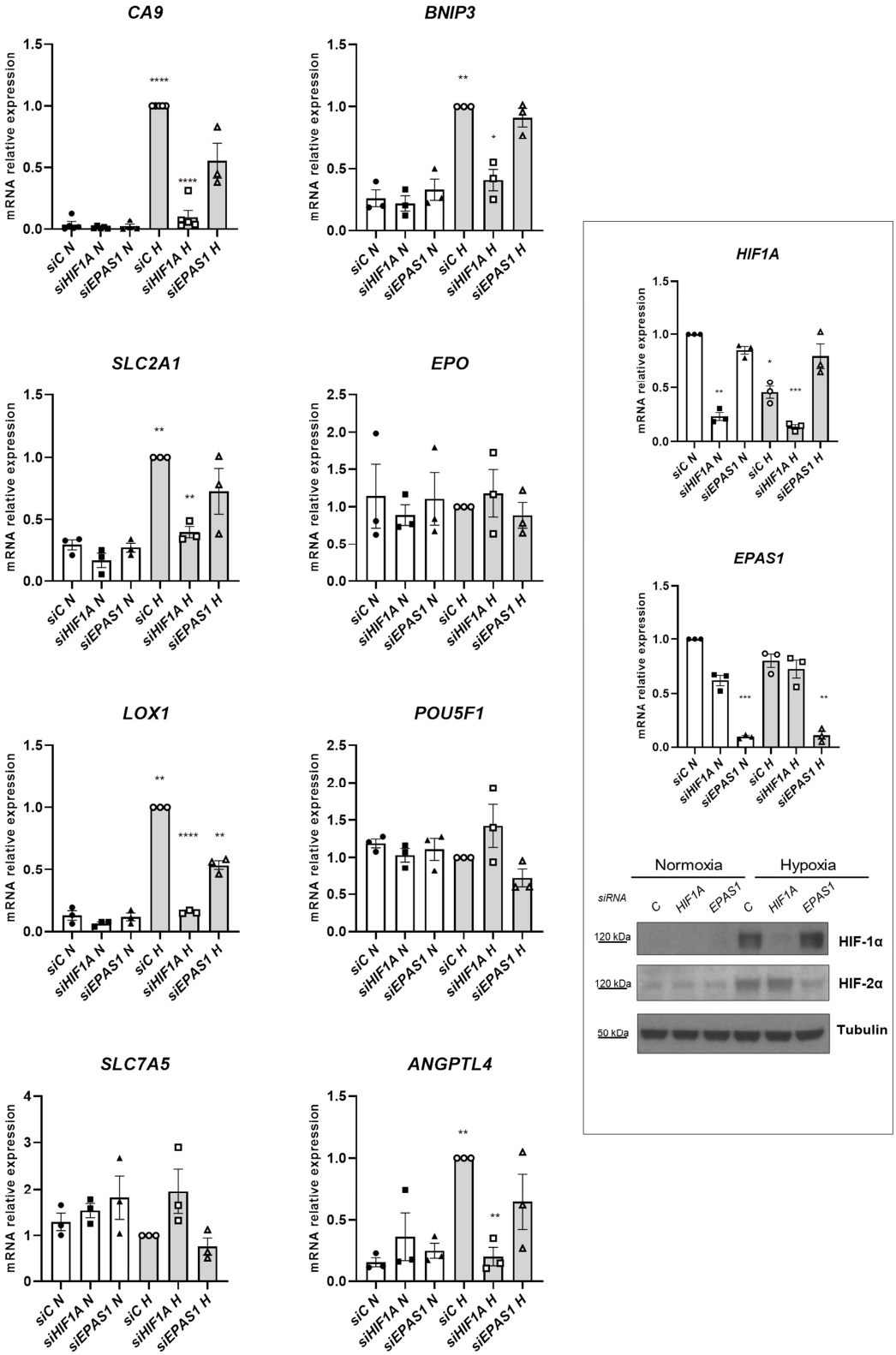

Figure R7: Looking for HIF-1- and HIF-2-dependent genes in HEK293 cells. HEK293 cells were transfected with *siC* (control), *siHIF1A* or *siEPAS1* during 48 hours. Then, after overnight normoxic (N; 20% O_2) or hypoxic (H; 1% O_2) incubation, mRNA and protein levels were harvested and analysed by RT-qPCR and WB, respectively. Results are normalized to *RPLP0* following $2^{-\Delta\Delta Ct}$ method and represented as relative values to hypoxic control cells. Silencing efficacy, by RT-qPCR and WB, is represented on the right inset. Figure shows the values corresponding to average ± s.e.m. (*p<0,03, **p<0,0021, ***p<0,0002, ****p<0,0001. One sample T-test)

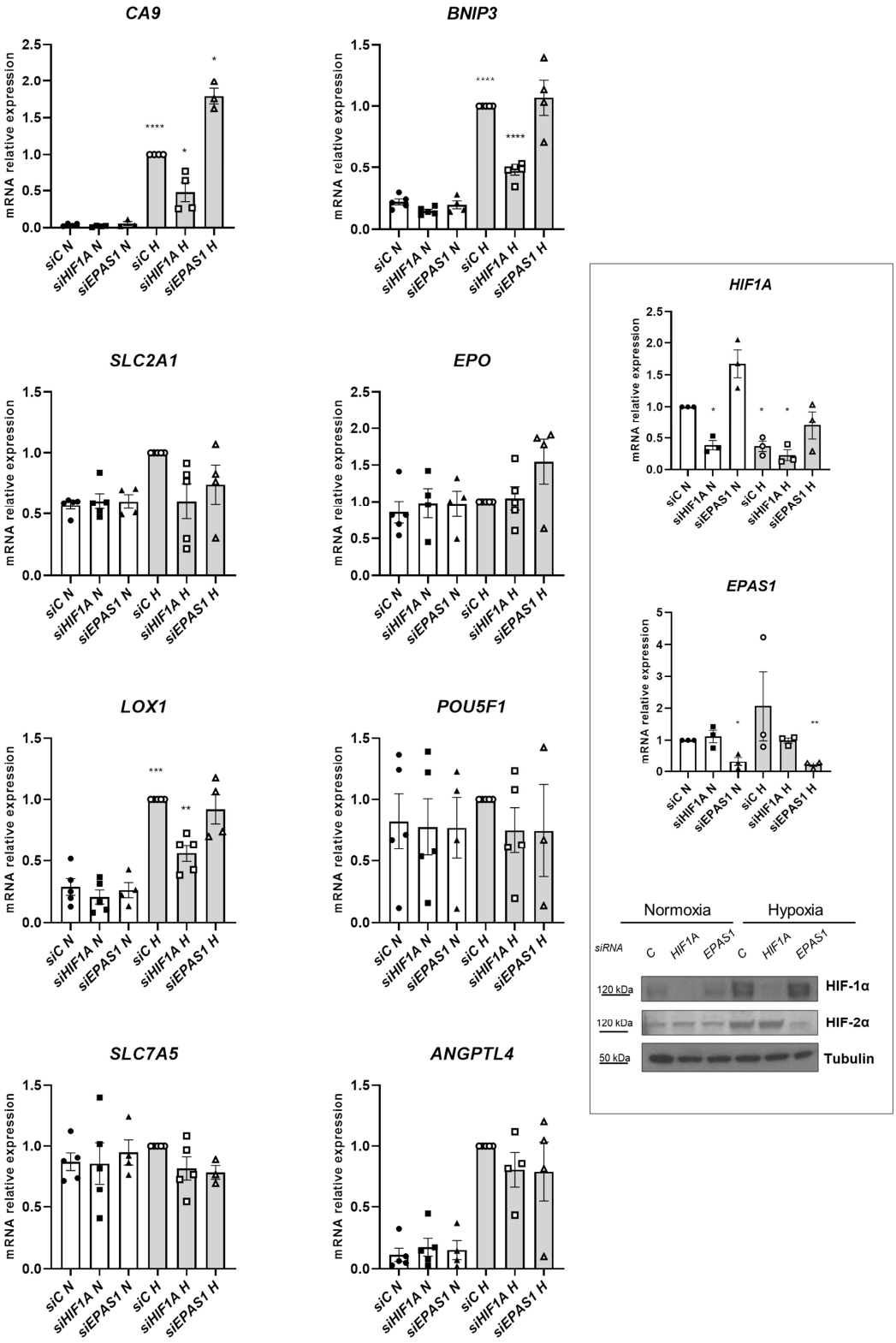

Figure R8: Looking for HIF-1- and HIF-2-dependent genes on MDA-MB-231 cells. MDA-MB-231 cells were transfected with *siC* (control), *siHIF1A* or *siEPAS1* during 48 hours. Then, after overnight normoxic (N; 20% O_2) or hypoxic (H; 1% O_2) incubation, mRNA and protein levels were analysed by RT-qPCR and WB, respectively. Results are normalized to *RPLP0* following $2^{-\Delta\Delta Ct}$ method and represented as relative values to hypoxic control cells. Silencing efficacy, by RT-qPCR and WB, is represented on the right inset. Figure shows the values corresponding to average ± s.e.m (*p<0,03, **p<0,0021, ***p<0,0002 ****p<0,0001. One sample T-test)

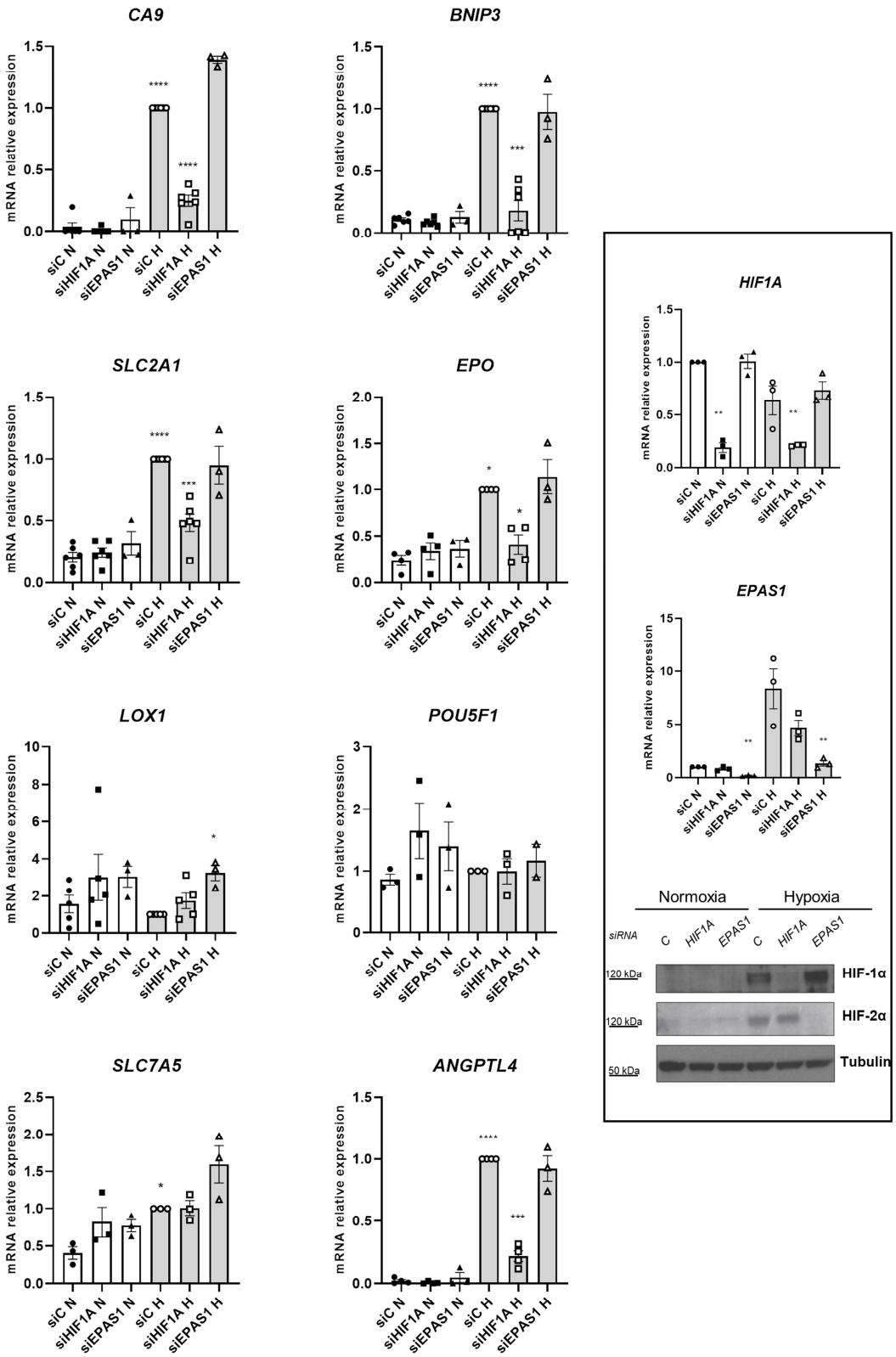

Figure R8: Looking for HIF-1- and HIF-2-dependent genes in A375 cells. A375 cells were transfected with *siC* (control), *siHIF1A* or *siEPAS1* during 48 hours. Then, after overnight normoxic (N; 20% O_2) or hypoxic (H; 1% O_2) incubation, mRNA and protein levels were analysed by RT-qPCR and WB, respectively. Results are normalized to *RPLP0* following $2^{-\Delta\Delta Ct}$ method and represented as relative values to hypoxic control cells. Silencing efficacy, by RT-qPCR and WB, is represented on the right inset. Figure shows the values corresponding to average ± s.e.m (*p<0,03, **p<0,0021, ***p<0,0002, ****p<0,0001. One sample T-test)

The second strategy benefits from *Cancertool*, a bioinformatic tool to study gene expression correlations (Cortazar *et al*, 2018). We searched for genes that were positively correlated with *EPAS1* but not *HIF1A* mRNA in breast cancer patient's datasets. We selected *MEF2C* (*Myocyte-specific enhancer factor 2C*), *TXNIP* (Thioredoxin-interacting protein), *PPAP2B (PLPP3* (Phospholipid phosphatase 3)), *GSN* (Gelsolin), *GPR116 (ADGRF5* (Adhesion G protein-coupled receptor F5)*), AKAP12* (A-kinase anchor protein 12), *PDGFRB* (Platelet-derived growth factor receptor beta), *PCOLCE* (Procollagen C-endopeptidase enhancer 1) and *COL18A1* (Collagen alpha-1(XVIII) chain), which were positively and consistently correlated with *EPAS1* mRNA levels in at least 4 of the 6 different Breast cancer (BCa) databases included in *Cancertool* (Table R1 and Figure R10).

Table R1: BCa databases of Cancertool.

BCa databases of Cancertool					
Cancer Study	*Reference*	*GEO*	*Platform*	*Contains*	*Cohort size*
Ivshina et al.	*PMID: 17079448*	*GSE4922*	*Affx HG-U133A, Affx HG-U133B*	*mRNA, LINCs*	*249*
Lu et al.	*PMID: 18297396*	*GSE5460*	*Affx HG-U133_Plus_2*	*mRNA, cds, LINCs*	*131*
METABRIC	*PMID: 22522925*	*EGAS00000000098*	*Illumina HumanHT-12 v3*	*mRNA, LINCs*	*1980*
Pawitan et al.	*PMID: 16280042*	*GSE1456*	*Affx HG-U133A, Affx HG-U133B*	*mRNA, LINCs*	*159*
TCGA	*raw data at TCGA*	*GSE62944*	*Agilent G450A_07 array*	*mRNA, LINCs*	*522*
Wang et al.	*PMID: 15721472*	*GSE2034*	*Affx HG-U133A*	*mRNA, LINCs*	*286*

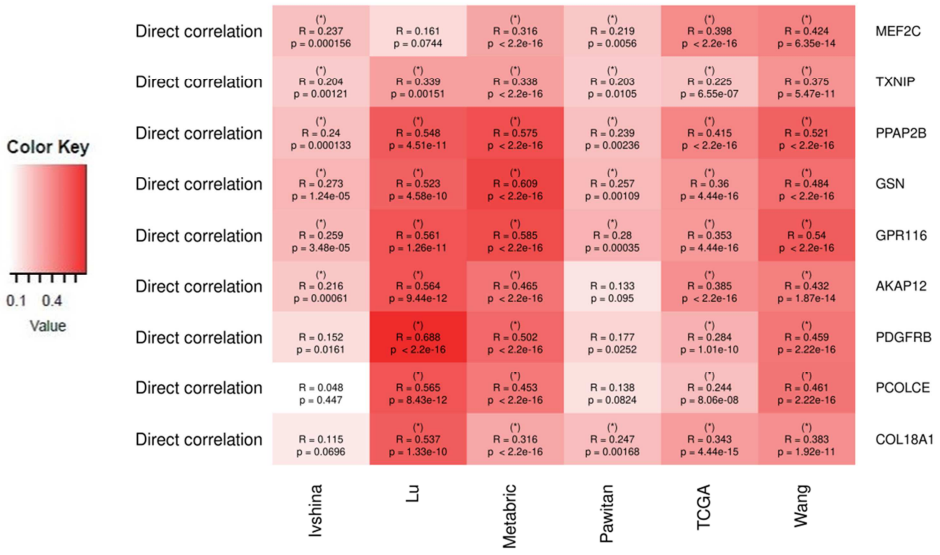

Figure R10: Genes that positively correlated with *EPAS1* mRNA levels. Pearson correlations of the genes that strongly positively correlated with *EPAS1* mRNA levels using Cancertool BCa databases.

As an example, Figure R10 summarizes the graphics for *PDGFRB* correlation with *EPAS1* and *HIF1A* as depicted in *Cancertool* (Figure R11).

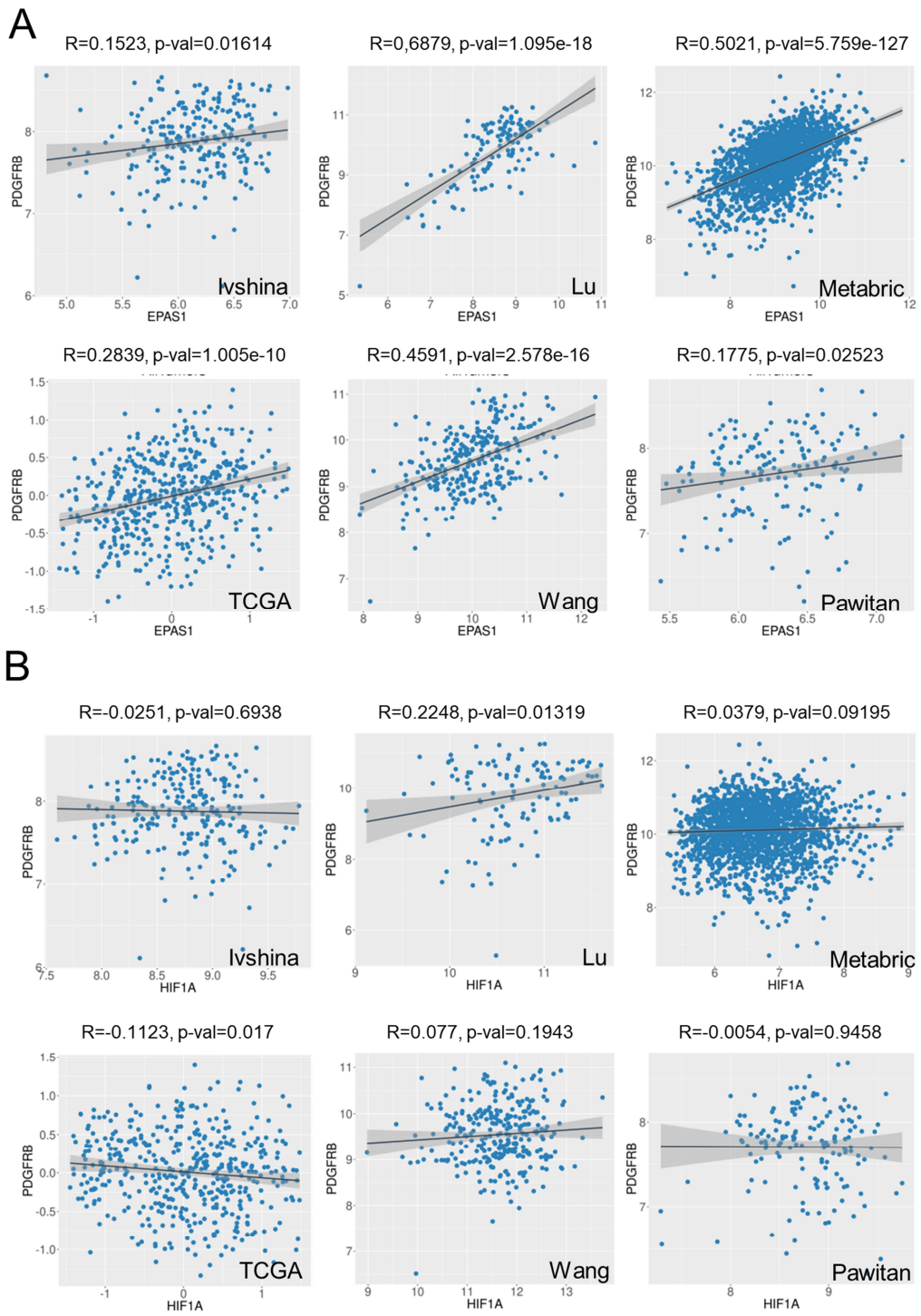

Figure R11: *PDGFRB* correlates with *EPAS1* but not with *HIF1A*. Graphical repressentation of *PDGFRB* correlation with *EPAS1* (a) and *HIF1A* (B) mRNAs.

Then, the hypoxic induction of these genes was assessed in control or *HIF1A*/*EPAS1* silenced HEK293 and MDA-MB-231 cells. After analysing the mRNA levels in that context, we excluded any hypoxic induction in the expression of the above-mentioned genes except for *PCOLCE* mRNA, which was significantly induced by hypoxia in MDA-MB-231 cells. However, the hypoxic induction of *PCOLCE* was regulated neither by HIF-1 nor by HIF-2 (Figure R12).

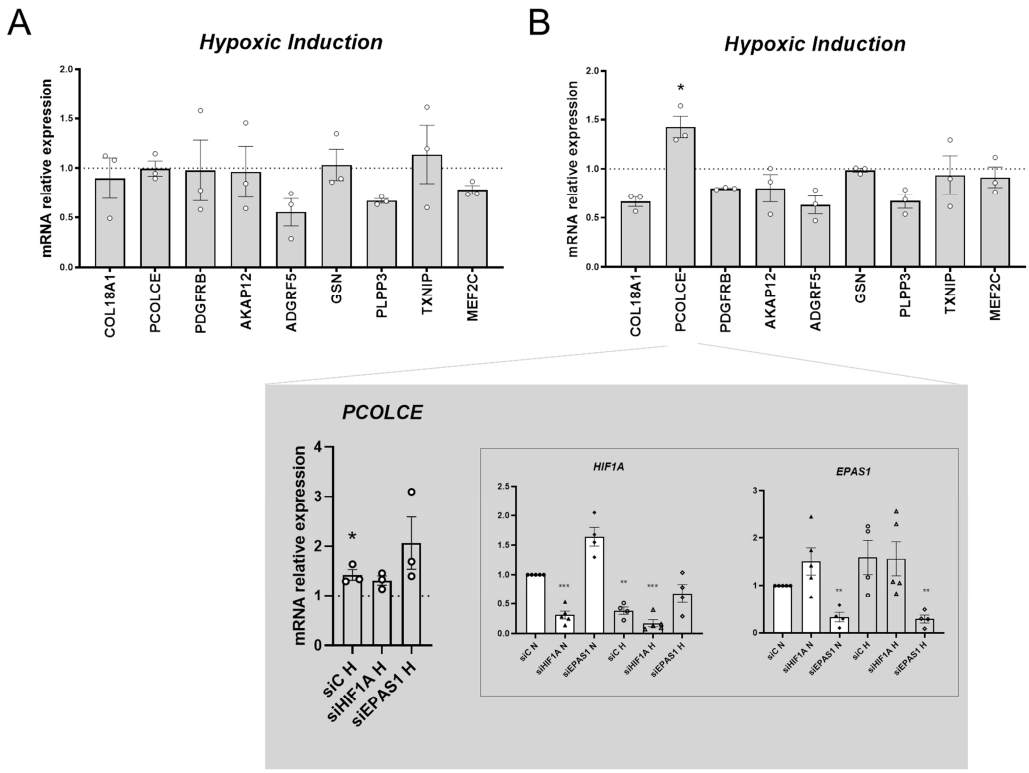

Figure R12: Hypoxic regulation of genes whose expression positively and exclusively correlates with *EPAS1* in breast cancer tumor patients. A) Hypoxic induction of the indicated genes in HEK293 cell line **B)** Hypoxic induction of the indicated genes in MDA-MB-231 cell line. MDA-MB-231 cells were transfected with *siC* (control), *siHIF1A* or *siEPAS1* during 48 hours. After overnight normoxic (N; 20% O_2) or hypoxic (H; 1%O_2) incubation, mRNA levels were analysed by RT-qPCR. Results are normalized to *RPLP0* following $2^{-\Delta\Delta Ct}$ method and represented as relative values to normoxic control cells. Silencing efficacy of is represented on the inset. Figure shows the values corresponding to average ± sS.E.M.. (*p<0,03, **p<0,0021, ***p<0,0002. One sample T-test)

2.4 Mitoxantrone inhibits HIF-1α accumulation

The significant decrease on hypoxia-induced target genes expression and HIF-1α hypoxic accumulation triggered by *USP11* silencing opens a novel and promising target to modulate the hypoxia-signalling pathway. We therefore used Mitoxantrone, a FDA-approved drug previously described as an USP11 pharmacological inhibitor (Burkhart *et al*, 2013). Cells were treated with 1µM of Mitoxantrone for 24 hour, and as a result, Mitoxantrone blocked the hypoxic induction of HIF-1α without affecting USP11 protein levels significantly (Figure R13 A). Accordingly, Mitoxantrone also blocked the hypoxic induction of HIF-1 target genes *BNIP3* and *SLC2A1*, but not *CA9* (Figure R13 B).

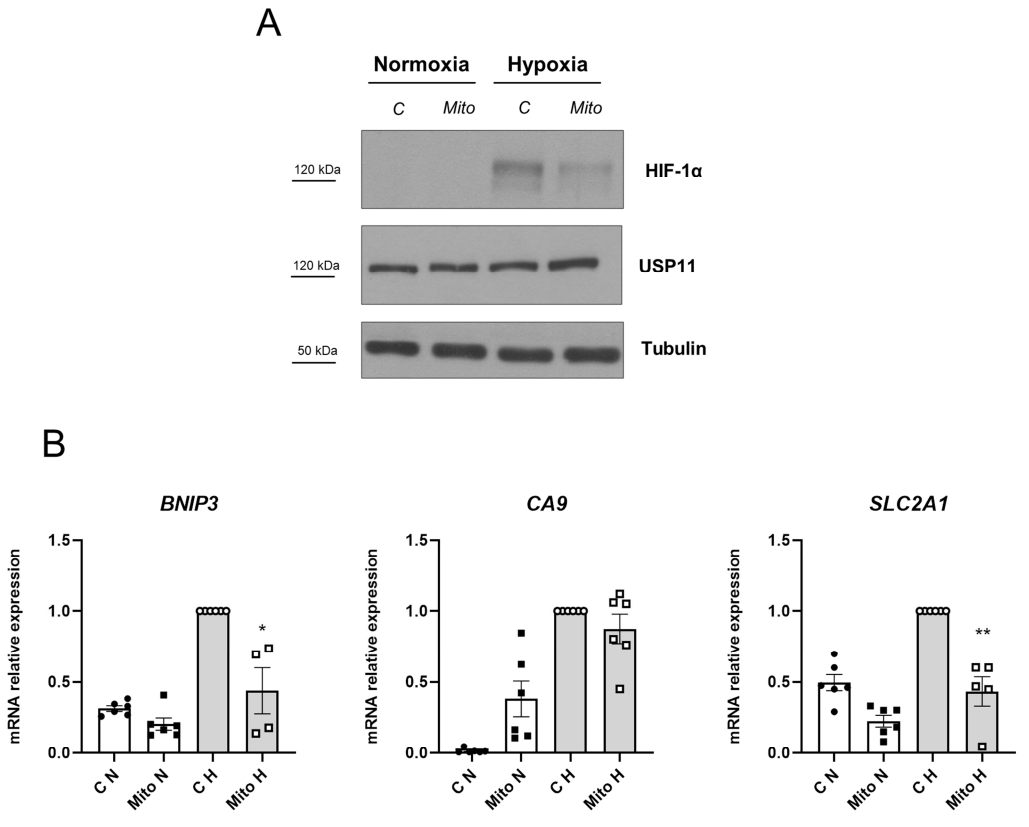

Figure R13: Effect of Mitoxantrone treatment on hypoxia signalling pathway. HEK293 cells were treated with 1uM of Mitoxantrone (Mito) for 24 hours and incubated in normoxia (N; 20% O_2) or hypoxia (H; 1% O_2) during 2 hours before protein collection or overnight before mRNA collection. **A)** Total protein extracts were analysed by western blot using the indicated antibodies. Tubulin was used as a loading control. This is a representative figure of at least three independent experiments. **B)** Total mRNA levels were analysed by RT-qPCR. Results are normalized to *RPLP0* following $2^{-\Delta\Delta Ct}$ method and represented as relative values to hypoxic control cells . Figure shows the values corresponding to average ± S.E.M. (*p<0,03, **p<0,0021. One sample T-test)

Mitoxantrone inhibitory role on the hypoxia signalling cascade was also tested on MDA-MB-231 cells. In this model, only 0.5µM of Mitoxantrone treatment was sufficient to nicely impeded HIF-1α hypoxic accumulation. At the same time a significant decrease of the hypoxic induction of HIF-1 target genes *BNIP3*, *CA9* and *LOX1* was observed (Figure R14).

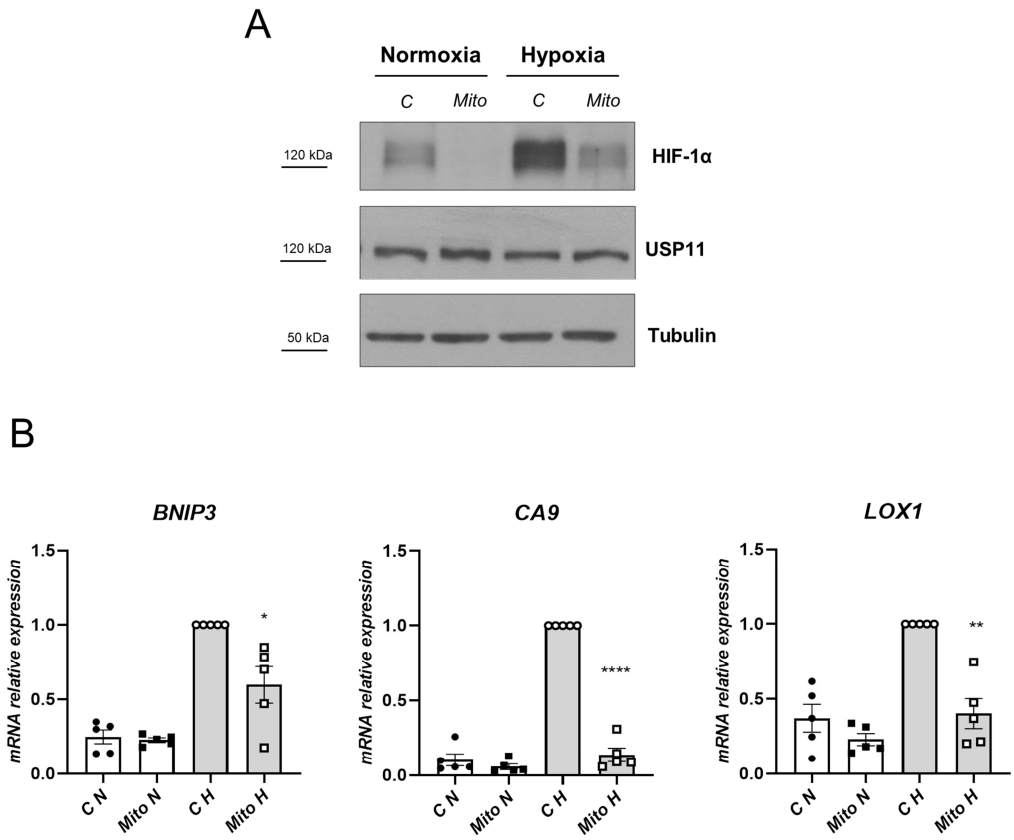

Figure R14: Effect of Mitoxantrone treatment on hypoxia signalling pathway in MDA-MB-231 cell line. MDA-MB-231 cells were treated with 0,5uM of Mitoxantrone (Mito) for 24 hours and incubated in normoxia (N; 20% O_2) or hypoxia (H; 1% O_2) during 2 hours before protein collection or overnight before mRNA collection. **A)** Total protein extracts were analysed by western blot using the indicated antibodies. Tubulin was used as a loading control. This is a representative figure of at least three independent experiments. **B)** Total mRNA levels were analysed by RT-qPCR. Results are normalized to *RPLP0* following $2^{-\Delta\Delta Ct}$ method and represented as relative values to hypoxic control cells . Figure shows the values corresponding to average ± S.E.M. (*p<0,03, **p<0,0021, ****p<0,0001. One sample T-test)

3 HIF1α regulation by USP11

3.1 USP11 controls HIF1A mRNA

Although the analysis was initially proposed as a control, we realized that *USP11* knockdown reduced not only hypoxia-induced accumulation of HIF-1α but also *HIF1A* mRNA levels in both, normoxic and hypoxic conditions. This decrease, again, resulted specific of *HIF1A* isoform as the levels of *EPAS1* mRNA were even increased (Figure R15 A). Moreover, pharmacological inhibition of USP11 with Mitoxantrone also results in a significant decrease of *HIF1A* specifically in conditions, normoxia and hypoxia (Figure R15 B).

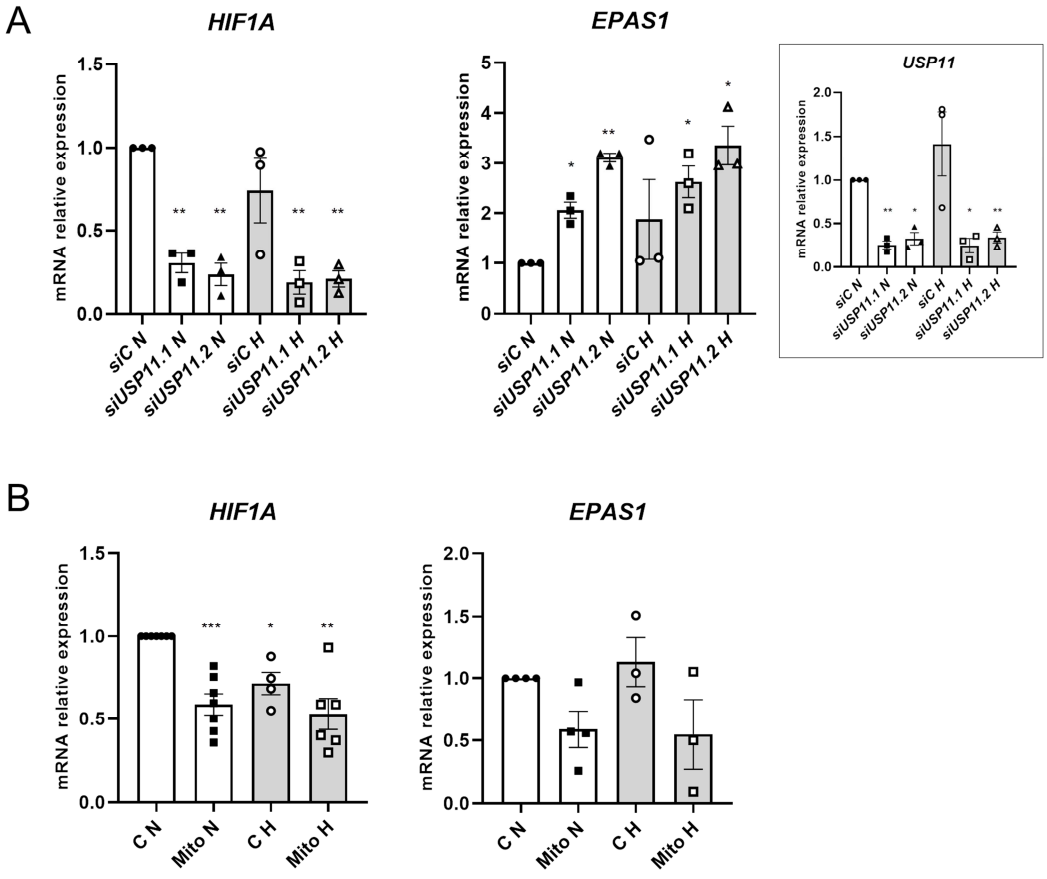

Figure R15: *USP11* repression specifically decreases *HIF1A* mRNA. A) HEK293 cells were transfected with *siC* (control), *siUSP11.1* or *siUSP11.2* during 48 hours. After overnight normoxic (N; 20% O_2) or hypoxic (H; 1% O_2) incubation, mRNA was collected. **B)** HEK293 cells were treated with 1uM of Mitoxantrone (Mito) for 24 hours and incubated in normoxia (N; 20% O_2) or hypoxia (H; 1% O_2) overnight before mRNA collection. Levels of mRNA were analysed by RT-qPCR. Results are normalized to *RPLP0* following $2^{-\Delta\Delta Ct}$ method and represented as relative values to normoxic control cells. Silencing efficacy is represented on the right inset. Figure shows the values corresponding to average ± S.E.M. (*p<0,03, **p<0,002, ***p<0,0002. One sample T-test)

3.2 *USP11 and HIF1A mRNA transcriptional regulation*

Based on our previous data, *HIF1A* mRNA regulation seemed to be the target of USP11-mediated regulation. Therefore, the next question to tackle was whether USP11 was controlling *HIF1A* transcription. We first used a luciferase reporter construct driven by the *HIF1A* promoter (Minet *et al*, 1999) to analyse its activity in a *USP11* knockdown context. However, when *USP11* was down regulated, the *HIF1A* promoter-triggered luciferase activity was not reduced and even significantly increased, which is the opposite outcome we expected (Figure R16 A). In addition, these results were confirmed by measuring the levels of *HIF1A* pre-mRNA (Figure R16 B).

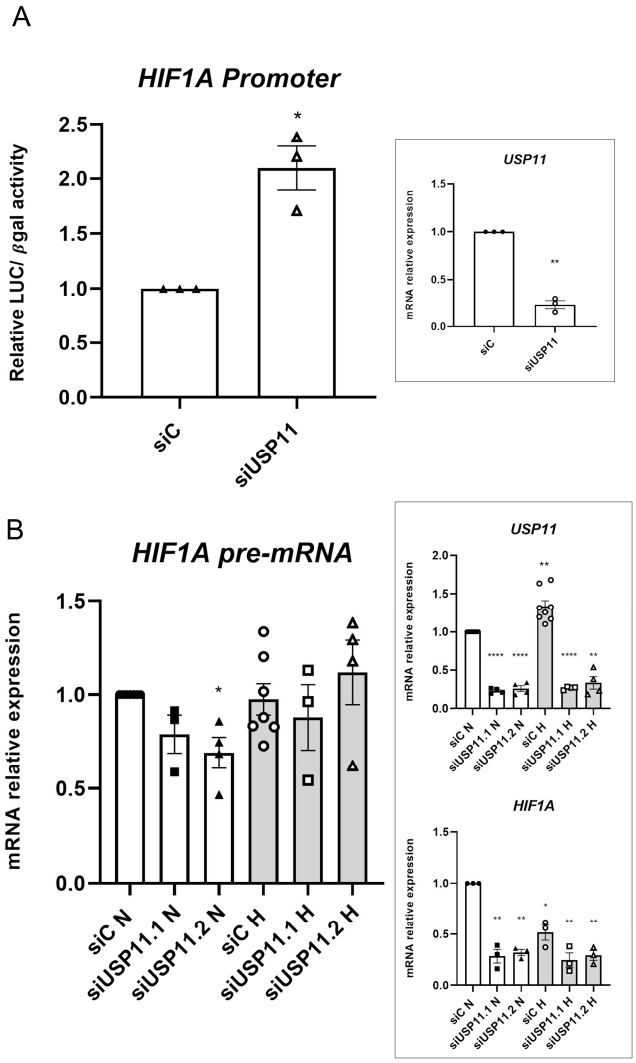

Figure R16. Effect of *USP11* knockdown on *HIF1A* transcription. A) HEK293 cells were transfected with *siC* (control) or *siUSP11* during 24 hours before transfecting *HIF1A*prom-LUC and CMV-βgal. After additional 24 hours, luciferase activity was meassured and normalized to β-galactosidase activity. Results are represented as relative values to control cells. **B)** HEK293 cells were transfected with *siC* (control), *siUSP11.1* or *siUSP11.2* during 48 hours. After overnight normoxic (N; 20% O_2) or hypoxic (H; 1% O_2) incubation, mRNA levels were analysed by RT-qPCR. Results are normalized to *RPLP0* following the $2^{-\Delta\Delta Ct}$ method and represented as relative values to normoxic control. The right insets shows *USP11* silencing efficacy and *HIF1A* mature transcript levels. Figure shows the values corresponding to average ± s.e.m (*p<0,03, **p<0,0021, ****p<0,0001. One sample T-test)

3.3 *USP11 and HIF1A mRNA stability*

Once the impact of USP11 on *HIF1A* mRNA transcription was discarded as the major mechanism regulating USP11-mediated decrease of *HIF1A*, we aim to study *HIF1A* mRNA posttranscriptional regulation. As a key element of such mRNA regulation, we focused on the 3'UTR. Thus, using a luciferase reporter construct fused to the 3'UTR region of *HIF1A* mRNA (Chamboredon *et al*, 2011b), we were able to detect a decrease in the luciferase activity when *USP11* was knocked down (Figure R17).

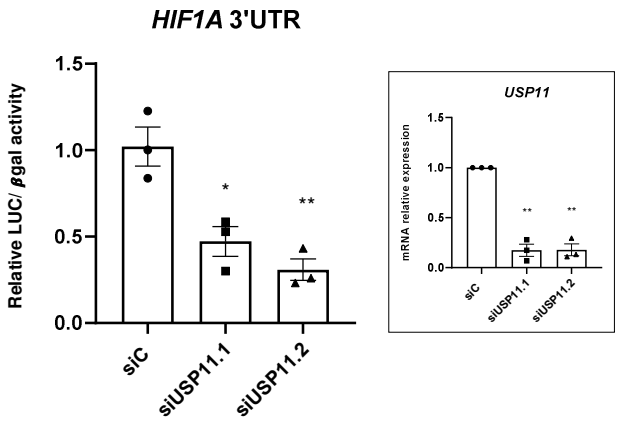

Figure R17: USP11 silencing decreases the luciferase activity of the *HIF1A* 3'UTR reporter construct. HEK293 cells were silenced with *siC* (control), *siUSP11.1* or *siUSP11.2* during 24 hours before transfecting LUC-*HIF1A* 3'UTR and CMV-βgal. After additional 24 hours, luciferase activity was meassured and normalized to β-galactosidasa activity. Results are represented as relative values to control cells. On the right inset, *USP11* silencing efficacy was assessed by RT-qPCR. Figure shows the values corresponding to average ± S.E.M. (*p<0,03, **p<0,0021,. One sample T-test)

According to these data, the impact of *USP11* silencing on the ectopic expression of a HIF-1α construct, which contained the full-length coding sequence but lack the regulatory 3' UTR (Myc-HIF-1α), was almost negligible (Figure R18).

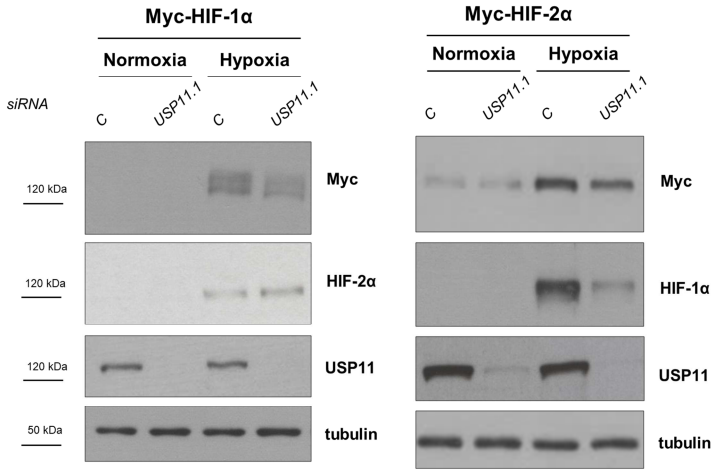

Figure R18. USP11 knockdown does not affect HIF-1α at protein level. HEK293 cells were silenced with *siC* (control) or *siUSP11* during 24 hours before transfecting Myc-HIF-1α or Myc-HIF-2α for additional 24 hours. After that, cells were incubated either in (N; 20% O_2) or hypoxia (H; 1% O_2) overnight before harvesting. Total protein extracts were analysed by western blot using the indicated antibodies. Tubulin was used as a loading control. This is a representative figure of at least three independent experiments.

RNA biology often links 3'UTR regulation to mRNA stability. Therefore, the half-life of *HIF1A* mRNA was analysed after transcription blockade with Actinomycin D. Interestingly, a significant decrease in the *HIF1A* half-life was detected upon *USP11* knockdown (Figure R19). Similar results were obtained using DRB (5,6-Dichlorobenzimidazole 1-β-D-ribofuranoside) as an inhibitor of transcription (data not shown).

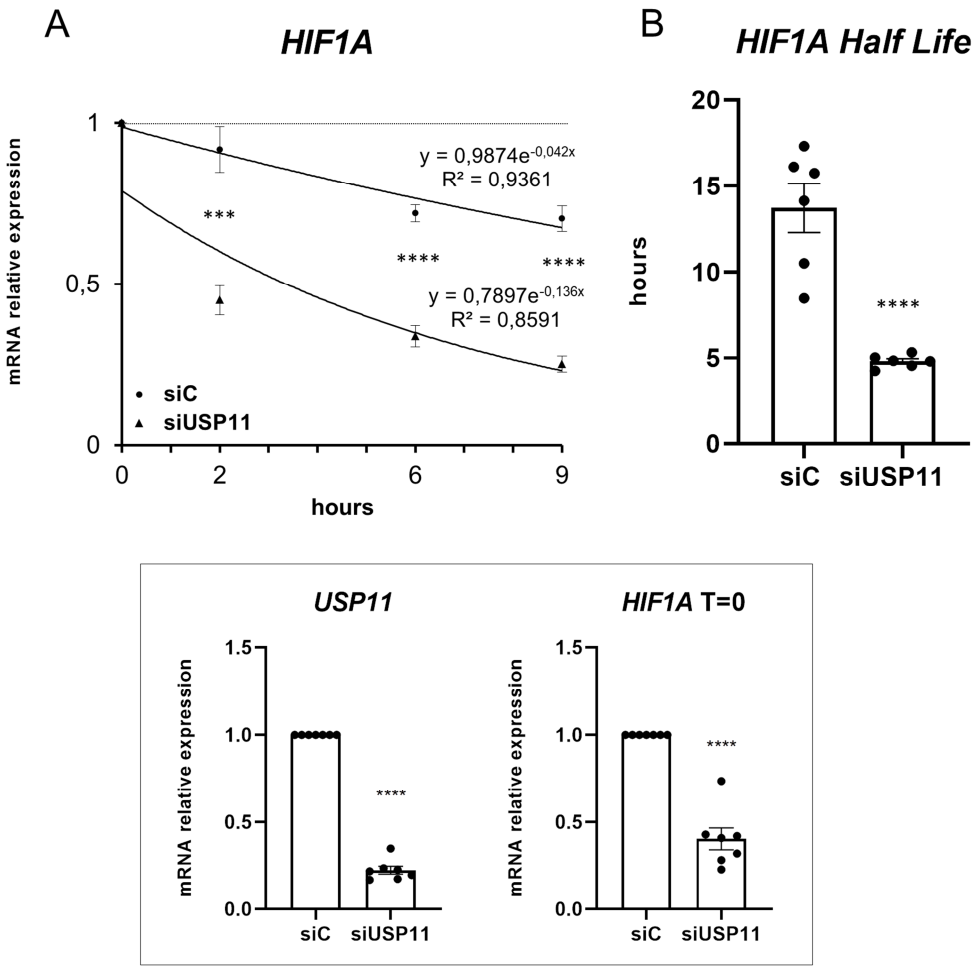

Figure R19*: USP11 regulates HIF1A* mRNA stability. A) *HIF1A decay* and **B)** derived *HIF1A* mRNA half life. HEK293 cells were transfected with *siC* (control) or *siUSP11*, incubated 48 hours in normoxia and then treated with Actinomycin D (5mg/ml) before collecting them after 0, 2, 6 and 9 hours. Total mRNA cell extracts were analysed by RT-qPCR. Results are normalized to *RPLP0* following the $2^{-\Delta\Delta Ct}$ method and represented as relative values to time 0 of each condition. The bottom inset corresponds to the silencing efficacy and the *HIF1A* mRNA levels at time 0. Figure shows the values corresponding to average ± S.E.M. (***p<0,002, ****p<0,0001. One sample T-test)

3.4 The impact of USP11 in HIF1A mRNA stability in MDA-MB-231

The results obtained so far pointing to a posttranscriptional regulation of *HIF1A* by USP11 on HEK293 cells. Similarly, *HIF1A* mRNA levels decreased when *USP11* was silenced or inhibited with Mitoxantrone treatment in MDA-MB-231 cells (Figure R20).

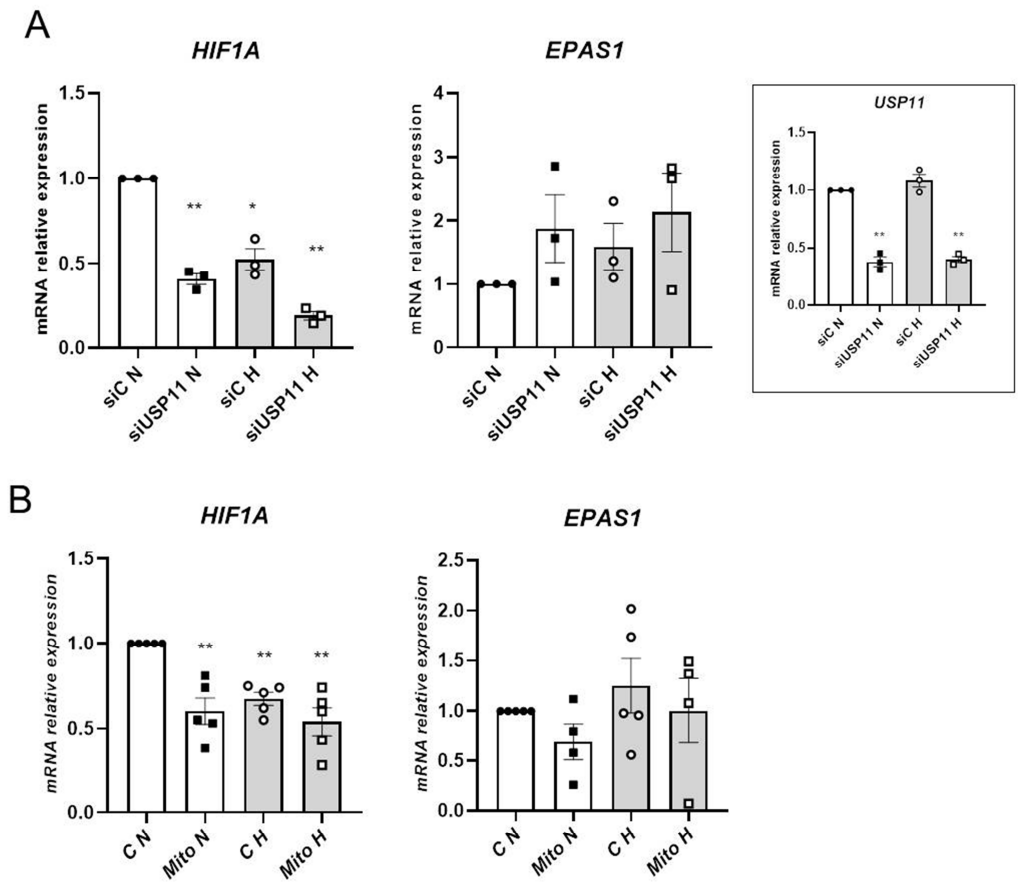

Figure R20: *USP11* repression specifically decreases *HIF1A* mRNA in MDA-MB-231. A) MDA-MB-231 cells were transfected with *siC* (control) or *siUSP11.1* during 48 hours and incubated in normoxia (N; 20% O_2) or hypoxia (H; 1% O_2) overnight before mRNA collection and mRNA analysis by RT-qPCR. **B)** MDA-MB-231 cells were treated with 0,5 uM of Mitoxantrone for 24 hours and incubated in normoxia (N; 20% O_2) or hypoxia (H; 1% O_2) overnight before mRNA collection and mRNA analysis by RT-qPCR. Results are normalized to *RPLP0* following $2^{-\Delta\Delta Ct}$ method and represented as relative values to normoxic control cells. Silencing efficacy is represented on the right inset. Figure shows the values corresponding to average ± S.E.M. (*p<0,03, **p<0,002. One sample T-test)

Furthermore, as expected, the luciferase-reporter gene activity driven by the *HIF1A* promoter did not change in *USP11* knockdown cells (Figure R21 A). On the contrary, silencing of *USP11* significantly decreased the *HIF1A* 3'UTR-

driven luciferase reporter gene activity (Figure R21 B) and *HIF1A* mRNA half-life decreased upon *USP11* silencing (Figure R21 C).

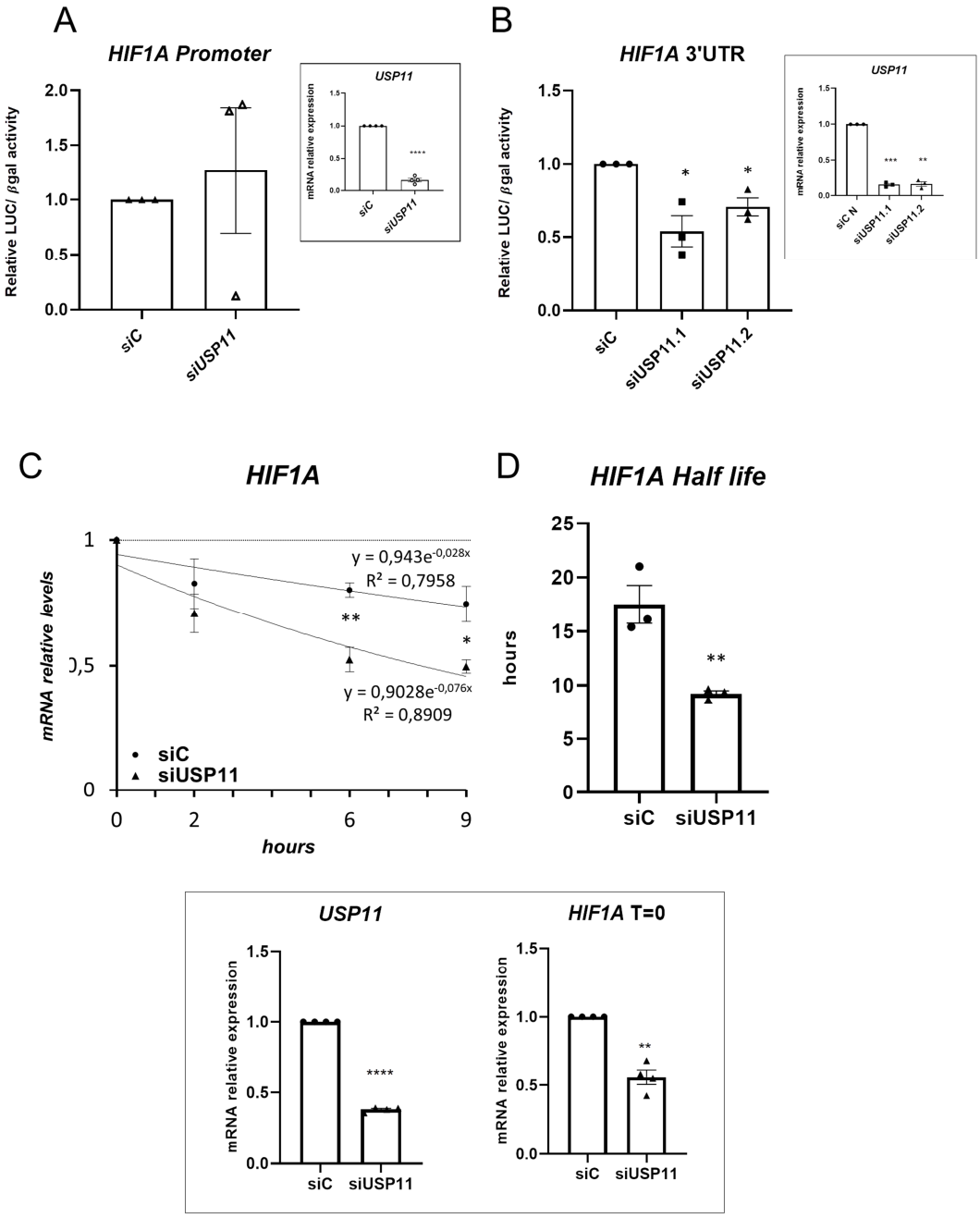

Figure R21. **USP11 regulates *HIF1A* half-life in MDA-MB-231 cells. A)** MDA-MB-231 cells were transfected with *siC* (control) or *siUSP11* during 24 hours before transfecting HIF1A prom-LUC and CMV-βgal. After additional 24 hours, luciferase activity was meassured and normalized to β-galactosidase activity. Results are represented as relative values to control cells. **B)** MDA-MB-231 cells were silenced with *siC* (control), *siUSP11.1* or *siUSP11.2* during 24 hours before transfecting LUC-*HIF1A* 3'UTR and CMV-βgal. After additional 24 hours, luciferase activity was meassured and normalized to β-galactosidase activity. Results are represented as relative values to control cells. **C)** *HIF1A decay* and **D)** derived *HIF1A* mRNA half life. MDA-MB-231 cells were transfected with *siC* (control) or *siUSP11*, incubated 48 hours in normoxia and then treated with Actinomycin D (5mg/ml) before collecting them after 0, 2, 6 and 9 hours. mRNA cell extracts were analysed by RT-qPCR. Results are normalized to *RPLP0* following the $2^{-\Delta\Delta Ct}$ method and represented as relative values to time 0 of each condition. Insets shows the silencing efficacy as well as *HIF1A* mRNA levels at time 0. Figure shows the values corresponding to average ± S.E.M.. (*p<0,03, **p<0,0021, ***p<0,0002, ****p<0,0001. One sample T-test)

3.5 Searching for the ribonucleoprotein complex that controls HIF1A mRNA stability

In view of the above-mentioned results, we wondered how USP11 was regulating HIF1A mRNA stability. Our first approach was focused on *aHIF,* which is a natural antisense mRNA reported to bind the 3'UTR of *HIF1A* and to down regulate its expression (Rossignol *et al*, 2002). Furthermore, the expression of *aHIF* has been shown to be increased under hypoxia due to the presence of putative hypoxia response elements in its promoter. However, *USP11* knockdown did not significantly alter *a HIF* expression (Figure R22).

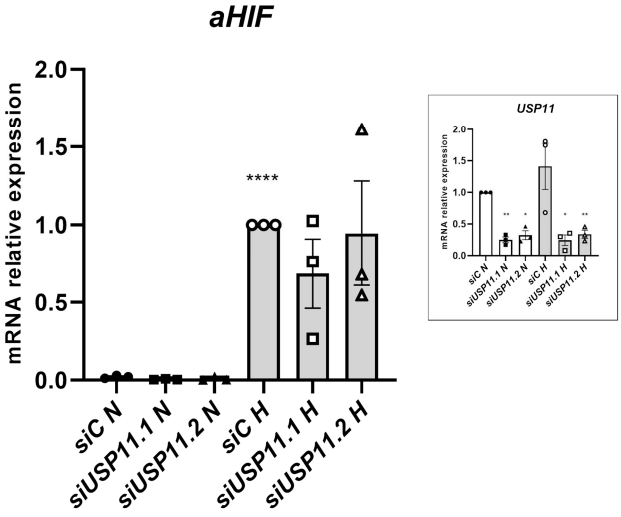

Figure R22: ***USP11* knockdown does not alter *aHIF* expression.** HEK293 cells were transfected with *siC* (control), *siUSP11.1* or *siUSP11.2* during 48 hours. Then, after overnight normoxic (N; 20% O_2) or hypoxic (H; 1% O_2) incubation, mRNA levels were analysed by RT-qPCR. Results were normalized to *RPLP0* following the $2^{-\Delta\Delta Ct}$ method, and represented as relative values to control cells in hypoxia. The right inset correspond to the silencing efficacy. Figure shows the values corresponding to average ± S.E.M.. (*p<0,03, **p<0,0021, ****p<0,0001. One sample T-test)

HIF1A regulators previously described in the literature concentrated our next attempt to identify the USP11-driven molecular mediator(s):

ELAVL1 (ELAV-like protein 1), is an RNA-binding protein reported to regulate the stability and translation of many different mRNAs (Srikantan *et al*, 2012). In particular, ELAVL1 has been reported to bind AU-rich elements presents within the 3'UTR and 5'UTR of *HIF1A* and thus, to increase *HIF1A* mRNA stability and translation rate (Yasuda *et al*, 2014b; Galbán *et al*, 2008).

Nucleolin (NCL) is a nuclear protein that associates with chromatin and pre-ribosomal particles (Dempsey *et al*, 1998). NCL has been reported to bind AU-rich elements within different mRNAs and in particular, it has been described to increase *HIF1A* mRNA stability (Zhang *et al*, 2012b).

PML is a central component of the nuclear bodies, which primary function is to store transcripts and RNA-processing proteins (Borden & Culjkovic, 2009). PML has also been linked to HIF signalling modulation. Indeed, PML inhibits *HIF1A* translation while HIF-1α promotes PML transcription (Ponente *et al*, 2017; Bernardi *et al*, 2006).

FBXO11 is a component of an E3 ubiquitin-protein ligase complex that has been reported to inhibit de novo synthesis of HIF-1α protein by destabilizing *HIF1A* mRNA (Ju *et al*, 2015a).

In addition, we selected for RNA-binding proteins or Ub E3 ubiquitin-ligases among the publicly available USP11 interactome data base (BioGrid)(Oughtred *et al*, 2016):

Heterogeneous nuclear ribonucleoprotein D0 (hnRNPD), also called AUF1, is a RNA-binding protein reported to bind AU-rich elements within the 3'UTR region of different mRNAs and to regulate their turnover, usually by enhancing mRNA decay (Yoon *et al*, 2014), although hnRNPD has also been described as a transcription factor (Panda *et al*, 2014).

RAE1 is a RNA-binding protein whose main function is exporting mRNAs from nucleus to cytoplasm (Funasaka *et al*, 2011). Interestingly, USP11 has been reported to deubiquitinate RAE1 (Stockum *et al*, 2018b).

RBM15B is an RNA-binding protein that plays a role in N6-methyladenosine methylation of RNAs, thereby regulating processes such as alternative splicing and X chromosome inactivation(Majerciak *et al*, 2010).

RNF4 is an Ub E3 ubiquitin ligase that recognizes and binds poly-sumoylated chains, and USP11 has been reported to bind RNF4 (Hendriks *et al*, 2015b). Furthermore, RNF4 has been involved in ubiquitination and degradation of well know members of the hypoxia signalling pathway: HIF-2α (van Hagen *et al*, 2010) and FIH (Sallais *et al*, 2017).

We silenced all the above mentioned potential candidates, and measured the expression of *HIF1A* mRNA. However, no significant change on *HIF1A* mRNA levels were detected with the exception of *hnRNPD* silencing. Indeed,

mimicking the effect of *USP11* silencing, *HIF1A* but not *EPAS1* mRNA levels decreased upon *hnRNPD* silencing (Figure R23).

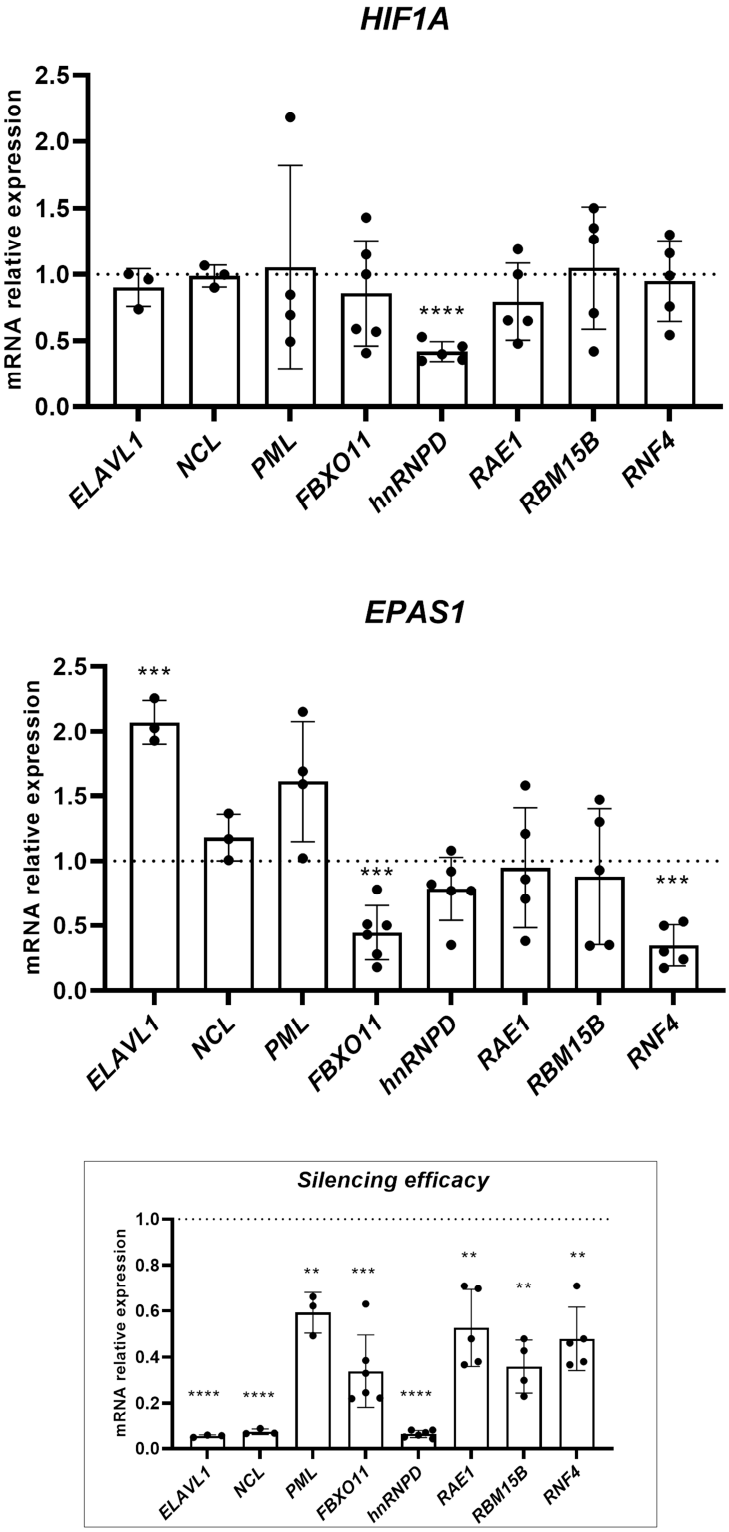

Figure R23: hnRNPD is a potential mediator of USP11. HEK293 cells were transfected with *siC* or the indicated *siRNAs* during 48 hours. Then, mRNA levels were analysed by RT-qPCR. Results were normalized to *RPLP0* following the $2^{-\Delta\Delta Ct}$ method, and represent relative values to control cells. The inset corresponds to the silencing efficacy. Figure shows the values corresponding to average ± S.E.M.. (*p<0,03, **p<0,0021, ***p<0,0002, ****p<0,0001. One sample T-test).

3.5.1 *hnRNPD activates the hypoxia-signalling cascade*

We next analysed the impact of hnRNPD on the hypoxia signalling pathway by quantifying the expression of HIF-1 target genes. As expected, the hypoxic induction of *BNIP3, CA9* and *SLC2A1* was significantly abrogated when *hnRNPD* was silenced (Figure 24).

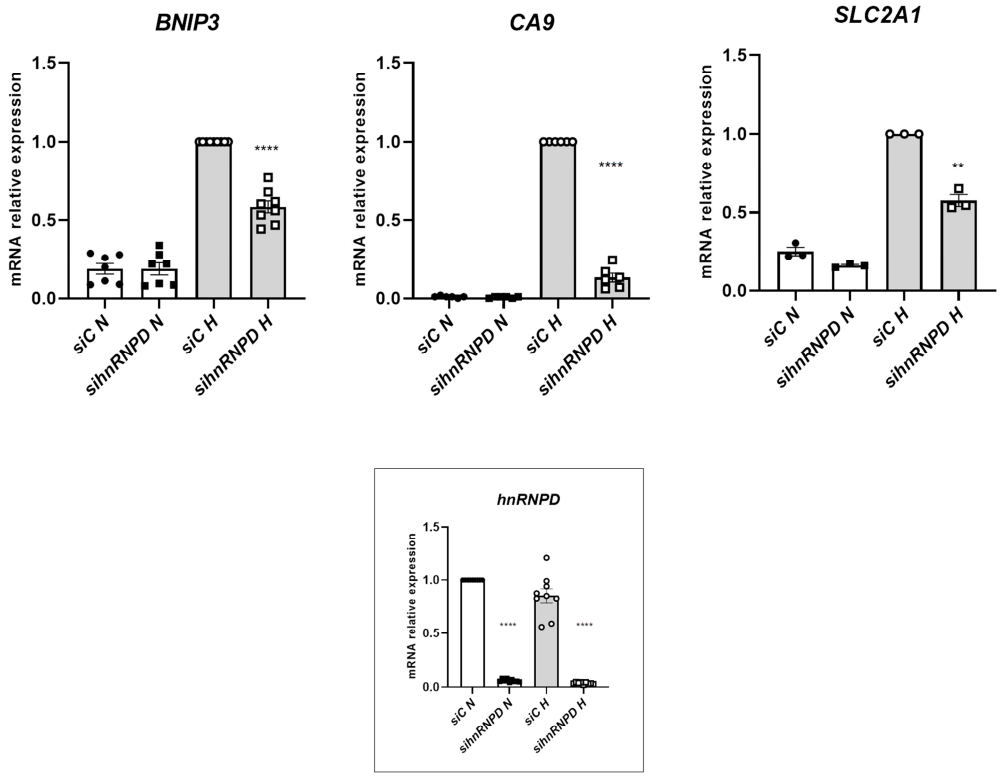

Figure R24: hnNRPD controls the hypoxic induction of HIF target genes. HEK293 cells were transfected with *siC* (control) or *sihnRNPD* during 48 hours and incubated in normoxia (N; 20% O_2) or hypoxia (H; 1% O_2) overnight before mRNA collection and analysis of mRNA levels by RT-qPCR. Results were normalized to *RPLP0* following the $2^{-\Delta\Delta Ct}$ method are represented as relative values to hypoxic control cells. The inset corresponds to the silencing efficacy normalized to nomoxic control cells. Figure shows the values corresponding to average ± S.E.M. (**p<0,0021, ****p<0,0001. One sample T-test).

According to the previous data, and similar to the impact of *USP11* silencing that we used as an internal control, the hypoxic accumulation of HIF-1α together with EGLN1/PHD2 decreased upon *hnRNPD* silencing, while HIF-2α was not affected (Figure R25).

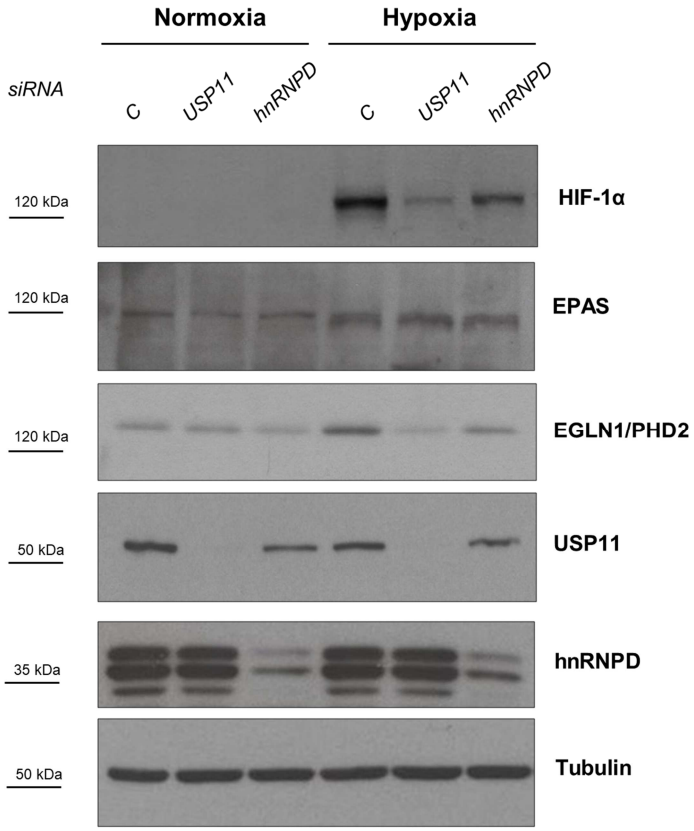

Figure R25: **Silencing of *hnRNPD* decreases HIF-1α hypoxic accumulation.** HEK293 cells were transfected with *siC* (control), *siUSP11* or *sihnNRPD* during 48 hours. After overnight normoxic (N; 20% O_2) or hypoxic (H; 1% O_2) incubation, cells were collected and protein levels were analysed by western blot using the indicated antibodies. Tubulin was used as a loading control. This is a representative figure of at least three independent experiments.

To decipher the molecular mechanisms underlying hnRNPD-mediated *HIF1A* regulation, we tackled a strategy similar to the one we used to characterise USP11. Thus, we first confirmed that hnRNPD does not affect *HIF1A* mRNA transcription (Figure R26).

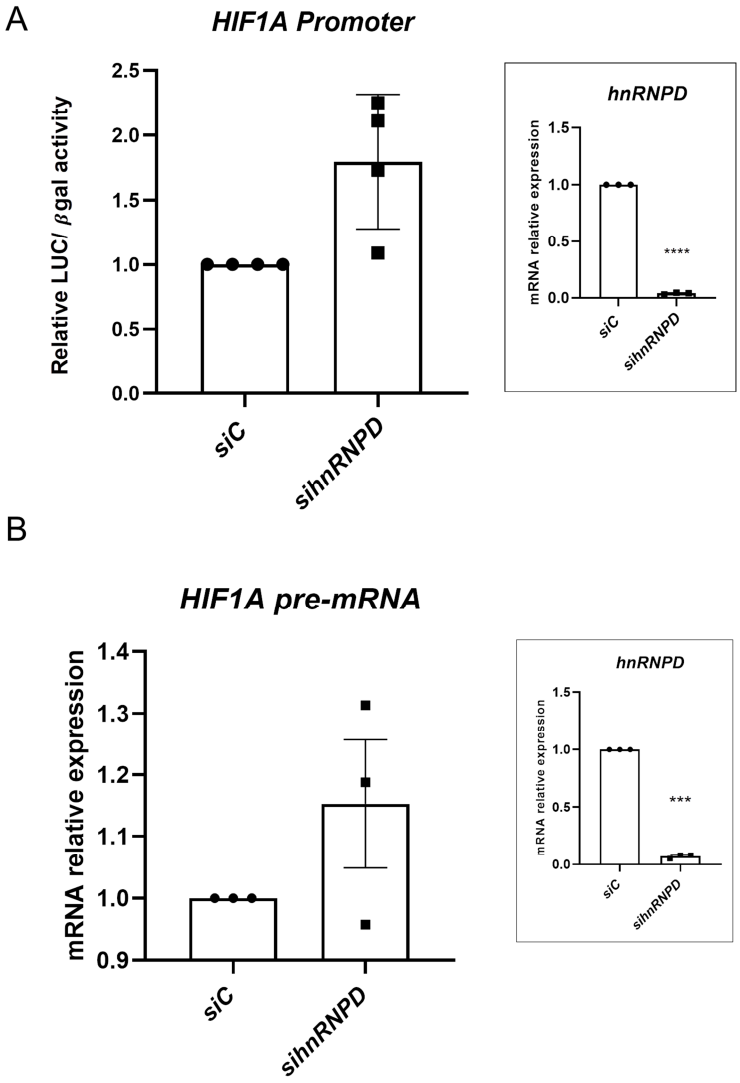

Figure R26: hnRNPD does not control *HIF1A* mRNA transcription. A) HEK293 cells were transfected with *siC* (control) or *sihnRNPD* during 24 hours before transfecting *HIF1A* prom-LUC and CMV-βgal. After additional 24 hours, luciferase activity was meassured and normalized to β-galactosidase activity. Results are represented as relative values to the control cells. **B)** HEK293 cells were transfected with *siC* (control) or *sihnRNPD* during 48 hours before analysing mRNA levels by RT-qPCR. Results were normalized to *RPLP0* following the $2^{-\Delta\Delta Ct}$ method, and represented as relative values to control cells. The right insets correspond to *hnRNPD* silencing. Figure shows the values corresponding to average ± S.E.M.. (***p<0,0002. ****p<0,0001. One sample T-test)

Next, we confirmed that hnRNPD, similar to USP11, controls *HIF1A* mRNA stability through the use of the HIF1A 3'UTR-driven luciferase reporter and the transcription block to measure *HIF1A* half-life (Figure R27).

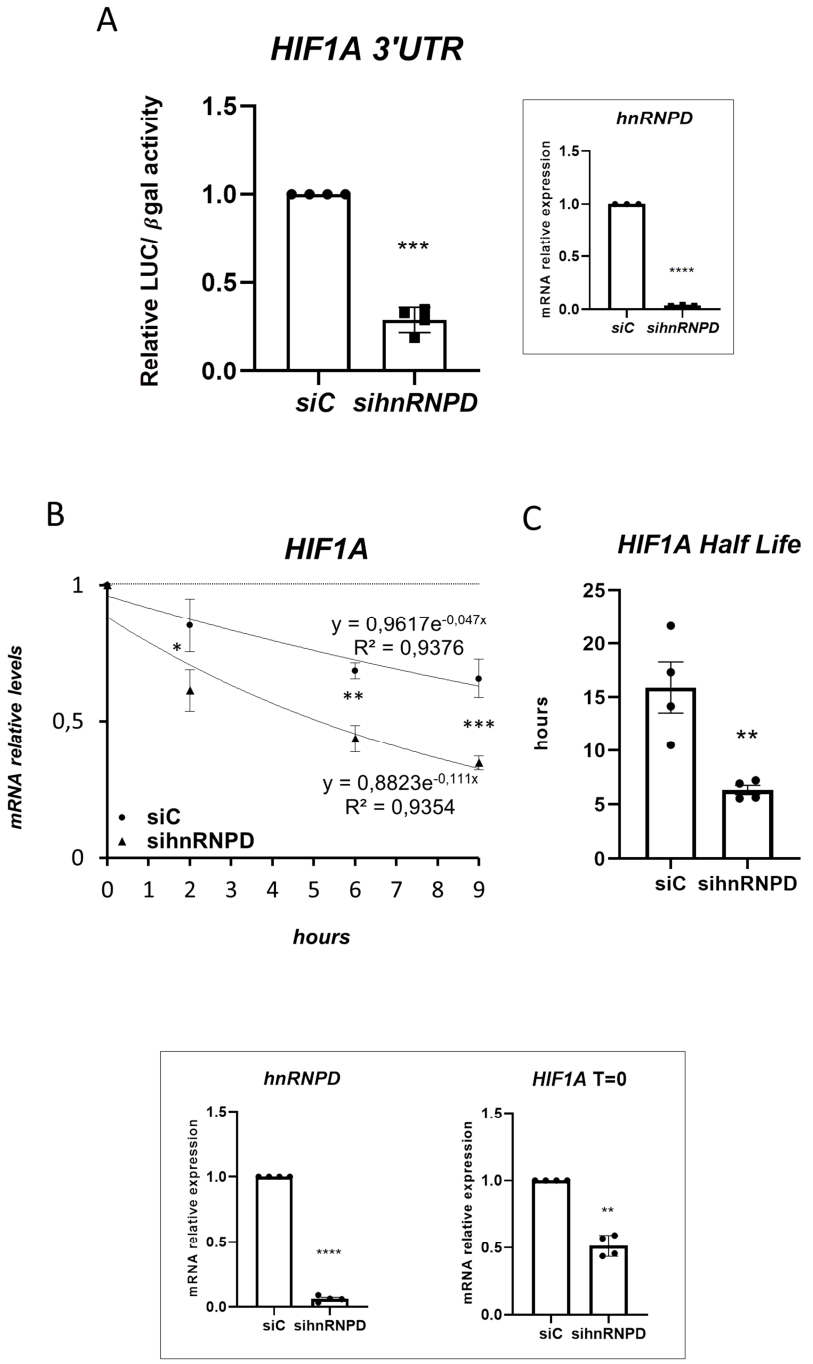

Figure R27: *hnRNPD* regulates *HIF1A* half-life. A) HEK293 cells were transfected with *siC* (control) or *sihnRNPD* during 24 hours before transfecting before transfecting the LUC-*HIF1A* 3'UTR and CMV-βgal reporters. After additional 24 hours, luciferase activity was meassured and normalized to β-galactosidase activity. Results are represented as relative values to the control cells. Insets describes the silencing efficacy. **B)** *HIF1A decay* and **C)** derived *HIF1A* mRNA half life. HEK293 cells were transfected with *siC* (control) or *sihnRNPD*, incubated 48 hours in normoxia and then treated with Actinomycin D (5 mg/ml) before collecting them after 0, 2, 6 and 9 hours. mRNA cell extracts were analysed by RT-qPCR. Results are normalized to *RPLP0* following the $2^{-\Delta\Delta Ct}$ method, and represented as relative values to time 0 of each condition. Insets describe the silencing efficacy as well as *HIF1A* mRNA levels at time 0. Figure shows the values corresponding to average ±S.E.M. (**p<0,00021, ***p<0,0002, ****p<0,0001. One sample T-test)

Finally, and in accordance with the USP11 data extrapolation previously shown, we have confirmed the impact of hnRNPD over *HIF1A* control on the MDA-MB-231 cells (Figure R29). As expected, and similarly to USP11, *hnRNPD* silencing was able to decrease hypoxia induced HIF-1α accumulation and *HIF1A* mRNA levels either in normoxia or hypoxia without affecting *EPAS1* (Figure R29). Also, the hypoxic induction of HIF-1 target genes, such as *BNIP3* and *CA9,* was significantly decreased upon *hnRNPD* silencing (Figure R29 B).

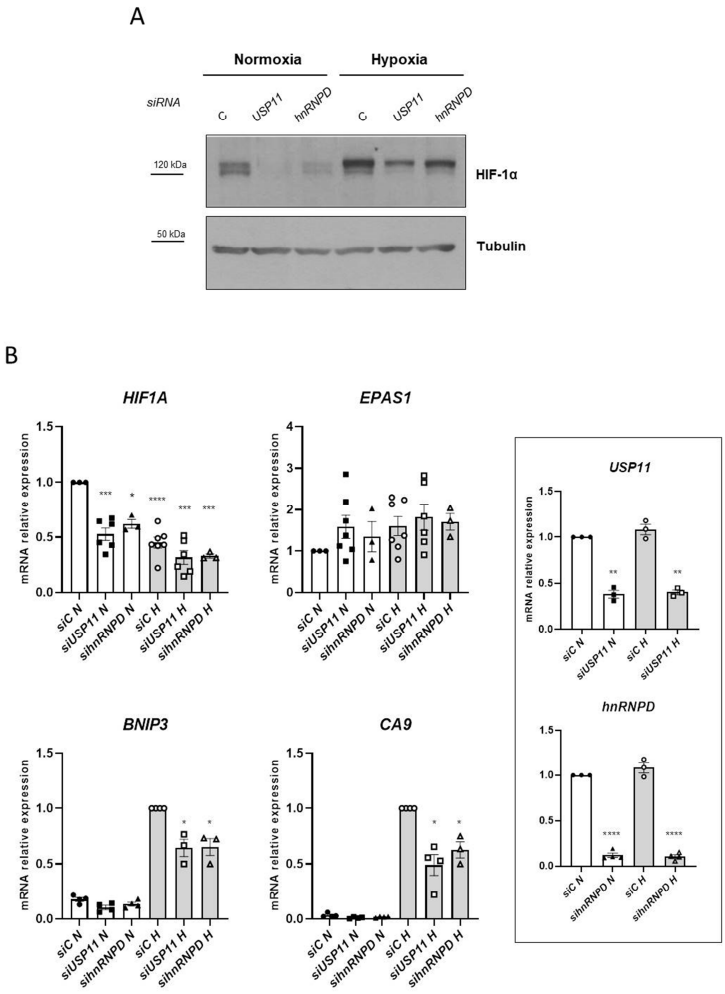

Figure R29: hnRNPD regulates the hypoxia signaling pathway in MDA-MB-231. MDA-MB-231 cells were transfected with *siC* (control), *siUSP11.1* or *sihnNRPD* during 48 hours. After that, cells were incubated either in (N; 20% O_2) or hypoxia (H; 1% O_2) overnight before harvesting. **A)** Total protein extracts were analysed by western blot. Tubulin was used as a loading control. This is a representative figure of at least three independent experiments. **B)** mRNA levels were analysed by RT-qPCR. Results are normalized to *RPLP0* following the $2^{-\Delta\Delta Ct}$ method, and represented as relative values to the the normoxic or the hypoxic control cells, in the case of HIF-1 target genes . Silencing efficacy is shown in the right inset. Figure shows the values corresponding to average ± S.E.M.. (*p<0,03, **p<0,00021, ***p<0,0002, ****p<0,0001. One sample T-test)

3.6 hnRNPD and USP11 interact in cellulo

Given the overlapping in the hnRNPD- and USP11-mediated regulatory mechanisms on *HIF1A*, we hypothesized that hnRNPD could be a target for USP11 and therefore, both proteins could interact. Indeed, endogenous hnRNPD was detected by IP of the ectopically expressed GFP-USP11 (Figure R30).

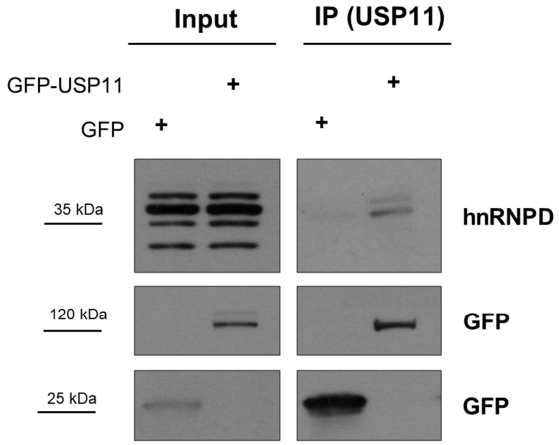

Figure R30: USP11 and hnRNPD co-precipitate in cells. HEK293 cells were transfected with GFP or GFP-USP11 during 24 hours before harvesting. Cell extracts were incubated with GFP-traps overnight. Input and eluted samples were analysed by western blot with the indicated antibodies. Tubulin was used as input loading control. This is a representative figure of at least three independent experiments.

hnRNPD consists of four isoforms (p37, p40, p42 and p45) produced by alternative splicing of exons 2 and 7 (Zucconi *et al*, 2010) . It has been reported that the isoforms work as dimers, which bind and modify targeted mRNAs and therefore, regulate the recruitment of additional RBPs. We have analysed the intracellular distribution of the different isoforms by immune-staining and cell-fractioning followed by Western blot (Figure R31). As suggested in a previous report (Moore *et al*, 2014), p37 and p40 are located in the nucleus and the cytoplasm, while p42 and p45 are mainly located in the nucleus.

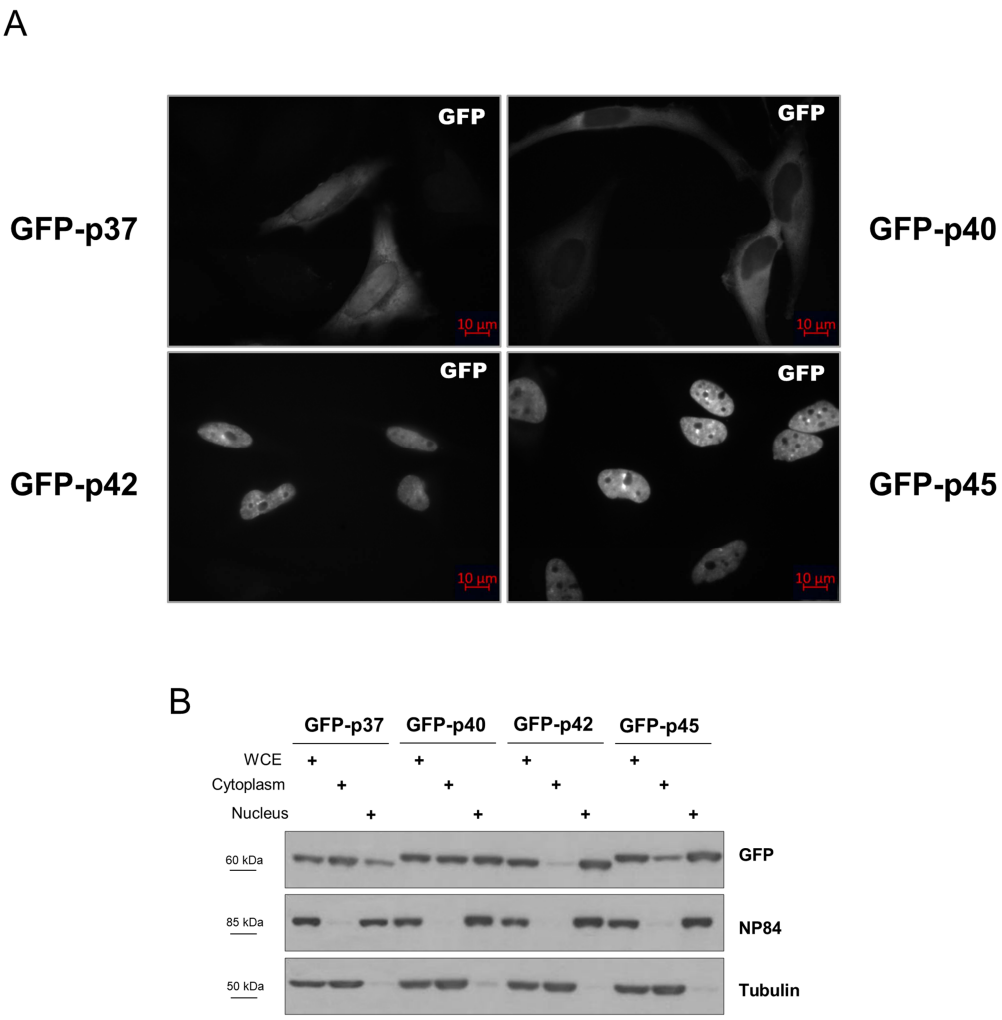

Figure R31: Intracellular distribution of the hnRNPD isoforms. A) HeLa cells were seeded on coverlips and transfected with GFP-p37, GFP-p40, GFP-p42 or GFP-p50 during 24 hours before fixing and mounting into microscope slides. GFP fluorescence is detected in this image using Axioimager D1 (Zeiss). **B)** HeLa cells were transfected with GFP-p37, GFP-p40, GFP-p42 or GFP-p50 during 24 hours before cell fractioning. Proteins from the total celll extracts and the different subcellular fractions were analysed by western blot. Tubulin and NP84 were used as citoplasm and nuclear fraction controls, respectively. This is a representative figure of at least three independent experiments.

Once confirmed the interaction between USP11 and hnRNPD and the different location of the hnRNPD isoforms, their potential specificity to bind USP11 was assessed. Thus, the hnRNPD isoforms were immunoprecipitated, individually or in combination, and USP11 analysed by WB. USP11 was indeed detected in all the different experimental conditions suggesting that the four isoforms similarly bind USP11 (Figure R32).

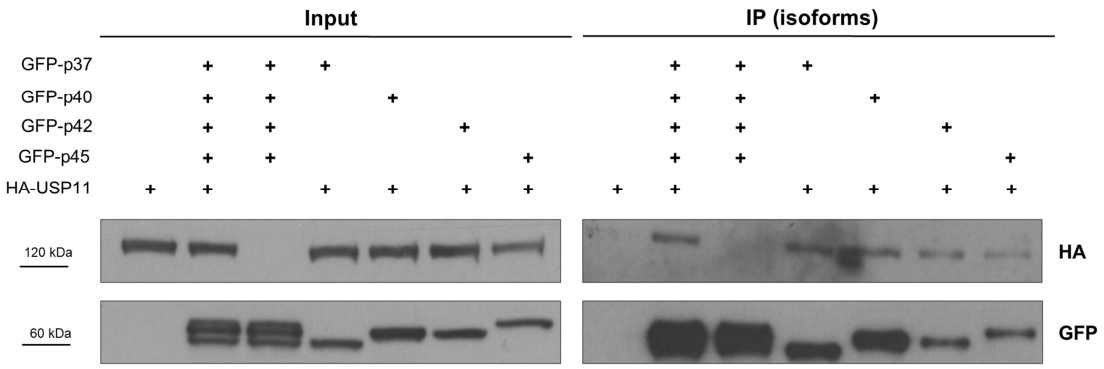

Figure R32: USP11 and all hnRNPD isoforms co-precipitate in cells. HEK293 cells were transfected with HA-USP11 and GFP or GFP-p37, GFP-p40, GFP-p42 and GFP-p45, (individually or all together) during 24 hours before harvesting. Cell extracts were incubated with GFP-traps overnight. Input and eluted samples were analysed by western blot with the indicated antibodies. This is a representative figure of at least three independent experiments.

3.6.1 hnRNPD binds HIF1A mRNA

As hnRNPD is a RBP, it was tempting to speculate about the possibility that hnRNPD directly binds *HIF1A* mRNA. Thus, biotinylated overlapping RNA probes spanning the entire *HIF1A* mRNA [5'UTR, the coding region (CR) and the 3'UTR] (Figure 33A and 33B) were synthesized by *in vitro* transcription. Then, biotinylated RNA probes were incubated with cellular extracts and the 'pulldown' complex was assessed by Western blot analysis. Despite variability in the intensity of the protein signal among experiments, we consistently observed preferential binding to the 3'UTR region of *HIF1A,* and in particular to fragments 6 and 9 (Figure R33).

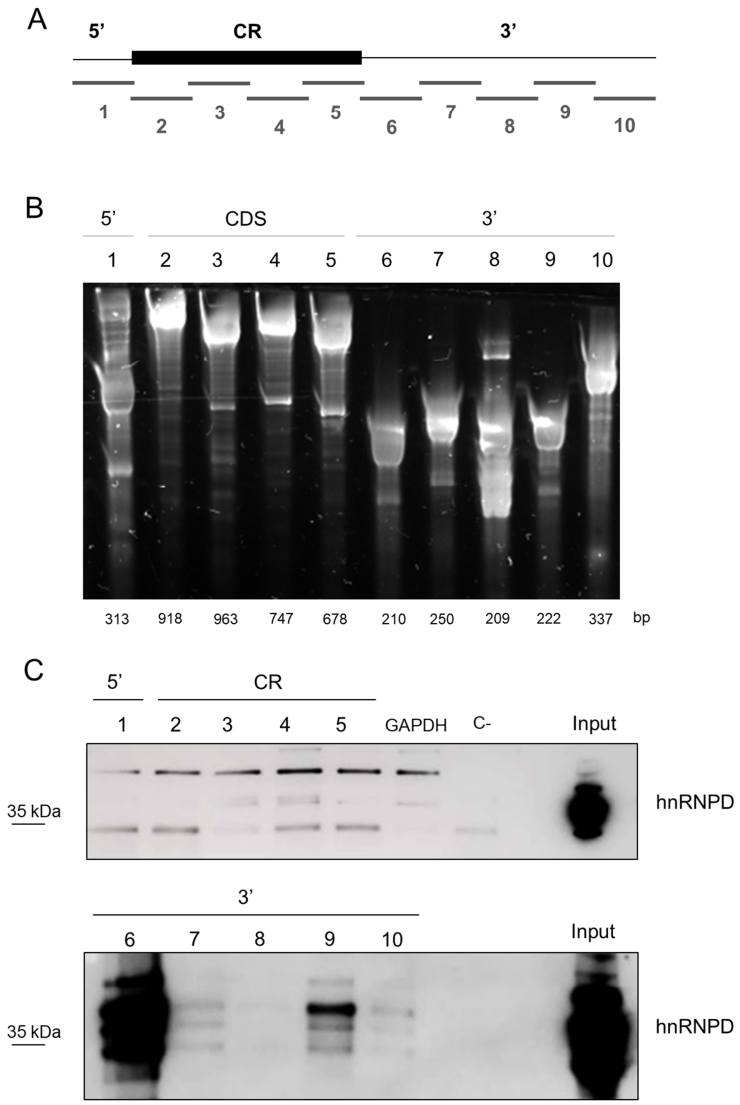

Figure R33: hnRNPD interacts with the 3'UTR region of *HIF1A* mRNA. A) Schematic representation of the biotinylated RNA probes covering the 5'UTR, the coding region and the 3'UTR of *HIF1A* mRNA that were generated. **B)** *HIF1A* biotinylated probes synthetized by *in vitro* transcription were visualized in an agarose gel prior to gel purification. **C)** HEK293 cell lysates were incubated with the biotinylated *HIF1A* probes and then with streptavidin beads. Input and eluted samples were analysed by western blot with the hnRNPD antibody. This is a representative figure of ten independent experiments.

In the same line, *HIF1A* mRNA enrichment was assessed after hnRNPD immunoprecipitation by Ribonucleoprotein Immunoprecititation assays (RIPs). Indeed, compared with a control IgG, the hnRNPD RIP showed a significant enrichment on *HIF1A* mRNA similarly to *ME2FC* and *VEGFA*, two well-known mRNAs that bind hnRNPD, while *RPLP0* and *GAPDH*, used as negative controls, were not enriched (Figure R34 A). In addition, we examined the

specificity of the different hnRNPD isoforms towards *HIF1A* mRNA. Interestingly, the p37 RIP showed a greater enrichment in *HIF1A* mRNA greater than the rest of the hnRNPD isoforms (Figure R34 B).

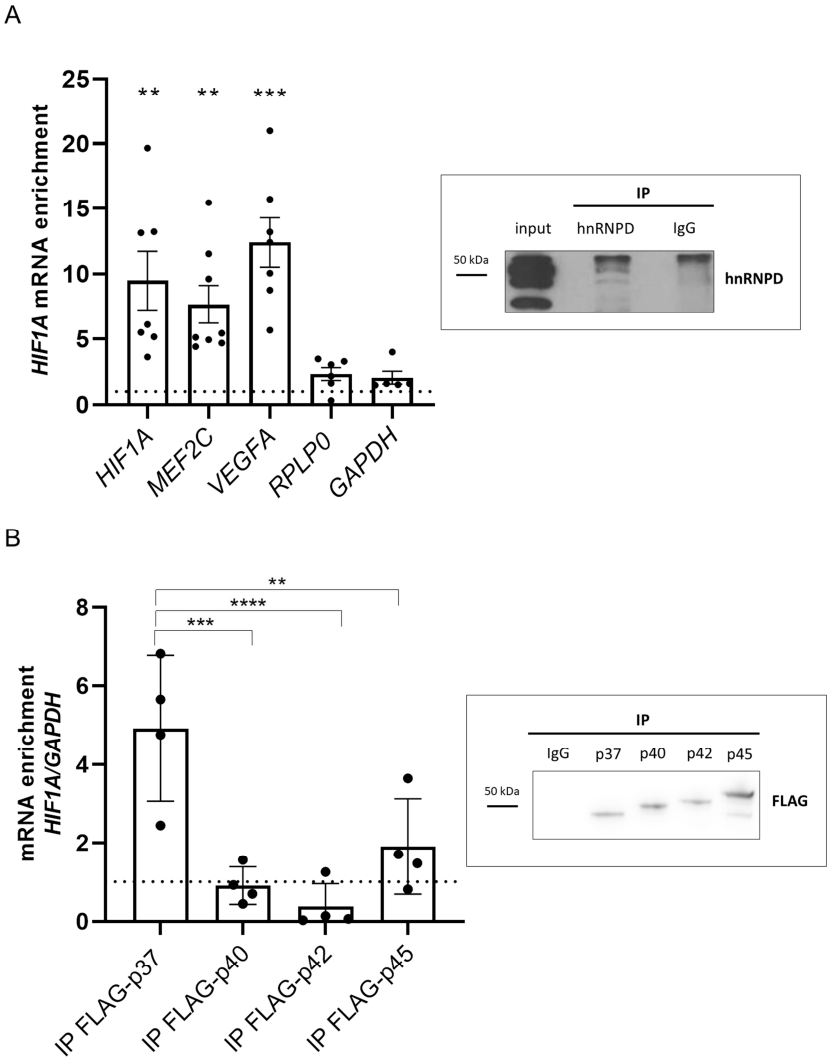

Figure R34: hnRNPD binds *HIF1A* mRNA. A) HEK293 mRNA extracts were obtained to perform RIP followed by RT-qPCR to determinate hnRNPD direct binding to *HIF1A* mRNA. Results are represented as relative values to non-reactive IgG antibody following the $2^{-\Delta Ct}$ method. The right inset shows a representative western blot of the IP efficiency analysed by western blot using the hnRNPD antibody. **B)** RIP followed by RT-qPCR to determinate the individual FLAG-tagged hnRNPD isoforms binding to *HIF1A* mRNA. Results are represented as relative values to GAPDH and non-reactive IgG antibody following $2^{-\Delta Ct}$ method. The right insets show a representative western blot of the IP efficiency analysed by western blot using the corresponding antibodies.

3.6.2 *USP11 binds HIF1A mRNA*

As hnRNPD directly binds *HIF1A* and also interacts with USP11, we next evaluated the potential interaction of USP11 with *HIF1A* mRNA. Thus, we performed new RIP experiments. The USP11 RIP significantly enriched *HIF1A* mRNA, though failed to enrich *RPLP0* and *GAPDH* that we used as negative controls, and even more interestingly *ME2FC* and *VEGFA* (Figure R35).

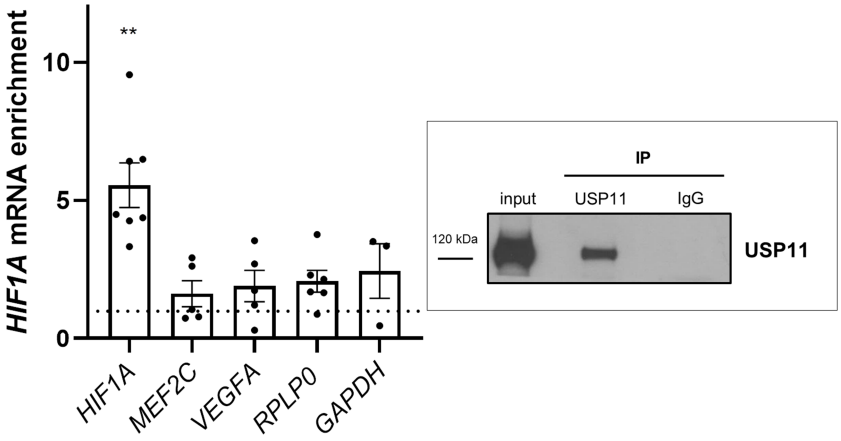

Figure R35: USP11 binds *HIF1A* mRNA. HEK293 total cell extracts were obtained to perform RIP followed by RT-qPCR. Results are represented as relative values to non-reactive IgG antibody following $2^{-\Delta Ct}$ method. The right inset shows a representative western blot of the IP efficiency analysed by western blot using the USP11 antibody.

In order to go deeper into the understanding of the hnRNPD-USP11 complex, we next assessed the potential hierarchy between both proteins to shape the ribonucleoprotein complex that governs *HIF1A* stability. To address this question, we performed new RIP experiments: hnRNPD- and USP11-RIP in control or upon USP11 and hnRNPD silencing, respectively. The hnRNPD RIP showed a significant enrichment in *HIF1A* mRNA independently of the silencing of USP11 (Figure R36). On the contrary, *HIF1A* mRNA was not significantly enriched in the USP11 RIP upon silencing of hnRNPD.

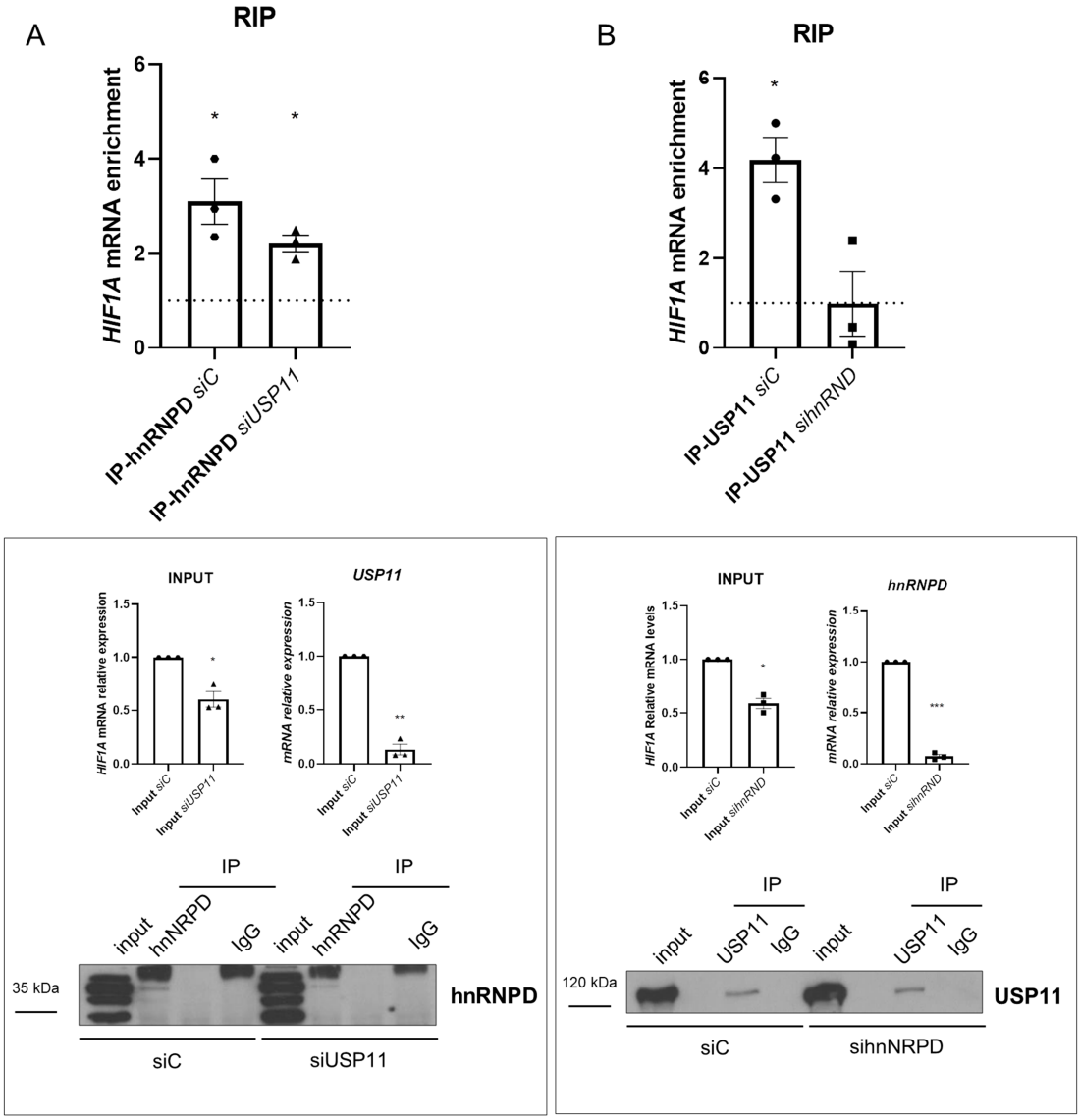

Figure R36: hnRNPD is required for the binding of USP11 to *HIF1A*. HEK293 cells were transfected with *siC* (control), *siUSP11.1* or *sihnNRPD* during 48 hours. Total cell extracts were obtained to perform RIP followed by RT-qPCR to determinate **A)** hnRNPD and **B)** USP11 direct binding to *HIF1A* mRNA. Results are represented as relative values to non-reactive IgG antibody following the $2^{-\Delta Ct}$ method. Lower insets corresponds to the mRNA expression levels of *HIF1A, hnRNPD* or *USP11* that were assessed by RT-qPCR in the inputs to analyse the impact of *hnRNPD* and *USP11* and the silencing efficacy, respectively. Results are normalized to *RPLP0* following the $2^{-\Delta\Delta Ct}$ method, and represented as relative values to control cells. Finally, representative experiments of both IP efficiencies were analysed by western blot using hnRNPD or USP11 antibodies.

3.6.3 hnRNPD is not a direct target of USP11

We next wanted to further elucidate whether hnRNPD is a direct target of hnRNPD. As shown in Figure 30 and according with the preferential role of USP11 towards Lys63-ubiquitin chains, USP11 knockdown did not impact on hnRNPD protein levels (Figure R37). We next performed ubiquitination assays under denaturing conditions to analyse the presence of ubiquitin chains on

hnRNPD and their putative modulation by USP11. We analysed the ubiquitination status of two different hnRNPD isoforms (p37 and p45, the shortest and the longest isoforms, respectively) upon control or USP11 knockdown conditions. Although the proteins were successfully pulled-down, we did not detect hnRNPD ubiquitination (data not shown). However, we detected ubiquitination on a HIF-2α ectopically expressed plasmid that we used as a positive control.

To solve sensitivity problems of the ubiquitination assays, we analysed new equivalent samples by Mass Spectrometry (MS) in collaboration with Dr. Ugo Mayor (UPV/EHU). Data arising from this analysis confirmed hnRNPD as the main protein present in all samples followed by ubiquitin among the endogenous proteins (Figure R37).

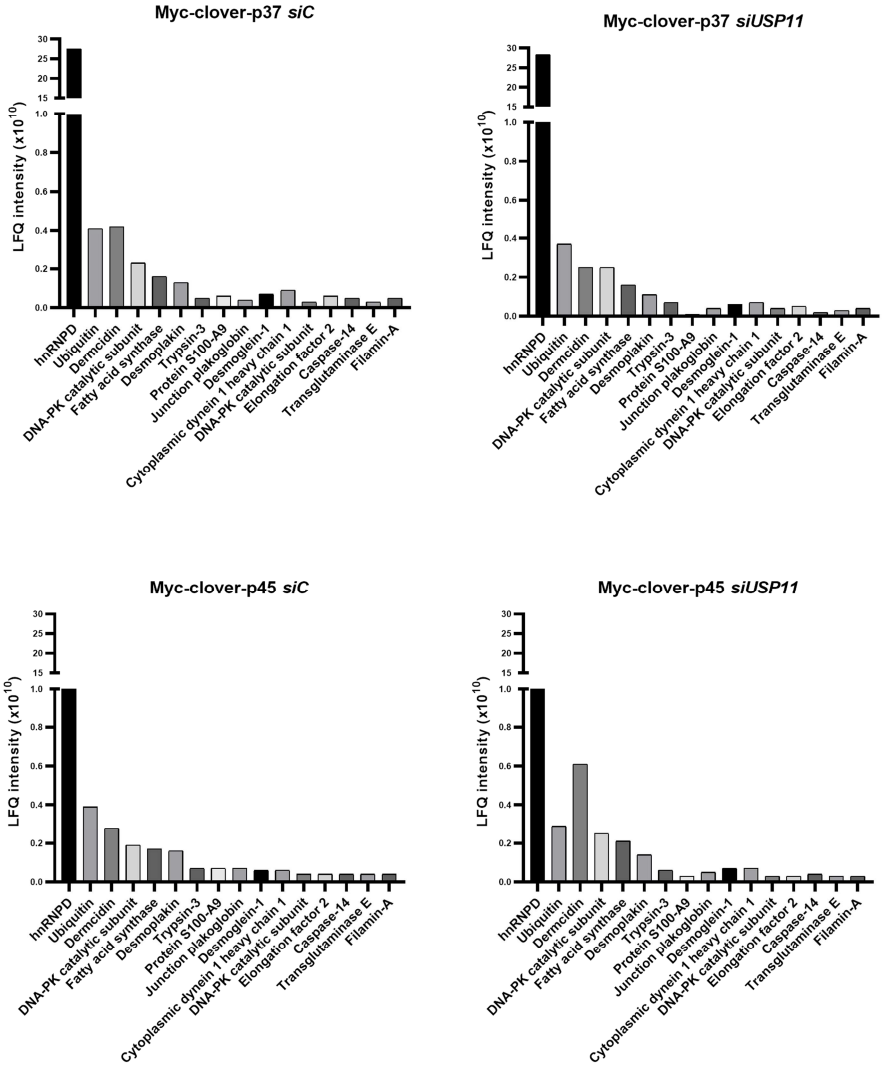

Figure R37. Analysis of p37 and p45 ubiquitin assay by MS. Frequency histograms indicating the proteins (X axis) vs the higher LFQ intensities (Y axis) corresponding to the four samples analysed.

MS data allowed us to identify two common peptides within the two hnRNPD isoforms that were ubiquitinated (Lys72 and Lys178 or Lys197). Interestingly, two populations of ubiquitin chains were detected: Lys48 and Lys63 (Table R2).

Table R2: Summary of the ubiquitinated peptides identified by MS.

Protein	Isoform	Peptide sequence	Position of di-glycine
hnNRPD	p37	IDASK(G-G)NEEDEGK	
	p45	IDASK(G-G)NEEDEGK	**Lys72**
	p37	IFVGGLSPDTPEEK(G-G)IR	**Lys 178**
	p45	IFVGGLSPDTPEEK(G-G)IR	**Lys 197**
Polyubiquitin		LIFAGK(G-G)QLEDGR	**Lys 48**
		TLSDYNIQK(G-G)ESTLHLVLR	**Lys 63**

However, the amount of neither total hnRNPD peptides nor total polyubiquitin peptides were altered upon *USP11* silencing. Regarding polyubiquitin peptides, K63 polyubiquitin peptide is slightly increased upon USP11 silencing in both samples. However, the increase in K63-ubiquitin chains is not translated into a rise of hnRNPD ubiquitinated peptides, which precludes USP11 regulation of hnRNPD ubiquitination (Table R3).

Table R3: Ratio of ubiquitinated peptides USP11-silenced vs control cells.

Protein	Peptide sequence	**Myc-clover-p37 siUSP11/siC** (Ratio LFQ intensities)	**Myc-clover-p37 siUSP11/siC** (Ratio LFQ intensities)
hnRNPD	Total	**0,97**	**0,81**
	IDASK(G-G)NEEDEGK	**0,20**	**N/A**
	IFVGGLSPDTPEEK(G-G)IR	**0,79**	**1,05**
Polyubiquitin	Total	**1,12**	**0,73**
	LIFAGK(G-G)QLEDGR	**0,63**	**0,65**
	TLSDYNIQK(G-G)ESTLHLVLR	**1,41**	**1,31**

4 Hypoxic regulation of the hnRNPD/USP11 ribonucleoprotein complex

4.1 Hypoxia and USP11

Given the important role of USP11 and hnRNPD in activating the hypoxia signalling cascade, it was tempting to study their potential regulation upon changes in oxygen availability.

All the above shown data ruled out a transcriptional regulation of USP11 by hypoxia (Figures R3, R6, R15, R16 R20, and R29) and suggested that hypoxia does not impact on USP11 protein levels. In order to confirm these results, we analysed USP11 protein level at different hypoxia time points including also cells treated with the pan prolyl-hydroxylase inhibitor Dimetiloaxil glicine (DMOG). Indeed, no significant changes were observed on USP11 protein levels under any of the aforementioned conditions compared to control cells (Figure R38).

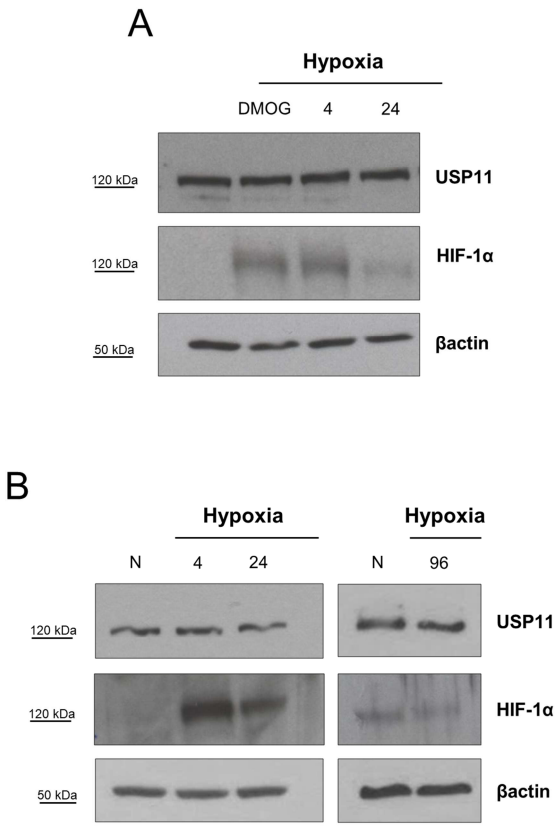

Figure R38: USP11 protein levels are not affected by hypoxia. HEK293 **A)** or MDA-MB-231 **B)** cells were treated with DMOG (1mM; 4h) or incubated in normoxic (N; 20% O_2) or hypoxic (H; 1% O_2) conditions during the specified times. Total protein levels were analysed by western blot with the indicated antibodies. β-actin was used as a loading control.This is a representative figure of at least three independent experiments.

In addition, we analysed the potential role of the proteasome in the control of USP11 protein levels as such regulation has been reported in the case of many different DUBs (Mei *et al*, 2011). Neither USP11 wild type nor the catalytically inactive USP11 protein levels were affected by MG132, in spite of the HIF-1α accumulation that we used as a positive control (Figure R39).

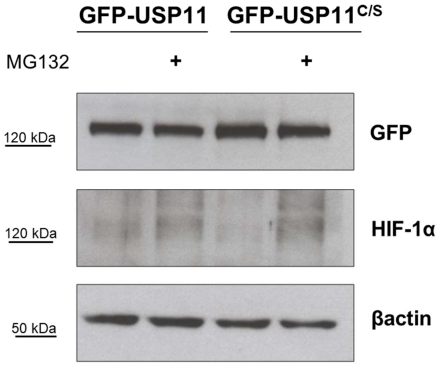

Figure R39: **The protein levels of USP11 are not regulated by the proteasome.** HEK293 cells were transfected with GFP-USP11 (wild type) or GFP-USP11$^{C/S}$ (catalytically inactive) during 24 hours before blocking the proteasome with MG132 (10μM; 4h). Total protein extracts were analysed by western blot with the indicated antibodies. β-actin was used as a loading control. This is a representative figure of at least three independent experiments.

We next aimed to analyse the putative impact of hypoxia on USP11 catalytic activity by using an Ub-derived activity based probe (ABP) assay. Thus, we utilized the HA-tagged ubiquitin vinyl sulfone (HA-Ub-VS) probe that contains modified ubiquitin with an electrophilic trap (vinyl sulfone), which covalently and irreversibly reacts with the active cysteine of the DUBs. We first tuned the experimental conditions to profile USP11 activity by testing the probe binding to ectopically expressed wild type or inactive USP11. As expected, HA-Ub-VS probe exclusively bound wild type USP11 (Figure R40).

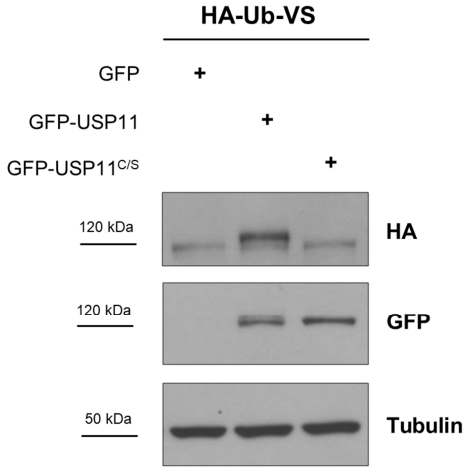

Figure R40: Utility of the HA-Ub-VS probe to measure USP11 catalytic activity. HEK293 were transfected with GFP, GFP-USP11 (wild type) or GFP-USP11^{C318S} (catalytically inactive) during 24 hours. Cells were harvested and incubated with the HA-Ub-VS. Total protein as well as HA-Ub-VS probe levels were detected with the indicated antibodies by western blot. Tubulin was used as a loading control. This is a representative figure of at least three independent experiments.

.

We next overexpressed GFP-USP11 in cells that were then incubated in normoxia, hypoxia or hypoxia followed by re-oxygenation. Interestingly, hypoxia correlated with a strong decrease in USP11 activity as shown by the drop in the binding of the HA-Ub-VS probe (Figure R41 A). Furthermore, this inhibition in USP11 activity by hypoxia appears to be reversible once restored oxygen availability (Figure R41 A). However, the use of DMOG does not mimic USP11 inhibition and thus, we exclude the involvement of PHDs, as well as other members of the family of 2-oxoglutarate-dependent dioxygenases in the hypoxia-driven inhibition of USP11 catalytic activity (Figure 41 B).

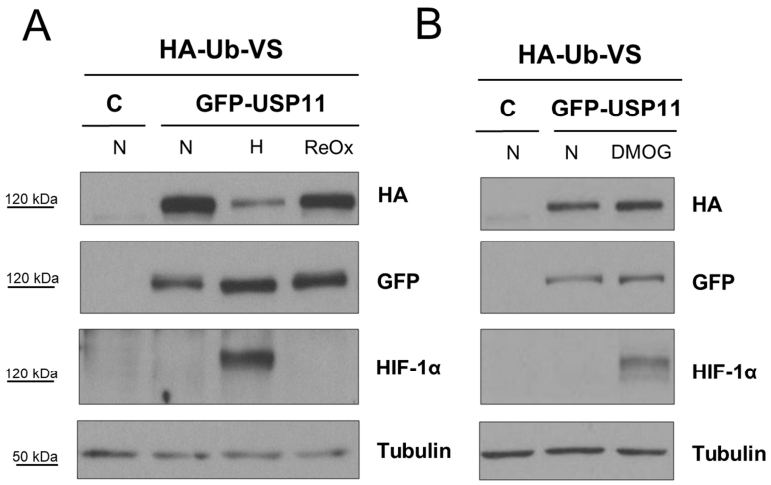

Figure R41: **Hypoxia regulates the activity of USP11. A)** HEK293 were transfected with GFP (C) or GFP-USP11 and incubated in normoxia (N; 20% O_2), hypoxia (H; 1% O_2) for 24 hours or hypoxia (24h) followed by 1h of re-oxygenation. **B)** HEK293 cells were transfected with GFP (C) or GFP-USP11 and untreated or treated with DMOG (1mM; 4h). Harvested cells were incubated with the HA-Ub-VS. Total protein as well as HA-Ub-VS probe levels were detected with the indicated antibodies by western blot. Tubulin was used as a loading control. This is a representative figure of at least three independent experiments.
.

Many DUBs have been reported to be able to auto-deubiquitinate. For instance, USP4, USP19, USP29 and UCH-L1 have been shown to reverse their own ubiquitination (Wada & Kamitani, 2006; Mei *et al*, 2011; Meray & Lansbury, 2007; Schober *et al.,* manuscript in preparation). On the basis of the inhibitory impact of hypoxia on USP11 catalytic activity, we hypothesized an increase in the ubiquitination pattern of USP11 upon hypoxia. Thus, we ectopically expressed USP11 and performed an ubiquitination assay under denaturing

conditions in cells incubated in normoxia or hypoxia. The presence of USP11-ubiquitinated forms, which were apparent as a higher molecular weight smear, was already detected in normoxia but much more visible in hypoxia (Figure R42).

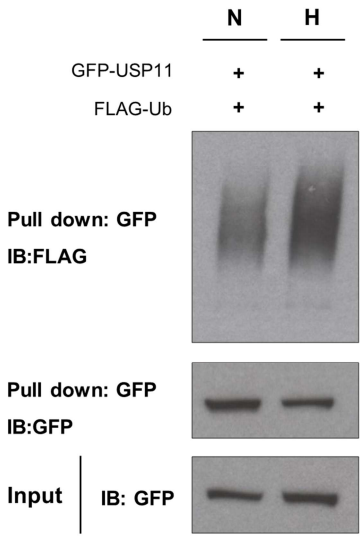

Figure R42. Hypoxia promotes USP11 ubiquitination. HEK293 cells were co-transfected with FLAG-ubiquitin and GFP-USP11 during 24 hours. After that, HEK293 were incubated in normoxia (N; 20% O_2) or hypoxia (H; 1% O_2) overnight before MG132 (10µM) treatment during 4 hours. GFP-tagged proteins were pulled-down under denaturing conditions with GFP-traps. Total protein extracts and eluted proteins were run on gradient gels (4-12% acrylamide). Non-modified and ubiquitinated proteins were detected by western blot using the corresponding antibodies.

As mentioned in the introduction, it has been recently suggested that USP11 activity depends on the phosphorylation of the Ser452 by S6K1 in diffuse large B-cell lymphoma (Kapadia *et al*, 2018). Thus, we hypothesized a role for such phosphorylation in the hypoxia-mediated inhibition of USP11 catalytic activity.

We first confirmed previous reports showing that S6K1 activity is reduced upon hypoxia in our system (Lee *et al*, 2009). Indeed, S6K1 phosphorylation as well as the phosphorylation of RPS6, its direct target, decreased along a hypoxia kinetic as a read-out of the inhibition of the PI3K-Akt-mTOR pathway (Figure R43).

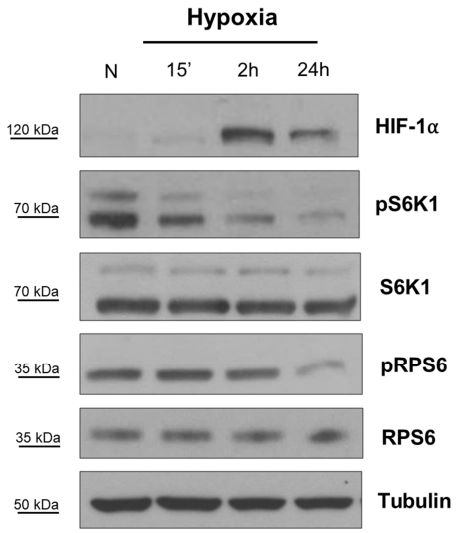

Figure R43: **Hypoxia inactivates S6K1.** HEK293 cells were incubated in normoxia (N; 20% O_2) or hypoxia (H; 1% O_2) for the indicated times before harvesting. Total protein levels were analysed by WB with the indicated antibodies. Tubulin was used as a loading control. This is a representative figure of at least three independent experiments.

However, our attempts to measure the phosphorylation status of endogenous USP11 using anti-phosphoSer/Thr/Tyr antibodies in these experimental conditions have been unsuccessful so far. We initially attempted to detect USP11 phosphorylation in normoxia or hypoxia using PhosTag gels. PhosTag gels retain phosphorylated proteins and thus provoke a slower migration than that of the non- phosphorylated counterparts. We migrated total cellular extracts in pre-cast (7,5% and 50mM PhosTag) or home-made (5% and 50mM PhosTag) gels and analysed by Western Blot. While the shift on AMPKα2, whose phosphorylation is decreased by hypoxia (Romero-Ruiz *et al*, 2012), was easily detected (Figure R44 A), no clear shift was detected in the case of USP11 (Figure R44 B).

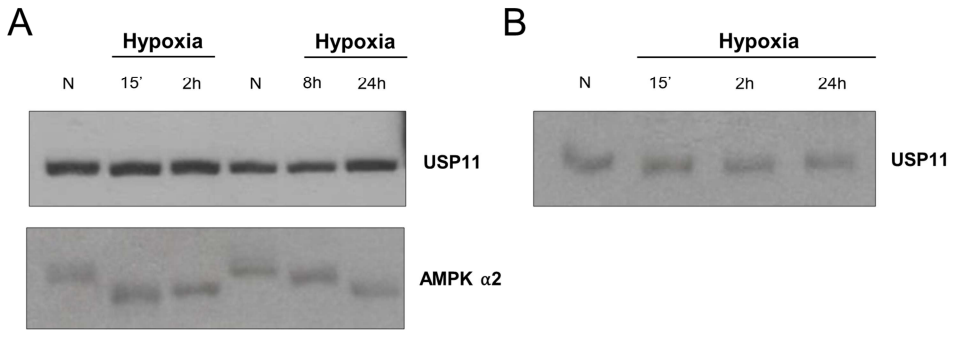

Figure R44: **Detection of USP11 phosphorylation.** HEK293 cells were incubated in normoxia (N; 20% O_2) or hypoxia (H; 1% O_2) overnight before harvesting.Total protein extracts were migrated in **A)** pre-cast or **B)** home-made PhosTag gels and analysed by WB with the indicated antibodies.

Despite the failure to detect USP11 phosphorylation, we generated the phosphorylation death mutant by replacing the Ser452 by an Ala452 ($USP11^{S452A}$) and profiled its activity as previously. Similar to the $USP11^{C318S}$, the catalytic activity of $USP11^{S452A}$ was completely abolished (FigureR45).

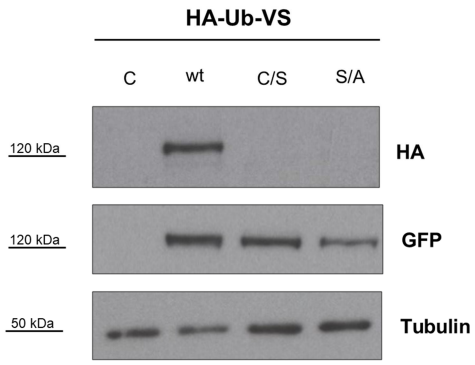

Figure R45: **Phosphorylation of USP11 Ser452 is necessary for the catalytic activity.** HEK293 cells were transfected with GFP or the different GFP-USP11 constructs during 24 hours. Cells were harvested and incubated with the HA-Ub-VS. Total protein as well as HA-Ub-VS probe levels were detected with the indicated antibodies by western blot. Tubulin was used as a loading control. This is a representative figure of at least three independent experiments.

In line with the inverse correlation previously shown between USP11 activity and the ubiquitination status, $USP11^{C318S}$ and $USP11^{S452A}$'s ubiquitinated forms were highly increased compared to the wild type protein (Figure R46).

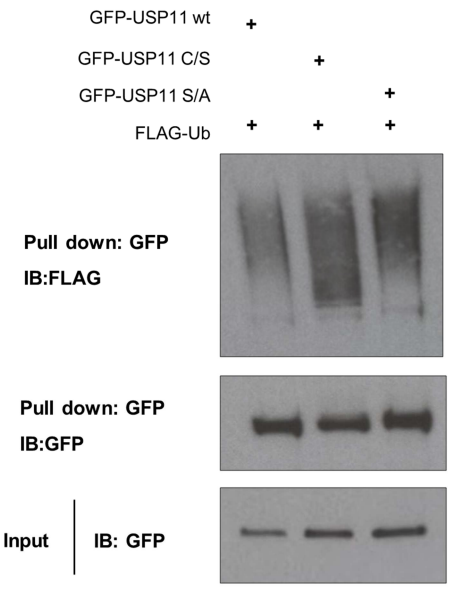

Figure R46: **USP11 catalitic activity and ubiquitination inversely correlate.** HEK293 cells were co-transfected with FLAG-ubiquitin and the different GFP-USP11 constructs during 24 hours. Cells were treated with MG132 (10µM) for 4 hours before GFP-tagged proteins were pulled-down under denaturing conditions with GFP-traps. Total protein extracts and eluted proteins were run on gradient gels (4-12% acrylamide) and non-modified and ubiquitinated forms detected by western blot.

4.2 Hypoxia and hnRNPD

Our previous data (Figure R24 or R25) also precluded a role for hypoxia in the control of *hnRNPD* mRNA levels. However, such analysis was aimed to amplify the 4 hnRNPD isoforms at the same time, and thus we set up experimental conditions to specifically amplify each of the different isoforms. However, , neither mRNA levels nor protein levels changed upon hypoxic conditions (Figure R47).

Curiously, when subcellular localization of the different hnRNPD isoforms was analysed, we could observe that p37 distribution changed. In normoxia, GFP-p37 is uniformly located along nucleus and cytoplasm. However during hypoxia, GFP-p37 is significantly accumulated into the nuclear compartment. In contrast, the cellular localization of the rest of the hnRNPD isoforms remained unaltered (Figure R48).

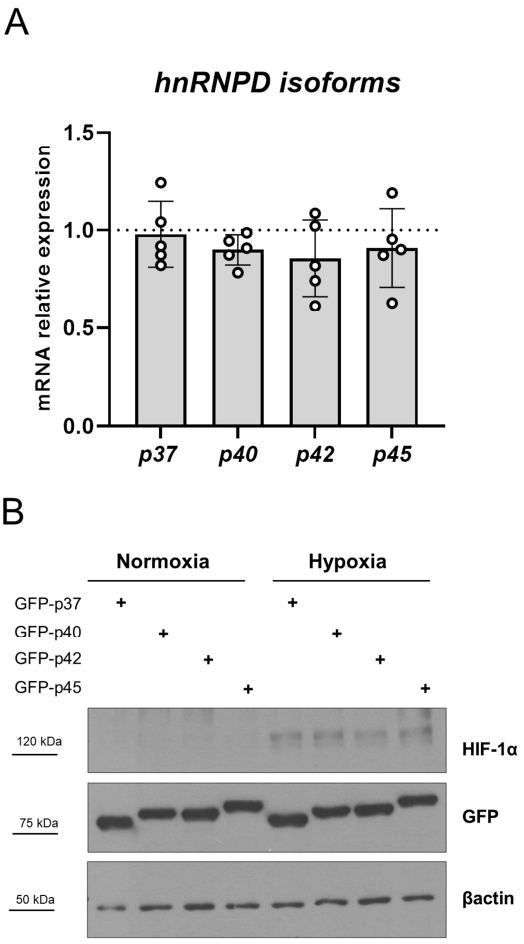

Figure R47: Hypoxia does not affect hnRNPD isoform expression levels. A) HEK293 cells were incubated either in normoxia (N; 20% O_2) or hypoxia (H; 1% O_2) overnight before analysing mRNA levels using directed RT followed by qPCR to amplify the *hnRNPD* isoforms individually. Results are normalized to *RPLP0* following the $2^{-\Delta\Delta Ct}$ method, and represented as relative values to the normoxic control cells. **B)** 293 cells were transfected with GFP-p37, GFP-p40, GFP-p42, GFP-p45 during 24 hours before overnight incubation in normoxia or hypoxia. Total protein extracts were analysed by western blot. β-actin was used as a loading control. This is a representative figure of at least three independent experiments.

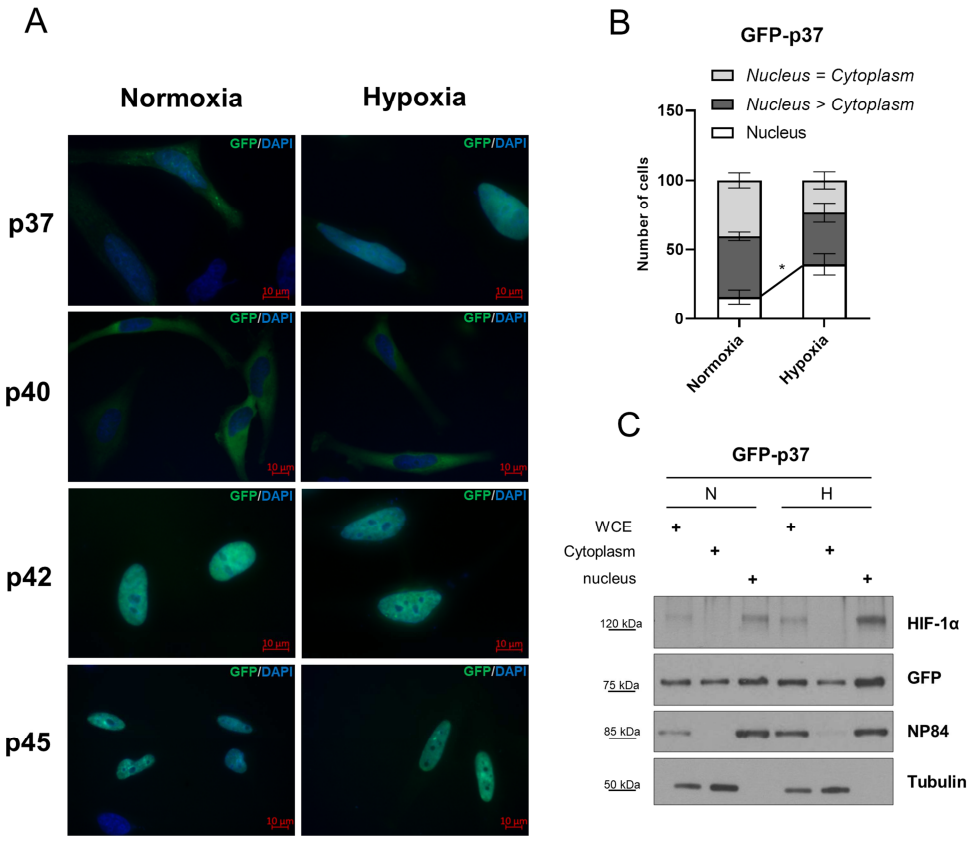

Figure R48: GFP-p37 swicth form nuclear and cytoplasmic distribution to mostly nuclear localization upon hypoxia. A) HeLa cells were seeded on coverlips and transfected with GFP-p37, GFP-p40, GFP-p42 or GFP-p50 during 24 hours and incubated either in normoxia (N; 20% O_2) or hypoxia (H; 1% O_2) overnight before fixing and mounting into microscope slides. GFP fluorescence was detected in this image in green and nuclear staining in blue (DAPI) using Axioimager D1 (Zeiss). **B)** Quantification of GFP-p37 fluorescence images. **C)** HeLa cells were transfected with GFP-p37, GFP-p40, GFP-p42 or GFP-p50 during 24 hours and incubated either in normoxia (N; 20% O_2) or hypoxia (H; 1% O_2) overnight before harvesting. Total protein extracts as well as the extracts corresponding to the different subcellular fractions were analysed by western blot. Tubulin and NP84 were used as citoplasm and nuclear fraction controls, respectively. This is a representative figure of at least three independent experiments.

The behaviour of *HIF1A* mRNA upon hypoxia (*HIF1A* pre-mRNA is not affected while total *HIF1A* mRNA levels are significantly decreased; Figure R44) is perfectly consistent with the inhibition of USP11, which exacerbates *HIF1A* turnover and also correlates with the nuclear accumulation of p37.

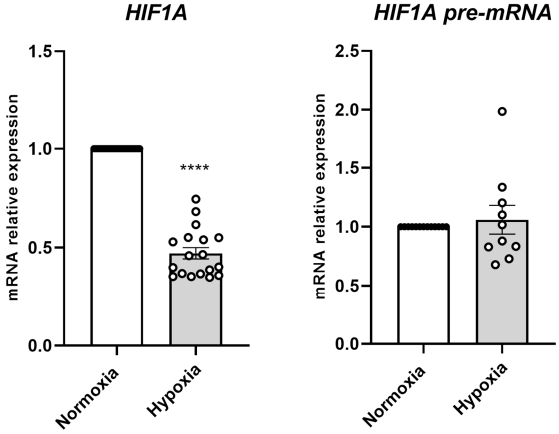

Figure R49: **Hypoxia regulates *HIF1A* mRNA posttranscriptionally.** HEK293 cells were incubated in normoxia (N; 20% O_2) or hypoxia (H; 1% O_2) overnight before harvesting. Total mRNA levels were analysed by RT-qPCR. Results are normalized to *RPLP0* following the $2^{-\Delta\Delta Ct}$ method, and represented as relative values to normoxic cells. (****p<0,0001. One sample T-test)

5 Relevance of USP11 in innate immune memory

The dogma of an innate immune system incapable of mounting adaptive responses has been contradicted by observations in BCG-vaccinated individuals in which a level of protection against disparate pathogens was identified (Netea *et al*, 2016). Indeed, the existence of long-term consequences of the stimulation of macrophages with certain simple (e.g. β-glucans, the major *Candida Albicans* cell wall constituent) or complex (e.g. BCG, the mycobacterial vaccine strain) stimuli has been recently recognized and termed 'innate immune memory or trained immunity' (Dominguez - Andres & Netea, 2019; Netea *et al*, 2016). Although the mechanisms underlying the development of innate immune memory are not completely known, both variations in metabolism (Warburg effect) mediated by the Akt/mTOR/HIF axis, and epigenetic changes are known to occur (Arts *et al*, 2016a; Kelly & O'Neill, 2015; Arts *et al*, 2016b).

The PI3K-Akt-mTOR pathway has been classically linked to the control of *HIF1A* transcription and/or HIF-1α translation. However, based in our previous data, we anticipated a further role for the USP11-mediated posttranscriptional regulation of *HIF1A* mRNA in this pathway. We therefore used torin (T, Tocris Bioscience) and rapamicin (R, LC Laboratories) to inhibit the mTOR pathway. While USP11 protein levels were not affected, the hypoxic accumulation of HIF-1α as well as the hypoxic induction of HIF1 target genes was reduced (Figure R50A). These results are consistent with the previous publications and the effect of both inhibitors on mTOR measured as the phosphorylation status of RPS6 (Figure R50A and B). Interestingly, and in agreement with our hypothesis, *HIF1A* mRNA levels were reduced upon T and R treatment, while *HIF1A* pre-mRNA levels were not affected (Figure R50C).

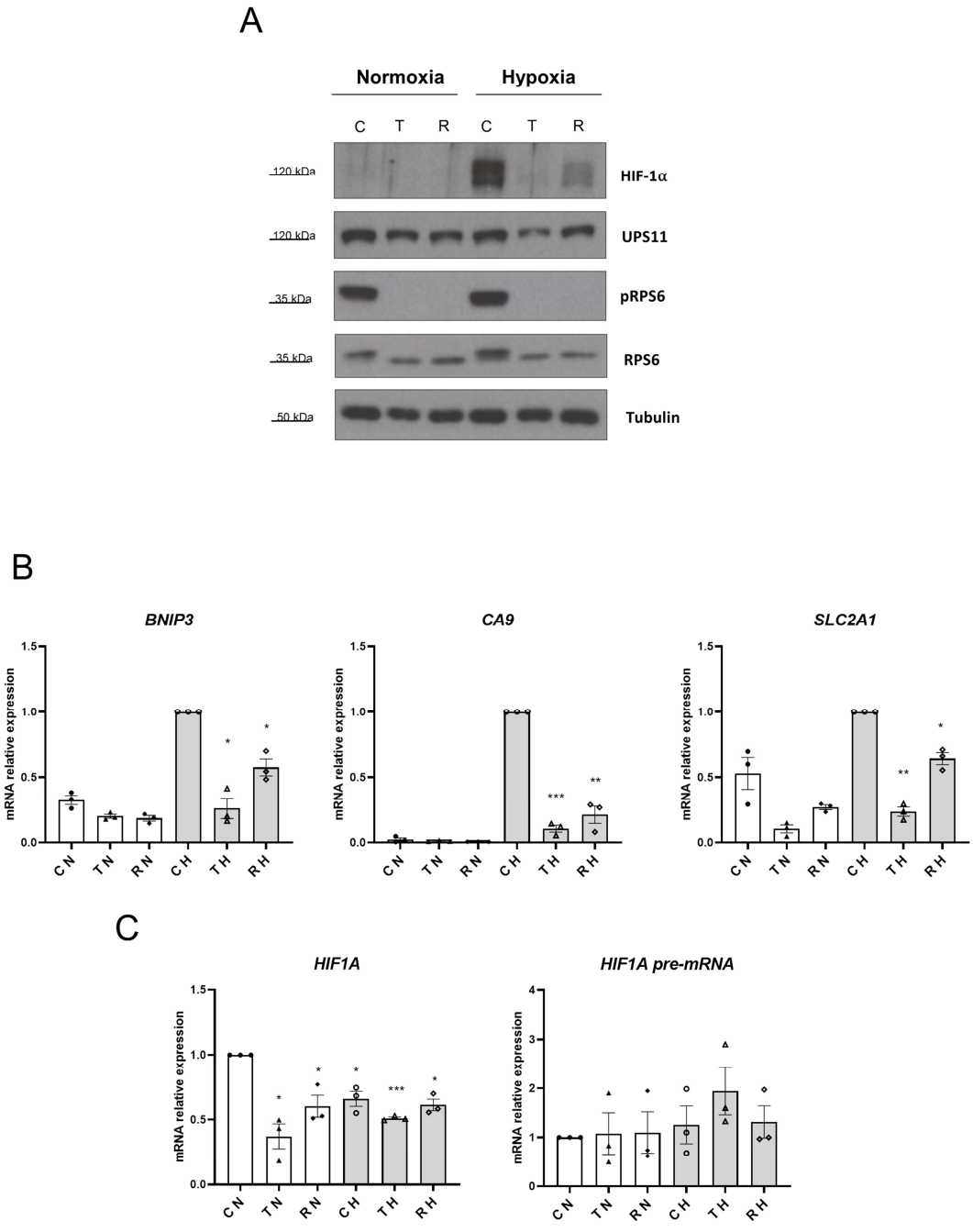

Figure R50: **mTOR inhibition decreases *HIF1A* mRNA *post-transcriptionally*.** HEK293 were untreated or treated in the presence of Torin (T, 0,25 µM) or Rapamicin (R, 0,02 µM) for 24 hours and incubated in normoxia (N; 20% O_2) or hypoxia (H; 1% O_2) overnight before harvesting. **A)** Total protein levels were analysed by WB with the indicated antibodies. Tubulin was used as a loading control. This is a representative figure of at least three independent experiments. HIF-1 target genes (B) and *HIF1A* and *pre-mRNA* mRNA levels (**C**) mRNA levels were analysed by RT-qPCR. Results are normalized to *RPLP0* following the $2^{-\Delta\Delta Ct}$ method, and represented as relative values to hypoxic or normoxic control cells (*p<0,03, **p<0,0021, ***p<0,0002. (One sample T-test One sample T-test)

Accordingly, we have hypothesized that USP11 could be implicated in the regulation of the glycolytic switch mediated by the Akt/mTOR/HIF axis in the context of trained immunity. In collaboration with Dr Anguita's lab, we have focused in the study of the trained innate memory-triggered by *Borrelia burgdorferi,* the causative agent of Lyme borreliosis.

B. burgdorferi is one of the few extracellular pathogens that are able to establish persistent infections, in part because of the need to remain in the mammalian host until ticks acquire the microorganism, which can take several months (Sprong *et al*, 2018). Interestingly, Anguita's lab has recently reported that *B. burgdorferi* triggers macrophage memory to limit host inflammation and facilitate the persistence of the infection (Barriales *et al., submitted to Virulence, KVIR-2019-0158*).

Innate immune memory is replicated *in vitro* by the use of a primary stimulus, a period of resting, and a secondary, different, stimulus. Thus, we have analyzed mRNA extracts kindly provided by Dr Anguita'lab from unstimulated or mouse bone marrow-derived macrophages (BMMs) that have been stimulated with the spirochete (48h), rested (16-20h) and restimulated (48h). As expected, an increase of the glycolytic gene *SLC2A1* was observed in experienced BMMs (Figure R51). Interestingly, experienced monocytes induced *HIF1A* upon *B. burgdorferi,* which nicely correlated with an induction of *USP11* mRNA.

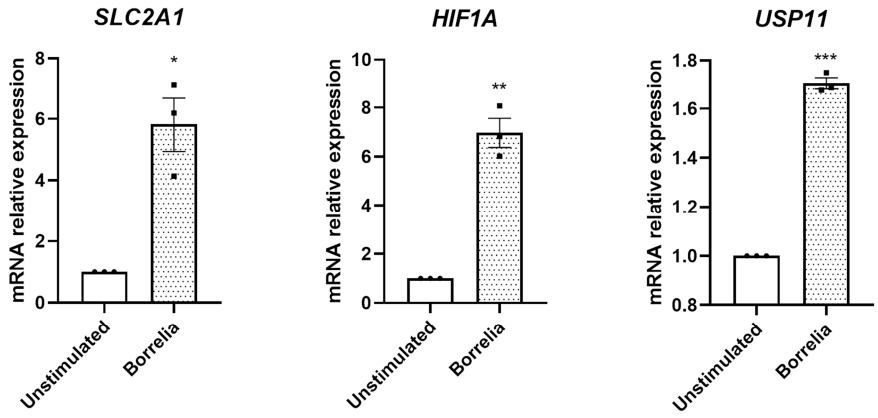

Figure R51: *Borrelia burgdorferi* induces *USP11*. Bone marrow derived monocytes were isolated from mice and differentiated to macrophages. Then, macrophages were chronically infected with *Borrelia burgdorferi* and mRNA levels analysed by RT-qPCR. Results are normalized to *RPLP0* following the $2^{-\Delta\Delta Ct}$ method, and represented as relative values to unestimulated macrophages (*p<0,03, **p<0,002. (One sample T-test One sample T-test)

We obtained similar results using human peripheral blood monocytes that were exposed to *Borrelia burgdorferi.* Upon Borrelia stimulation, human macrophages presented an induction of the glycolytic genes *LDHA* and *SLC2A1* that perfectly correlated with *HIF1A* and *USP11* mRNA induction (Figure 52A). Interestingly, when monocytes were exposed to *Lactobacillus plantarum,* a well-known probiotic and symbiotic microorganism, the induction of the above-mentioned glycolytic genes was not produced. Moreover, neither *HIF1A* nor *USP11* were induced upon *L. plantarum* stimulation (Figure 52B). This preliminary study might point to an important role of *HIF1A* post-transcriptional regulation in monocytes immune response.

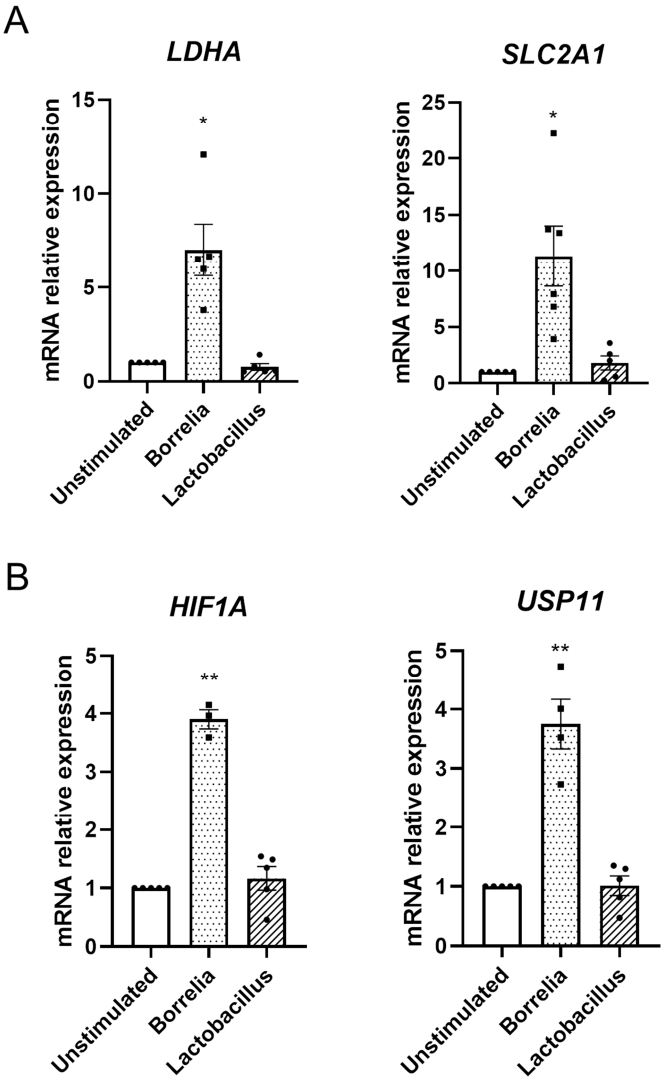

Figure R52: *USP11* induction correlates with the innate immune memory phenotype. Bone marrow derived monocytes were isolated from human healthy donors and differenced to macrophages. Then, macrophages were infected twice (48h) with *Borrelia burgdorferi* or *Lactobacillus plantarum,* leaving a resting period of 16-20 hours between infections. Total mRNA levels were analysed by RT-qPCR. **A)** *LDHA* and *SLC2A1* and **B)** *HIF1A* and *USP11* mRNA levels. Results are normalized to *RPLP0* following the $2^{-\Delta\Delta Ct}$ method, and represented as relative values to unestimulated macrophages (*p<0,03, **p<0,002. (One sample T-test One sample T-test)

Discussion:

1 RNAi screen of DUBs that modulate the hypoxia signalling cascade

Oxygen homeostasis is vital and impacts on devastating diseases of great incidence in our society. During the last 30 years, we have reached seminal contributions to the comprehension on how hypoxia triggers specific adaptive mechanisms at the physiological and molecular levels. Moreover, clinical settings such as anaemia, vascular dysfunction or tumour angiogenesis, have directly benefited from these discoveries. However, it is fair to state that we still need to go deeper into the understanding of the intricate mechanisms that remain unknown for future implications, in short, medium and long terms.

In that regard, we postulated the DUBs as essential mediators of the hypoxia signalling pathway. Furthermore, DUBs are evolutionary linked with proteases and promising targets for pharma companies as their conserved catalytic domains facilitate the use of high throughput screening assays for drug discovery. Interestingly, several inhibitors have been designed against DUBs, including several hypoxia-related DUBs, and are being tested in preclinical and/or clinical trials (Table D1).

Table D1: DUBs inhibitors that are being tested on preclinical trials.

Target	DUB	Inhibitor	Disease Indication	Stage of development	References
HIF-1α	USP20	GSK2643943A	Oncology	Preclinical	(Deng *et al*, 2012)
	USP8	HBX41108	Oncology	Preclinical	(Weinstock *et al*, 2012)
	UCHL1	LDN-57444	Cancer	Preclinical	(Gu *et al*, 2018)
	USP7	ADC-01, ADC-03	Oncology, Immuno-oncology	Preclinical	(Gavory *et al*, 2015)
		HBX41108			(Reverdy *et al*, 2012) (Colland *et al*, 2009)
		P5091			(Weinstock *et al*, 2012)
		P22077			(Weinstock *et al*, 2012)
VHL	USP9x	WP1130	Oncology	Preclinical	(Kapuria *et al*, 2010)

Based on the aforementioned arguments, a loss of function screening using a HRE-driven luciferase reporter gene was performed in our laboratory to identify new DUBs that regulate the hypoxia signalling pathway. Our results confirmed some of the DUBs reported in the meantime as mediators of the hypoxia signalling pathway (UCHL1, USP8, USP28 and OTUD7B) and identified 12 additional hits for further validation and characterization: USP10, USP11, USP13, USP29, USP32, USP40, USP47 and OTUD4 were chosen as hypoxia signalling-activating DUBs while UCHL5, USP16, STAMBPL1 and PRPF8 were chosen as hypoxia-signalling inhibiting DUBs.

We have previously shown that USP29 is indeed a novel DUB that controls HIF-1α and HIF-2α stability through a PHD/pVHL-independent mechanism implying proteasome-mediated degradation (Schober et al. manuscript in preparation). Now, by measuring the effect of the silencing of these hits on endogenous HIF-dependent genes, we directly discarded OTUD4, STAMBPL1, USP32, USP40 and USP47. Indeed, their silencing had no significant effect in the hypoxic induction of *BNIP3* or *CA9.* As expected, none of this DUBs has been related with the regulation of the hypoxia signalling pathway.

Surprisingly *PRPF8*, *USP13, USP10* or *USP16* knockdown showed some apparently contradictory results on different hypoxia-induced genes. The hypoxia-induced down-regulation of *PRPF8*, *USP10* and *USP16* as well as potential negative feedback loops could explain for these controversial results. In any case, these inconsistent results prompted us to discard these candidates.

In contrast with the screening data, UCHL5 seemed to activate the hypoxia signalling cascade. UCHL5 has been associated with the 19S regulatory subunit of the 26S proteasome (Yao *et al*, 2006), which meant a pleiotropic effect on hypoxia signalling.

Finally, the effect on HIF-target genes upon *USP11* validated the results obtained on the screening. Hence, the strong and consistent down-regulation of the hypoxia signalling cascade upon *USP11* silencing argued our decision to focus on this specific DUB and further characterize USP11 mechanism of

action. Furthermore, in spite of the prominent number of USP11 targets, there was no report connecting USP11 with hypoxia.

2 USP11 is an activator of the hypoxia-signalling cascade.

Regulation of cell cycle and apoptosis or the control of DNA damage response is among the most important cellular process controlled by USP11. Our most recent data point to USP11 as a new activator of hypoxia-driven adaptation. Therefore, it is tempting to speculate that USP11 could act as signal hub integrating vital information that allows cells to deal with stress.

In vitro results showed the preferential affinity of USP11 towards K63- and K6-Ub chains over the different types of Ub-chains (Harper *et al*, 2014). By contrast, most of the reports attribute a role for USP11 as a stabilizing DUB, which is classically mediated through K48-Ub chains. Hence, it is tempting to speculate about the relevance of some of the above mentioned targets. The simplest explanation could be the unfortunately too extensive use of inappropriate ubiquitination assays that very often omit the basic and essential requirement of this type of assays: the use of denaturing conditions. Nevertheless, we can't exclude at this point the implication of K48/K63 branched Ub-chains that target for proteasomal degradation (Ohtake *et al*, 2018) and therefore, further and accurate MS studies will be required to clarify the complexity of Ub-chains and USP11 functionality.

3 HIF1α regulation by USP11

HIF-α canonical regulation mediated by the O_2/PHD/pVHL axis can be bypass by a number of mechanisms. For example, an increase in transcription or translation is able to produce an accumulation of HIF-1α in normoxic conditions in spite of proficient PHDs-mediated degradation (See section 1.1.2.2.1 and 1.1.2.2.3). Thus, deciphering new mechanisms, which fine tune

HIF-α accumulation independently of the canonical regulation is of paramount importance.

In this project we have characterized how USP11 is essential to maintain *HIF1A* mRNA stability. Accordingly, *USP11* knockdown and *HIF1A* mRNA destabilization are sufficient to abolish the hypoxia-dependent transcriptional response. Our data clearly state a specific role for USP11 in HIF-1α regulation in spite of the problems we have had to validate this effect on HIF-2-dependent genes. Thus, USP11 joins the list of DUBS that regulate HIF-1α towards different mechanisms. Indeed, USP8, USP29, Cezanne and MCPIP1 have been reported to control HIF-1α and HIF-2α (Troilo *et al*, 2014; Bremm *et al*, 2014a; Moniz *et al*, 2015; Sun *et al*, 2018a; Ligeza *et al*, 2017; Schober et al., manuscript in preparation). However, USP20, UCHL1, USP9x, USP28, USP7 and USP19 have been reported to target specific HIF-α isoforms as it is the case for USP11 (Li *et al*, 2005; Goto *et al*, 2015; Zhang *et al*, 2016a; Flugel *et al*, 2012; Wu *et al*, 2016a; Lu *et al*, 2011).

To our knowledge, USP11 is the first DUB to be reported as a post-transcriptional regulator of HIF-1α. We licence to discard the previously reported contribution of USP52 and MCPIP1 on *HIF1A* and *EPAS1* mRNA stability, respectively (Bett *et al*, 2013b; Sun *et al*, 2018b). Indeed, USP52 is not really a DUB enzyme and the results supporting the role of MCPIP1 to up regulate *EPAS1* mRNA levels in a post-transcriptional manner are more than questionable.

Although our data strongly support USP11-mediated post-transcriptional regulation of *HIF1A* as playing the major role in USP11-driven HIF signalling regulation, we cannot discard the minor effect of USP11 silencing on the ectopic expression of HIF-1α as well as HIF-2α. Such impact could be consistent with the recently report suggesting that USP11 promotes DLBCL proliferation by enhancing eIF4B-dependent protein translation (Kapadia *et al*, 2018).

USP11 regulation of *HIF1A* mRNA stability involves a RNP complex composed of at least hnRNPD and USP11, though we could anticipate a RNP complex composed by additional RNA-regulatory proteins. USP11 and hnRNPD as a complex appear to specifically control *HIF1A* mRNA stability, as USP11 is not present on the RNP complex containing hnRNPD that targets *VEGFA* or *MEF2C* (Xin *et al*, 2012; Panda *et al*, 2014). Hence, our results strongly suggest that USP11 is not present by default in every RNP complex containing hnRNPD.

hnRNPD is indeed an essential partner of the complex and validates previous PAR-CLIP *in silico* data from Dr Gorospe's laboratory (Yoon *et al*, 2014). However, the presence of USP11 is much more surprising and unexpected. In this regard, it would be really interesting to study whether USP11 is directly regulating any other transcripts at posttranscriptional level and analyse the landscape of such interactions. Only two DUBs have been reported to bind mRNAs: MCPIP1, which holds RNAse activity and directly control *IL6ST* mRNA (Matsushita *et al*, 2009) and OTUD4 that has recently proposed as an essential component of neuronal RNA stress and mobile granules by interacting with RBPs as HuB and SMN1, and to directly bind its own mRNA (Das *et al*, 2019).

USP11 does not affect hnRNPD protein levels according with USP11 regulating protein signalling rather than protein stability. While our preliminary data suggest that USP11 silencing did not affect hnRNPD polyubiquitination, further replicates should be required to confirm these data. Similarly, it could be interesting to characterize the RNP complex and to analyse whether USP11 is directly regulating specific partner(s) of the RNP complex.

4 Hypoxic regulation of the hnRNPD/USP11 ribonucleoprotein complex

We propose that hypoxia tends to destabilize *HIF1A* mRNA in order to avoid sustained activation of HIF similar to the negative feedback loops already described(Connolly *et al*, 2006; Liu *et al*, 2006; Ginouves *et al*, 2008; Stiehl *et al*, 2012; Moore *et al*, 2015). Furthermore, the behaviour of *HIF1A* mRNA and the role of USP11 and hnRNPD in regulating *HIF1A* mRNA turnover prompted us to analyse the potential impact of hypoxia on both mediators. Hypoxia did not impact on USP11 or hnRNPD mRNA and protein levels, but interestingly, hypoxia modulates USP11 catalytic activity and the cellular location of p37, the hnRNPD isoform that preferentially binds *HIF1A* mRNA.

Hypoxia inhibits USP11 activity in a reversible manner, which is further independent of oxygen sensor activity. Information of USP11 catalytic activity regulation by cellular stimulus is scarce. Very recently, USP11 serine 452 (S452), whose phosphorylation is catalysed by S6K1, has been described as an essential residue for USP11 enzymatic activity. Ser452 is located in the UBL2 domain within the USP11 bipartite catalytic domains and therefore, such phosphorylation could impair Ub binding. However, the exact localization of Ser452 on USP11 structure is not known, as USP11 3D structure has not been solved. Surprisingly, it has been suggested that phosphorylation of Ser452 is required for USP11 to be catalytically active based on *in cellulo* studies. However, *in vitro* ubiquitination studies using recombinant USP11 protein contradict such *in cellulo* assays (Kapadia *et al*, 2018). In this regard, our data based on ABP assays clearly state that the mutation of the Ser452 by an Ala residue really abolished USP11 enzymatic activity. Despite we were not able to detect direct changes in Ser452 phosphorylation, a nice correlation between decrease of both, S6K1 and USP11 activities is observed upon hypoxia. However, more accurate experiments are needed in order to confirm the of Ser452 phosphorylation in hypoxia-induced inhibition of USP11 activity. MS analyses of USP11 from normoxic or hypoxic cells are on-going to clarify this point.

In addition, hypoxia increased USP11 polyubiquitination raise new questions about USP11 regulation. Whether USP11 ubiquitination is a read-out of the compromised USP11 catalytic activity upon hypoxia or USP11 ubiquitination directly contributes to USP11 activity and/or USP11 interaction landscape is still uncertain and further studies are required.

A very recent paper, reported that PTEN activity is required to maintain USP11 protein levels (Park *et al*, 2019). By contrast, we could not detect changes in USP11 levels comparing prostate samples of PTEN KO and control mice as well as prostate cancer cell lines in which the expression of PTEN has been genetically manipulated (data not shown).

Similar to our findings, shuttling of RBPs has been previously reported. In the case of HuR, for instance, cytoplasm localization has been shown to be essential to stabilize its targeted mRNAs, and nuclear sequestration impedes its function(von Roretz *et al*, 2011). We have identified a nuclear accumulation of p37 upon hypoxia that has not been previously described in the literature. hnRNPD isoforms, p37 and p40, have been reported to shuttle (Sarkar *et al*, 2003a) and 14-3-3σ up-regulation has been shown to maintain hnRNPD on the cytoplasmic fraction(He & Schneider, 2006; Rizou *et al*, 2018). Whether such mechanisms might be implicated in hypoxia-induced p37 nuclear accumulation remains to be addressed. While, we discard a role for USP11-mediated p37 ubiquitination, we cannot rule out the possibility that changes in the USP11 ubiquitination status could affect the affinity to bind p37 and therefore, to regulate p37 shuttling.

5 Relevance of USP11 in innate immune memory

HIF-1α up-regulation during immune responses have been thought to occur transcriptionally through NF-κB (Frede *et al*, 2006; Rius *et al*, 2008). Furthermore, HIF-1-mediated aerobic glycolysis essential to develop macrophage trained immune response was reported to involve mTOR transcriptional and post-translational effects (Cheng *et al*, 2014b; Majumder *et*

al, 2004). Our data show a good correlation between *HIF1A* and *USP11* up-regulation that is specific for *Borrelia burgdorferi* infection. These results point to a role of *HIF1A* posttranscriptional regulation to control monocytes, although we are confident that those are preliminary results and that more experiments are required to confirm these results. In this regard, in addition to directly analyse the levels of *HIF1A* pre-mRNA to confirm the relevance of *HIF1A* posttranscriptional regulation and to analyse the transcription factors induced by *B. burgdorferi* that could be mediating USP11 upregulation, we currently generate a colony of *usp11*$^{-/-}$ mice in our animal facility. Hopefully, this animal model will help us to understand the implication of USP11 on pathogen-host responses as well as the different immune responses elicit by macrophages depending on pathogen and symbiont microorganism infection, using *Borrelia burgdorferi* and *Lactobacillus plantarum,* respectively.

6 Outlook and perspectives

In accordance with the aforementioned results, we propose a model summarized in Figure D1. In this model, active USP11 is part of the *HIF1A* RNP complex, whose main function is to stabilize *HIF1A* in normoxia by either recruiting stabilizing elements (X, Y or Z from Figure D1) or competing with destabilizing components including miRNA(s) that target *HIF1A 3'UTR*. hnRNPD and in particular, the p37 isoform, is an additional and essential partner of the complex assuring *HIF1A* mRNA steady state levels in well oxygenated cells. Upon hypoxia, USP11 deubiquitinating activity is inhibited and p37 accumulates into the nucleus. We still don't know whether these two hypoxia-induced responses are directly linked or not. Anyway, we propose that USP11 inhibition leads to increased ubiquitination of USP11 and eventually of additional partner(s) of the *HIF1A* RNP complex. This increased in ubiquitination could undo the recruitment of stabilizing elements and/or favouring the binding of destabilizing components (D from Figure D1). Alternatively, the switch in the recruitment of stabilizing versus destabilizing elements could be dictated by the presence of p37 into the *HIF1A* RNP complex that depends on oxygen availability.

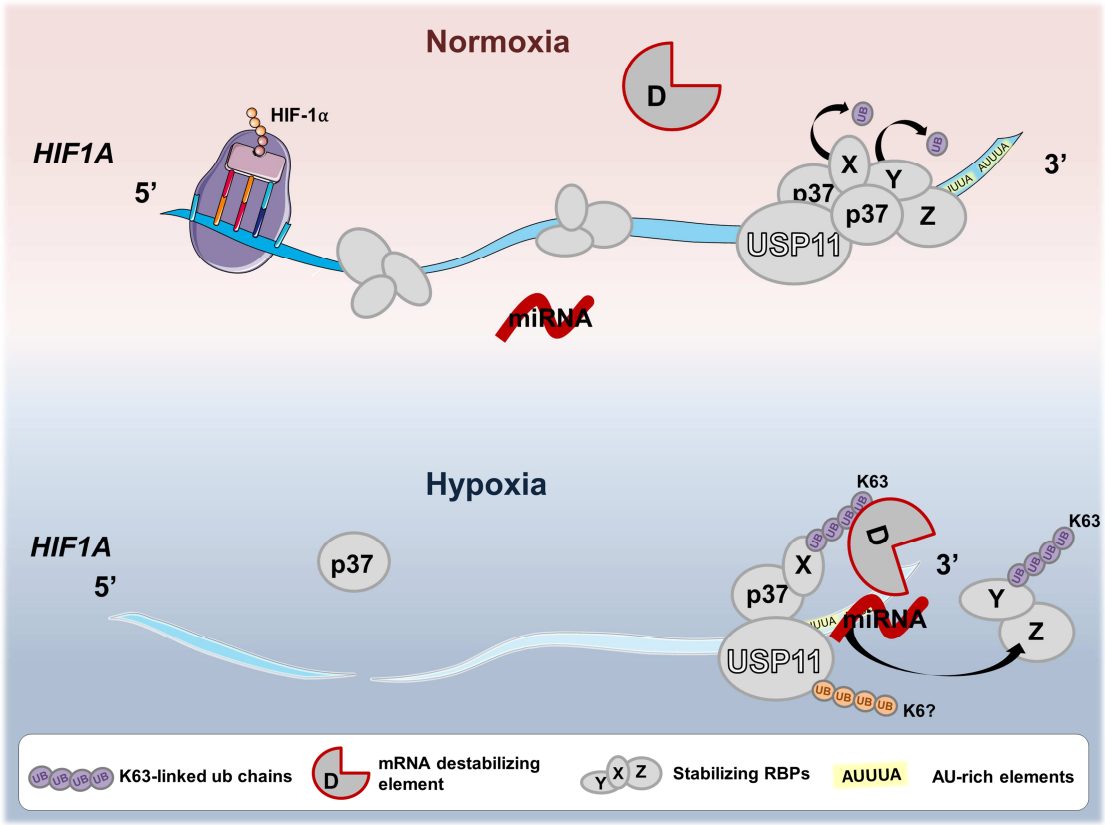

Figure D1: Depicted model for *HIF1A* mRNA stability regulation by USP11.

Identifying a new regulatory pathway as we have described in this research project is certainly a challenging task. However at the end of the project, new and demanding question arise: what are the partners of *HIF1A* RNP complex and which one, if any, is regulated by USP11 catalytic activity? How *HIF1A* decreases during hypoxia? Is *HIF1A* posttranscriptional regulation a good target to modulate the hypoxia pathway and/or the innate immune response? How is USP11 catalytic activity and hnRNPD/p37 shuttling regulated by hypoxia? We can speculate but the real answers will have to wait.

Conclusions

In summary, the results obtained throughout this project lead to the following conclusions:

1) USP11 is an activator of the hypoxia signalling cascade in different cellular contexts. Indeed, USP11 is necessary to sustain hypoxia-driven signalling.

2) USP11 exclusively controls HIF-1α by regulating *HIF1A* mRNA stability.

3) USP11 can be pharmacologically inhibited with Mitoxantrone, which also exacerbates *HIF1A* turnover and prevents HIF-signalling without affecting *EPAS1* mRNA.

4) USP11 binds hnRNPD and promote *HIF1A* mRNA stability, towards hnRNPD-mediated interaction with *HIF1A* 3'UTR.

5) Hypoxia decreases USP11 activity as well as promotes hnRNPD/p37 localization into the nuclear compartment.

6) USP11-mediated *HIF1A* up-regulation upon *Borrelia burgdorferi* chronic infection may present a new opportunity to understand the pathology of Lyme disease.

Bibliography

Abdelmohsen K, Pullmann R, Lal A, Kim HH, Galban S, Yang X, Blethrow JD, Walker M, Shubert J, Gillespie DA, Furneaux H, Gorospe M & Gorospe M (2007) Phosphorylation of HuR by Chk2 regulates SIRT1 expression. *Mol. Cell* **25:** 543–57 Available at: http://www.ncbi.nlm.nih.gov/pubmed/17317627 [Accessed September 19, 2019]

Adamovich Y, Ladeuix B, Golik M, Koeners MP & Asher G (2017) Rhythmic Oxygen Levels Reset Circadian Clocks through HIF1α. *Cell Metab.* **25:** 93–101 Available at: http://www.ncbi.nlm.nih.gov/pubmed/27773695 [Accessed September 5, 2019]

Akutsu M, Dikic I & Bremm A (2016) Ubiquitin chain diversity at a glance. *J. Cell Sci.* **129:** 875–880 Available at: http://www.ncbi.nlm.nih.gov/pubmed/26906419 [Accessed September 8, 2019]

Altun M, Zhao B, Velasco K, Liu H, Hassink G, Paschke J, Pereira T & Lindsten K (2012) Ubiquitin-specific protease 19 (USP19) regulates hypoxia-inducible factor 1α (HIF-1α) during hypoxia. *J. Biol. Chem.* **287:** 1962–9 Available at: http://www.jbc.org/lookup/doi/10.1074/jbc.M111.305615 [Accessed September 14, 2019]

Amelio I, Inoue S, Markert EK, Levine AJ, Knight RA, Mak TW & Melino G (2015) TAp73 opposes tumor angiogenesis by promoting hypoxia-inducible factor 1α degradation. *Proc. Natl. Acad. Sci.* **112:** 226–231

An J, Mo D, Liu H, Veena MS, Srivatsan ES, Massoumi R & Rettig MB (2008) Inactivation of the CYLD Deubiquitinase by HPV E6 Mediates Hypoxia-Induced NF-κB Activation. *Cancer Cell* **14:** 394–407 Available at: http://www.ncbi.nlm.nih.gov/pubmed/18977328 [Accessed August 23, 2019]

Aprelikova O, Wood M, Tackett S, Chandramouli GVR & Barrett JC (2006) Role of ETS Transcription Factors in the Hypoxia-Inducible Factor-2 Target Gene Selection. *Cancer Res.* **66:** 5641–5647 Available at: http://cancerres.aacrjournals.org/lookup/doi/10.1158/0008-5472.CAN-05-3345 [Accessed September 6, 2019]

Arts RJW, Carvalho A, La Rocca C, Palma C, Rodrigues F, Silvestre R, Kleinnijenhuis J, Lachmandas E, Gonçalves LG, Belinha A, Cunha C, Oosting M, Joosten LAB, Matarese G, van Crevel R & Netea MG (2016a) Immunometabolic Pathways in BCG-Induced Trained Immunity. *Cell Rep.* **17:** 2562–2571 Available at: https://linkinghub.elsevier.com/retrieve/pii/S2211124716315522 [Accessed September 19, 2019]

Arts RJW, Novakovic B, Ter Horst R, Carvalho A, Bekkering S, Lachmandas E, Rodrigues F, Silvestre R, Cheng S-C, Wang S-Y, Habibi E, Gonçalves LG, Mesquita I, Cunha C, van Laarhoven A, van de Veerdonk FL, Williams DL, van der Meer JWM, Logie C, O'Neill LA, et al (2016b) Glutaminolysis and Fumarate Accumulation Integrate Immunometabolic and Epigenetic Programs in Trained Immunity. *Cell Metab.* **24:** 807–819 Available at: https://linkinghub.elsevier.com/retrieve/pii/S1550413116305393 [Accessed September 19, 2019]

Barreau C, Paillard L & Osborne HB (2005) AU-rich elements and associated factors: are there unifying principles? *Nucleic Acids Res.* **33:** 7138–50

Available at: http://www.ncbi.nlm.nih.gov/pubmed/16391004 [Accessed August 22, 2019]
Batie M, Frost J, Frost M, Wilson JW, Schofield P & Rocha S (2019) Hypoxia induces rapid changes to histone methylation and reprograms chromatin. *Science* **363:** 1222–1226 Available at: http://www.sciencemag.org/lookup/doi/10.1126/science.aau5870 [Accessed September 6, 2019]
Bayraktar S, Gutierrez Barrera AM, Liu D, Pusztai L, Litton J, Valero V, Hunt K, Hortobagyi GN, Wu Y, Symmans F & Arun B (2013) USP-11 as a Predictive and Prognostic Factor Following Neoadjuvant Therapy in Women With Breast Cancer. *Cancer J.* **19:** 10–17 Available at: http://www.ncbi.nlm.nih.gov/pubmed/23337751 [Accessed July 30, 2019]
Bernardi R, Guernah I, Jin D, Grisendi S, Alimonti A, Teruya-Feldstein J, Cordon-Cardo C, Celeste Simon M, Rafii S & Pandolfi PP (2006) PML inhibits HIF-1α translation and neoangiogenesis through repression of mTOR. *Nature* **442:** 779–785 Available at: http://www.ncbi.nlm.nih.gov/pubmed/16915281 [Accessed July 16, 2019]
Berra E, Benizri E, Ginouvès A, Volmat V, Roux D & Pouysségur J (2003) HIF prolyl-hydroxylase 2 is the key oxygen sensor setting low steady-state levels of HIF-1 in normoxia. *EMBO J.* **22:** 4082–4090 Available at: http://www.ncbi.nlm.nih.gov/pubmed/12912907 [Accessed September 6, 2019]
Bett JS, Ibrahim AFM, Garg AK, Kelly V, Pedrioli P, Rocha S & Hay RT (2013a) The P-body component USP52/PAN2 is a novel regulator of HIF1A mRNAstability. *Biochem. J.* **451:** 185 Available at: https://www.ncbi.nlm.nih.gov/pmc/articles/PMC3632086/ [Accessed August 22, 2019]
Bett JS, Ibrahim AFM, Garg AK, Kelly V, Pedrioli P, Rocha S & Hay RT (2013b) The P-body component USP52/PAN2 is a novel regulator of *HIF1A* mRNA stability. *Biochem. J.* **451:** 185–194 Available at: http://biochemj.org/lookup/doi/10.1042/BJ20130026 [Accessed February 20, 2019]
Bomberger JM, Ye S, MacEachran DP, Koeppen K, Barnaby RL, O'Toole GA & Stanton BA (2011) A Pseudomonas aeruginosa toxin that hijacks the host ubiquitin proteolytic system. *PLoS Pathog.* **7:**
Bonello S, Zähringer C, BelAiba RS, Djordjevic T, Hess J, Michiels C, Kietzmann T & Görlach A (2007) Reactive Oxygen Species Activate the HIF-1α Promoter Via a Functional NFκB Site. *Arterioscler. Thromb. Vasc. Biol.* **27:** 755–761 Available at: http://www.ncbi.nlm.nih.gov/pubmed/17272744 [Accessed September 6, 2019]
Borden KLB & Culjkovic B (2009) Perspectives in PML: a unifying framework for PML function. *Front. Biosci. (Landmark Ed.* **14:** 497–509 Available at: http://www.ncbi.nlm.nih.gov/pubmed/19273081 [Accessed August 30, 2019]
Bremm A, Moniz S, Mader J, Rocha S & Komander D (2014a) Cezanne (OTUD7B) regulates HIF-1α homeostasis in a proteasome-independent manner. *EMBO Rep.* **15:** 1268–77 Available at: http://www.ncbi.nlm.nih.gov/pubmed/25355043 [Accessed September 9, 2019]

Bremm A, Moniz S, Mader J, Rocha S & Komander D (2014b) Cezanne (OTUD 7B) regulates HIF -1α homeostasis in a proteasome-independent manner. *EMBO Rep.* **15:** 1268–1277 Available at: http://www.ncbi.nlm.nih.gov/pubmed/25355043 [Accessed August 23, 2019]

Bruick RK & McKnight SL (2001) A Conserved Family of Prolyl-4-Hydroxylases That Modify HIF. *Science (80-.).* **294:** 1337–1340 Available at: http://www.ncbi.nlm.nih.gov/pubmed/11598268 [Accessed August 15, 2019]

Bruning U, Cerone L, Neufeld Z, Fitzpatrick SF, Cheong A, Scholz CC, Simpson DA, Leonard MO, Tambuwala MM, Cummins EP & Taylor CT (2011) MicroRNA-155 Promotes Resolution of Hypoxia-Inducible Factor 1 Activity during Prolonged Hypoxia. *Mol. Cell. Biol.* **31:** 4087–4096 Available at: http://www.ncbi.nlm.nih.gov/pubmed/21807897 [Accessed September 8, 2019]

Burkhart RA, Peng Y, Norris ZA, Tholey RM, Talbott VA, Liang Q, Ai Y, Miller K, Lal S, Cozzitorto JA, Witkiewicz AK, Yeo CJ, Gehrmann M, Napper A, Winter JM, Sawicki JA, Zhuang Z & Brody JR (2013) Mitoxantrone Targets Human Ubiquitin-Specific Peptidase 11 (USP11) and Is a Potent Inhibitor of Pancreatic Cancer Cell Survival. *Mol. Cancer Res.* **11:** 901–911 Available at: http://www.ncbi.nlm.nih.gov/pubmed/23696131 [Accessed August 24, 2019]

Buscà R, Berra E, Gaggioli C, Khaled M, Bille K, Marchetti B, Thyss R, Fitsialos G, Larribère L, Bertolotto C, Virolle T, Barbry P, Pouysségur J, Ponzio G & Ballotti R (2005) Hypoxia-inducible factor 1α is a new target of microphthalmia-associated transcription factor (MITF) in melanoma cells. *J. Cell Biol.* **170:** 49–59 Available at: http://www.ncbi.nlm.nih.gov/pubmed/15983061 [Accessed August 12, 2019]

Chakraborty AA, Laukka T, Myllykoski M, Ringel AE, Booker MA, Tolstorukov MY, Meng YJ, Meier SR, Jennings RB, Creech AL, Herbert ZT, McBrayer SK, Olenchock BA, Jaffe JD, Haigis MC, Beroukhim R, Signoretti S, Koivunen P & Kaelin WG (2019) Histone demethylase KDM6A directly senses oxygen to control chromatin and cell fate. *Science (80-.).* **363:** 1217–1222 Available at: https://science.sciencemag.org/content/363/6432/1217.long [Accessed September 6, 2019]

Chamboredon S, Ciais D, Desroches-Castan A, Savi P, Bono F, Feige J-J & Cherradi N (2011a) Hypoxia-inducible factor-1α mRNA: a new target for destabilization by tristetraprolin in endothelial cells. *Mol. Biol. Cell* **22:** 3366–78 Available at: http://www.ncbi.nlm.nih.gov/pubmed/21775632 [Accessed August 12, 2019]

Chamboredon S, Ciais D, Desroches-Castan A, Savi P, Bono F, Feige J-J & Cherradi N (2011b) Hypoxia-inducible factor-1α mRNA: a new target for destabilization by tristetraprolin in endothelial cells. *Mol. Biol. Cell* **22:** 3366–78 Available at: http://www.ncbi.nlm.nih.gov/pubmed/21775632 [Accessed August 20, 2019]

Chamboredon S, Ciais D, Desroches-Castan A, Savi P, Bono F, Feige J-J & Cherradi N (2011c) Hypoxia-inducible factor-1α mRNA: a new target for destabilization by tristetraprolin in endothelial cells. *Mol. Biol. Cell* **22:**

3366–3378 Available at: https://www.molbiolcell.org/doi/10.1091/mbc.e10-07-0617 [Accessed August 12, 2019]
Chegini N & Safa AR (1987) Influence of mitoxantrone on nucleolar function in MDA-MB-231 human breast tumor cell line. *Cancer Lett.* **37:** 327–336 Available at: http://www.ncbi.nlm.nih.gov/pubmed/3677064 [Accessed September 9, 2019]
Cheng D, Zhao H, Yang Y, Hu T & Yang Q (2014a) GSK3β negatively regulates HIF1α mRNA stability via nucleolin in the MG63 osteosarcoma cell line. *Biochem. Biophys. Res. Commun.* **443:** 598–603 Available at: http://www.ncbi.nlm.nih.gov/pubmed/24333432 [Accessed August 22, 2019]
Cheng S-C, Quintin J, Cramer RA, Shepardson KM, Saeed S, Kumar V, Giamarellos-Bourboulis EJ, Martens JHA, Rao NA, Aghajanirefah A, Manjeri GR, Li Y, Ifrim DC, Arts RJW, van der Veer BMJW, van der Meer BMJW, Deen PMT, Logie C, O'Neill LA, Willems P, et al (2014b) mTOR- and HIF-1α-mediated aerobic glycolysis as metabolic basis for trained immunity. *Science* **345:** 1250684 Available at: http://www.ncbi.nlm.nih.gov/pubmed/25258083 [Accessed September 18, 2019]
Cheng Y-C, Liou J-P, Kuo C-C, Lai W-Y, Shih K-H, Chang C-Y, Pan W-Y, Tseng JT & Chang J-Y (2013) MPT0B098, a novel microtubule inhibitor that destabilizes the hypoxia-inducible factor-1α mRNA through decreasing nuclear-cytoplasmic translocation of RNA-binding protein HuR. *Mol. Cancer Ther.* **12:** 1202–12 Available at: http://mct.aacrjournals.org/cgi/doi/10.1158/1535-7163.MCT-12-0778 [Accessed November 22, 2018]
Choi B-J, Park S-A, Lee S-Y, Cha YN & Surh Y-J (2017) Hypoxia induces epithelial-mesenchymal transition in colorectal cancer cells through ubiquitin-specific protease 47-mediated stabilization of Snail: A potential role of Sox9. *Sci. Rep.* **7:** 15918 Available at: http://www.ncbi.nlm.nih.gov/pubmed/29162839 [Accessed August 23, 2019]
Chun Y-S, Choi E, Kim T-Y, Kim M-S & Park J-W (2002) A dominant-negative isoform lacking exons 11 and 12 of the human hypoxia-inducible factor-1alpha gene. *Biochem. J.* **362:** 71–9 Available at: http://www.ncbi.nlm.nih.gov/pubmed/11829741 [Accessed August 20, 2019]
Chun Y-S, Lee K-H, Choi E, Bae S-Y, Yeo E-J, Huang LE, Kim M-S & Park J-W (2003) Phorbol ester stimulates the nonhypoxic induction of a novel hypoxia-inducible factor 1alpha isoform: implications for tumor promotion. *Cancer Res.* **63:** 8700–7 Available at: http://www.ncbi.nlm.nih.gov/pubmed/14695184 [Accessed August 20, 2019]
Chun YS, Choi E, Yeo EJ, Lee JH, Kim MS & Park JW (2001) A new HIF-1 alpha variant induced by zinc ion suppresses HIF-1-mediated hypoxic responses. *J. Cell Sci.* **114:** 4051–61 Available at: http://www.ncbi.nlm.nih.gov/pubmed/11739637 [Accessed September 8, 2019]
Clague MJ, Barsukov I, Coulson JM, Liu H, Rigden DJ & Urbé S (2013) Deubiquitylases From Genes to Organism. *Physiol. Rev.* **93:** 1289–1315

Available at: http://www.ncbi.nlm.nih.gov/pubmed/23899565 [Accessed September 8, 2019]
Clague MJ, Urbé S & Komander D (2019) Breaking the chains: deubiquitylating enzyme specificity begets function. *Nat. Rev. Mol. Cell Biol.* **20:** 338–352 Available at: http://www.ncbi.nlm.nih.gov/pubmed/30733604 [Accessed September 8, 2019]
Colland F, Formstecher E, Jacq X, Reverdy C, Planquette C, Conrath S, Trouplin V, Bianchi J, Aushev VN, Camonis J, Calabrese A, Borg-Capra C, Sippl W, Collura V, Boissy G, Rain J-C, Guedat P, Delansorne R & Daviet L (2009) Small-molecule inhibitor of USP7/HAUSP ubiquitin protease stabilizes and activates p53 in cells. *Mol. Cancer Ther.* **8:** 2286–2295 Available at: http://www.ncbi.nlm.nih.gov/pubmed/19671755 [Accessed September 10, 2019]
Coltella N, Percio S, Valsecchi R, Cuttano R, Guarnerio J, Ponzoni M, Pandolfi PP, Melillo G, Pattini L & Bernardi R (2014) HIF factors cooperate with PML - RAR α to promote acute promyelocytic leukemia progression and relapse. *EMBO Mol. Med.* **6:** 640–650 Available at: http://www.ncbi.nlm.nih.gov/pubmed/24711541 [Accessed August 22, 2019]
Compernolle V, Brusselmans K, Acker T, Hoet P, Tjwa M, Beck H, Plaisance S, Dor Y, Keshet E, Lupu F, Nemery B, Dewerchin M, Van Veldhoven P, Plate K, Moons L, Collen D & Carmeliet P (2002) Loss of HIF-2α and inhibition of VEGF impair fetal lung maturation, whereas treatment with VEGF prevents fatal respiratory distress in premature mice. *Nat. Med.* **8:** 702–710 Available at: http://www.nature.com/articles/nm721 [Accessed September 6, 2019]
Connolly E, Braunstein S, Formenti S & Schneider RJ (2006) Hypoxia Inhibits Protein Synthesis through a 4E-BP1 and Elongation Factor 2 Kinase Pathway Controlled by mTOR and Uncoupled in Breast Cancer Cells. *Mol. Cell. Biol.* **26:** 3955–3965 Available at: http://www.ncbi.nlm.nih.gov/pubmed/16648488 [Accessed September 7, 2019]
Cortazar AR, Torrano V, Martín-Martín N, Caro-Maldonado A, Camacho L, Hermanova I, Guruceaga E, Lorenzo-Martín LF, Caloto R, Gomis RR, Apaolaza I, Quesada V, Trka J, Gomez-Muñoz A, Vincent S, Bustelo XR, Planes FJ, Aransay AM & Carracedo A (2018) CANCERTOOL: A Visualization and Representation Interface to Exploit Cancer Datasets. *Cancer Res.* **78:** 6320–6328 Available at: http://cancerres.aacrjournals.org/lookup/doi/10.1158/0008-5472.CAN-18-1669 [Accessed August 30, 2019]
Covello KL, Simon MC & Keith B (2005) Targeted Replacement of Hypoxia-Inducible Factor-1α by a Hypoxia-Inducible Factor-2α Knock-in Allele Promotes Tumor Growth. *Cancer Res.* **65:** 2277–2286 Available at: http://cancerres.aacrjournals.org/lookup/doi/10.1158/0008-5472.CAN-04-3246 [Accessed September 6, 2019]
Cox J, Hein MY, Luber CA, Paron I, Nagaraj N & Mann M (2014) Accurate Proteome-wide Label-free Quantification by Delayed Normalization and Maximal Peptide Ratio Extraction, Termed MaxLFQ. *Mol. Cell. Proteomics* **13:** 2513–2526 Available at: http://www.ncbi.nlm.nih.gov/pubmed/24942700 [Accessed October 10,

2019]
Cox J & Mann M (2008) MaxQuant enables high peptide identification rates, individualized p.p.b.-range mass accuracies and proteome-wide protein quantification. *Nat. Biotechnol.* **26:** 1367–1372 Available at: http://www.ncbi.nlm.nih.gov/pubmed/19029910 [Accessed August 5, 2019]
Cox J, Neuhauser N, Michalski A, Scheltema RA, Olsen J V. & Mann M (2011) Andromeda: A Peptide Search Engine Integrated into the MaxQuant Environment. *J. Proteome Res.* **10:** 1794–1805 Available at: http://www.ncbi.nlm.nih.gov/pubmed/21254760 [Accessed August 5, 2019]
Cuende J, Moreno S, Bolaños JP & Almeida A (2008) Retinoic acid downregulates Rae1 leading to APC(Cdh1) activation and neuroblastoma SH-SY5Y differentiation. *Oncogene* **27:** 3339–44 Available at: http://www.nature.com/articles/1210987 [Accessed August 5, 2019]
Cui J, Duan B, Zhao X, Chen Y, Sun S, Deng W, Zhang Y, Du J, Chen Y & Gu L (2016) MBD3 mediates epigenetic regulation on EPAS1 promoter in cancer. *Tumor Biol.* **37:** 13455–13467 Available at: http://www.ncbi.nlm.nih.gov/pubmed/27465550 [Accessed September 22, 2019]
Das R, Schwintzer L, Vinopal S, Aguado Roca E, Sylvester M, Oprisoreanu A-M, Schoch S, Bradke F & Broemer M (2019) New roles for the de-ubiquitylating enzyme OTUD4 in an RNA–protein network and RNA granules. *J. Cell Sci.* **132:** jcs229252 Available at: http://www.ncbi.nlm.nih.gov/pubmed/31138677 [Accessed September 16, 2019]
Dempsey LA, Hanakahi LA & Maizels N (1998) A Specific Isoform of hnRNP D Interacts with DNA in the LR1 Heterodimer: Canonical RNA Binding Motifs in a Sequence-specific Duplex DNA Binding Protein. *J. Biol. Chem.* **273:** 29224–29229 Available at: http://www.ncbi.nlm.nih.gov/pubmed/9786934 [Accessed July 24, 2019]
Deng H, O'Keefe H, Davie CP, Lind KE, Acharya RA, Franklin GJ, Larkin J, Matico R, Neeb M, Thompson MM, Lohr T, Gross JW, Centrella PA, O'Donovan GK, Bedard KL (Sargent), van Vloten K, Mataruse S, Skinner SR, Belyanskaya SL, Carpenter TY, et al (2012) Discovery of Highly Potent and Selective Small Molecule ADAMTS-5 Inhibitors That Inhibit Human Cartilage Degradation via Encoded Library Technology (ELT). *J. Med. Chem.* **55:** 7061–7079 Available at: http://www.ncbi.nlm.nih.gov/pubmed/22891645 [Accessed September 10, 2019]
Deng T, Yan G, Song X, Xie L, Zhou Y, Li J, Hu X, Li Z, Hu J, Zhang Y, Zhang H, Sun Y, Feng P, Wei D, Hu B, Liu J, Tan W & Ye M (2018) Deubiquitylation and stabilization of p21 by USP11 is critical for cell-cycle progression and DNA damage responses. *Proc. Natl. Acad. Sci.* **115:** 4678–4683 Available at: http://www.ncbi.nlm.nih.gov/pubmed/29666278 [Accessed August 24, 2019]
Dhingra R, Margulets V, Chowdhury SR, Thliveris J, Jassal D, Fernyhough P, Dorn GW & Kirshenbaum LA (2014) Bnip3 mediates doxorubicin-induced cardiac myocyte necrosis and mortality through changes in mitochondrial signaling. *Proc. Natl. Acad. Sci. U. S. A.* **111:** E5537-44 Available at: http://www.pnas.org/lookup/doi/10.1073/pnas.1414665111 [Accessed November 19, 2018]

Dioum EM, Chen R, Alexander MS, Zhang Q, Hogg RT, Gerard RD & Garcia JA (2009) Regulation of Hypoxia-Inducible Factor 2 Signaling by the Stress-Responsive Deacetylase Sirtuin 1. *Science (80-.).* **324:** 1289–1293 Available at: http://www.ncbi.nlm.nih.gov/pubmed/19498162 [Accessed September 22, 2019]

Dominguez-Andres J & Netea MG (2019) Long-term reprogramming of the innate immune system. *J. Leukoc. Biol.* **105:** 329–338 Available at: http://www.ncbi.nlm.nih.gov/pubmed/29999546 [Accessed September 19, 2019]

Dunwoodie SL (2009) The Role of Hypoxia in Development of the Mammalian Embryo. *Dev. Cell* **17:** 755–773 Available at: https://linkinghub.elsevier.com/retrieve/pii/S1534580709004821 [Accessed September 5, 2019]

Ehrlich ES, Wang T, Luo K, Xiao Z, Niewiadomska AM, Martinez T, Xu W, Neckers L & Yu X-F (2009) Regulation of Hsp90 client proteins by a Cullin5-RING E3 ubiquitin ligase. *Proc. Natl. Acad. Sci.* **106:** 20330–20335 Available at: http://www.ncbi.nlm.nih.gov/pubmed/19933325 [Accessed August 23, 2019]

Elorza A, Soro-Arnáiz I, Meléndez-Rodríguez F, Rodríguez-Vaello V, Marsboom G, de Cárcer G, Acosta-Iborra B, Albacete-Albacete L, Ordóñez A, Serrano-Oviedo L, Giménez-Bachs JM, Vara-Vega A, Salinas A, Sánchez-Prieto R, Martín del Río R, Sánchez-Madrid F, Malumbres M, Landázuri MO & Aragonés J (2012) HIF2α Acts as an mTORC1 Activator through the Amino Acid Carrier SLC7A5. *Mol. Cell* **48:** 681–691 Available at: https://linkinghub.elsevier.com/retrieve/pii/S1097276512008179 [Accessed August 16, 2019]

Elvert G, Kappel A, Heidenreich R, Englmeier U, Lanz S, Acker T, Rauter M, Plate K, Sieweke M, Breier G & Flamme I (2003) Cooperative Interaction of Hypoxia-inducible Factor-2α (HIF-2α) and Ets-1 in the Transcriptional Activation of Vascular Endothelial Growth Factor Receptor-2 (Flk-1). *J. Biol. Chem.* **278:** 7520–7530 Available at: http://www.jbc.org/lookup/doi/10.1074/jbc.M211298200 [Accessed September 6, 2019]

Ema M, Taya S, Yokotani N, Sogawa K, Matsuda Y & Fujii-Kuriyama Y (1997) A novel bHLH-PAS factor with close sequence similarity to hypoxia-inducible factor 1 regulates the VEGF expression and is potentially involved in lung and vascular development. *Proc. Natl. Acad. Sci.* **94:** 4273–4278 Available at: http://www.pnas.org/cgi/doi/10.1073/pnas.94.9.4273 [Accessed September 6, 2019]

Epstein AC, Gleadle JM, McNeill LA, Hewitson KS, O'Rourke J, Mole DR, Mukherji M, Metzen E, Wilson MI, Dhanda A, Tian YM, Masson N, Hamilton DL, Jaakkola P, Barstead R, Hodgkin J, Maxwell PH, Pugh CW, Schofield CJ & Ratcliffe PJ (2001) C. elegans EGL-9 and mammalian homologs define a family of dioxygenases that regulate HIF by prolyl hydroxylation. *Cell* **107:** 43–54 Available at: http://www.ncbi.nlm.nih.gov/pubmed/11595184 [Accessed August 15, 2019]

Faesen AC, Luna-Vargas MPA & Sixma TK (2012) The role of UBL domains in ubiquitin-specific proteases. *Biochem. Soc. Trans.* **40:** 539–545 Available

at: http://www.ncbi.nlm.nih.gov/pubmed/22616864 [Accessed August 24, 2019]
Flugel D, Gorlach A & Kietzmann T (2012) GSK-3 regulates cell growth, migration, and angiogenesis via Fbw7 and USP28-dependent degradation of HIF-1. *Blood* **119:** 1292–1301 Available at: http://www.ncbi.nlm.nih.gov/pubmed/22144179 [Accessed August 23, 2019]
Frede S, Stockmann C, Freitag P & Fandrey J (2006) Bacterial lipopolysaccharide induces HIF-1 activation in human monocytes via p44/42 MAPK and NF-κB. *Biochem. J* **396:** 517–527 Available at: http://www.biochemj.org/content/396/3/517.full-text.pdf [Accessed August 20, 2019]
Funasaka T, Nakano H, Wu Y, Hashizume C, Gu L, Nakamura T, Wang W, Zhou P, Moore MAS, Sato H & Wong RW (2011) RNA export factor RAE1 contributes to NUP98-HOXA9-mediated leukemogenesis. *Cell Cycle* **10:** 1456–1467 Available at: http://www.ncbi.nlm.nih.gov/pubmed/21467841 [Accessed July 23, 2019]
Galbán S, Kuwano Y, Pullmann R, Martindale JL, Kim HH, Lal A, Abdelmohsen K, Yang X, Dang Y, Liu JO, Lewis SM, Holcik M & Gorospe M (2008) RNA-binding proteins HuR and PTB promote the translation of hypoxia-inducible factor 1alpha. *Mol. Cell. Biol.* **28:** 93–107 Available at: http://www.ncbi.nlm.nih.gov/pubmed/17967866 [Accessed July 23, 2019]
Garcia DA, Baek C, Estrada MV, Tysl T, Bennett EJ, Yang J & Chang JT (2018) USP11 Enhances TGFβ-Induced Epithelial–Mesenchymal Plasticity and Human Breast Cancer Metastasis. *Mol. Cancer Res.* **16:** 1172–1184 Available at: http://www.ncbi.nlm.nih.gov/pubmed/29724812 [Accessed August 24, 2019]
Gavory G, O'dowd C, McClelland K & Odrzywol E (2015) Abstract LB-257: Discovery and characterization of novel, highly potent and selective USP7 inhibitors. Available at: http://cancerres.aacrjournals.org/content/75/15_Supplement/LB-257.short [Accessed September 10, 2019]
Ghosh G, Subramanian I V., Adhikari N, Zhang X, Joshi HP, Basi D, Chandrashekhar YS, Hall JL, Roy S, Zeng Y & Ramakrishnan S (2010) Hypoxia-induced microRNA-424 expression in human endothelial cells regulates HIF-α isoforms and promotes angiogenesis. *J. Clin. Invest.* **120:** 4141–4154 Available at: http://www.ncbi.nlm.nih.gov/pubmed/20972335 [Accessed September 8, 2019]
Ginouves A, Ilc K, Macias N, Pouyssegur J & Berra E (2008) PHDs overactivation during chronic hypoxia "desensitizes" HIF and protects cells from necrosis. *Proc. Natl. Acad. Sci.* **105:** 4745–4750 Available at: http://www.ncbi.nlm.nih.gov/pubmed/18347341 [Accessed September 6, 2019]
Giraud-Triboult K, Rochon-Beaucourt C, Nissan X, Champon B, Aubert S & Piétu G (2011) Combined mRNA and microRNA profiling reveals that miR-148a and miR-20b control human mesenchymal stem cell phenotype via EPAS1. *Physiol. Genomics* **43:** 77–86 Available at: http://www.ncbi.nlm.nih.gov/pubmed/21081659 [Accessed September 22, 2019]
Goldstein G, Scheid M, Hammerling U, Schlesinger DH, Niall HD & Boyse EA

(1975) Isolation of a polypeptide that has lymphocyte-differentiating properties and is probably represented universally in living cells. *Proc. Natl. Acad. Sci. U. S. A.* **72:** 11–5 Available at: http://www.pnas.org/cgi/doi/10.1073/pnas.72.1.11 [Accessed September 8, 2019]

Gothié E, Richard DE, Berra E, Pagès G & Pouysségur J (2000) Identification of Alternative Spliced Variants of Human Hypoxia-inducible Factor-1α. *J. Biol. Chem.* **275:** 6922–6927 Available at: http://www.ncbi.nlm.nih.gov/pubmed/10702253 [Accessed August 20, 2019]

Goto Y, Zeng L, Yeom CJ, Zhu Y, Morinibu A, Shinomiya K, Kobayashi M, Hirota K, Itasaka S, Yoshimura M, Tanimoto K, Torii M, Sowa T, Menju T, Sonobe M, Kakeya H, Toi M, Date H, Hammond EM, Hiraoka M, et al (2015) UCHL1 provides diagnostic and antimetastatic strategies due to its deubiquitinating effect on HIF-1α. *Nat. Commun.* **6:** 6153 Available at: http://www.ncbi.nlm.nih.gov/pubmed/25615526 [Accessed September 9, 2019]

Gruber M, Hu C-J, Johnson RS, Brown EJ, Keith B & Simon MC (2007) Acute postnatal ablation of Hif-2 results in anemia. *Proc. Natl. Acad. Sci.* **104:** 2301–2306 Available at: http://www.pnas.org/cgi/doi/10.1073/pnas.0608382104 [Accessed September 6, 2019]

Gu Y, Ding X, Huang J, Xue M, Zhang J, Wang Q, Yu H, Wang Y, Zhao F, Wang H, Jin M, Wu Y & Zhang Y (2018) The deubiquitinating enzyme UCHL1 negatively regulates the immunosuppressive capacity and survival of multipotent mesenchymal stromal cells. *Cell Death Dis.* **9:** 459 Available at: http://www.ncbi.nlm.nih.gov/pubmed/29686406 [Accessed September 10, 2019]

Guo J, Shinriki S, Su Y, Nakamura T, Hayashi M, Tsuda Y, Murakami Y, Tasaki M, Hide T, Takezaki T, Kuratsu J, Yamashita S, Ueda M, Li J-D, Ando Y & Jono H (2014) Hypoxia suppresses cylindromatosis (CYLD) expression to promote inflammation in glioblastoma: possible link to acquired resistance to anti-VEGF therapy. *Oncotarget* **5:** 6353–64 Available at: http://www.ncbi.nlm.nih.gov/pubmed/25071012 [Accessed August 23, 2019]

Guzzo CM & Matunis MJ (2013) Expanding SUMO and ubiquitin-mediated signaling through hybrid SUMO-ubiquitin chains and their receptors. *Cell Cycle* **12:** 1015–1017 Available at: http://www.ncbi.nlm.nih.gov/pubmed/23511166 [Accessed September 8, 2019]

Hägele S, Kühn U, Böning M & Katschinski DM (2009) Cytoplasmic polyadenylation-element-binding protein (CPEB)1 and 2 bind to the *HIF-1* α mRNA 3′-UTR and modulate HIF-1α protein expression. *Biochem. J.* **417:** 235–246 Available at: http://www.ncbi.nlm.nih.gov/pubmed/18752464 [Accessed August 22, 2019]

van Hagen M, Overmeer RM, Abolvardi SS & Vertegaal ACO (2010) RNF4 and VHL regulate the proteasomal degradation of SUMO-conjugated Hypoxia-Inducible Factor-2alpha. *Nucleic Acids Res.* **38:** 1922–31 Available at: http://www.ncbi.nlm.nih.gov/pubmed/20026589 [Accessed July 16, 2019]

Haglund K, Di Fiore PP & Dikic I (2003) Distinct monoubiquitin signals in

receptor endocytosis. *Trends Biochem. Sci.* **28:** 598–604 Available at: http://www.ncbi.nlm.nih.gov/pubmed/14607090 [Accessed September 8, 2019]
Hao S & Baltimore D (2009) The stability of mRNA influences the temporal order of the induction of genes encoding inflammatory molecules. *Nat. Immunol.* **10:** 281–288 Available at: http://www.ncbi.nlm.nih.gov/pubmed/19198593 [Accessed September 8, 2019]
Hara S, Hamada J, Kobayashi C, Kondo Y & Imura N (2001) Expression and Characterization of Hypoxia-Inducible Factor (HIF)-3α in Human Kidney: Suppression of HIF-Mediated Gene Expression by HIF-3α. *Biochem. Biophys. Res. Commun.* **287:** 808–813 Available at: https://linkinghub.elsevier.com/retrieve/pii/S0006291X01956591 [Accessed September 6, 2019]
Harper S, Gratton HE, Cornaciu I, Oberer M, Scott DJ, Emsley J & Dreveny I (2014) Structure and catalytic regulatory function of ubiquitin specific protease 11 N-terminal and ubiquitin-like domains. *Biochemistry* **53:** 2966–78 Available at: http://www.ncbi.nlm.nih.gov/pubmed/24724799 [Accessed August 24, 2019]
He C & Schneider R (2006) 14-3-3sigma is a p37 AUF1-binding protein that facilitates AUF1 transport and AU-rich mRNA decay. *EMBO J.* **25:** 3823–31 Available at: http://www.ncbi.nlm.nih.gov/pubmed/16902409 [Accessed September 22, 2019]
He Q, Johnston J, Zeitlinger J, City K & City K (2015) HHS Public Access Author manuscript Oncogene. Author manuscript; available in PMC 2015 April 30. Published in final edited form as: Oncogene. 2013 August 29; 32(35): 4057–4063. doi:10.1038/onc.2012.578. Cancer-Stromal Cell Interactions Mediated by Hypoxia. **33:** 395–401
Hendriks IA, Schimmel J, Eifler K, Olsen J V. & Vertegaal ACO (2015a) Ubiquitin-specific Protease 11 (USP11) Deubiquitinates Hybrid Small Ubiquitin-like Modifier (SUMO)-Ubiquitin Chains to Counteract RING Finger Protein 4 (RNF4). *J. Biol. Chem.* **290:** 15526–15537 Available at: http://www.ncbi.nlm.nih.gov/pubmed/25969536 [Accessed August 24, 2019]
Hendriks IA, Schimmel J, Eifler K, Olsen J V & Vertegaal ACO (2015b) Ubiquitin-specific Protease 11 (USP11) Deubiquitinates Hybrid Small Ubiquitin-like Modifier (SUMO)-Ubiquitin Chains to Counteract RING Finger Protein 4 (RNF4). *J. Biol. Chem.* **290:** 15526–37 Available at: http://www.ncbi.nlm.nih.gov/pubmed/25969536 [Accessed July 23, 2019]
Hershko A, Heller H, Elias S & Ciechanover A (1983) Components of ubiquitin-protein ligase system. Resolution, affinity purification, and role in protein breakdown. *J. Biol. Chem.* **258:** 8206–14 Available at: http://www.ncbi.nlm.nih.gov/pubmed/6305978 [Accessed September 8, 2019]
Hicke L (2001) A new ticket for entry into budding vesicles-ubiquitin. *Cell* **106:** 527–30 Available at: http://www.ncbi.nlm.nih.gov/pubmed/11551499 [Accessed September 8, 2019]
Hirsilä M, Koivunen P, Günzler V, Kivirikko KI & Myllyharju J (2003) Characterization of the human prolyl 4-hydroxylases that modify the hypoxia-inducible factor. *J. Biol. Chem.* **278:** 30772–80 Available at:

http://www.ncbi.nlm.nih.gov/pubmed/12788921 [Accessed August 15, 2019]
Hornbeck P V., Kornhauser JM, Tkachev S, Zhang B, Skrzypek E, Murray B, Latham V & Sullivan M (2012) PhosphoSitePlus: a comprehensive resource for investigating the structure and function of experimentally determined post-translational modifications in man and mouse. *Nucleic Acids Res.* **40:** D261–D270 Available at: http://www.ncbi.nlm.nih.gov/pubmed/22135298 [Accessed September 24, 2019]
Hu C-J, Wang L-Y, Chodosh LA, Keith B & Simon MC (2003) Differential roles of hypoxia-inducible factor 1alpha (HIF-1alpha) and HIF-2alpha in hypoxic gene regulation. *Mol. Cell. Biol.* **23:** 9361–74 Available at: http://www.ncbi.nlm.nih.gov/pubmed/14645546 [Accessed August 18, 2019]
Hu M, Li P, Li M, Li W, Yao T, Wu J-W, Gu W, Cohen RE & Shi Y (2002) Crystal Structure of a UBP-Family Deubiquitinating Enzyme in Isolation and in Complex with Ubiquitin Aldehyde. *Cell* **111:** 1041–1054 Available at: https://linkinghub.elsevier.com/retrieve/pii/S0092867402011996 [Accessed September 8, 2019]
Huang J, Zhao Q, Mooney SM & Lee FS (2002) Sequence Determinants in Hypoxia-inducible Factor-1α for Hydroxylation by the Prolyl Hydroxylases PHD1, PHD2, and PHD3. *J. Biol. Chem.* **277:** 39792–39800 Available at: http://www.ncbi.nlm.nih.gov/pubmed/12181324 [Accessed September 6, 2019]
Huang LE, Gu J, Schau M & Bunn HF (1998) Regulation of hypoxia-inducible factor 1 is mediated by an O2-dependent degradation domain via the ubiquitin-proteasome pathway. *Proc. Natl. Acad. Sci.* **95:** 7987–7992 Available at: http://www.pnas.org/cgi/doi/10.1073/pnas.95.14.7987 [Accessed September 6, 2019]
Huang TT, Nijman SMB, Mirchandani KD, Galardy PJ, Cohn MA, Haas W, Gygi SP, Ploegh HL, Bernards R & D'Andrea AD (2006) Regulation of monoubiquitinated PCNA by DUB autocleavage. *Nat. Cell Biol.* **8:** 341–347 Available at: http://www.ncbi.nlm.nih.gov/pubmed/16531995 [Accessed August 23, 2019]
Hubbi ME, Hu H, Kshitiz, Ahmed I, Levchenko A & Semenza GL (2013) Chaperone-mediated Autophagy Targets Hypoxia-inducible Factor-1α (HIF-1α) for Lysosomal Degradation. *J. Biol. Chem.* **288:** 10703–10714 Available at: http://www.ncbi.nlm.nih.gov/pubmed/23457305 [Accessed August 23, 2019]
Ideguchi H, Ueda A, Tanaka M, Yang J, Tsuji T, Ohno S, Hagiwara E, Aoki A & Ishigatsubo Y (2002) Structural and functional characterization of the USP11 deubiquitinating enzyme, which interacts with the RanGTP-associated protein RanBPM. *Biochem. J.* **367:** 87–95 Available at: http://www.ncbi.nlm.nih.gov/pubmed/12084015 [Accessed August 24, 2019]
Ivan M, Kondo K, Yang H, Kim W, Valiando J, Ohh M, Salic A, Asara JM, Lane WS & Kaelin WG (2001) HIFalpha Targeted for VHL-Mediated Destruction by Proline Hydroxylation: Implications for O2 Sensing. *Science (80-.).* **292:** 464–468 Available at: http://www.ncbi.nlm.nih.gov/pubmed/11292862 [Accessed September 6, 2019]

Iyer N V., Kotch LE, Agani F, Leung SW, Laughner E, Wenger RH, Gassmann M, Gearhart JD, Lawler AM, Yu AY & Semenza GL (1998a) Cellular and developmental control of O2 homeostasis by hypoxia-inducible factor 1alpha. *Genes Dev.* **12:** 149–162 Available at: http://www.ncbi.nlm.nih.gov/pubmed/9436976 [Accessed August 18, 2019]

Iyer N V., Leung SW & Semenza GL (1998b) The Human Hypoxia-Inducible Factor 1α Gene:HIF1AStructure and Evolutionary Conservation. *Genomics* **52:** 159–165 Available at: http://www.ncbi.nlm.nih.gov/pubmed/9782081 [Accessed August 20, 2019]

Jaakkola P, Mole DR, Tian Y-M, Wilson MI, Gielbert J, Gaskell SJ, Kriegsheim A v., Hebestreit HF, Mukherji M, Schofield CJ, Maxwell PH, Pugh CW & Ratcliffe PJ (2001) Targeting of HIF-alpha to the von Hippel-Lindau Ubiquitylation Complex by O2-Regulated Prolyl Hydroxylation. *Science (80-.).* **292:** 468–472 Available at: http://www.ncbi.nlm.nih.gov/pubmed/11292861 [Accessed September 6, 2019]

Jacko AM, Nan L, Li S, Tan J, Zhao J, Kass DJ & Zhao Y (2016) De-ubiquitinating enzyme, USP11, promotes transforming growth factor β-1 signaling through stabilization of transforming growth factor β receptor II. *Cell Death Dis.* **7:** e2474–e2474 Available at: http://www.ncbi.nlm.nih.gov/pubmed/27853171 [Accessed August 24, 2019]

Jiang B-H, Rue E, Wang GL, Roe R & Semenza GL (1996) Dimerization, DNA Binding, and Transactivation Properties of Hypoxia-inducible Factor 1. *J. Biol. Chem.* **271:** 17771–17778 Available at: http://www.jbc.org/content/271/30/17771.long [Accessed September 6, 2019]

Jiang B-H, Zheng JZ, Leung SW, Roe R & Semenza GL (1997a) Transactivation and Inhibitory Domains of Hypoxia-inducible Factor 1α. *J. Biol. Chem.* **272:** 19253–19260 Available at: http://www.jbc.org/content/272/31/19253.long [Accessed September 6, 2019]

Jiang BH, Agani F, Passaniti A, Semenza GL, Hanrahan C, Georgescu M-M, Simons JW & Semenza GL (1997b) V-SRC induces expression of hypoxia-inducible factor 1 (HIF-1) and transcription of genes encoding vascular endothelial growth factor and enolase 1: involvement of HIF-1 in tumor progression. *Cancer Res.* **57:** 5328–35 Available at: http://www.ncbi.nlm.nih.gov/pubmed/9393757 [Accessed August 20, 2019]

Joo HY, Zhai L, Yang C, Nie S, Erdjument-Bromage H, Tempst P, Chang C & Wang H (2007) Regulation of cell cycle progression and gene expression by H2A deubiquitination. *Nature* **449:** 1068–1072

Joshi S, Singh AR & Durden DL (2014a) MDM2 Regulates Hypoxic Hypoxia-inducible Factor 1α Stability in an E3 Ligase, Proteasome, and PTEN-Phosphatidylinositol 3-Kinase-AKT-dependent Manner. *J. Biol. Chem.* **289:** 22785–22797 Available at: http://www.ncbi.nlm.nih.gov/pubmed/24982421 [Accessed July 16, 2019]

Joshi S, Singh AR & Durden DL (2014b) MDM2 Regulates Hypoxic Hypoxia-inducible Factor 1α Stability in an E3 Ligase, Proteasome, and PTEN-Phosphatidylinositol 3-Kinase-AKT-dependent Manner. *J. Biol. Chem.* **289:** 22785–22797 Available at: http://www.ncbi.nlm.nih.gov/pubmed/24982421

[Accessed August 23, 2019]
Ju U-I, Park J-W, Park H-S, Kim SJ & Chun Y-S (2015a) FBXO11 represses cellular response to hypoxia by destabilizing hypoxia-inducible factor-1α mRNA. *Biochem. Biophys. Res. Commun.* **464:** 1008–1015 Available at: https://linkinghub.elsevier.com/retrieve/pii/S0006291X15302680 [Accessed August 20, 2019]
Ju U-I, Park J-W, Park H-S, Kim SJ & Chun Y-S (2015b) FBXO11 represses cellular response to hypoxia by destabilizing hypoxia-inducible factor-1α mRNA. *Biochem. Biophys. Res. Commun.* **464:** 1008–1015 Available at: http://www.ncbi.nlm.nih.gov/pubmed/26187670 [Accessed July 16, 2019]
Kang HJ, Kim HJ, Rih J-K, Mattson TL, Kim KW, Cho C-H, Isaacs JS & Bae I (2006) BRCA1 Plays a Role in the Hypoxic Response by Regulating HIF-1α Stability and by Modulating Vascular Endothelial Growth Factor Expression. *J. Biol. Chem.* **281:** 13047–13056 Available at: http://www.ncbi.nlm.nih.gov/pubmed/16543242 [Accessed September 9, 2019]
Kapadia B, Nanaji NM, Bhalla K, Bhandary B, Lapidus R, Beheshti A, Evens AM & Gartenhaus RB (2018) Fatty Acid Synthase induced S6Kinase facilitates USP11-eIF4B complex formation for sustained oncogenic translation in DLBCL. *Nat. Commun.* **9:** 829 Available at: http://www.nature.com/articles/s41467-018-03028-y [Accessed September 2, 2019]
Kapuria V, Peterson LF, Fang D, Bornmann WG, Talpaz M & Donato NJ (2010) Deubiquitinase Inhibition by Small-Molecule WP1130 Triggers Aggresome Formation and Tumor Cell Apoptosis. *Cancer Res.* **70:** 9265–9276 Available at: http://www.ncbi.nlm.nih.gov/pubmed/21045142 [Accessed September 10, 2019]
Ke J, Dai C, Wu W, Gao J, Xia A, Liu G, Lv K & Wu C (2014) USP11 regulates p53 stability by deubiquitinating p53. *J. Zhejiang Univ. Sci. B* **15:** 1032–1038 Available at: http://www.ncbi.nlm.nih.gov/pubmed/25471832 [Accessed August 24, 2019]
Kelly B & O'Neill LA (2015) Metabolic reprogramming in macrophages and dendritic cells in innate immunity. *Cell Res.* **25:** 771–784 Available at: http://www.ncbi.nlm.nih.gov/pubmed/26045163 [Accessed September 19, 2019]
Kim TW, Yim S, Choi BJ, Jang Y, Lee JJ, Sohn BH, Yoo H-S, Yeom Y Il & Park KC (2010) Tristetraprolin regulates the stability of HIF-1α mRNA during prolonged hypoxia. *Biochem. Biophys. Res. Commun.* **391:** 963–968 Available at: http://www.ncbi.nlm.nih.gov/pubmed/19962963 [Accessed August 22, 2019]
Kim Y, Noren Hooten N, Dluzen DF, Martindale JL, Gorospe M & Evans MK (2015) Posttranscriptional Regulation of the Inflammatory Marker C-Reactive Protein by the RNA-Binding Protein HuR and MicroRNA 637. *Mol. Cell. Biol.* **35:** 4212–21 Available at: http://mcb.asm.org/lookup/doi/10.1128/MCB.00645-15 [Accessed August 5, 2019]
Koh MY, Darnay BG & Powis G (2008) Hypoxia-Associated Factor, a Novel E3-Ubiquitin Ligase, Binds and Ubiquitinates Hypoxia-Inducible Factor 1 , Leading to Its Oxygen-Independent Degradation. *Mol. Cell. Biol.* **28:** 7081–7095 Available at: http://www.ncbi.nlm.nih.gov/pubmed/18838541

[Accessed August 23, 2019]
Koivunen P, Hirsilä M, Günzler V, Kivirikko KI & Myllyharju J (2004) Catalytic Properties of the Asparaginyl Hydroxylase (FIH) in the Oxygen Sensing Pathway Are Distinct from Those of Its Prolyl 4-Hydroxylases. *J. Biol. Chem.* **279:** 9899–9904 Available at: http://www.jbc.org/lookup/doi/10.1074/jbc.M312254200 [Accessed September 19, 2019]
Kurtovic-Kozaric A, Przychodzen B, Singh J, Konarska MM, Clemente MJ, Otrock ZK, Nakashima M, Hsi ED, Yoshida K, Shiraishi Y, Chiba K, Tanaka H, Miyano S, Ogawa S, Boultwood J, Makishima H, Maciejewski JP & Padgett RA (2015) PRPF8 defects cause missplicing in myeloid malignancies. *Leukemia* **29:** 126–136 Available at: http://dx.doi.org/10.1038/leu.2014.144
Lando D, Peet DJ, Gorman JJ, Whelan DA, Whitelaw ML & Bruick RK (2002) FIH-1 is an asparaginyl hydroxylase enzyme that regulates the transcriptional activity of hypoxia-inducible factor. *Genes Dev.* **16:** 1466–71 Available at: http://www.ncbi.nlm.nih.gov/pubmed/12080085 [Accessed September 6, 2019]
Laughner E, Taghavi P, Chiles K, Mahon PC & Semenza GL (2001) HER2 (neu) Signaling Increases the Rate of Hypoxia-Inducible Factor 1 (HIF-1) Synthesis: Novel Mechanism for HIF-1-Mediated Vascular Endothelial Growth Factor Expression. *Mol. Cell. Biol.* **21:** 3995–4004 Available at: http://mcb.asm.org/cgi/doi/10.1128/MCB.21.12.3995-4004.2001 [Accessed September 8, 2019]
Lavorgna A & Harhaj EW (2012) An RNA Interference Screen Identifies the Deubiquitinase STAMBPL1 as a Critical Regulator of Human T-Cell Leukemia Virus Type 1 Tax Nuclear Export and NF- B Activation. *J. Virol.* **86:** 3357–3369
Lee E-W, Seong D, Seo J, Jeong M, Lee H-K & Song J (2015) USP11-dependent selective cIAP2 deubiquitylation and stabilization determine sensitivity to Smac mimetics. *Cell Death Differ.* **22:** 1463–1476 Available at: http://www.ncbi.nlm.nih.gov/pubmed/25613375 [Accessed August 24, 2019]
Lee K-H, Park J-W & Chun Y-S (2004) Non-hypoxic transcriptional activation of the aryl hydrocarbon receptor nuclear translocator in concert with a novel hypoxia-inducible factor-1alpha isoform. *Nucleic Acids Res.* **32:** 5499–511 Available at: http://www.ncbi.nlm.nih.gov/pubmed/15479785 [Accessed August 20, 2019]
Lee SY, Ramirez J, Franco M, Lectez B, Gonzalez M, Barrio R & Mayor U (2014) Ube3a, the E3 ubiquitin ligase causing Angelman syndrome and linked to autism, regulates protein homeostasis through the proteasomal shuttle Rpn10. *Cell. Mol. Life Sci.* **71:** 2747–58 Available at: http://link.springer.com/10.1007/s00018-013-1526-7 [Accessed August 1, 2019]
Lee WH, Kim YW, Choi JH, Brooks SC, Lee M-O & Kim SG (2009) Oltipraz and dithiolethione congeners inhibit hypoxia-inducible factor-1 activity through p70 ribosomal S6 kinase-1 inhibition and H2O2-scavenging effect. *Mol. Cancer Ther.* **8:** 2791–2802 Available at: http://www.ncbi.nlm.nih.gov/pubmed/19789218 [Accessed October 14, 2019]

Li C, Xiong W, Liu X, Xiao W, Guo Y, Tan J & Li Y (2019) Hypomethylation at non-CpG/CpG sites in the promoter of HIF-1α gene combined with enhanced H3K9Ac modification contribute to maintain higher HIF-1α expression in breast cancer. *Oncogenesis* **8:** 26 Available at: http://www.nature.com/articles/s41389-019-0135-1 [Accessed September 6, 2019]

Li Z, Wang D, Messing EM & Wu G (2005) VHL protein-interacting deubiquitinating enzyme 2 deubiquitinates and stabilizes HIF-1α. *EMBO Rep.* **6:** 373–378 Available at: http://www.ncbi.nlm.nih.gov/pubmed/15776016 [Accessed September 9, 2019]

Liao T-L, Wu C-Y, Su W-C, Jeng K-S & Lai MMC (2010) Ubiquitination and deubiquitination of NP protein regulates influenza A virus RNA replication. *EMBO J.* **29:** 3879–3890 Available at: http://www.ncbi.nlm.nih.gov/pubmed/20924359 [Accessed September 23, 2019]

Ligeza J, Marona P, Gach N, Lipert B, Miekus K, Wilk W, Jaszczynski J, Stelmach A, Loboda A, Dulak J, Branicki W, Rys J & Jura J (2017) MCPIP1 contributes to clear cell renal cell carcinomas development. *Angiogenesis* **20:** 325–340 Available at: http://www.ncbi.nlm.nih.gov/pubmed/28197812 [Accessed September 21, 2019]

Lim K-H, Suresh B, Park J-H, Kim Y-S, Ramakrishna S & Baek K-H (2016) Ubiquitin-specific protease 11 functions as a tumor suppressor by modulating Mgl-1 protein to regulate cancer cell growth. *Oncotarget* **7:** 14441–57 Available at: http://www.ncbi.nlm.nih.gov/pubmed/26919101 [Accessed August 24, 2019]

Lin C-H, Chang H-S & Yu WCY (2008) USP11 Stabilizes HPV-16E7 and Further Modulates the E7 Biological Activity. *J. Biol. Chem.* **283:** 15681–15688 Available at: http://www.ncbi.nlm.nih.gov/pubmed/18408009 [Accessed August 24, 2019]

Liu J, Xia H, Kim M, Xu L, Li Y, Zhang L, Cai Y, Norberg HV, Zhang T, Furuya T, Jin M, Zhu Z, Wang H, Yu J, Li Y, Hao Y, Choi A, Ke H, Ma D & Yuan J (2011) Beclin1 controls the levels of p53 by regulating the deubiquitination activity of USP10 and USP13. *Cell* **147:** 223–234 Available at: http://dx.doi.org/10.1016/j.cell.2011.08.037

Liu L, Cash TP, Jones RG, Keith B, Thompson CB & Simon MC (2006) Hypoxia-Induced Energy Stress Regulates mRNA Translation and Cell Growth. *Mol. Cell* **21:** 521–531 Available at: http://www.ncbi.nlm.nih.gov/pubmed/16483933 [Accessed September 7, 2019]

Liu Y V, Baek JH, Zhang H, Diez R, Cole RN & Semenza GL (2007) RACK1 competes with HSP90 for binding to HIF-1alpha and is required for O(2)-independent and HSP90 inhibitor-induced degradation of HIF-1alpha. *Mol. Cell* **25:** 207–17 Available at: http://www.ncbi.nlm.nih.gov/pubmed/17244529 [Accessed August 23, 2019]

López-Barneo J, del Toro R, Levitsky KL, Chiara MD & Ortega-Sáenz P (2004) Regulation of oxygen sensing by ion channels. *J. Appl. Physiol.* **96:** 1187–1195 Available at: https://www.physiology.org/doi/10.1152/japplphysiol.00929.2003 [Accessed

September 19, 2019]
Lu J-Y, Bergman N, Sadri N & Schneider RJ (2006) Assembly of AUF1 with eIF4G-poly(A) binding protein complex suggests a translation function in AU-rich mRNA decay. *RNA* **12:** 883–93 Available at: http://www.ncbi.nlm.nih.gov/pubmed/16556936 [Accessed August 12, 2019]
Lu Y, Bedard N, Chevalier S & Wing SS (2011) Identification of Distinctive Patterns of USP19-Mediated Growth Regulation in Normal and Malignant Cells. *PLoS One* **6:** e15936 Available at: http://www.ncbi.nlm.nih.gov/pubmed/21264218 [Accessed September 9, 2019]
Luo G, Gu YZ, Jain S, Chan WK, Carr KM, Hogenesch JB & Bradfield CA (1997) Molecular characterization of the murine Hif-1 alpha locus. *Gene Expr.* **6:** 287–99 Available at: http://www.ncbi.nlm.nih.gov/pubmed/9368100 [Accessed August 20, 2019]
Luo W, Zhong J, Chang R, Hu H, Pandey A & Semenza GL (2010) Hsp70 and CHIP selectively mediate ubiquitination and degradation of hypoxia-inducible factor (HIF)-1alpha but Not HIF-2alpha. *J. Biol. Chem.* **285:** 3651–63 Available at: http://www.ncbi.nlm.nih.gov/pubmed/19940151 [Accessed September 9, 2019]
Luong LA, Fragiadaki M, Smith J, Boyle J, Lutz J, Dean JLE, Harten S, Ashcroft M, Walmsley SR, Haskard DO, Maxwell PH, Walczak H, Pusey C & Evans PC (2013) Cezanne Regulates Inflammatory Responses to Hypoxia in Endothelial Cells by Targeting TRAF6 for Deubiquitination. *Circ. Res.* **112:** 1583–1591 Available at: http://www.ncbi.nlm.nih.gov/pubmed/23564640 [Accessed September 8, 2019]
Maertens GN, El Messaoudi-Aubert S, Elderkin S, Hiom K & Peters G (2010) Ubiquitin-specific proteases 7 and 11 modulate Polycomb regulation of the INK4a tumour suppressor. *EMBO J.* **29:** 2553–2565 Available at: http://www.ncbi.nlm.nih.gov/pubmed/20601937 [Accessed September 2, 2019]
Mahon PC, Hirota K & Semenza GL (2001) FIH-1: a novel protein that interacts with HIF-1alpha and VHL to mediate repression of HIF-1 transcriptional activity. *Genes Dev.* **15:** 2675–86 Available at: http://www.ncbi.nlm.nih.gov/pubmed/11641274 [Accessed September 6, 2019]
Majerciak V, Deng M & Zheng Z-M (2010) Requirement of UAP56, URH49, RBM15, and OTT3 in the expression of Kaposi sarcoma-associated herpesvirus ORF57. *Virology* **407:** 206–12 Available at: https://linkinghub.elsevier.com/retrieve/pii/S0042682210005441 [Accessed August 5, 2019]
Majumder PK, Febbo PG, Bikoff R, Berger R, Xue Q, McMahon LM, Manola J, Brugarolas J, McDonnell TJ, Golub TR, Loda M, Lane HA & Sellers WR (2004) mTOR inhibition reverses Akt-dependent prostate intraepithelial neoplasia through regulation of apoptotic and HIF-1-dependent pathways. *Nat. Med.* **10:** 594–601 Available at: http://www.nature.com/articles/nm1052 [Accessed September 22, 2019]
Makino Y, Cao R, Svensson K, Bertilsson G, Asman M, Tanaka H, Cao Y, Berkenstam A & Poellinger L (2001) Inhibitory PAS domain protein is a negative regulator of hypoxia-inducible gene expression. *Nature* **414:** 550–

554 Available at: http://www.nature.com/articles/35107085 [Accessed September 6, 2019]
Matsushita K, Takeuchi O, Standley DM, Kumagai Y, Kawagoe T, Miyake T, Satoh T, Kato H, Tsujimura T, Nakamura H & Akira S (2009) Zc3h12a is an RNase essential for controlling immune responses by regulating mRNA decay. *Nature* **458:** 1185–1190 Available at: http://www.ncbi.nlm.nih.gov/pubmed/19322177 [Accessed September 21, 2019]
Maurer U, Preiss F, Brauns-Schubert P, Schlicher L & Charvet C (2014) GSK-3 - at the crossroads of cell death and survival. *J. Cell Sci.* **127:** 1369–78 Available at: http://www.ncbi.nlm.nih.gov/pubmed/24687186 [Accessed September 20, 2019]
Maxwell PH, Wiesener MS, Chang G-W, Clifford SC, Vaux EC, Cockman ME, Wykoff CC, Pugh CW, Maher ER & Ratcliffe PJ (1999) The tumour suppressor protein VHL targets hypoxia-inducible factors for oxygen-dependent proteolysis. *Nature* **399:** 271–275 Available at: http://www.ncbi.nlm.nih.gov/pubmed/10353251 [Accessed September 6, 2019]
Maynard MA, Qi H, Chung J, Lee EHL, Kondo Y, Hara S, Conaway RC, Conaway JW & Ohh M (2003) Multiple Splice Variants of the Human HIF-3α Locus Are Targets of the von Hippel-Lindau E3 Ubiquitin Ligase Complex. *J. Biol. Chem.* **278:** 11032–11040 Available at: http://www.jbc.org/lookup/doi/10.1074/jbc.M208681200 [Accessed September 6, 2019]
Mei Y, Hahn AA, Hu S & Yang X (2011) The USP19 deubiquitinase regulates the stability of c-IAP1 and c-IAP2. *J. Biol. Chem.* **286:** 35380–7 Available at: http://www.jbc.org/lookup/doi/10.1074/jbc.M111.282020 [Accessed September 3, 2019]
Meray RK & Lansbury PT (2007) Reversible Monoubiquitination Regulates the Parkinson Disease-associated Ubiquitin Hydrolase UCH-L1. *J. Biol. Chem.* **282:** 10567–10575 Available at: http://www.ncbi.nlm.nih.gov/pubmed/17259170 [Accessed September 3, 2019]
Miller JL (2000) Mitoxantrone receives multiple-sclerosis indication. *Am. J. Heal. Pharm.* **57:** 2038–2040 Available at: http://www.ncbi.nlm.nih.gov/pubmed/11098301 [Accessed September 9, 2019]
Mills DB, Francis WR, Vargas S, Larsen M, Elemans CP, Canfield DE & Wörheide G (2018) The last common ancestor of animals lacked the HIF pathway and respired in low-oxygen environments. *Elife* **7:** Available at: https://www.ncbi.nlm.nih.gov/pmc/articles/PMC5800844/ [Accessed September 5, 2019]
Minamishima YA, Moslehi J, Bardeesy N, Cullen D, Bronson RT, Kaelin WG & Jr (2008) Somatic inactivation of the PHD2 prolyl hydroxylase causes polycythemia and congestive heart failure. *Blood* **111:** 3236–44 Available at: http://www.ncbi.nlm.nih.gov/pubmed/18096761 [Accessed September 19, 2019]
Minchenko OH, Tsymbal DO, Minchenko DO, Riabovol OO, Halkin O V. & Ratushna OO (2016) IRE-1α regulates expression of ubiquitin specific peptidases during hypoxic response in U87 glioma cells. *Endoplasmic*

Reticulum Stress Dis. **3:** Available at: https://www.degruyter.com/view/j/ersc.2016.3.issue-1/ersc-2016-0003/ersc-2016-0003.xml [Accessed September 8, 2019]
Mines MA, Goodwin JS, Limbird LE, Cui F-F & Fan G-H (2009) Deubiquitination of CXCR4 by USP14 is critical for both CXCL12-induced CXCR4 degradation and chemotaxis but not ERK ativation. *J. Biol. Chem.* **284:** 5742–52 Available at: http://www.ncbi.nlm.nih.gov/pubmed/19106094 [Accessed August 23, 2019]
Minet E, Ernest I, Michel G, Roland I, Remacle J, Raes M & Michiels C (1999) HIF1A Gene Transcription Is Dependent on a Core Promoter Sequence Encompassing Activating and Inhibiting Sequences Located Upstream from the Transcription Initiation Site and cis Elements Located within the 5′UTR. *Biochem. Biophys. Res. Commun.* **261:** 534–540 Available at: http://www.ncbi.nlm.nih.gov/pubmed/10425220 [Accessed August 12, 2019]
Mohlin S, Hamidian A, von Stedingk K, Bridges E, Wigerup C, Bexell D & Påhlman S (2015) PI3K–mTORC2 but not PI3K–mTORC1 Regulates Transcription of HIF2A/EPAS1 and Vascularization in Neuroblastoma. *Cancer Res.* **75:** 4617–4628 Available at: http://www.ncbi.nlm.nih.gov/pubmed/26432405 [Accessed September 22, 2019]
Mole DR, Blancher C, Copley RR, Pollard PJ, Gleadle JM, Ragoussis J & Ratcliffe PJ (2009) Genome-wide Association of Hypoxia-inducible Factor (HIF)-1α and HIF-2α DNA Binding with Expression Profiling of Hypoxia-inducible Transcripts. *J. Biol. Chem.* **284:** 16767–16775 Available at: http://www.ncbi.nlm.nih.gov/pubmed/19386601 [Accessed August 10, 2019]
Mole DR & Ratcliffe PJ (2008) Cellular oxygen sensing in health and disease. *Pediatr. Nephrol.* **23:** 681–694 Available at: http://link.springer.com/10.1007/s00467-007-0632-x [Accessed September 5, 2019]
Moniz S, Bandarra D, Biddlestone J, Campbell KJ, Komander D, Bremm A & Rocha S (2015) Cezanne regulates E2F1-dependent HIF2 expression. *J. Cell Sci.* **128:** 3082–3093 Available at: http://www.ncbi.nlm.nih.gov/pubmed/26148512 [Accessed September 9, 2019]
Moore AE, Chenette DM, Larkin LC & Schneider RJ (2014) Physiological networks and disease functions of RNA-binding protein AUF1. *Wiley Interdiscip. Rev. RNA* **5:** 549–64 Available at: http://doi.wiley.com/10.1002/wrna.1230 [Accessed August 30, 2019]
Moore CEJ, Mikolajek H, Regufe da Mota S, Wang X, Kenney JW, Werner JM & Proud CG (2015) Elongation Factor 2 Kinase Is Regulated by Proline Hydroxylation and Protects Cells during Hypoxia. *Mol. Cell. Biol.* **35:** 1788–804 Available at: http://www.ncbi.nlm.nih.gov/pubmed/25755286 [Accessed September 7, 2019]
Moroz E, Carlin S, Dyomina K, Burke S, Thaler HT, Blasberg R & Serganova I (2009) Real-Time Imaging of HIF-1α Stabilization and Degradation. *PLoS One* **4:** e5077 Available at: http://www.ncbi.nlm.nih.gov/pubmed/19347037 [Accessed August 17, 2019]
Netea MG, Joosten LAB, Latz E, Mills KHG, Natoli G, Stunnenberg HG, ONeill

LAJ & Xavier RJ (2016) Trained immunity: A program of innate immune memory in health and disease. *Science (80-.).* **352:** aaf1098–aaf1098 Available at: http://www.ncbi.nlm.nih.gov/pubmed/27102489 [Accessed September 19, 2019]

Nijman SMB, Huang TT, Dirac AMG, Brummelkamp TR, Kerkhoven RM, D'Andrea AD & Bernards R (2005) The Deubiquitinating Enzyme USP1 Regulates the Fanconi Anemia Pathway. *Mol. Cell* **17:** 331–339 Available at: http://www.ncbi.nlm.nih.gov/pubmed/15694335 [Accessed August 23, 2019]

Nishi R, Wijnhoven P, Le Sage C, Tjeertes J, Galanty Y, Forment J V., Clague MJ, Urbé S & Jackson SP (2014) Systematic characterization of deubiquitylating enzymes for roles in maintaining genome integrity. *Nat. Cell Biol.* **16:** 1016–1026

Ohh M, Park CW, Ivan M, Hoffman MA, Kim T-Y, Huang LE, Pavletich N, Chau V & Kaelin WG (2000) Ubiquitination of hypoxia-inducible factor requires direct binding to the β-domain of the von Hippel–Lindau protein. *Nat. Cell Biol.* **2:** 423–427 Available at: http://www.ncbi.nlm.nih.gov/pubmed/10878807 [Accessed September 6, 2019]

Ohtake F, Tsuchiya H, Saeki Y & Tanaka K (2018) K63 ubiquitylation triggers proteasomal degradation by seeding branched ubiquitin chains. *Proc. Natl. Acad. Sci.* **115:** E1401–E1408 Available at: http://www.ncbi.nlm.nih.gov/pubmed/29378950 [Accessed September 12, 2019]

Ortiz-Barahona A, Villar D, Pescador N, Amigo J & del Peso L (2010) Genome-wide identification of hypoxia-inducible factor binding sites and target genes by a probabilistic model integrating transcription-profiling data and in silico binding site prediction. *Nucleic Acids Res.* **38:** 2332–2345 Available at: http://www.ncbi.nlm.nih.gov/pubmed/20061373 [Accessed August 18, 2019]

Oughtred R, Chatr-aryamontri A, Breitkreutz B-J, Chang CS, Rust JM, Theesfeld CL, Heinicke S, Breitkreutz A, Chen D, Hirschman J, Kolas N, Livstone MS, Nixon J, O'Donnell L, Ramage L, Winter A, Reguly T, Sellam A, Stark C, Boucher L, et al (2016) BioGRID: A Resource for Studying Biological Interactions in Yeast: Table 1. *Cold Spring Harb. Protoc.* **2016:** pdb.top080754 Available at: http://www.ncbi.nlm.nih.gov/pubmed/26729913 [Accessed September 16, 2019]

Paatero I, Jokilammi A, Heikkinen PT, Iljin K, Kallioniemi O-P, Jones FE, Jaakkola PM & Elenius K (2012) Interaction with ErbB4 Promotes Hypoxia-inducible Factor-1α Signaling. *J. Biol. Chem.* **287:** 9659–9671 Available at: http://www.ncbi.nlm.nih.gov/pubmed/22308027 [Accessed August 23, 2019]

Panda AC, Abdelmohsen K, Yoon J-H, Martindale JL, Yang X, Curtis J, Mercken EM, Chenette DM, Zhang Y, Schneider RJ, Becker KG, de Cabo R & Gorospe M (2014) RNA-Binding Protein AUF1 Promotes Myogenesis by Regulating MEF2C Expression Levels. *Mol. Cell. Biol.* **34:** 3106–3119 Available at: http://www.ncbi.nlm.nih.gov/pubmed/24891619 [Accessed July 24, 2019]

Park E-J, Lee Y-M, Oh T-I, Kim B, Lim B-O & Lim J-H (2017) Vanillin

Suppresses Cell Motility by Inhibiting STAT3-Mediated HIF-1α mRNA Expression in Malignant Melanoma Cells. *Int. J. Mol. Sci.* **18:** 532 Available at: http://www.mdpi.com/1422-0067/18/3/532 [Accessed August 20, 2019]

Park MK, Yao Y, Xia W, Setijono SR, Kim JH, Vila IK, Chiu H-H, Wu Y, Billalabeitia EG, Lee MG, Kalb RG, Hung M-C, Pandolfi PP, Song SJ & Song MS (2019) PTEN self-regulates through USP11 via the PI3K-FOXO pathway to stabilize tumor suppression. *Nat. Commun.* **10:** 636 Available at: http://www.nature.com/articles/s41467-019-08481-x [Accessed August 24, 2019]

Peng Y, Cui C, He Y, Ouzhuluobu, Zhang H, Yang D, Zhang Q, Bianbazhuoma, Yang L, He Y, Xiang K, Zhang X, Bhandari S, Shi P, Yangla, Dejiquzong, Baimakangzhuo, Duojizhuoma, Pan Y, Cirenyangji, et al (2017) Down-Regulation of *EPAS1* Transcription and Genetic Adaptation of Tibetans to High-Altitude Hypoxia. *Mol. Biol. Evol.* **34:** msw280 Available at: http://www.ncbi.nlm.nih.gov/pubmed/28096303 [Accessed September 22, 2019]

Petroski MD & Deshaies RJ (2005) Function and regulation of cullin–RING ubiquitin ligases. *Nat. Rev. Mol. Cell Biol.* **6:** 9–20 Available at: http://www.ncbi.nlm.nih.gov/pubmed/15688063 [Accessed September 8, 2019]

Pickart CM & Fushman D (2004) Polyubiquitin chains: polymeric protein signals. *Curr. Opin. Chem. Biol.* **8:** 610–616 Available at: http://www.ncbi.nlm.nih.gov/pubmed/15556404 [Accessed September 8, 2019]

Ponente M, Campanini L, Cuttano R, Piunti A, Delledonne GA, Coltella N, Valsecchi R, Villa A, Cavallaro U, Pattini L, Doglioni C & Bernardi R (2017) PML promotes metastasis of triple-negative breast cancer through transcriptional regulation of HIF1A target genes. *JCI Insight* **2:** e87380 Available at: http://www.ncbi.nlm.nih.gov/pubmed/28239645 [Accessed August 22, 2019]

Pontes MH, Sevostyanova A & Groisman EA (2015) When Too Much ATP Is Bad for Protein Synthesis. *J. Mol. Biol.* **427:** 2586–2594 Available at: http://www.ncbi.nlm.nih.gov/pubmed/26150063 [Accessed October 11, 2019]

Pore N, Jiang Z, Shu H-K, Bernhard E, Kao GD & Maity A (2006) Akt1 Activation Can Augment Hypoxia-Inducible Factor-1 Expression by Increasing Protein Translation through a Mammalian Target of Rapamycin-Independent Pathway. *Mol. Cancer Res.* **4:** 471–479 Available at: http://www.ncbi.nlm.nih.gov/pubmed/16849522 [Accessed September 2, 2019]

Ramanathan HN & Ye Y (2012) Cellular strategies for making monoubiquitin signals. *Crit. Rev. Biochem. Mol. Biol.* **47:** 17–28 Available at: http://www.ncbi.nlm.nih.gov/pubmed/21981143 [Accessed September 8, 2019]

Rane S, He M, Sayed D, Vashistha H, Malhotra A, Sadoshima J, Vatner DE, Vatner SF & Abdellatif M (2009) Downregulation of MiR-199a Derepresses Hypoxia-Inducible Factor-1α and Sirtuin 1 and Recapitulates Hypoxia Preconditioning in Cardiac Myocytes. *Circ. Res.* **104:** 879–886 Available at: http://www.ncbi.nlm.nih.gov/pubmed/19265035 [Accessed September 8, 2019]

Ravi R, Mookerjee B, Bhujwalla ZM, Sutter CH, Artemov D, Zeng Q, Dillehay LE, Madan A, Semenza GL & Bedi A (2000) Regulation of tumor angiogenesis by p53-induced degradation of hypoxia-inducible factor 1alpha. *Genes Dev.* **14:** 34–44 Available at: http://www.ncbi.nlm.nih.gov/pubmed/10640274 [Accessed August 23, 2019]

Reverdy C, Conrath S, Lopez R, Planquette C, Atmanene C, Collura V, Harpon J, Battaglia V, Vivat V, Sippl W & Colland F (2012) Discovery of Specific Inhibitors of Human USP7/HAUSP Deubiquitinating Enzyme. *Chem. Biol.* **19:** 467–477 Available at: http://www.ncbi.nlm.nih.gov/pubmed/22520753 [Accessed September 10, 2019]

Reyes-Reyes EM, Šalipur FR, Shams M, Forsthoefel MK & Bates PJ (2015) Mechanistic studies of anticancer aptamer AS1411 reveal a novel role for nucleolin in regulating Rac1 activation. *Mol. Oncol.* **9:** 1392–405 Available at: http://doi.wiley.com/10.1016/j.molonc.2015.03.012 [Accessed August 5, 2019]

Richter K, Paakkola T, Mennerich D, Kubaichuk K, Konzack A, Ali-Kippari H, Kozlova N, Koivunen P, Haapasaari K-M, Jukkola-Vuorinen A, Teppo H-R, Dimova EY, Bloigu R, Szabo Z, Kerkelä R & Kietzmann T (2018) USP28 Deficiency Promotes Breast and Liver Carcinogenesis as well as Tumor Angiogenesis in a HIF-independent Manner. *Mol. Cancer Res.* **16:** 1000–1012 Available at: http://www.ncbi.nlm.nih.gov/pubmed/29545478 [Accessed August 23, 2019]

Rius J, Guma M, Schachtrup C, Akassoglou K, Zinkernagel AS, Nizet V, Johnson RS, Haddad GG & Karin M (2008) NF-κB links innate immunity to the hypoxic response through transcriptional regulation of HIF-1α. *Nature* **453:** 807–811 Available at: http://www.ncbi.nlm.nih.gov/pubmed/18432192 [Accessed August 20, 2019]

Rizou M, Frangou EA, Marineli F, Prakoura N, Zoidakis J, Gakiopoulou H, Liapis G, Kavvadas P, Chatziantoniou C, Makridakis M, Vlahou A, Boletis J, Vlahakos D, Goumenos D, Daphnis E, Iatrou C & Charonis AS (2018) The family of 14-3-3 proteins and specifically 14-3-3σ are up-regulated during the development of renal pathologies. *J. Cell. Mol. Med.* **22:** 4139–4149 Available at: http://www.ncbi.nlm.nih.gov/pubmed/29956451 [Accessed September 22, 2019]

Romero-Ruiz A, Bautista L, Navarro V, Heras-Garvín A, March-Díaz R, Castellano A, Gómez-Díaz R, Castro MJ, Berra E, López-Barneo J & Pascual A (2012) Prolyl hydroxylase-dependent modulation of eukaryotic elongation factor 2 activity and protein translation under acute hypoxia. *J. Biol. Chem.* **287:** 9651–8 Available at: http://www.ncbi.nlm.nih.gov/pubmed/22308030 [Accessed September 3, 2019]

von Roretz C, Beauchamp P, Di Marco S & Gallouzi I-E (2011) HuR and myogenesis: Being in the right place at the right time. *Biochim. Biophys. Acta - Mol. Cell Res.* **1813:** 1663–1667 Available at: http://www.ncbi.nlm.nih.gov/pubmed/21315776 [Accessed September 22, 2019]

Rossignol F, Vaché C & Clottes E (2002) Natural antisense transcripts of hypoxia-inducible factor 1alpha are detected in different normal and tumour human tissues. *Gene* **299:** 135–40 Available at:

http://www.ncbi.nlm.nih.gov/pubmed/12459261 [Accessed July 16, 2019]
Saini NY, Cerny J, Furtado VF, Desmond A, Zhou Z, Raffel G, Puthawala I, Bednarik J, Shanahan L, Miron PM, Woda B, Ramanathan M & Nath R (2019) Elderly do benefit from induction chemotherapy: High dose mitoxantrone-based ("5 + 1") induction chemotherapy regimen in newly diagnosed acute myeloid leukemia. *Am. J. Hematol.* **94:** 209–215 Available at: http://www.ncbi.nlm.nih.gov/pubmed/30417942 [Accessed September 9, 2019]
Sallais J, Alahari S, Tagliaferro A, Bhattacharjee J, Post M & Caniggia I (2017) Factor inhibiting HIF1–A novel target of SUMOylation in the human placenta. *Oncotarget* **8:** 114002–114018 Available at: http://www.ncbi.nlm.nih.gov/pubmed/29371964 [Accessed July 16, 2019]
Sánchez-Elsner T, Ramírez JR, Rodriguez-Sanz F, Varela E, Bernabéu C & Botella LM (2004) A Cross-Talk Between Hypoxia and TGF-β Orchestrates Erythropoietin Gene Regulation Through SP1 and Smads. *J. Mol. Biol.* **336:** 9–24 Available at: https://linkinghub.elsevier.com/retrieve/pii/S0022283603015262 [Accessed September 6, 2019]
Sanchez M, Galy B, Muckenthaler MU & Hentze MW (2007) Iron-regulatory proteins limit hypoxia-inducible factor-2α expression in iron deficiency. *Nat. Struct. Mol. Biol.* **14:** 420–426 Available at: http://www.ncbi.nlm.nih.gov/pubmed/17417656 [Accessed September 22, 2019]
Sarkar B, Lu J-Y & Schneider RJ (2003a) Nuclear Import and Export Functions in the Different Isoforms of the AUF1/Heterogeneous Nuclear Ribonucleoprotein Protein Family. *J. Biol. Chem.* **278:** 20700–20707 Available at: http://www.ncbi.nlm.nih.gov/pubmed/12668672 [Accessed September 23, 2019]
Sarkar B, Xi Q, He C & Schneider RJ (2003b) Selective degradation of AU-rich mRNAs promoted by the p37 AUF1 protein isoform. *Mol. Cell. Biol.* **23:** 6685–93 Available at: http://www.ncbi.nlm.nih.gov/pubmed/12944492 [Accessed September 18, 2019]
Schoenfeld AR, Apgar S, Dolios G, Wang R & Aaronson SA (2004) BRCA2 Is Ubiquitinated In Vivo and Interacts with USP11, a Deubiquitinating Enzyme That Exhibits Prosurvival Function in the Cellular Response to DNA Damage. *Mol. Cell. Biol.* **24:** 7444–7455 Available at: http://www.ncbi.nlm.nih.gov/pubmed/15314155 [Accessed August 30, 2019]
Scholz CC, Rodriguez J, Pickel C, Burr S, Fabrizio J-A, Nolan KA, Spielmann P, Cavadas MAS, Crifo B, Halligan DN, Nathan JA, Peet DJ, Wenger RH, Von Kriegsheim A, Cummins EP & Taylor CT (2016) FIH Regulates Cellular Metabolism through Hydroxylation of the Deubiquitinase OTUB1. *PLoS Biol.* **14:** e1002347 Available at: http://www.ncbi.nlm.nih.gov/pubmed/26752685 [Accessed August 23, 2019]
Scortegagna M, Subtil T, Qi J, Kim H, Zhao W, Gu W, Kluger H & Ronai ZA (2011) USP13 Enzyme Regulates Siah2 Ligase Stability and Activity via Noncatalytic Ubiquitin-binding Domains. *J. Biol. Chem.* **286:** 27333–27341 Available at: http://www.ncbi.nlm.nih.gov/pubmed/21659512 [Accessed August 23, 2019]

Semenza GL (2012) Hypoxia-inducible factors in physiology and medicine. *Cell* **148:** 399–408 Available at: http://www.ncbi.nlm.nih.gov/pubmed/22304911 [Accessed September 5, 2019]
Semenza GL & Wang GL (1992) A nuclear factor induced by hypoxia via de novo protein synthesis binds to the human erythropoietin gene enhancer at a site required for transcriptional activation. *Mol. Cell. Biol.* **12:** 5447–5454 Available at: http://mcb.asm.org/lookup/doi/10.1128/MCB.12.12.5447 [Accessed September 6, 2019]
Senft D, Qi J & Ronai ZA (2018) Ubiquitin ligases in oncogenic transformation and cancer therapy. *Nat. Rev. Cancer* **18:** 69–88 Available at: http://www.ncbi.nlm.nih.gov/pubmed/29242641 [Accessed September 19, 2019]
Shafee N, Kaluz S, Ru N & Stanbridge EJ (2009) PI3K/Akt activity has variable cell-specific effects on expression of HIF target genes, CA9 and VEGF, in human cancer cell lines. *Cancer Lett.* **282:** 109–115 Available at: http://www.ncbi.nlm.nih.gov/pubmed/19342157 [Accessed August 30, 2019]
Shah P, Qiang L, Yang S, Soltani K & He Y-Y (2017) Regulation of XPC deubiquitination by USP11 in repair of UV-induced DNA damage. *Oncotarget* **8:** 96522–96535 Available at: http://www.ncbi.nlm.nih.gov/pubmed/29228550 [Accessed August 24, 2019]
Sheflin LG, Zou A-P & Spaulding SW (2004) Androgens regulate the binding of endogenous HuR to the AU-rich 3′UTRs of HIF-1α and EGF mRNA. *Biochem. Biophys. Res. Commun.* **322:** 644–651 Available at: https://www.sciencedirect.com/science/article/pii/S0006291X04016298?via%3Dihub [Accessed August 21, 2019]
Shin CH, Lee H, Kim HR, Choi KH, Joung J-G & Kim HH (2017) Regulation of PLK1 through competition between hnRNPK, miR-149-3p and miR-193b-5p. *Cell Death Differ.* **24:** 1861–1871 Available at: http://www.ncbi.nlm.nih.gov/pubmed/28708135 [Accessed August 22, 2019]
Spiliotopoulos A, Blokpoel Ferreras L, Densham RM, Caulton SG, Maddison BC, Morris JR, Dixon JE, Gough KC & Dreveny I (2019) Discovery of peptide ligands targeting a specific ubiquitin-like domain–binding site in the deubiquitinase USP11. *J. Biol. Chem.* **294:** 424–436 Available at: http://www.ncbi.nlm.nih.gov/pubmed/30373771 [Accessed August 24, 2019]
Sprong H, Azagi T, Hoornstra D, Nijhof AM, Knorr S, Baarsma ME & Hovius JW (2018) Control of Lyme borreliosis and other Ixodes ricinus-borne diseases. *Parasit. Vectors* **11:** 145 Available at: http://www.ncbi.nlm.nih.gov/pubmed/29510749 [Accessed September 19, 2019]
Srikantan S, Tominaga K & Gorospe M (2012) Functional interplay between RNA-binding protein HuR and microRNAs. *Curr. Protein Pept. Sci.* **13:** 372–9 Available at: http://www.ncbi.nlm.nih.gov/pubmed/22708488 [Accessed August 30, 2019]
Staudacher JJ, Naarmann-de Vries IS, Ujvari SJ, Klinger B, Kasim M, Benko E, Ostareck-Lederer A, Ostareck DH, Bondke Persson A, Lorenzen S, Meier JC, Blüthgen N, Persson PB, Henrion-Caude A, Mrowka R & Fähling M

(2015) Hypoxia-induced gene expression results from selective mRNA partitioning to the endoplasmic reticulum. *Nucleic Acids Res.* **43:** 3219–3236 Available at: http://www.ncbi.nlm.nih.gov/pubmed/25753659 [Accessed August 21, 2019]

Stiehl DP, Bordoli MR, Abreu-Rodríguez I, Wollenick K, Schraml P, Gradin K, Poellinger L, Kristiansen G & Wenger RH (2012) Non-canonical HIF-2α function drives autonomous breast cancer cell growth via an AREG–EGFR/ErbB4 autocrine loop. *Oncogene* **31:** 2283–2297 Available at: http://www.ncbi.nlm.nih.gov/pubmed/21927022 [Accessed September 23, 2019]

Stockum A, Snijders AP & Maertens GN (2018a) USP11 deubiquitinates RAE1 and plays a key role in bipolar spindle formation. *PLoS One* **13:** e0190513 Available at: http://www.ncbi.nlm.nih.gov/pubmed/29293652 [Accessed September 9, 2019]

Stockum A, Snijders AP & Maertens GN (2018b) USP11 deubiquitinates RAE1 and plays a key role in bipolar spindle formation. *PLoS One* **13:** e0190513 Available at: http://www.ncbi.nlm.nih.gov/pubmed/29293652 [Accessed July 23, 2019]

Su J, Li Z, Cui S, Ji L, Geng H, Chai K, Ma X, Bai Z, Yang Y, Wuren T, Ge RL & Rondina MT (2015) The Local HIF-2α/EPO Pathway in the Bone Marrow is Associated with Excessive Erythrocytosis and the Increase in Bone Marrow Microvessel Density in Chronic Mountain Sickness. *High Alt. Med. Biol.* **16:** 318–330

Sun H, Li X-B, Meng Y, Fan L, Li M & Fang J (2013) TRAF6 Upregulates Expression of HIF-1 and Promotes Tumor Angiogenesis. *Cancer Res.* **73:** 4950–4959 Available at: http://www.ncbi.nlm.nih.gov/pubmed/23722539 [Accessed September 7, 2019]

Sun H, Ou B, Zhao S, Liu X, Song L, Liu X, Wang R & Peng Z (2019) USP11 promotes growth and metastasis of colorectal cancer via PPP1CA-mediated activation of ERK/MAPK signaling pathway. *EBioMedicine* Available at: https://www.sciencedirect.com/science/article/pii/S2352396419305754 [Accessed September 23, 2019]

Sun P, Lu Y-X, Cheng D, Zhang K, Zheng J, Liu Y, Wang X, Yuan Y-F & Tang Y-D (2018a) Monocyte Chemoattractant Protein-Induced Protein 1 Targets Hypoxia-Inducible Factor 1α to Protect Against Hepatic Ischemia/Reperfusion Injury. *Hepatology* **68:** 2359–2375 Available at: http://www.ncbi.nlm.nih.gov/pubmed/29742804 [Accessed September 9, 2019]

Sun P, Lu Y-X, Cheng D, Zhang K, Zheng J, Liu Y, Wang X, Yuan Y-F & Tang Y-D (2018b) Monocyte Chemoattractant Protein-Induced Protein 1 Targets Hypoxia-Inducible Factor 1α to Protect Against Hepatic Ischemia/Reperfusion Injury. *Hepatology* **68:** 2359–2375 Available at: http://www.ncbi.nlm.nih.gov/pubmed/29742804 [Accessed September 2, 2019]

Sun W, Tan X, Shi Y, Xu G, Mao R, Gu X, Fan Y, Yu Y, Burlingame S, Zhang H, Rednam SP, Lu X, Zhang T, Fu S, Cao G, Qin J & Yang J (2010) USP11 negatively regulates TNFα-induced NF-κB activation by targeting on IκBα. *Cell. Signal.* **22:** 386–394 Available at: http://www.ncbi.nlm.nih.gov/pubmed/19874889 [Accessed August 24,

2019]
Swanson D, Freund CL, Ploder L, McInnes RR & Valle D (1996) A ubiquitin C-terminal hydrolase gene on the proximal short arm of the X chromosome: implications for X-linked retinal disorders. *Hum. Mol. Genet.* **5:** 533–538 Available at: http://www.ncbi.nlm.nih.gov/pubmed/8845848 [Accessed September 2, 2019]
Swatek KN & Komander D (2016) Ubiquitin modifications. *Cell Res.* **26:** 399–422 Available at: http://www.nature.com/articles/cr201639 [Accessed September 8, 2019]
Taguchi A, Yanagisawa K, Tanaka M, Cao K, Matsuyama Y, Goto H & Takahashi T (2008) Identification of Hypoxia-Inducible Factor-1 as a Novel Target for miR-17-92 MicroRNA Cluster. *Cancer Res.* **68:** 5540–5545 Available at: http://www.ncbi.nlm.nih.gov/pubmed/18632605 [Accessed September 8, 2019]
Taibi A, Singh N, Chen J, Arioli S, Guglielmetti S & Comelli EM (2017) Time- and strain-specific downregulation of intestinal *EPAS1* via miR-148a by *Bifidobacterium bifidum*. *Mol. Nutr. Food Res.* **61:** 1600596 Available at: http://www.ncbi.nlm.nih.gov/pubmed/27883285 [Accessed September 22, 2019]
Takano N, Sarfraz Y, Gilkes DM, Chaturvedi P, Xiang L, Suematsu M, Zagzag D & Semenza GL (2014) Decreased expression of cystathionine β-synthase promotes glioma tumorigenesis. *Mol. Cancer Res.* **12:** 1398–406 Available at: http://mcr.aacrjournals.org/lookup/doi/10.1158/1541-7786.MCR-14-0184 [Accessed August 30, 2019]
Tan B, Mu R, Chang Y, Wang Y-B, Wu M, Tu H-Q, Zhang Y-C, Guo S-S, Qin X-H, Li T, Li W-H, Zhang X-M, Li A-L & Li H-Y (2015) RNF4 negatively regulates NF-κB signaling by down-regulating TAB2. *FEBS Lett.* **589:** 2850–8 Available at: http://doi.wiley.com/10.1016/j.febslet.2015.07.051 [Accessed August 5, 2019]
Thomas JD & Johannes GJ (2007) Identification of mRNAs that continue to associate with polysomes during hypoxia. *RNA* **13:** 1116–1131 Available at: http://www.ncbi.nlm.nih.gov/pubmed/17488873 [Accessed August 21, 2019]
Tian H, Hammer RE, Matsumoto AM, Russell DW & McKnight SL (1998) The hypoxia-responsive transcription factor EPAS1 is essential for catecholamine homeostasis and protection against heart failure during embryonic development. *Genes Dev.* **12:** 3320–3324 Available at: http://www.ncbi.nlm.nih.gov/pubmed/9808618 [Accessed August 18, 2019]
Ting X, Xia L, Yang J, He L, Si W, Shang Y & Sun L (2019) USP11 acts as a histone deubiquitinase functioning in chromatin reorganization during DNA repair. *Nucleic Acids Res.* Available at: http://www.ncbi.nlm.nih.gov/pubmed/31504778 [Accessed September 23, 2019]
de Toeuf B, Soin R, Nazih A, Dragojevic M, Jurėnas D, Delacourt N, Vo Ngoc L, Garcia-Pino A, Kruys V & Gueydan C (2018) ARE-mediated decay controls gene expression and cellular metabolism upon oxygen variations. *Sci. Rep.* **8:** 5211 Available at: http://www.nature.com/articles/s41598-018-23551-8 [Accessed November 19, 2018]
Toschi A, Lee E, Gadir N, Ohh M & Foster DA (2008) Differential Dependence of Hypoxia-inducible Factors 1α and 2α on mTORC1 and mTORC2. *J. Biol.*

Chem. **283:** 34495–34499 Available at: http://www.ncbi.nlm.nih.gov/pubmed/18945681 [Accessed September 22, 2019]

Troilo A, Alexander I, Muehl S, Jaramillo D, Knobeloch K-P & Krek W (2014) HIF1α deubiquitination by USP8 is essential for ciliogenesis in normoxia. *EMBO Rep.* **15:** 77–85 Available at: http://embor.embopress.org/cgi/doi/10.1002/embr.201337688 [Accessed September 9, 2019]

Tuckerman JR, Zhao Y, Hewitson KS, Tian Y-M, Pugh CW, Ratcliffe PJ & Mole DR (2004) Determination and comparison of specific activity of the HIF-prolyl hydroxylases. *FEBS Lett.* **576:** 145–150 Available at: http://www.ncbi.nlm.nih.gov/pubmed/15474027 [Accessed September 6, 2019]

Tyanova S, Temu T, Sinitcyn P, Carlson A, Hein MY, Geiger T, Mann M & Cox J (2016) The Perseus computational platform for comprehensive analysis of (prote)omics data. *Nat. Methods* **13:** 731–740 Available at: http://www.ncbi.nlm.nih.gov/pubmed/27348712 [Accessed August 5, 2019]

Urbé S, Liu H, Hayes SD, Heride C, Rigden DJ & Clague MJ (2012) Systematic survey of deubiquitinase localization identifies USP21 as a regulator of centrosome- and microtubule-associated functions. *Mol. Biol. Cell* **23:** 1095–103 Available at: http://www.ncbi.nlm.nih.gov/pubmed/22298430 [Accessed August 12, 2019]

van der Veen AG & Ploegh HL (2012) Ubiquitin-Like Proteins. *Annu. Rev. Biochem.* **81:** 323–357 Available at: http://www.ncbi.nlm.nih.gov/pubmed/22404627 [Accessed September 8, 2019]

Vlasschaert C, Xia X, Coulombe J & Gray DA (2015) Evolution of the highly networked deubiquitinating enzymes USP4, USP15, and USP11. *BMC Evol. Biol.* **15:** 230 Available at: http://www.ncbi.nlm.nih.gov/pubmed/26503449 [Accessed August 24, 2019]

Wada K & Kamitani T (2006) UnpEL/Usp4 is ubiquitinated by Ro52 and deubiquitinated by itself. *Biochem. Biophys. Res. Commun.* **342:** 253–8 Available at: https://linkinghub.elsevier.com/retrieve/pii/S0006291X06002403 [Accessed September 3, 2019]

Wang D, Zhao J, Li S, Wei J, Nan L, Mallampalli RK, Weathington NM, Ma H & Zhao Y (2018a) Phosphorylated E2F1 is stabilized by nuclear USP11 to drive Peg10 gene expression and activate lung epithelial cells. *J. Mol. Cell Biol.* **10:** 60–73 Available at: http://www.ncbi.nlm.nih.gov/pubmed/28992046 [Accessed August 24, 2019]

Wang GL & Semenza GL (1993) General involvement of hypoxia-inducible factor 1 in transcriptional response to hypoxia. *Proc. Natl. Acad. Sci. U. S. A.* **90:** 4304 Available at: https://www.ncbi.nlm.nih.gov/pmc/articles/PMC46495/ [Accessed September 6, 2019]

Wang MJ & Lin S (2009) A Region within the 5′-Untranslated Region of Hypoxia-inducible Factor-1α mRNA Mediates Its Turnover in Lung Adenocarcinoma Cells. *J. Biol. Chem.* **284:** 36500–36510 Available at:

http://www.ncbi.nlm.nih.gov/pubmed/19887373 [Accessed August 20, 2019]
Wang W, Wang J, Yan H, Zhang K & Liu Y (2018b) Upregulation of USP11 promotes epithelial-to-mesenchymal transition by deubiquitinating Snail in ovarian cancer. *Oncol. Rep.* **41:** 1739–1748 Available at: http://www.ncbi.nlm.nih.gov/pubmed/30569152 [Accessed August 24, 2019]
Wang Z-D, Shen L-P, Chang C, Zhang X-Q, Chen Z-M, Li L, Chen H & Zhou P-K (2016) Long noncoding RNA lnc-RI is a new regulator of mitosis via targeting miRNA-210-3p to release PLK1 mRNA activity. *Sci. Rep.* **6:** 25385 Available at: http://www.ncbi.nlm.nih.gov/pubmed/27160062 [Accessed August 22, 2019]
Weinstock J, Wu J, Cao P, Kingsbury WD, McDermott JL, Kodrasov MP, McKelvey DM, Suresh Kumar KG, Goldenberg SJ, Mattern MR & Nicholson B (2012) Selective Dual Inhibitors of the Cancer-Related Deubiquitylating Proteases USP7 and USP47. *ACS Med. Chem. Lett.* **3:** 789–792 Available at: http://www.ncbi.nlm.nih.gov/pubmed/24900381 [Accessed September 10, 2019]
Wen Y-A, Stevens PD, Gasser ML, Andrei R & Gao T (2013) Downregulation of PHLPP Expression Contributes to Hypoxia-Induced Resistance to Chemotherapy in Colon Cancer Cells. *Mol. Cell. Biol.* **33:** 4594–4605 Available at: http://www.ncbi.nlm.nih.gov/pubmed/24061475 [Accessed August 23, 2019]
Wen Y, Zhou X, Lu M, He M, Tian Y, Liu L, Wang M, Tan W, Deng Y, Yang X, Mayer MP, Zou F & Chen X (2019) Bclaf1 promotes angiogenesis by regulating HIF-1α transcription in hepatocellular carcinoma. *Oncogene* **38:** 1845–1859 Available at: http://www.ncbi.nlm.nih.gov/pubmed/30367150 [Accessed September 6, 2019]
Wiltshire TD, Lovejoy CA, Wang T, Xia F, O'Connor MJ & Cortez D (2010a) Sensitivity to poly(ADP-ribose) polymerase (PARP) inhibition identifies ubiquitin-specific peptidase 11 (USP11) as a regulator of DNA double-strand break repair. *J. Biol. Chem.* **285:** 14565–14571
Wiltshire TD, Lovejoy CA, Wang T, Xia F, O'Connor MJ & Cortez D (2010b) Sensitivity to Poly(ADP-ribose) Polymerase (PARP) Inhibition Identifies Ubiquitin-specific Peptidase 11 (USP11) as a Regulator of DNA Double-strand Break Repair. *J. Biol. Chem.* **285:** 14565–14571 Available at: http://www.jbc.org/lookup/doi/10.1074/jbc.M110.104745 [Accessed August 30, 2019]
Wiseman LR & Spencer CM (1997) Mitoxantrone. *Drugs Aging* **10:** 473–485 Available at: http://www.ncbi.nlm.nih.gov/pubmed/9205852 [Accessed September 9, 2019]
Wong E & Cuervo AM (2010) Integration of Clearance Mechanisms: The Proteasome and Autophagy. *Cold Spring Harb. Perspect. Biol.* **2:** a006734–a006734 Available at: http://www.ncbi.nlm.nih.gov/pubmed/21068151 [Accessed September 22, 2019]
Wu H-C, Lin Y-C, Liu C-H, Chung H-C, Wang Y-T, Lin Y-W, Ma H-I, Tu P-H, Lawler SE & Chen R-H (2014) USP11 regulates PML stability to control Notch-induced malignancy in brain tumours. *Nat. Commun.* **5:** 3214 Available at: http://www.ncbi.nlm.nih.gov/pubmed/24487962 [Accessed

August 24, 2019]
Wu H-T, Kuo Y-C, Hung J-J, Huang C-H, Chen W-Y, Chou T-Y, Chen Y, Chen Y-J, Chen Y-J, Cheng W-C, Teng S-C & Wu K-J (2016a) K63-polyubiquitinated HAUSP deubiquitinates HIF-1α and dictates H3K56 acetylation promoting hypoxia-induced tumour progression. *Nat. Commun.* **7:** 13644 Available at: http://www.nature.com/articles/ncomms13644 [Accessed September 9, 2019]
Wu H, Ying W, Wang W, Li W & Feng X (2016b) HIF1α and HIF2α mediated UCHL1 upregulation in hypoxia-induced neuronal injury following neuronal hypoxic ischemic encephalopathy. *Int. J. Clin. Exp. Pathol.* **9:** 2677–2685 Available at: https://pdfs.semanticscholar.org/9b18/02beed0cf40d0126185ee0af8e864967263b.pdf [Accessed September 8, 2019]
Xin H, Brown JA, Gong C, Fan H, Brewer G & Gnarra JR (2012) Association of the von Hippel-Lindau Protein with AUF1 and Posttranscriptional Regulation of VEGFA mRNA. *Mol. Cancer Res.* **10:** 108–120 Available at: http://www.ncbi.nlm.nih.gov/pubmed/22086907 [Accessed July 24, 2019]
Xu Q, Briggs J, Park S, Niu G, Kortylewski M, Zhang S, Gritsko T, Turkson J, Kay H, Semenza GL, Cheng JQ, Jove R & Yu H (2005) Targeting Stat3 blocks both HIF-1 and VEGF expression induced by multiple oncogenic growth signaling pathways. *Oncogene* **24:** 5552–5560 Available at: http://www.nature.com/articles/1208719 [Accessed September 6, 2019]
Xu X-H, Bao Y, Wang X, Yan F, Guo S, Ma Y, Xu D, Jin L, Xu J & Wang J (2018) Hypoxic-stabilized EPAS1 proteins transactivate *DNMT1* and cause promoter hypermethylation and transcription inhibition of *EPAS1* in non-small cell lung cancer. *FASEB J.* **32:** 6694–6705 Available at: http://www.ncbi.nlm.nih.gov/pubmed/29920222 [Accessed September 22, 2019]
Xu Y, Li Y, Pang Y, Ling M, Shen L, Yang X, Zhang J, Zhou J, Wang X & Liu Q (2012) EMT and stem cell-like properties associated with HIF-2α are involved in arsenite-induced transformation of human bronchial epithelial cells. *PLoS One* **7:** 1–11
Yamaguchi T, Kimura J, Miki Y & Yoshida K (2007) The Deubiquitinating Enzyme USP11 Controls an I B Kinase (IKK)-p53 Signaling Pathway in Response to Tumor Necrosis Factor (TNF). *J. Biol. Chem.* **282:** 33943–33948 Available at: http://www.ncbi.nlm.nih.gov/pubmed/17897950 [Accessed August 24, 2019]
Yao T, Song L, Xu W, DeMartino GN, Florens L, Swanson SK, Washburn MP, Conaway RC, Conaway JW & Cohen RE (2006) Proteasome recruitment and activation of the Uch37 deubiquitinating enzyme by Adrm1. *Nat. Cell Biol.* **8:** 994–1002 Available at: http://www.ncbi.nlm.nih.gov/pubmed/16906146 [Accessed September 23, 2019]
Yasuda M, Hatanaka T, Shirato H & Nishioka T (2014a) Cell type-specific reciprocal regulation of HIF1A gene expression is dependent on 5′- and 3′-UTRs. *Biochem. Biophys. Res. Commun.* **447:** 638–643 Available at: https://linkinghub.elsevier.com/retrieve/pii/S0006291X14007001 [Accessed August 22, 2019]
Yasuda M, Hatanaka T, Shirato H & Nishioka T (2014b) Cell type-specific reciprocal regulation of HIF1A gene expression is dependent on 5'- and 3'-

UTRs. *Biochem. Biophys. Res. Commun.* **447:** 638–43 Available at: https://linkinghub.elsevier.com/retrieve/pii/S0006291X14007001 [Accessed August 22, 2019]
Yau R & Rape M (2016) The increasing complexity of the ubiquitin code. *Nat. Cell Biol.* **18:** 579–86 Available at: http://www.nature.com/articles/ncb3358 [Accessed September 8, 2019]
Ye Y, Scheel H, Hofmann K & Komander D (2009) Dissection of USP catalytic domains reveals five common insertion points. *Mol. Biosyst.* **5:** 1797 Available at: http://xlink.rsc.org/?DOI=b907669g [Accessed August 24, 2019]
Yoon J-H, De S, Srikantan S, Abdelmohsen K, Grammatikakis I, Kim J, Kim KM, Noh JH, White EJF, Martindale JL, Yang X, Kang M-J, Wood WH, Noren Hooten N, Evans MK, Becker KG, Tripathi V, Prasanth K V, Wilson GM, Tuschl T, et al (2014) PAR-CLIP analysis uncovers AUF1 impact on target RNA fate and genome integrity. *Nat. Commun.* **5:** 5248 Available at: http://www.nature.com/articles/ncomms6248 [Accessed August 5, 2019]
Yu M, Liu K, Mao Z, Luo J, Gu W & Zhao W (2016) USP11 Is a Negative Regulator to γH2AX Ubiquitylation by RNF8/RNF168. *J. Biol. Chem.* **291:** 959–967 Available at: http://www.ncbi.nlm.nih.gov/pubmed/26507658 [Accessed August 24, 2019]
Yuan J, Luo K, Zhang L, Cheville JC & Lou Z (2010) USP10 Regulates p53 Localization and Stability by Deubiquitinating p53. *Cell* **140:** 384–396 Available at: http://www.ncbi.nlm.nih.gov/pubmed/20096447 [Accessed August 23, 2019]
Zhang C, Peng Z, Zhu M, Wang P, Du X, Li X, Liu Y, Jin Y, McNutt MA & Yin Y (2016a) USP9X destabilizes pVHL and promotes cell proliferation. *Oncotarget* **7:** 60519–60534 Available at: http://www.ncbi.nlm.nih.gov/pubmed/27517496 [Accessed September 9, 2019]
Zhang D, Li J, Zhang M, Gao G, Zuo Z, Yu Y, Zhu L, Gao J & Huang C (2012a) The Requirement of c-Jun N-terminal Kinase 2 in Regulation of Hypoxia-inducing Factor-1α mRNA Stability. *J. Biol. Chem.* **287:** 34361–34371 Available at: http://www.ncbi.nlm.nih.gov/pubmed/22910906 [Accessed August 22, 2019]
Zhang D, Li J, Zhang M, Gao G, Zuo Z, Yu Y, Zhu L, Gao J & Huang C (2012b) The Requirement of c-Jun N-terminal Kinase 2 in Regulation of Hypoxia-inducing Factor-1α mRNA Stability. *J. Biol. Chem.* **287:** 34361–34371 Available at: http://www.ncbi.nlm.nih.gov/pubmed/22910906 [Accessed July 30, 2019]
Zhang E, Shen B, Mu X, Qin Y, Zhang F, Liu Y, Xiao J, Zhang P, Wang C, Tan M & Fan Y (2016b) Ubiquitin-specific protease 11 (USP11) functions as a tumor suppressor through deubiquitinating and stabilizing VGLL4 protein. *Am. J. Cancer Res.* **6:** 2901–2909 Available at: http://www.ncbi.nlm.nih.gov/pubmed/28042509 [Accessed September 9, 2019]
Zhang S, Xie C, Li H, Zhang K, Li J, Wang X & Yin Z (2018a) Ubiquitin-specific protease 11 serves as a marker of poor prognosis and promotes metastasis in hepatocellular carcinoma. *Lab. Investig.* **98:** 883–894 Available at: http://www.ncbi.nlm.nih.gov/pubmed/29545598 [Accessed August 24, 2019]

Zhang X, Liu L, Wei X, Tan YS, Tong L, Chang, BS R, Ghanamah MS, Reinblatt M, Marti GP, Harmon JW & Semenza GL (2010) Impaired angiogenesis and mobilization of circulating angiogenic cells in HIF-1α heterozygous-null mice after burn wounding. *Wound Repair Regen.* **18:** 193–201 Available at: http://www.ncbi.nlm.nih.gov/pubmed/20163569 [Accessed September 5, 2019]

Zhang Y, Luo Y, Wang Y, Liu H, Yang Y & Wang Q (2018b) Effect of deubiquitinase USP8 on hypoxia/reoxygenation-induced inflammation by deubiquitination of TAK1 in renal tubular epithelial cells. *Int. J. Mol. Med.* **42:** 3467–3476 Available at: http://www.spandidos-publications.com/10.3892/ijmm.2018.3881 [Accessed August 23, 2019]

Zhao J, Wei J, Dong S, Bowser RK, Zhang L, Jacko AM & Zhao Y (2016) Destabilization of Lysophosphatidic Acid Receptor 1 Reduces Cytokine Release and Protects Against Lung Injury. *EBioMedicine* **10:** 195–203 Available at: http://www.ncbi.nlm.nih.gov/pubmed/27448760 [Accessed September 9, 2019]

Zhao Y, Majid MC, Soll JM, Brickner JR, Dango S & Mosammaparast N (2015) Noncanonical regulation of alkylation damage resistance by the OTUD4 deubiquitinase. *EMBO J.* **34:** 1687–1703

Zheng X, Zhai B, Koivunen P, Shin SJ, Lu G, Liu J, Geisen C, Chakraborty AA, Moslehi JJ, Smalley DM, Wei X, Chen X, Chen Z, Beres JM, Zhang J, Tsao JL, Brenner MC, Zhang Y, Fan C, DePinho RA, et al (2014) Prolyl hydroxylation by EglN2 destabilizes FOXO3a by blocking its interaction with the USP9x deubiquitinase. *Genes Dev.* **28:** 1429–44 Available at: http://www.ncbi.nlm.nih.gov/pubmed/24990963 [Accessed August 23, 2019]

Zhong H, Chiles K, Feldser D, Laughner E, Hanrahan C, Georgescu MM, Simons JW & Semenza GL (2000) Modulation of hypoxia-inducible factor 1alpha expression by the epidermal growth factor/phosphatidylinositol 3-kinase/PTEN/AKT/FRAP pathway in human prostate cancer cells: implications for tumor angiogenesis and therapeutics. *Cancer Res.* **60:** 1541–5 Available at: http://www.ncbi.nlm.nih.gov/pubmed/10749120 [Accessed August 20, 2019]

Zhou X, Guo X, Chen M, Xie C & Jiang J (2018) HIF-3α Promotes Metastatic Phenotypes in Pancreatic Cancer by Transcriptional Regulation of the RhoC–ROCK1 Signaling Pathway. *Mol. Cancer Res.* **16:** 124–134 Available at: http://mcr.aacrjournals.org/lookup/doi/10.1158/1541-7786.MCR-17-0256 [Accessed September 6, 2019]

Zhou Z, Luo A, Shrivastava I, He M, Huang Y, Bahar I, Liu Z & Wan Y (2017) Regulation of XIAP Turnover Reveals a Role for USP11 in Promotion of Tumorigenesis. *EBioMedicine* **15:** 48–61 Available at: http://www.ncbi.nlm.nih.gov/pubmed/28040451 [Accessed August 24, 2019]

Zimmer M, Ebert BL, Neil C, Brenner K, Papaioannou I, Melas A, Tolliday N, Lamb J, Pantopoulos K, Golub T & Iliopoulos O (2008) Small-Molecule Inhibitors of HIF-2a Translation Link Its 5′UTR Iron-Responsive Element to Oxygen Sensing. *Mol. Cell* **32:** 838–848 Available at: http://www.ncbi.nlm.nih.gov/pubmed/19111663 [Accessed September 22, 2019]

Zucconi BE, Ballin JD, Brewer BY, Ross CR, Huang J, Toth EA & Wilson GM

(2010) Alternatively Expressed Domains of AU-rich Element RNA-binding Protein 1 (AUF1) Regulate RNA-binding Affinity, RNA-inducedfile:///Y:/Y - GBEdurne/Teresa/BEFORE 2018/DUBs regulators of HITs validation/siRNA/OTUD4/sh only.pdf Protein Oligomerization, and th. *J. Biol. Chem.* **285:** 39127–39139 Available at: http://www.ncbi.nlm.nih.gov/pubmed/20926381 [Accessed August 5, 2019]

Apendix 1: Posters presented during the thesis

Deubiquitinating enzymes (DUBs) as new regulators of the Hypoxia Pathway

Teresa Martín-Mateos, Encarnación Pérez-Andrés, Onintza Carlevaris, Sara Pozo, Edurne Berra

CIC bioGUNE, Derio, ES

State of the art

Oxygen homeostasis is crucial for aerobic organisms. Hypoxia can produce irreversible damages, even when transient and is associated with pathologies such as ischemic diseases, inflammatory and metabolic disorders, Alzheimer and cancer. Thus, a crucial cellular adaptive response is quickly triggered by the hypoxia signalling pathway, which is tightly controlled by the ubiquitin-proteasome system (UPS). The family of DeUbiquitinating enzymes (DUBs) specifically deconjugates ubiquitin from targeted Proteins, playing major roles in the UPS control.

Objective

To find DUBs that modulate this pathway to be used as therapeutic targets

Hypothesis

DUBs should play an important role in the subtle regulation of the hypoxia signalling

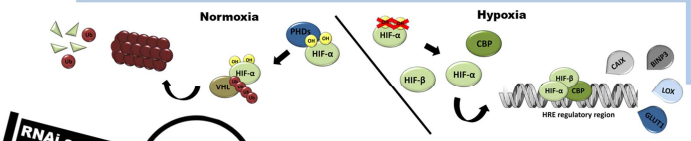

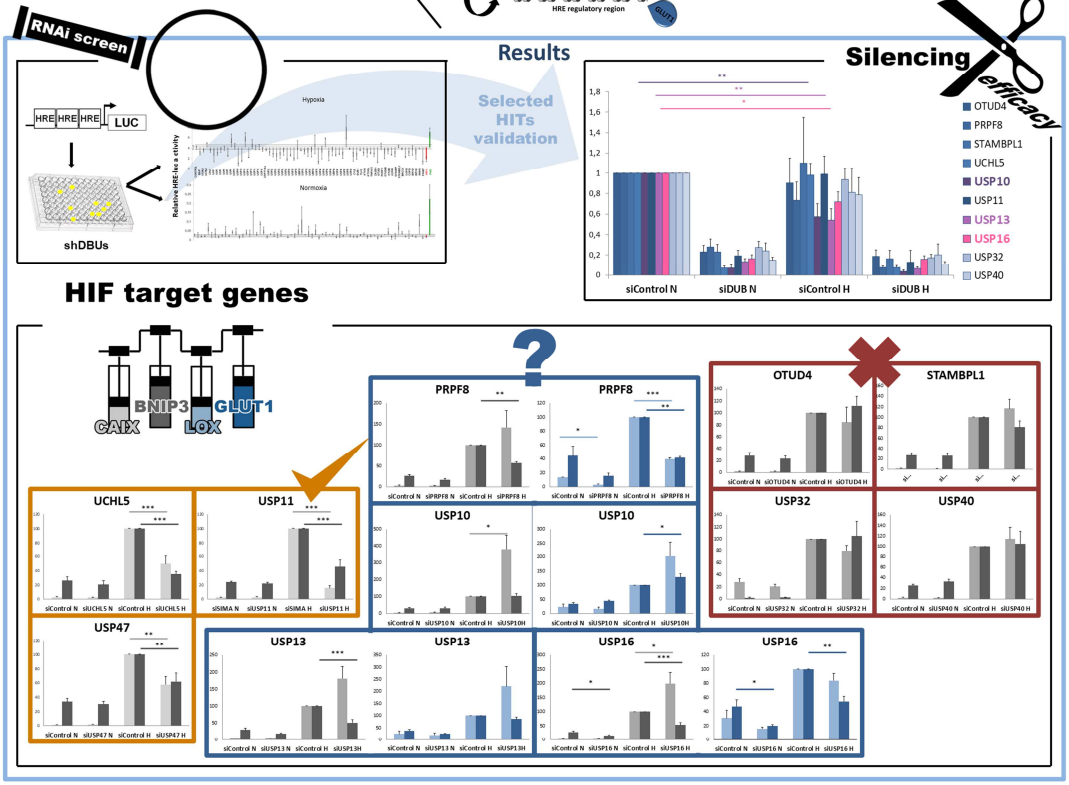

Conclusions

We have identified three DUBs whose mRNA levels are regulated by hypoxia

We have successfully validated three DUBs that activate the hypoxia signalling pathway

Further work is required to clarify the role of PRPPF8, USP10, USP13 and USP16

USP10 ⬇mRNA

USP13 ⬇mRNA

USP16 ⬇mRNA

Activators UCHL5

USP11

USP47

This work has been supported by

BES_2014_070406 BFU_2013_46647_R

Deubiquitinating enzymes (DUBs) to target the Hypoxia Pathway

Amelie Schober, Teresa Martín-Mateos, Encarnación Pérez-Andrés, Onintza Carlevaris, Sara Pozo, Edurne Berra

CIC bioGUNE, Derio, ES

INTRODUCTION

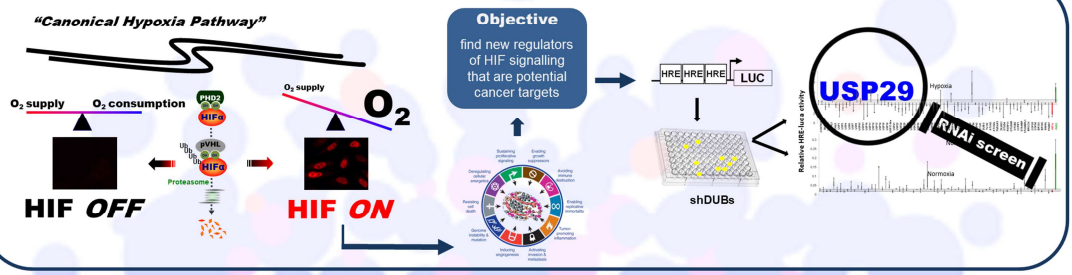

RESULTS

USP29 induces endogenous HIF-1α accumulation

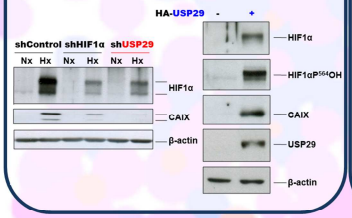

USP29 is a non-canonical regulator of HIF-1α

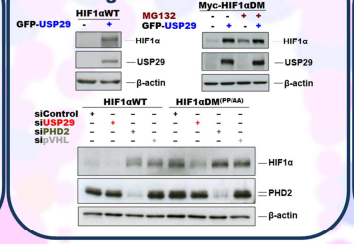

USP29 universal effect

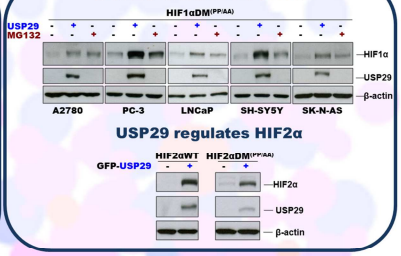

USP29 regulates HIF2α

USP29 physically interacts with HIF-α

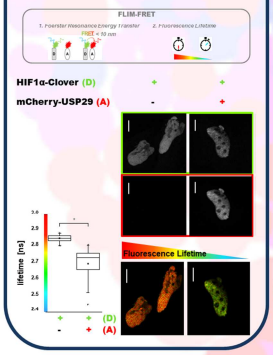

USP29 deubiquitinates HIF-1α

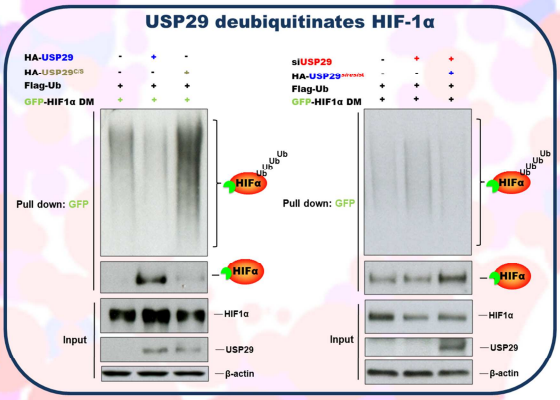

USP29: oncogene in prostate cancer

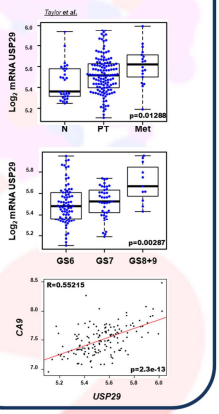

CONCLUSION

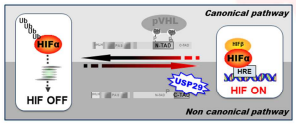

✓ **USP29 is a novel HIF-α activator**

✓ **USP29 deubiquitinates HIF-α and protects it from proteasome-mediated degradation in an O_2/PHD/pVHL independent way**

This work has been supported by

BES_2014_070406 BFU_2013_46647_R

The challenge of finding specific HIF-1 or HIF-2 dependent genes

Teresa Martín-Mateos, Onintza Carlevaris & Edurne Berra

CIC bioGUNE, Derio, ES

STATE OF THE ART

The Hypoxia Inducible Factor (HIF) is the master cellular regulator that controls adaptation to hypoxia. HIF transcription factor works as a dimer, binding the Hypoxia Responsive Elements (HRE) within the regulatory regions of the target genes. The dimer is composed by an alpha subunit (HIF-α), which stability and function are tightly controlled by oxygen levels, and a beta subunit (HIF-β) that is ubiquitously present in the cell. Among the three HIF-α isoforms, HIF-3α generates different slicing products, which are poorly studied. By contrast, HIF-1α and HIF-2α are best characterized and considered the master regulators of the hypoxic transcriptional response. Although HIF-1 and HIF-2 functions are clearly non-redundant, the identification of specific target genes is still controversial in the hypoxia field. By using two independent strategies, we have tried to validate HIF-1 or HIF-2 target genes in three different models: embryonic kidney (HEK293), malignant melanoma (A375) and breast adenocarcinoma (MDA-MB-231) cell lines.

RESULTS

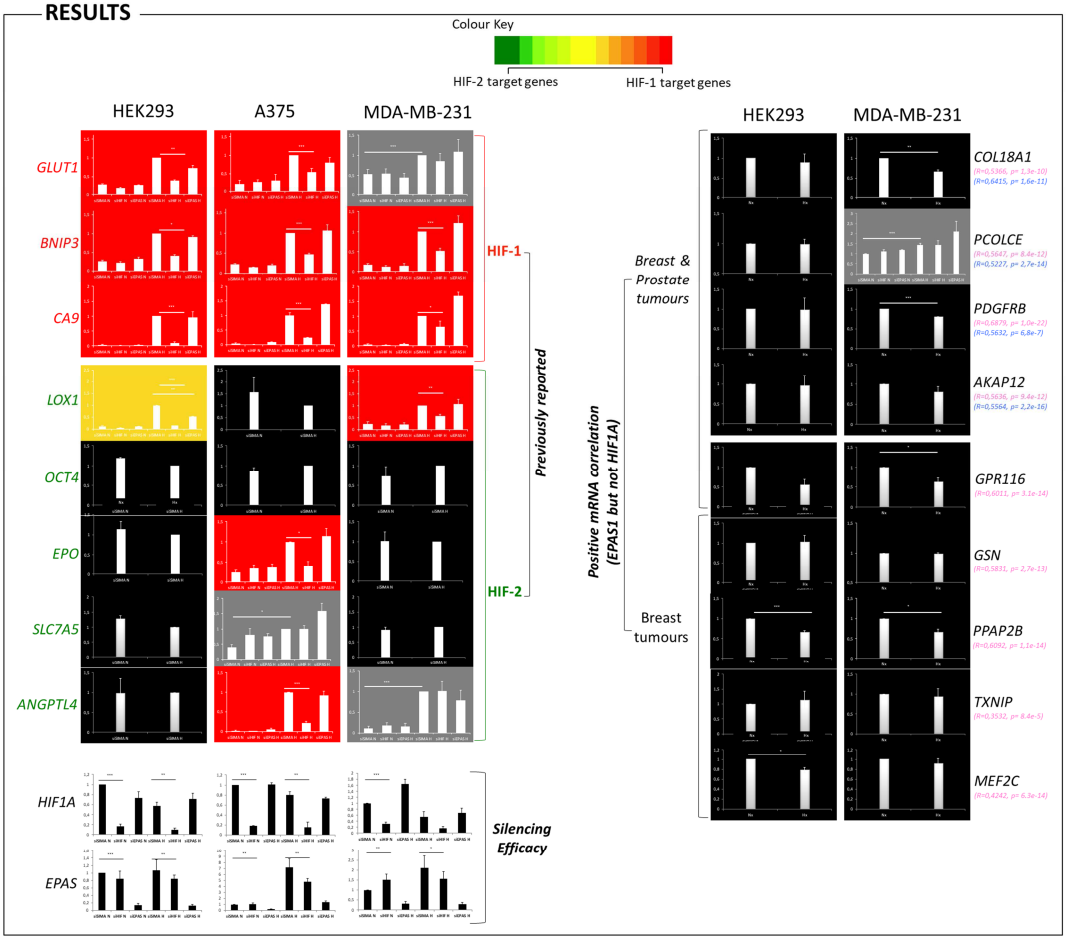

CONCLUSION

We have confirmed most of the previously reported HIF-1 target genes. However, we have failed to validate any described HIF2-dependent gene in three independent cell models. Interestingly, we have found that the hypoxic induction of LOX1 appears to be mediated by both HIF-1 and HIF-2 in HEK293 cell line.

We have failed our approach to identify new HIF2-specific target genes based on a positive correlation with *EPAS*1 but not with *HIF1A* expression in at least 5 different data bases of breast and/or prostate cancer patients. Furthermore, among all the genes we have analyzed, only *PCOLCE* expression has been shown to be induced by hypoxia.

This work has been supported by

Post-transcriptional HIF1A regulation:

a new target to control the hypoxia signalling pathway

Teresa Martín-Mateos, Inés Martín-Barros, Peio Azkoaga, Onintza Carlevaris, Laura Martínez-Pérez and Edurne Berra

CIC bioGUNE, Derio, ES

STATE OF THE ART

Adaptation to hypoxia is a puzzling and tightly regulated challenge that can produce irreversible damages, even when transient. In fact, hypoxia is associated with pathologies such as ischemic diseases, inflammatory and metabolic disorders, Alzheimer and cancer. This adaptability involves a severe gene expression rewiring (e.x: induction of *BNIP3, CA9, SLC2A1* and *LOX*), which is mainly triggered by the Hypoxia Inducible transcription Factor (HIF). HIF acts as a heterodimer composed by a ubiquitously expressed β subunit (HIF-β) that binds to the O_2-sensitive α subunit (HIF-α). The regulation of the hypoxia signalling pathway canonically relies on HIF-α protein stability, which has been described to be exquisitely regulated through the Ubiquitin Proteasome System (UPS). Accordingly, we argue that key UPS components as DeUbiquitinating enzymes (DUBs) might contribute to the adaptive programme. Here, we report a novel and robust mechanism of HIF-α regulation that relies on *HIF1A* transcript processing and turnover and that could shed light on new targets to fine tune the hypoxia signalling pathway.

1 RNAi-BASED SCREEN OF DUBs

Hypoxic induction of *BNIP3* and *CA9*

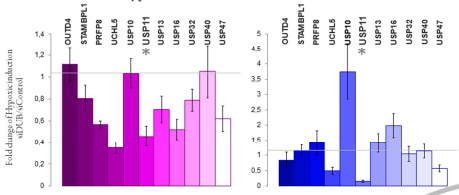

DUB knockdown

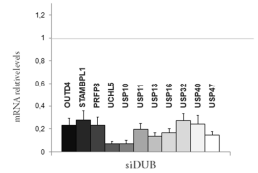

2 USP11 ACTIVATES HIF-1 SIGNALLING

siUSP11.1 and 2 decrease HIF target genes' hypoxic induction

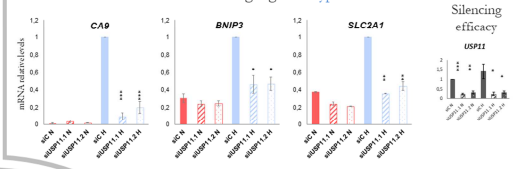

siUSP11.1 and *specifically* 2 blocks HIF-1α hypoxic accumulation

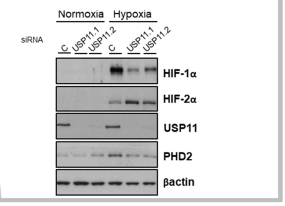

5 DRUGABILITY

USP11 INHIBITOR : MITOXANTRONE

Blocks HIF-1 signalling

FDA APPROVED

- Hematological malignancies
- Prostate cancer
- Multiple sclerosis

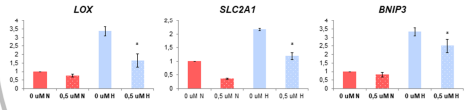

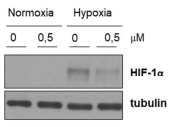

3 THROUGH *HIF1A*

USP11 controls *HIF1A* mRNA *individually*

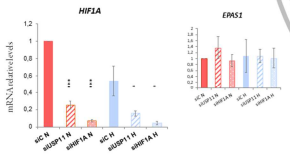

USP11 controls *HIF1A* mRNA at posttranscriptional level

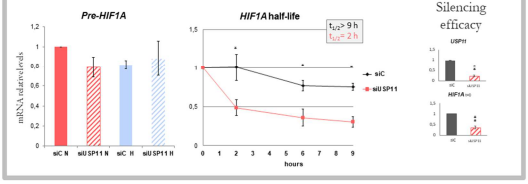

4 USP11 BINDS RBPs

RNA Binding Proteins

USP11 interacts with hnRNPD

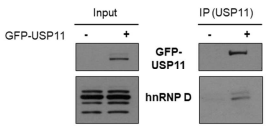

hnRNPD also stabilizes *HIF1A*

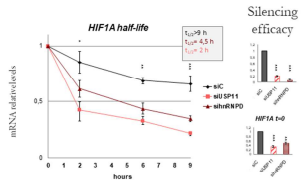

hnRNPD binds *HIF1A*

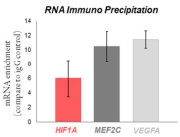

CONCLUSION

- USP11 is an activator of the hypoxia signalling cascade.
- USP11 controls *HIF1A* stability, which is necessary for triggering the hypoxic transcriptional programme.
- USP11 interacts with hnRNPD, that binds *HIF1A* directly to enhance its stability.
- MITOXANTRONE, a USP11 pharmacological inhibitor, recapitulates the effect of USP11 knockdown on cells.

WORKING MODEL

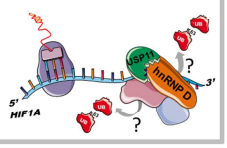

CIC bioGUNE
CENTER FOR COOPERATIVE RESEARCH IN BIOSCIENCES
EXCELENCIA SEVERO OCHOA
Red HYPOX
SAF2017-90794-REDT
This work has been supported by
BES_2014_070406 BFU_2013_46647_R
EEBB-I-17-12687 BFU_2016_76872_R

Apendix 2: Scientific Contributions

The persistent stimulation of macrophages with *Borrelia burgdorferi* results in increased glycolysis and the regulation of phagocytosis and inflammation

Diego Barriales [1], Itziar Martín [1], Ana Carreras-González [1], Marta Montesinos-Robledo [1], Teresa Martín-Mateos [2], Estibaliz Atondo [1], Ainhoa Palacios [1], Monika Gonzalez [3], Diana Cabrera [4], Ainize Peña-Cearra [1], Sebastiaan M. van Liempd [4], Juan M. Falcón-Pérez [4,5], Miguel A. Pascual-Itoiz [1], Leticia Abecia [1], Aize Pellon [1], Maria Luz Martínez-Chantar [6], Ana M. Aransay [3,7], Alberto Pascual [8], Edurne Berra [2], José Luis Lavín [9], Héctor Rodríguez [1], Juan Anguita [1,5,*]

[1] Inflammation and Macrophage Plasticity laboratory, CIC bioGUNE, Derio, Spain 48160

[2] Physiopathology of the hypoxia-signaling pathway laboratory, CIC bioGUNE, Derio, Spain 48160

[3] Genomic Analysis platform, CIC bioGUNE, Derio, Spain 48160

[4] Metabolomics Platform, CIC bioGUNE, Derio, Spain 48160

[5] Ikerbasque, Basque Foundation for Science, Bilbao, Spain 48013

[6] Liver Diseases laboratory, CIC bioGUNE, Derio, Spain 48160

[7] CIBERehd, Instituto de Salud Carlos III, Madrid, 28029, Spain

[8] Instituto de Biomedicina de Sevilla, Hospital Universitario Virgen del Rocío/CSIC/Universidad de Sevilla, Seville, Spain

[9] Bioinformatics Service, CIC bioGUNE, Derio, Spain 48160

***Correspondence to*:** Juan Anguita, PhD. Inflammation and Macrophage Plasticity laboratory, CIC bioGUNE. Parque Tecnológico de Bizkaia, Bldg. 801A. Derio, Spain 48160.

janguita@cicbiogune.es

Abstract

Macrophage exposure to vaccine or vaccine-like formulations results in disparate secondary responses. However, little is known about the long-term consequences of the interaction between macrophages and persistent infectious agents. We have identified the transcriptomic and metabolic changes associated with the long-term response of macrophages to *Borrelia burgdorferi*, an extracellular pathogen able to establish persistent infections in mammals. Chronically-stimulated macrophages show an enhanced ability to bind and internalize the spirochete, while producing reduced amounts of proinflammatory factors. The transcriptional analysis of acutely and chronically stimulated macrophages shows the activation of similar inflammatory pathways, albeit with a limited response. In addition, experienced macrophages show the upregulation of HIF-induced genes and an augmented glycolytic output. Furthermore, the inhibition of glycolysis reduces the production of TNF by macrophages. We also show that, i*n vivo*, glycolysis inhibition results in decreased cardiac inflammation and reduced spirochetal persistence, when the animals are treated at the peak of the disease. These data show that *B. burgdorferi* induces long-term, memory-like responses in macrophages that are amenable to be manipulated *in vivo* and provide novel therapeutic targets for the treatment of infection and its associated inflammation.

Keywords: Lyme borreliosis, *Borrelia burgdorferi*, innate immune memory, metabolism, therapy, inflammation, phagocytosis

Background

Macrophages constitute the first line of defense of the immune system against infections. Since their identification as cells capable of ingesting microorganisms, their functional characterization has continuously evolved; yet much is still unknown about key aspects of their biology and how they are regulated. The existence of long-term consequences of the stimulation of macrophages with certain simple (e.g. beta glucans) or complex (e.g. BCG, the mycobacterial vaccine strain) stimuli has been termed *'innate immune memory'* [1, 2]. This concept originally evolved from observations in BCG-vaccinated individuals in which a level of protection against disparate pathogens was identified [3]. Innate immune memory has been defined in terms of the induction of proinflammatory cytokines [4]. Responses identified as memory have been divided into *innate immune training* and *tolerance*; the difference being the nature of the secondary response (heightened versus reduced). Innate immune memory is replicated *in vitro* by the use of a primary stimulus, a period of resting, and a different secondary stimulus. Although the mechanisms underlying the development of innate immune memory are not completely known, both variations in metabolism (Warburg effect) mediated by the AKT/mTOR/HIF axis, and epigenetic changes are known to occur [3, 5, 6]. The effect of this previous experience on the ability of monocytes/macrophages to internalize/phagocytose microorganisms has been, however, largely unaddressed, in spite of the importance of this process in the elimination of pathogens, and the intimate relationship between phagocytosis and the inflammatory output of macrophages [7, 8]. Moreover, the response to live and killed microorganisms is vastly different, both quantitatively and qualitatively [9-11]. Therefore, the phenotypic and regulatory mechanisms of innate immune memory cells against pathogens that are able to establish persistent infections are lacking, including the causative agent of Lyme borreliosis, *Borrelia burgdorferi* [12-14]. In spite of

persistently infecting mammalian hosts, including organs in which macrophages are the main responding immune cell such as the heart, the inflammatory response is known to vane over time albeit with bouts of exacerbation in experimentally infected animals [15] while long-term cardiac-related anomalies associated with infection with *B. burgdorferi* in humans are rare [16].

We have recently identified transcriptional traits and signaling pathways associated with the short-time stimulation of monocytes/macrophages from both human and murine origin with *B. burgdorferi* [17]. However, macrophages are likely exposed to *B. burgdorferi* during prolonged periods of time. Therefore, the response of these cells may be differentially modulated over time. Here, we show the long-term responses of macrophages to the spirochete with an emphasis on the ability to control bacterial phagocytosis and the ensuing proinflammatory response, as well as the regulatory control of these responses.

Methods

Mice

C57Bl/6 (B6) mice were purchased from Charles River Laboratories and bred in the Animal Facility at CIC bioGUNE. All the assays performed were approved by the competent authority (Diputación de Bizkaia) under European and Spanish directives. CIC bioGUNE´s Animal Facility is accredited by AAALAC Intl.

Human cells

Human monocytes were purified from buffy coats of healthy blood donors by positive selection using a human CD14 purification kit (Miltenyi Biotec), as described [17]. The cells were rested overnight before stimulation. All human samples were obtained after approval by the Basque Country's Ethics committee following the Helsinki convention. Donors signed an informed consent form and were anonymized to the authors.

Bacteria

B. burgdorferi s.s. Bb914 [18] and B31 clone 5A15 were used throughout. The spirochetes were grown in BSK-H medium (Sigma Aldrich) in 5-ml tubes at 34 ºC and used at a multiplicity of infection of 25.

Murine infections

Six to eight-week old B6 mice were infected with 10^5 *B. burgdorferi* B31 clone 5A15 subcutaneously, as described [19]. At the specified times, the mice were treated with dicholoroacetate (DCA; Thermo Fisher Scientific) (2 g/l) in the drinking water (changed twice a week) or intraperitoneally with 50 mg/kg of 3-(3-pyridinyl)-1-(4-pyridinyl)-2-propen-1-one (3PO), for a period of 14-28 days. The mice were sacrificed 4-5 weeks post infection. The hearts were cut in half through bisections across the atria and ventricles to isolate DNA and RNA using

the AllPrep DNA/RNA/miRNA Universal Kit (Qiagen) following the manufacturer's recommendations. Bacterial burdens were measured from heart DNA by qPCR targeting *recA* relative to the murine gene, *Rpl19.* RNA was reverse-transcribed and used to perform real-time PCR to determine the expression levels of *Tnf* and *Adgre1* relative to *Rpl19*, as before. The primers used are listed in Suppl. Table 1.

Cell culture

Bone marrow-derived macrophages (BMMs) were generated from 6-12-week-old B6 mice. Bone marrow cells were incubated in 100 mm x 15 mm non-treated Petri dishes (Falcon) for 6 days at 37 ºC with 5% CO_2 in DMEM supplemented with 10% FCS and 10% penicillin-streptomycin plus 30 ng/ml of M-CSF (Miltenyi Biotec, Pozuelo de Alarcón, Madrid, Spain). Non-adherent cells were then discarded and adherent macrophages were scraped, counted and seeded. The macrophage-like cell line, RAW 264.7, was maintained in DMEM supplemented with 10% FCS and 10% penicillin-streptomycin (Thermo Fisher Scientific).

Phagocytosis assays

Phagocytosis assays were performed as previously described [19]. BMMs and RAW 264.7 cells were cultured in serum- and antibiotic-free medium for 1 h. GFP expressing *B. burgdorferi* were then added to the cells at a multiplicity of infection of 25 and incubated at 4 °C for 15 min followed by 37 °C for 2 h. The cells were then washed to eliminate surface bacteria and analyzed by flow cytometry in a BD FACS Canto II cytometer (BD Biosciences, San Agustín de Guadalix, Madrid, Spain). The data were analyzed using FlowJo for Mac, version 10.5.3 (FlowJo, Ashland, OR). The phagocytic index was calculated following the formula: % GFP cells (Test) x MFI (Test) - % GFP cells (4 ºC control) x MFI (4 ºC control) [20].

Confocal microscopy

Following incubation with *B. burgdorferi* Bb914 at 4 ºC, the cells were washed, fixed with 4% paraformaldehyde for 20 min, permeabilized with PBS containing 0,3% Triton X-100 (VWR, Radnor, PA, USA) and stained with rhodamine-labelled phalloidin and DAPI for 10 min at 37 ºC (Thermo Fisher Scientific). After extensive washing with PBS, the cells were mounted using the Prolong Gold Antifade mounting reagent (Thermo Fisher Scientific). The images were obtained employing a Leica TCS SP8 confocal system (Leica Microsystems, Madrid, Spain).

Cytokine ELISA

The levels of murine and human TNF in the stimulation supernatants were determined by capture ELISA using the Mouse TNF ELISA Set II (BD Biosciences) and the human TNF ELISA set (Thermo Fisher Scientific), following the manufacturers' instructions.

RNA isolation

Total RNA was isolated using the NucleoSpin® RNA kit (Macherey-Nagel). The quantity and quality of the RNAs were assessed using the Qubit RNA Assay Kit (Thermo Fisher Scientific) and RNA Nano Chips in a 2100 Bioanalyzer (Agilent Technologies), respectively.

RNAseq transcriptomics

Libraries were prepared using the TruSeq RNA Sample Preparation Kit v2 (Illumina) following the instructions from the manufacturer. Single-read 50 nt sequencing of pooled libraries was carried out in a HiScanSQ platform (Illumina). The quality control of the sequenced samples was performed using the FASTQC software (www.bioinformatics.babraham.ac.uk/projects/fastq). Reads were mapped against the mouse (mm10) reference genome using Tophat [21] accounting for spliced junctions. The resulting BAM alignment files for the samples were then used to generate a table of raw counts by Rsubread [22], which was the input for the Differential Expression (DE) analysis, carried out by DESeq2 [23]. Transcriptomics data were analyzed using

QIAGEN´s Ingenuity® Pathway Analysis (IPA®, Qiagen). Validation of the RNAseq data was performed by real-time PCR (Suppl. Fig. 1). The RNAseq data are deposited under GEO accession number GSE125516.

Real-time PCR

RNA was reverse transcribed using M-MLV reverse transcriptase (Thermo Fisher Scientific). Real-time PCR was then performed using the PerfeCTa SYBR Green SuperMix low ROX (Quantabio) on a QuantStudio™ 6 Real-Time PCR System (Thermo Fisher Scientific). Fold induction of the genes was calculated relative to *Rpl19* using the $2^{-\Delta\Delta Ct}$ method.

Metabolic assays

The oxygen consumption (OCR) and extracellular acidification rates (ECAR) were measured in differentially stimulated BMMs employing an XF24 extracellular flux analyzer (Agilent). Unstimulated (4×10^5) and *B. burgdorferi*-stimulated cells (2×10^5) were seeded per well in a Cell-Tak coated plate (BD Biosciences), and the measurements were normalized to cellular protein amount. For ECAR determination, the cells were previously plated in XF Seahorse medium with 4 mM glutamine and 10 mM pyruvate, while for the mitochondrial stress test the cells were plated in medium containing 4 mM glutamine, 10 mM pyruvate and 25 mM glucose. After 1 hour at 37 °C without CO_2, three baseline oxidative consumption rate (OCR) and extracellular acidification rate (ECAR) measurements were performed. For glycolysis determination, ECAR was measured at baseline and after sequentially adding glucose (25 mM), Oligomycin (1 µM) and 2-DG (50 mM). In parallel experiments, OCR was determined at baseline and after sequentially adding oligomycin, FCCP, antimycin/rotenone at 1 µM. Lactate production was measured from stimulation supernatants using the Lactate (Trinity Biotech), Liquid L-Lactate Trinder (Biochemical Enterprise) and Lactate-Glo™ Assay kits (Promega).

Determination of metabolic intermediaries of the TCA metabolism

The levels of glutamine, glutamate, malate, citrate and succinate were determined in BMMs by liquid chromatography tandem mass spectrometry (LC-MS/MS). Cellular pellets were homogenized in 500 µl of ice-cold methanol/water (50/50 %v/v) containing 1 µM stable labelled ^{13}CD3-methionine (methionine-SL) as internal standard. The homogenate was shaken at 1,400 rpm for 30 minutes at 4 °C, centrifuged for 15 min at 13,000 rpm and 4 °C, and evaporated in a Speedvac. The resulting pellets were resuspended in equal volumes of water/acetonitrile (40/60 v/v). Samples were measured with a UPLC system (Acquity, Waters Inc.) coupled to a Time of Flight mass spectrometer (ToF MS, SYNAPT G2, Waters Inc.). A 2.1 x 100 mm, 1.7 µm BEH amide column (Waters Inc.), maintained at 40 °C, was used to separate the analytes before entering the MS. Mobile phase solvent A (aqueous phase) consisted of 99.5% water, 0.5% FA and 20 mM ammonium formate while solvent B (organic phase) consisted of 29.5% water, 70% acetonitrile, 0.5% FA and 1 mM ammonium formate. The following gradient was used: from 5% A to 50% A in 2.4 minutes in curved gradient (#8, as defined by Waters), from 50% A to 99.9% A in 0.2 minutes constant at 99.9% A for 1.2 minutes, back to 5% A in 0.2 minutes. The flow rate was 0.250 ml/min and the injection volume 2 µl. After every 6 injections QC low and QC high sample was injected. The MS was operated in positive and negative electrospray ionization, depending on analyte, in full scan mode. The cone voltage was 25 V and capillary voltage was 250 V. Source temperature was set to 120 °C and capillary temperature to 450 °C. The flow of the cone and desolvation gas (both nitrogen) were set to 5 L/h and 600 L/h, respectively. A 2 ng/mL leucine-enkephalin solution in water/acetonitrile/formic acid (49.9/50/0.1 %v/v/v) was infused at 10 µl/min and used for a lock mass which was measured each 36 seconds for 0.5 seconds. Spectral peaks were automatically corrected for deviations in the lock mass.

Results

***B. burgdorferi* induces long-term responses in macrophages affecting phagocytosis and proinflammatory cytokine production.** We first analyzed the response of macrophages stimulated acutely and those that had been previously exposed to *B. burgdorferi*. We stimulated murine bone marrow-derived macrophages (BMMs) for 48 h, washed them and re-stimulated them with the spirochete for 16 - 20h (condition BB; Suppl. Fig. 2A). Acutely stimulated macrophages were processed in parallel, except with no stimulation the first 48 h (condition UB). Non stimulated (condition UU) and stimulated and rested (condition BU) macrophages were also generated (Suppl. Fig. 2A). Previous exposure to the spirochete resulted in decreased TNF production in response to *B. burgdorferi*, compared to acutely activated cells (Fig. 1A). The analysis of purified $CD14^+$ cells from peripheral blood of healthy donors confirmed these results in human monocytes (Fig. 1A).

Macrophages previously activated with *B. burgdorferi* showed an augmented capacity to bind the spirochete at 4 ºC (Fig. 1B, Suppl. Fig. 2B), which resulted in their increased internalization when the cells were further incubated at 37 ºC (Fig. 1B). More binding of spirochetes to previously activated macrophages was also observed by confocal microscopy (Fig. 1C). In order to analyze the internalization rate of the spirochete, we compared the phagocytosis index of macrophages previously unexposed and stimulated with the spirochete. This analysis revealed similar internalization rates for *B. burgdorferi* (Fig. 1D), indicating that the higher internalization observed in macrophages previously activated was due to the increased ability of these cells to bind the bacterium. Overall, these data show that macrophages exposed to *B. burgdorferi* augment the capacity to bind and subsequently internalize the spirochete, albeit with the induction of reduced levels of TNF.

***B. burgdorferi* induces a differential transcriptional profile in acute and memory macrophages.** We then analyzed the transcription profiles of BMMs that had been stimulated with the spirochete under the 4 conditions shown in Suppl. Fig. 2A by RNAseq. The four conditions showed distinct transcriptional profiles, as seen in PCA (Fig. 2A) and sample distance matrix analysis (Suppl. Fig. 3A). The analysis of the 1,000 most regulated genes under the four conditions studied, showed similar patterns of expression for the conditions UU and BU, while UB and BB were also similar (Suppl. Fig. 3B). The comparison of genes up- and down-regulated under each condition versus unstimulated (UU) macrophages revealed that in spite of the similarities between the unstimulated (UU) and the previously stimulated (BU) conditions, 1334 genes were differentially regulated when using cut off values of 1 for the absolute $\log_2$ Fold Change and $p < 0.05$ (693 up and 641 down; Suppl. Fig. 3C). On the other hand, the comparison to unstimulated (UU) macrophages of acutely (UB) and re-stimulated (BB) cells revealed similar number of upregulated and downregulated genes (Suppl. Fig. 3D), of which a majority (2154; 1024 upregulated and 1130 downregulated) were common (Fig. 2B). Ingenuity Pathway Analysis (IPA) showed that the genes regulated in previously exposed macrophages (BB) were consistent with pathways activated by the acute stimulation of BMMs with *B. burgdorferi* (UB) [17], including interferons, TLRs, NOD and cytokines such as IL-1β (Fig. 2C). The transcriptional analysis of proinflammatory cytokine production (*Tnf*, *Il6*, *Il1b* and *Il12b*) confirmed the pattern observed for TNF by ELISA, while the levels of *Il10* transcripts were highly upregulated in previously activated cells (Suppl. Fig. 3E). However, as in acutely stimulated cells [17], the IL-10R-dependent signaling pathway was significantly repressed in memory macrophages (Fig. 2C**)**. A sizeable number of genes appeared differentially regulated in naïve (UB) and memory (BB) macrophages (Fig. 2D). The comparison of both conditions showed that 422 genes were upregulated in memory

macrophages, while 277 were downregulated compared to the acute stimulation of the cells (Fig. 2D).

Long-term stimulation with *B. burgdorferi* induces metabolic changes in macrophages. IPA identified the HIF1α pathway as upregulated in memory macrophages (Table 1). We therefore, analyzed the metabolic status of memory macrophages by Seahorse. Macrophages that had been previously exposed to the spirochete showed similar oxygen consumption rates (OCR) compared to acutely stimulated BMMs (Fig. 3A, Suppl. Fig. 4A), although memory macrophages showed lower maximal respiratory (MRC) and reserve capacities. In contrast, the glycolytic capacity of memory macrophages was significantly higher than in acutely stimulated cells (Fig. 3B, Suppl. Fig. 4B) and correlated with the presence of increased levels of lactate in the memory supernatants (Suppl. Fig. 4C) as well as the increased expression of the gene encoding the enzyme lactate dehydrogenase in both murine (log_2 Fold Induction = 1; p = 2.15E-18, between memory and acute macrophages**)** and human cells (Suppl. Fig. 4D). Moreover, the increased glycolytic capacity correlated with the augmented expression of several glycolytic genes (Fig. 3C) and the higher expression levels of *Pfkfb3*, the gene encoding the positive regulator of glycolysis, fructose-2,6-bisphosphatase 3 [24] (Suppl. Fig. 4E). On the other hand, the quantitative analysis by GC-MS of several intermediate metabolites of the tricarboxylic acic cycle (TCA) showed highly increased levels of glutamine, glutamate, succinate, citrate and malate (Fig. 3D). These data confirm previous reports [3, 6] and suggested increased glutaminolysis in re-stimulated macrophages and the conversion of malate to pyruvate to induce higher levels of lactate.

Glycolysis inhibition modulates the response of murine macrophages and inflammation during Lyme borreliosis. We then assessed whether the inhibition of the glycolytic output of

macrophages would affect the phagocytic and inflammatory capacity of these cells. Naïve and memory BMMs were stimulated in the presence of the glucose analogue, 2-deoxy glucose (2-DG). In both acute and memory macrophages, the use of 2-DG reduced the production of lactate (Fig. 4A). The inhibition of glycolysis resulted in a significant increased ability of naive macrophages to phagocytose *B. burgdorferi* (Fig. 4B), accompanied by decreased levels of TNF (Fig. 4C). The inhibition of glycolysis did not, however, affect the phagocytic capacity of memory macrophages (Fig. 4B) although it resulted in lower production of TNF (Fig. 4C). Interestingly, the presence of 2-DG only during the initial stimulation of BMMs (48 h) did not affect the production of TNF by memory macrophages (Fig. 4C).

In order to assess whether the inhibition of glycolysis *in vivo* during infection with *B. burgdorferi* would affect the levels of bacteria in the heart (where macrophage infiltration is most evident) or their inflammatory status, we treated the infected animals with the pyruvate dehydrogenase kinase inhibitor, dichloroacetate (DCA) [25] and the PFKFB3 inhibitor, 3-(3-pyridinyl)-1-(4-pyridinyl)-2-propen-1-one (3PO) [26]. The mice were treated either from day 0 relative to infection, or after 2 weeks of infection, at the peak of disease, for a period of 2-3 weeks. The treatment with DCA did not significantly affect spirochetemia in the heart (Fig. 5A). However, both macrophage infiltration (as measured by the expression of the *Adgre1* gene, which encodes for the surface protein F4/80, Fig. 5B) and *Tnf* expression (Fig. 5C) were reduced in mice treated with DCA for a period of 2 weeks compared to the controls. The increased in treatment time did not result in reduced macrophage infiltration (Fig. 5B) although *Tnf* expression remained significantly lower than in control animals (Fig. 5C). In contrast, treatment with 3PO for a period of 3 weeks starting week 2 of infection resulted in significant reduced levels of spirochetes, macrophage infiltration and *Tnf* expression, compared to control mice (Fig. 5). These results show

that the inhibition of glycolysis *in vivo* during an ongoing infection with *B. burgdorferi* results in a better control of infection, lower macrophage infiltration and reduced inflammation in the heart.

Discussion

Innate immune memory has been defined as the long-term modulation of monocyte/macrophage responses upon an initial encounter with primarily single PAMPs or dead bacteria [2, 4]. These responses have been studied in the context of proinflammatory cytokine induction [2]. Here, we have defined the long-term consequences of the encounter of macrophages with live *B. burgdorferi*, a spirochete able to establish persistent infections in mammals. Because the response of macrophages to live and dead spirochetes is both quantitatively and qualitatively distinct [9, 27] and involves the capacity of these cells to eliminate bacteria [8, 28], we provide a new perspective on the development and functional consequences of innate immune memory.

The continuous exposure to *B. burgdorferi* induces an increased capacity to internalize the spirochete albeit with a diminished production of proinflammatory cytokines. The induction of innate memory responses to the spirochete seem to constitute an advantage to the host, since it results in the control of the spirochete and a reduced inflammatory output. However, because *B. burgdorferi* is still able to persist under these conditions, a further modulation of ongoing innate immune memory responses provides and advantage for a better control of the spirochete and the ensuing inflammatory response.

The long-term responses induced by macrophage exposure to *B. burgdorferi* are characterized by metabolic changes that are consistent with 'classical' innate memory responses, including an increased glycolytic output [29]. Indeed, increased *PFKFB3, HK2* and *LDHA* gene expression has been observed in Lyme borreliosis patients, as well as increased levels of serum lactate [30]. Therefore, our results support the metabolic switch in infected patients and pinpoint these changes to monocyte/macrophages, albeit they do not discount metabolic shifts in other immune cells. Our results also imply the increased production of malate, among other components

of the tricarboxylic acid cycle (TCA) through enhanced glutaminolysis, which can be shuttled to its conversion to pyruvate in the absence of increased oxygen consumption, and the augmented production of lactate, in part because of increased *Ldha* expression. Importantly, we show that the inhibition of glycolysis *in vivo* through the use of the PFKFB3 inhibitor, 3PO, during an ongoing infection with *B. burgdorferi* results in a decreased cardiac inflammatory response and the control of bacterial burdens in the heart. Overall, these data show that the stimulation of macrophages with *B. burgdorferi* is dynamic and while affecting those pathways already described [17], it is modulated by the continuous stimulation with the spirochete, particularly affecting the metabolic status of the cells. They also show that the metabolic hallmarks of long-term responses to the spirochete can be therapeutically targeted during an ongoing infection, resulting in the control of inflammation and the persistence of the bacterium.

References

1. Dominguez-Andres J, Netea MG. Long-term reprogramming of the innate immune system. J Leukoc Biol **2019**; 105:329-38.

2. Netea MG, Joosten LA, Latz E, et al. Trained immunity: a program of innate immune memory in health and disease. Science **2016**; 352:aaf1098.

3. Arts RJW, Carvalho A, La Rocca C, et al. Immunometabolic Pathways in BCG-Induced Trained Immunity. Cell Rep **2016**; 17:2562-71.

4. Netea MG. Training innate immunity: the changing concept of immunological memory in innate host defence. Eur J Clin Invest **2013**; 43:881-4.

5. Kelly B, O'Neill LA. Metabolic reprogramming in macrophages and dendritic cells in innate immunity. Cell Res **2015**; 25:771-84.

6. Arts RJ, Novakovic B, Ter Horst R, et al. Glutaminolysis and fumarate accumulation integrate immunometabolic and epigenetic programs in trained immunity. Cell Metab **2016**; 24:807-19.

7. Ip WK, Sokolovska A, Charriere GM, et al. Phagocytosis and phagosome acidification are required for pathogen processing and MyD88-dependent responses to *Staphylococcus aureus*. J Immunol **2010**; 184:7071-81.

8. Cruz AR, Moore MW, La Vake CJ, Eggers CH, Salazar JC, Radolf JD. Phagocytosis of *Borrelia burgdorferi*, the Lyme disease spirochete, potentiates innate immune activation and induces apoptosis in human monocytes. Infect Immun **2008**; 76:56-70.

9. Cervantes JL, Dunham-Ems SM, La Vake CJ, et al. Phagosomal signaling by *Borrelia burgdorferi* in human monocytes involves Toll-like receptor (TLR) 2 and TLR8 cooperativity and TLR8-mediated induction of IFN-{beta}. Proc Natl Acad Sci U S A **2011**; 108:3683-8.

10. Petzke MM, Brooks A, Krupna MA, Mordue D, Schwartz I. Recognition of *Borrelia burgdorferi*, the Lyme disease spirochete, by TLR7 and TLR9 induces a type I IFN response by human immune cells. J Immunol **2009**; 183:5279-92.

11. Chong C, Bost KL, Clements JD. Differential production of interleukin-12 mRNA by murine macrophages in response to viable or killed *Salmonella* spp. Infect Immun **1996**; 64:1154-60.

12. Bernard Q, Smith AA, Yang X, et al. Plasticity in early immune evasion strategies of a bacterial pathogen. Proc Natl Acad Sci U S A **2018**; 115:E3788-E97.

13. Hodzic E, Imai D, Feng S, Barthold SW. Resurgence of persisting non-cultivable *Borrelia burgdorferi* following antibiotic treatment in mice. PLoS One **2014**; 9:e86907.

14. Embers ME, Barthold SW, Borda JT, et al. Persistence of *Borrelia burgdorferi* in rhesus macaques following antibiotic treatment of disseminated infection. PLoS One **2012**; 7:e29914.

15. Barthold SW, de Souza MS, Janotka JL, Smith AL, Persing DH. Chronic Lyme borreliosis in the laboratory mouse. Am J Pathol **1993**; 143:959-71.

16. Scheffold N, Herkommer B, Kandolf R, May AE. Lyme carditis--diagnosis, treatment and prognosis. Dtsch Arztebl Int **2015**; 112:202-8.

17. Carreras-Gonzalez A, Navasa N, Martin-Ruiz I, et al. A multi-omic analysis reveals the regulatory role of CD180 during the response of macrophages to Borrelia burgdorferi. Emerg Microbes Infect **2018**; 7:19.

18. Dunham-Ems SM, Caimano MJ, Pal U, et al. Live imaging reveals a biphasic mode of dissemination of *Borrelia burgdorferi* within ticks. J Clin Invest **2009**; 119:3652-65.

19. Hawley KL, Olson CM, Jr., Iglesias-Pedraz JM, et al. CD14 cooperates with complement receptor 3 to mediate MyD88-independent phagocytosis of *Borrelia burgdorferi*. Proc Natl Acad Sci U S A **2012**; 109:1228-32.

20. Hovius JW, Bijlsma MF, van der Windt GJ, et al. The urokinase receptor (uPAR) facilitates clearance of *Borrelia burgdorferi*. PLoS Pathog **2009**; 5:e1000447.

21. Trapnell C, Pachter L, Salzberg SL. TopHat: discovering splice junctions with RNA-Seq. Bioinformatics **2009**; 25:1105-11.

22. Liao Y, Smyth GK, Shi W. The Subread aligner: fast, accurate and scalable read mapping by seed-and-vote. Nucleic Acids Res **2013**; 41:e108.

23. Love MI, Huber W, Anders S. Moderated estimation of fold change and dispersion for RNA-seq data with DESeq2. Genome Biol **2014**; 15:550.

24. Calvo MN, Bartrons R, Castano E, Perales JC, Navarro-Sabate A, Manzano A. PFKFB3 gene silencing decreases glycolysis, induces cell-cycle delay and inhibits anchorage-independent growth in HeLa cells. FEBS Lett **2006**; 580:3308-14.

25. Caro-Maldonado A, Wang R, Nichols AG, et al. Metabolic reprogramming is required for antibody production that is suppressed in anergic but exaggerated in chronically BAFF-exposed B cells. J Immunol **2014**; 192:3626-36.

26. Schoors S, De Bock K, Cantelmo AR, et al. Partial and transient reduction of glycolysis by PFKFB3 blockade reduces pathological angiogenesis. Cell Metab **2014**; 19:37-48.

27. Salazar JC, Duhnam-Ems S, La Vake C, et al. Activation of human monocytes by live *Borrelia burgdorferi* generates TLR2-dependent and -independent responses which include induction of IFN-beta. PLoS Pathog **2009**; 5:e1000444.

28. Moore MW, Cruz AR, LaVake CJ, et al. Phagocytosis of *Borrelia burgdorferi* and *Treponema pallidum* potentiates innate immune activation and induces gamma interferon production. Infect Immun **2007**; 75:2046-62.

29. Cheng SC, Quintin J, Cramer RA, et al. mTOR- and HIF-1alpha-mediated aerobic glycolysis as metabolic basis for trained immunity. Science **2014**; 345:1250684.

30. Oosting M, Kerstholt M, Ter Horst R, et al. Functional and Genomic Architecture of *Borrelia burgdorferi*-Induced Cytokine Responses in Humans. Cell Host Microbe **2016**; 20:822-33.

Acknowledgments

This work was supported by grants from the Spanish Ministry of Science, Innovation and Universities (MCIU) co-financed with FEDER funds [SAF2015-65327-R and RTI2018-096494-B-100 to JA; BFU2016-76872-R to EB, AGL2017-86757-R to LA, SAF2017-87301-R to MLMC, SAF2015-64111-R to AP, SAF2015-73549-JIN to HR], Instituto de Salud Carlos III [PIE13/0004 to AP], the Basque Government Department of Health [2015111117 to LA], the Basque Foundation for Innovation and Health Research (BIOEF), through the EiTB Maratoia grant [BIO15/CA/016/BS to MLMC], the regional Government of Andalusia co-funded by CEC and FEDER funds [Proyectos de Excelencia P12-CTS-2232] and Fundación Domingo Martínez [to AP]. LA is supported by the Ramon y Cajal program [RYC-2013-13666]. DB, MMR, TMM and AP are recipients of MCIU FPI fellowships. ACG is a recipient of a fellowship form the Basque Government. APC is a recipient of a fellowship from the University of the Basque Country. We thank the MCIU for the Severo Ochoa Excellence accreditation [SEV-2016-0644], the Basque Department of Industry, Tourism and Trade [Etortek and Elkartek programs], the Innovation Technology Department of the Bizkaia Province and the CIBERehd network.

***Conflict of interests*:** The authors declare no conflict of interests.

Figure legends

Figure 1. *B. burgdorferi* induces long-term responses in macrophages that affect phagocytosis and proinflammatory cytokine production. (A) TNF production by murine BMMs (mBMM) and human peripheral blood monocytes (hMon) acutely (UB) and re-stimulated (BB) with *B. burgdorferi*, compared to unstimulated (UU) and stimulated and rested (BU) macrophages. (B) *B. burgdorferi* binding (upper panel) and internalization (lower panel) by naïve (black histograms) and memory (red histograms) BMMs. The grey histogram represents BMMs with no spirochetes added. (C) Confocal image showing binding of GFP-*B. burgdorferi* (Bb) to naïve (UB) and memory (BB) macrophages. The cells were incubated at 4 ºC for 2 hours, fixed and stained with phalloidin and DAPI. (D) Phagocytic index of naïve (UB) and memory (BB) macrophages.

Figure 2. Short- and long-term transcriptional regulation induced by *B. burgdorferi* in murine macrophages. (A) Principal component analysis of the transcriptome of unstimulated (UU), acutely stimulated (UB), stimulated and rested (BU) and re-stimulated (BB) macrophages. (B) Venn diagram representing genes that are co- and differentially regulated in naïve (UB) and re-stimulated (BB) macrophages versus unstimulated cells. The numbers at the top represent genes upregulated, while those at the bottom indicate the number of genes downregulated. (C) Upstream pathways regulated in acute (UB) and memory macrophages (BB) compared to unstimulated (UU) BMMs. Processes that showed activation are indicated in orange, whereas those that were repressed are presented in blue. The color intensities are representative of the calculated Z value for each process. (D) Volcano plot showing the differential expression of genes when comparing acute and memory macrophages. The red dots represent genes upregulated in BB macrophages and the blue dots indicate genes that are upregulated in acutely stimulated macrophages.

Fig. 3. *B. burgdorferi*-induced metabolic changes in memory macrophages. (A) Normalized oxygen consumption rate (OCR) and (B) glycolysis of acute and memory murine macrophages. FCCP: carbonyl cyanide-4-(trifluoromethoxy)phenylhydrazone; Rot: rotenone. (C) Variation in gene expression levels of components of glycolysis between acute and memory macrophages. The colors indicate changes in gene expression when comparing acute and memory macrophages with unstimulated cells. An internal asterisk (*) indicates that the differences are > 2 fold and $p < 0.05$. Those genes significantly increased in memory compared to acute macrophages are marked in bold, while those significantly reduced are marked in bold and underlined. (D) Intermediate metabolites of the TCA in acute and memory murine macrophages. *; Student´s t test, $p < 0.05$.

Fig. 4. Glycolysis inhibition modulates the response of murine macrophages to *B. burgdorferi*. (A) Lactate production (B) Phagocytosis and (C) TNF induction by *B. burgdorferi* in acute and memory macrophages in the presence or absence of the glycolysis inhibitor, 2-deoxyglucose (DG), during the phase of memory generation (48h) or the restimulation period (20h).

Fig. 5. Glycolysis inhibition modulates the response of murine macrophages and decreases inflammation during Lyme borreliosis. (A) *B. burgdorferi* burdens in the heart of infected mice as determined by DNA real-time PCR using primers specific for *recA* and relateive to the house-keeping gene, *Rpl19*. The mice were treated with DCA or 3PO starting the same day (0+4) or 2 weeks after infection (2+2; 2+3). The mice were treated for 2 (2+2), 3 (2+3) or 4 (0+4) weeks. (E) Macrophage infiltration and (F) *Tnf* gene expression in infected mouse hearts treated with DCA or 3PO, using the same regimes as in A. Uninf.: uninfected controls. The results shown represent 5-10 mice per group. The results were analyzed by ANOVA, followed by pairwise comparisons. *; $p < 0.05$.

Table 1. **Upstream pathways regulated in memory macrophages compared to acutely stimulated cells.** Pathways activated (z-score >2) and repressed (z-score < -2) were identified using the Ingenuity Pathway Analysis tool. The table represents the ten most upregulated and ten most repressed upstream regulator pathways. The full list is provided in Table S2.

Upstream Regulator	Expr Log Ratio	Activation z-score	p-value of overlap
Prostaglandin E2		3.843	5.92E-29
Il6	1.569	3.7	5.67E-35
Cg		3.294	4.86E-14
Hif1a	0.685	3.223	2.74E-15
Stat3	0.479	3.165	1.63E-25
Ca^{2+}		3.156	1.1E-10
FGF2		3.084	1.98E-15
Forskolin		3.045	4.73E-19
Mek		3.04	2.76E-09
Cd38	1.002	3.003	7.84E-07
Androgen		-2.646	3.86E-05
NS-398		-2.673	1.11E-7
Silibinin		-2.742	1.26E-03
CD3		-2.811	3.3E-15
Salirasib		-2.813	1.26E-04

Stk11	0.089	-2.88	9.04E-04
AP5		-2.882	2.09E-05
EGTA		-2.961	2.91E-07
Linsidomine		-2.961	5.92E-07
H89		-3.285	1,01E-13

1
2

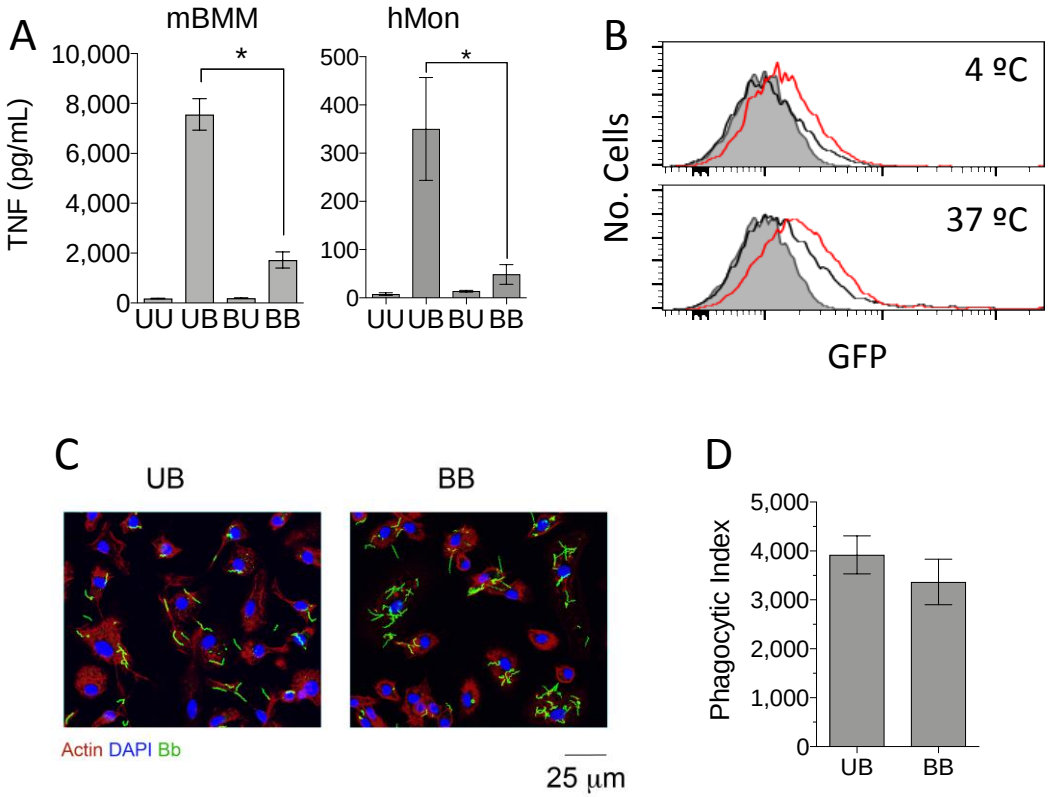

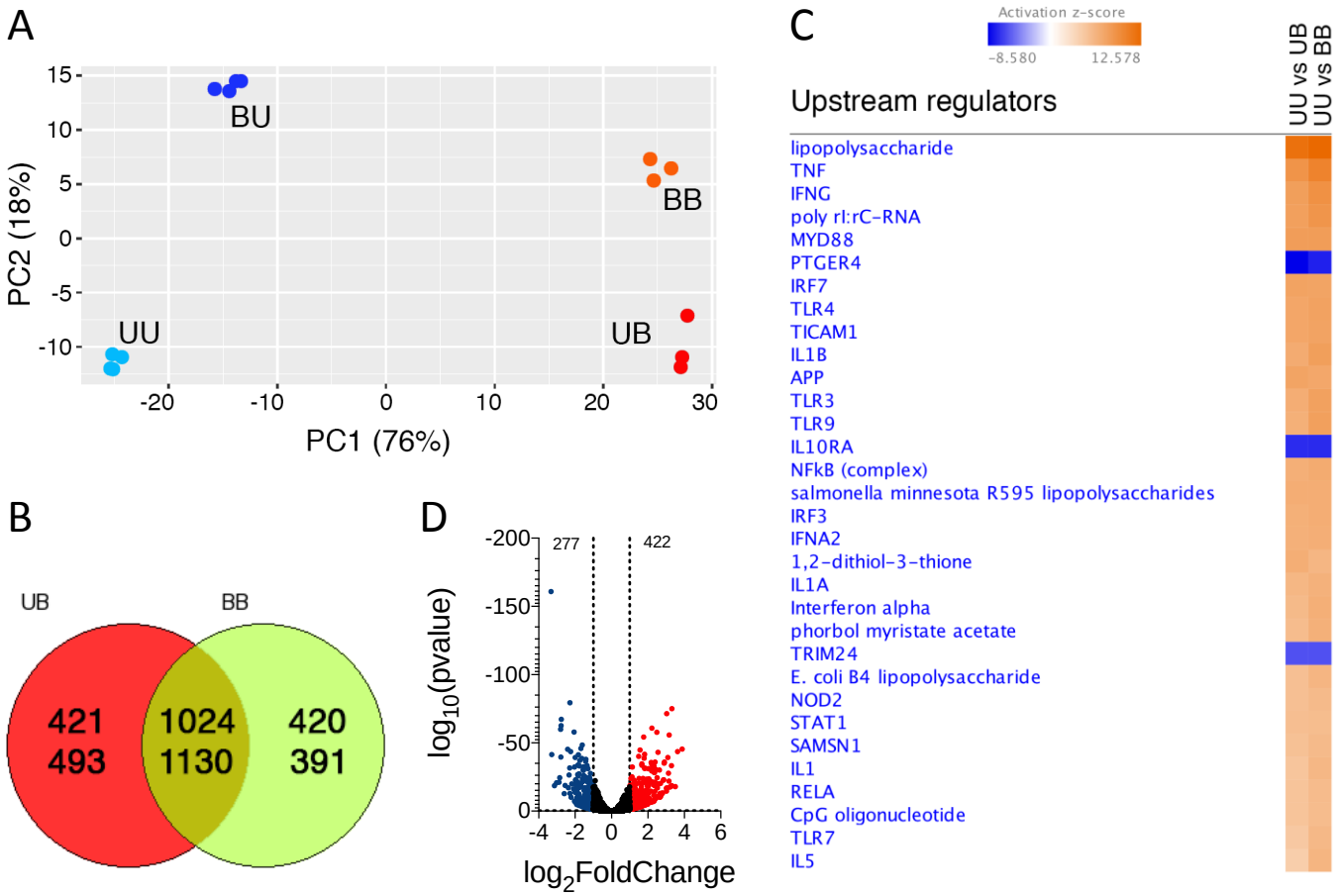
A
15
10
5
0
-5
-10
PC2 (18%)
BU
BB
UU
UB
-20
-10
0
10
20
30
PC1 (76%)
B
UB
BB
421
493
1024
1130
420
391
D
-200
-150
-100
-50
0
277
422
log10(pvalue)
-4
-2
0
2
4
6
log2FoldChange
C
Activation z-score
-8.580
12.578
Upstream regulators
UU vs UB
UU vs BB
lipopolysaccharide
TNF
IFNG
poly rI:rC-RNA
MYD88
PTGER4
IRF7
TLR4
TICAM1
IL1B
APP
TLR3
TLR9
IL10RA
NFkB (complex)
salmonella minnesota R595 lipopolysaccharides
IRF3
IFNA2
1,2-dithiol-3-thione
IL1A
Interferon alpha
phorbol myristate acetate
TRIM24
E. coli B4 lipopolysaccharide
NOD2
STAT1
SAMSN1
IL1
RELA
CpG oligonucleotide
TLR7
IL5

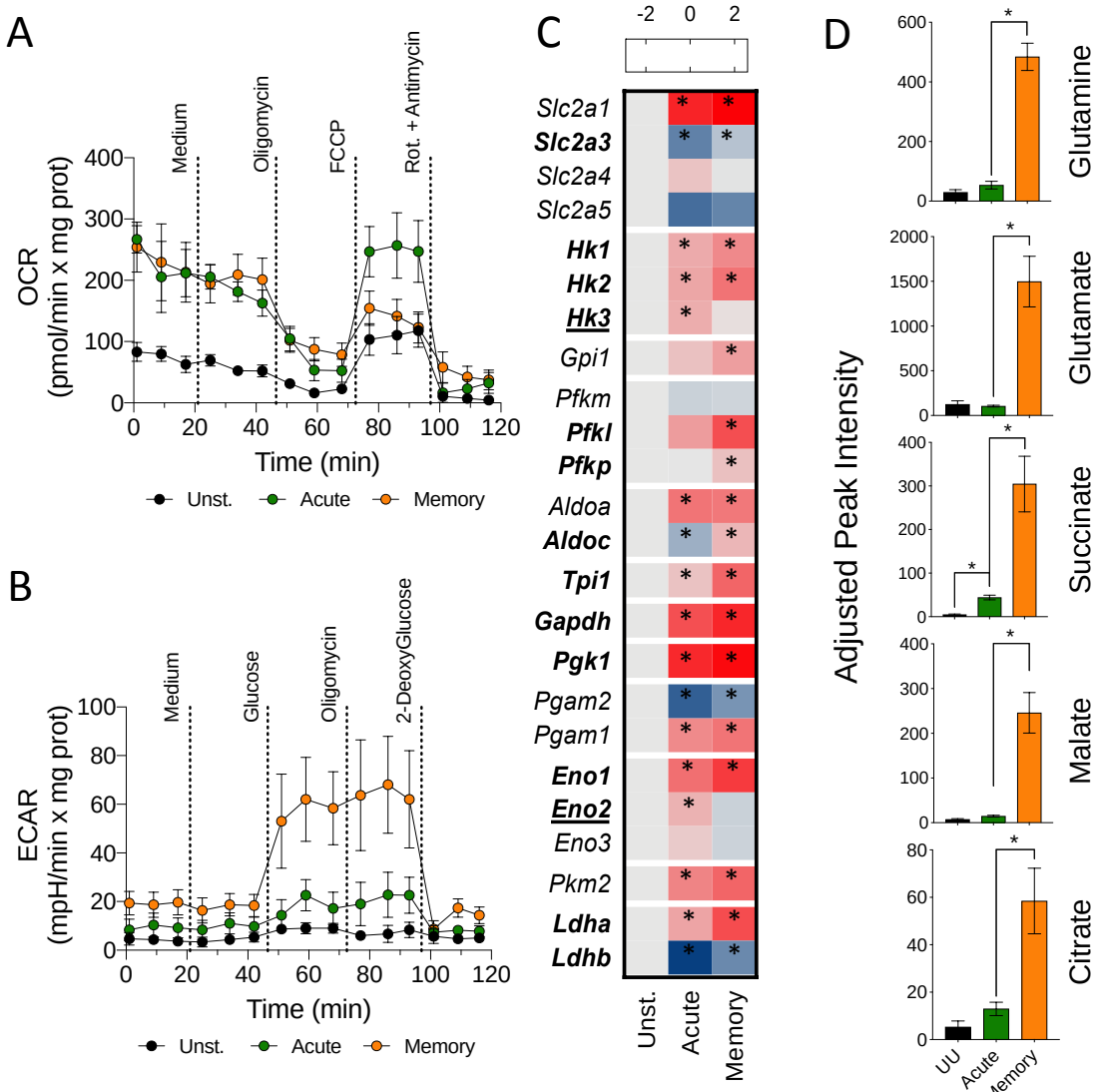
A
OCR
(pmol/min x mg prot)
Medium
Oligomycin
FCCP
Rot. + Antimycin
Time (min)
Unst.
Acute
Memory
B
ECAR
(mpH/min x mg prot)
Medium
Glucose
Oligomycin
2-DeoxyGlucose
Time (min)
Unst.
Acute
Memory
C
-2
0
2
Slc2a1
Slc2a3
Slc2a4
Slc2a5
Hk1
Hk2
Hk3
Gpi1
Pfkm
Pfkl
Pfkp
Aldoa
Aldoc
Tpi1
Gapdh
Pgk1
Pgam2
Pgam1
Eno1
Eno2
Eno3
Pkm2
Ldha
Ldhb
Unst.
Acute
Memory
D
Adjusted Peak Intensity
Glutamine
Glutamate
Succinate
Malate
Citrate
UU
Acute
Memory

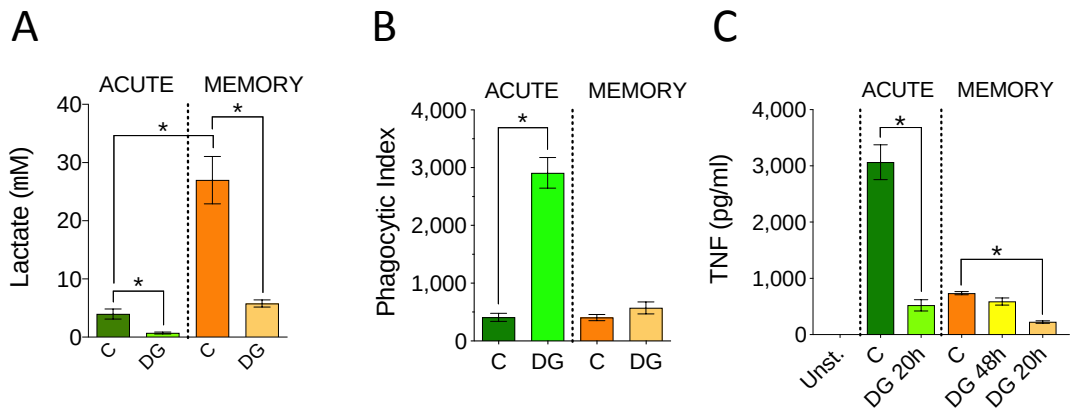
A
ACUTE
MEMORY
Lactate (mM)
40
30
20
10
0
*
*
*
C
DG
C
DG
B
ACUTE
MEMORY
Phagocytic Index
4,000
3,000
2,000
1,000
0
*
C
DG
C
DG
C
ACUTE
MEMORY
TNF (pg/ml)
4,000
3,000
2,000
1,000
0
*
*
Unst.
C
DG 20h
C
DG 48h
DG 20h

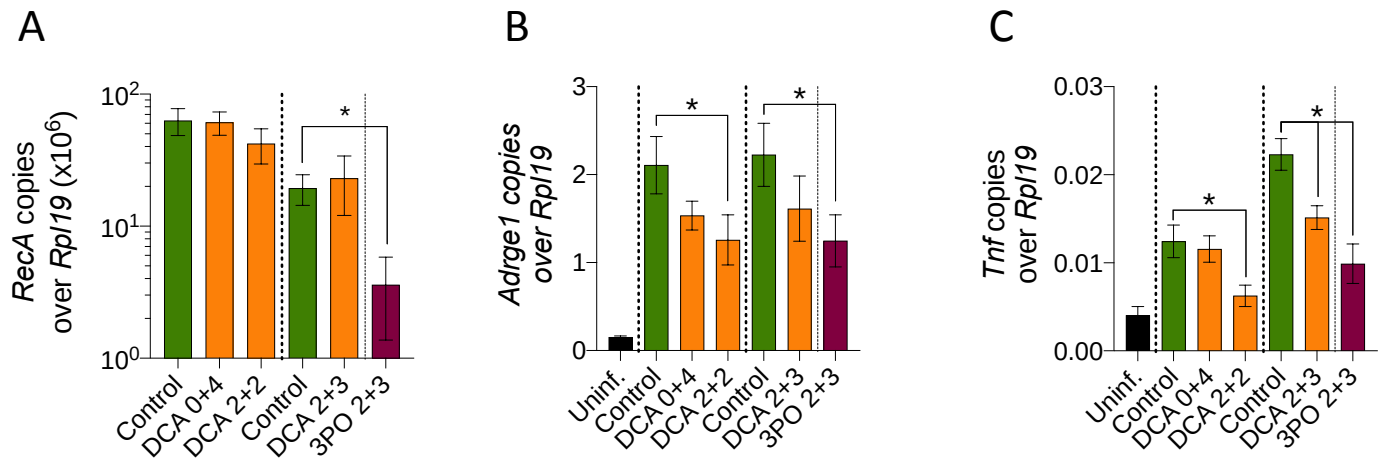
A
RecA copies over Rpl19 (x10^6)
10^2
10^1
10^0
*
Control
DCA 0+4
DCA 2+2
Control
DCA 2+3
3PO 2+3
B
Adrge1 copies over Rpl19
3
2
1
0
*
*
Uninf.
Control
DCA 0+4
DCA 2+2
Control
DCA 2+3
3PO 2+3
C
Tnf copies over Rpl19
0.03
0.02
0.01
0.00
*
*
Uninf.
Control
DCA 0+4
DCA 2+2
Control
DCA 2+3
3PO 2+3

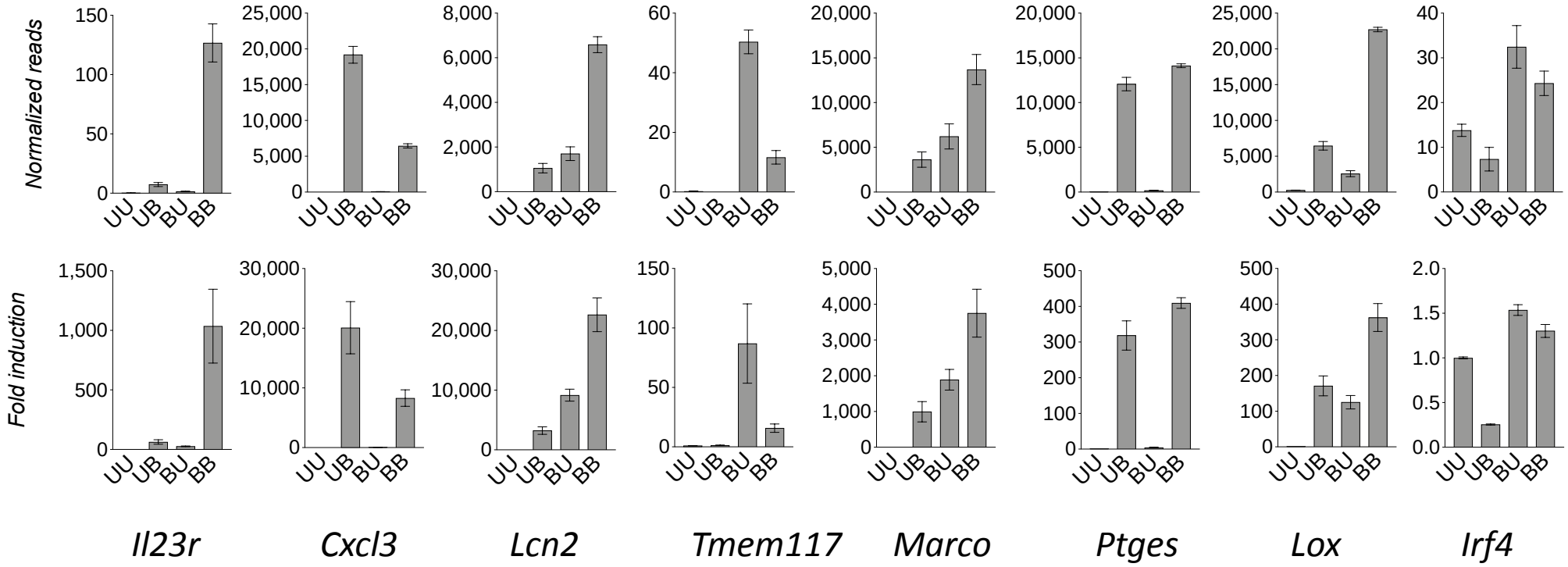

Supplementary Figure 1. Validation of the RNAseq. The upper graphs show normalized reads of a group of selected genes differentially regulated in BMMs from 4 independent mice, as determined by the RNA-seq analysis. The bottom graphs show the fold induction of the same genes determined by qRT-PCR using BMMs from 4 mice. BMMs were stimulated following the schedule from figure 1A.

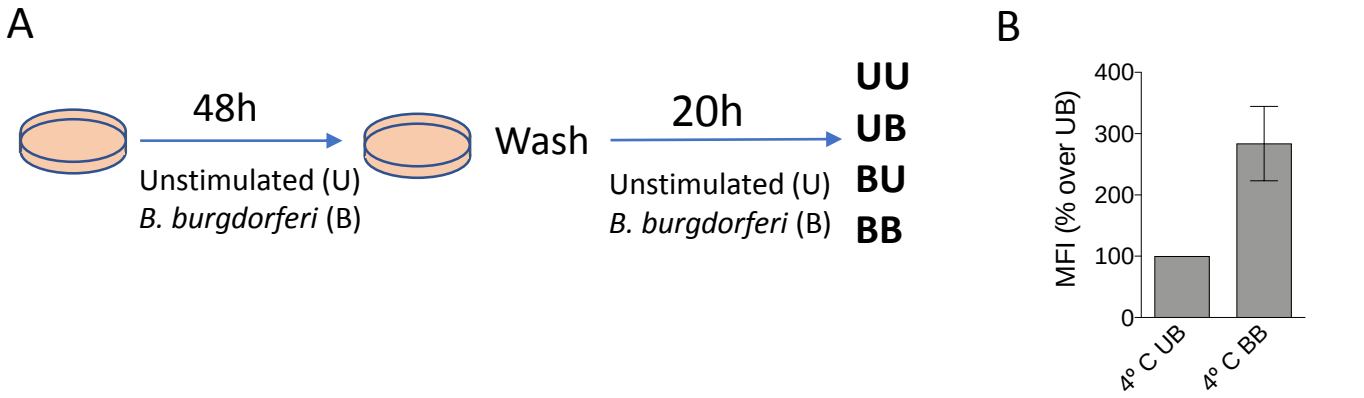

Supplementary Figure 2. *B. burgdorferi* induces long-term responses in macrophages that affect phagocytosis and proinflammatory cytokine production. (A) Schematic representation of the working conditions to assess long-term effects of the stimulation of BMMs with *B. burgdorferi*. The four conditions were defined by the first and secondary stimulations, yielding the conditions UU, UB, BU and BB. (B) TNF production by BMMs acutely (UB) and re-stimulated (BB) with *B. burgdorferi*, compared to unstimulated (UU) and stimulated and rested (BU) macrophages. (B) Increased mean fluorescence intensity (MFI) of memory macrophages over naïve cells, incubated for 2 h at 4 ºC. The data are presented as percentage increase over acutely stimulated macrophages (UB).

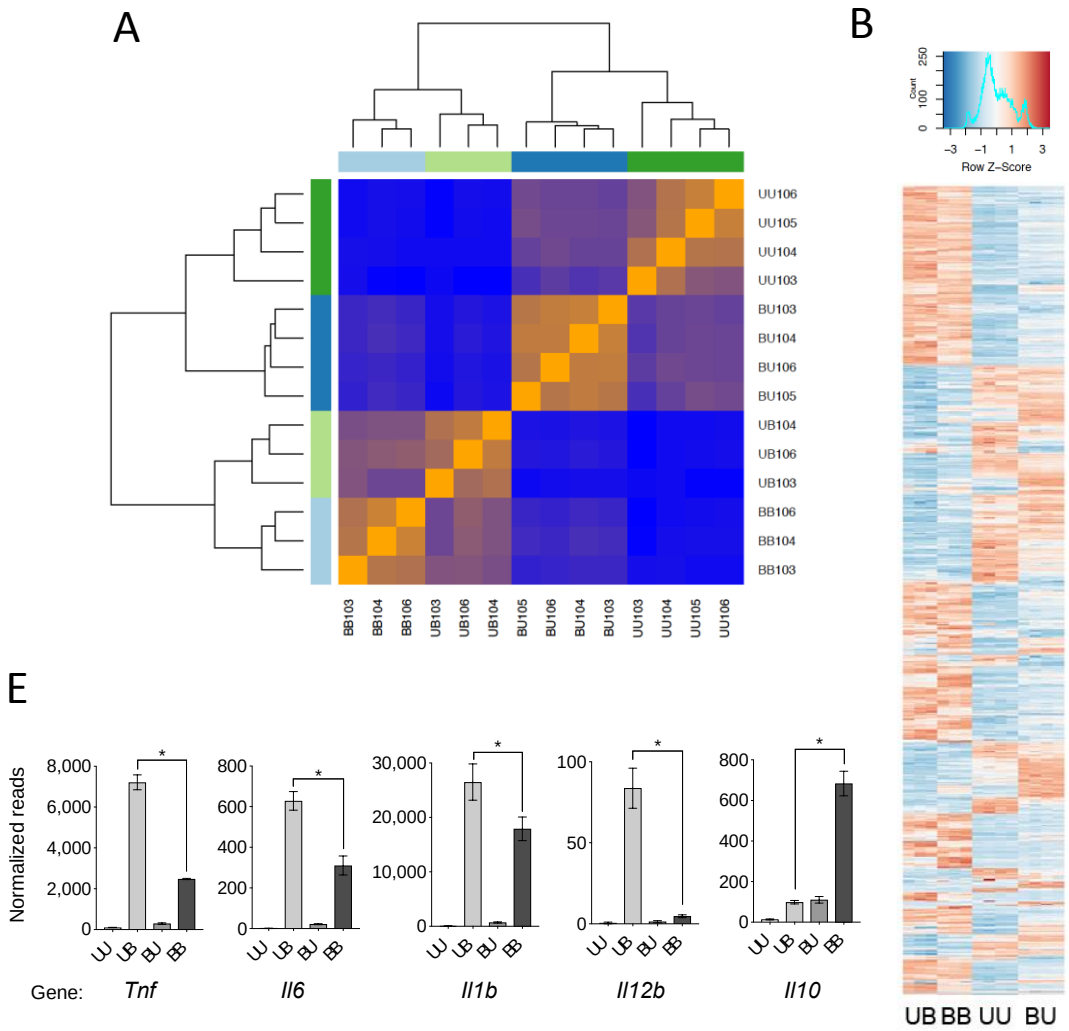

Supplementary Figure 3. Short- and long-term transcriptional regulation induced by *B. burgdorferi* in murine macrophages. (A) Sample distance matrix of BMMs stimulated with *B. burgdorferi* under the conditions described in Fig. 1A. (B) Heat map representing the most 1,000 regulated genes in BMMs differentially exposed to *B burgdorferi*. (C) Volcano plot showing genes differentially regulated between unstimulated (UU) and stimulated and rested (BU) BMMs. The red dots represent upregulated genes in BU macrophages, whereas the blue dots correspond to downregulated genes. The cut-off values to determine differential expression were set at an absolute value of $\log_2$ Fold Induction of 1 and $p < 0.05$. (D) Volcano plots representing genes differentially expressed by acutely stimulated (Condition UB; left panel) and re-stimulated (Condition BB; right panel) macrophages versus unstimulated cells. (E) mRNA expression levels of pro- and anti-inflammatory cytokines in BMMs differentially exposed to *B. burgdorferi*.

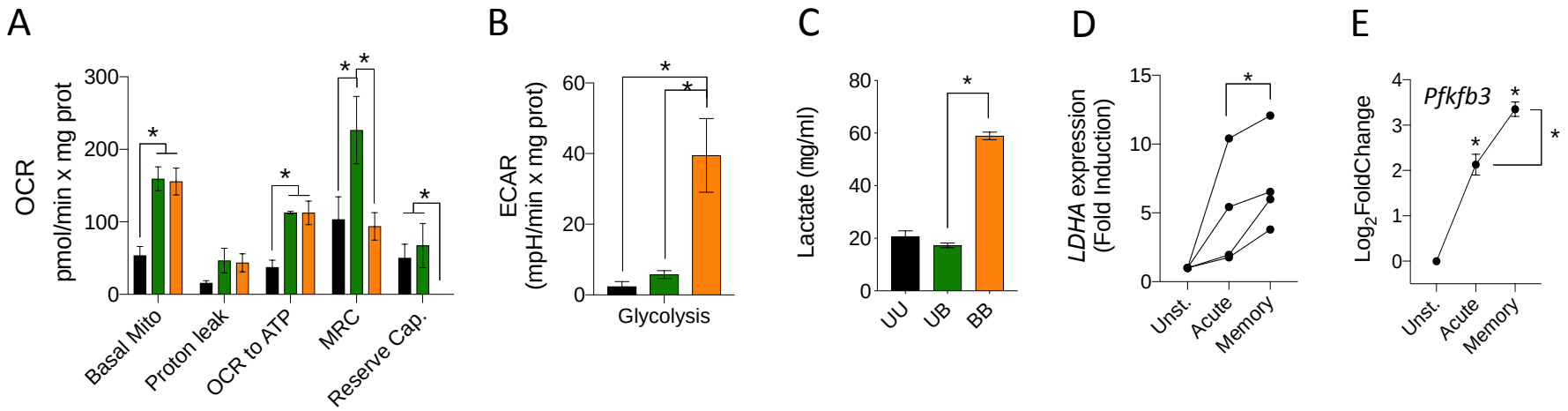

Supplementary Figure 4. *B. burgdorferi*-induced metabolic changes in memory macrophages. (A) Normalized oxygen consumption rate (OCR) and (B) glycolysis of acute and memory murine macrophages. MRC: maximal respiratory capacity. (C) Lactate production by acute and memory murine macrophages, measured in the supernatants of cells stimulated following the experimental design described in Fig. 1A. *; Student´s t tes, $p < 0.05$. (D) *LDHA* expression in acute and memory human peripheral blood monocytes, as determined by real-time PCR. *; paired Student´s t test, $p < 0.05$. (E) *Pfkfb3* gene expression changes in acute and memory macrophages in response to B. burgdorferi stimulation. *, $p < 0.05$.